

UNIVERSITY OF SOUTHAMPTON

**FACULTY OF MEDICINE, HEALTH AND
BIOLOGICAL SCIENCES**

SCHOOL OF MEDICINE

Division of Infection Inflammation and Repair

**Molecular and Functional Characterisations of
UTE-1 Binding Proteins involved in the Regulation
of the Human *TIMP1* Gene**

Marie-Anne Bertrand

Thesis for the degree of Doctor of Philosophy

December 2004

ABSTRACT

FACULTY OF MEDICINE, HEALTH AND BIOLOGICAL SCIENCES

SCHOOL OF MEDICINE

DIVISION OF INFLAMMATION, INFECTION AND REPAIR

Doctor of Philosophy

MOLECULAR AND FUNCTIONAL CHARACTERISATIONS OF UTE-1
BINDING PROTEINS INVOLVED IN THE REGULATION OF THE HUMAN
TIMP1 GENE

By Marie-Anne Bertrand

Liver fibrosis is characterised by an excessive deposition of ECM proteins disrupting the normal architecture of the liver. In normal tissues, ECM degradation is finely controlled by a balance between the activities of matrix metalloproteinases (MMP) and their inhibitors, tissue specific of metalloproteinases (TIMP). In contrast, in the fibrotic liver, the overexpression of TIMP1 by hepatic Stellate cells (HSC) leads to an impaired ECM degradation. Therefore, the regulation of *TIMP1* gene expression is a key process in the development of the disease. Within the *TIMP1* promoter, a DNA binding element essential for the promoter activity, named upstream TIMP-1 element (UTE-1), has been identified. This DNA region is the binding site of an unknown 30 kDa protein. The aim of this thesis was to identify this protein and its role in the control of *TIMP1* expression in HSC.

The key finding of this work was the identification of RUNX proteins as the transcription factors that bind to the UTE-1. RUNX proteins are three important transcription regulators involved in the pathology of several cancers. This study demonstrated that HSC expressed several spliced forms of RUNX1 and RUNX2 and that, at least, RUNX1 was associated with the *TIMP1* promoter *in situ*. Reporter gene assays demonstrated that overexpression of the main variant of RUNX1 (RUNX1B) inhibited *TIMP1* transcription whereas RUNX1A, which lacked the C-terminal region, and RUNX2 functioned as stimulators. In addition JunD and MOZ-induced transcription of *TIMP1* was inhibited by RUNX1B but not RUNX1A suggesting that the C-terminal domain of RUNX1B was responsible for the repression. This effect was associated with a lack of interaction between RUNX1B and JunD whereas RUNX1A could directly interact with JunD. These data suggested that, RUNX1B recruits, via its C-terminal domain, transcriptional repressors within the *TIMP1* promoter, resulting in the inhibition of both interaction with JunD and activation of the transcription. In contrast, RUNX1B repression of transcription is reverted in the presence of CBP. Hence, RUNX1B have stimulatory or inhibitory effect on *TIMP1* transcription depending on the nature of its interaction with other cofactors.

During this study, we also demonstrated the utility of baculovirus as a vector for the delivery, to both mammalian cell lines and primary cells, of a shRNA-generating cassette and the consequent RNAi-mediated silencing of the *Lamin* gene. This new technology could be used to silence endogenous *RUNX* genes in primary HSC in order to have a complete understanding of the regulation of *TIMP1* expression by RUNX and therefore identifying potential therapeutic targets.

List of contents

Abstract	ii
List of contents	iii
List of Tables and Figures	viii
Author's declaration	x
Acknowledgements	xi
Abbreviations	xii
Chapter 1: Introduction	1
1.1. The liver and liver fibrosis	2
1.1.1. Function of the liver	2
1.1.2. Cell composition of the liver	3
1.1.2.1. Hepatocytes, the major cells of the liver and sinusoids	3
1.1.2.2. Hepatic Stellate Cells, source of ECM and cytokines	3
1.1.3. Quiescent HSC : not that quiet	5
1.1.3.1. Change in HSC characteristics during activation	5
1.1.3.2. Stimuli inducing HSC activation	5
1.1.3.3. Transcription regulation associated with HSC activation	5
1.1.4. Molecular changes during liver fibrosis	6
1.2. Matrix metalloproteinases, ECM degrading enzymes	9
1.2.1. Characteristics of MMP	9
1.2.1.1. Nomenclature, substrate and structure of MMP	9
1.2.1.2. Role of MMP: ECM digestion...and more	11
1.2.1.3. MMP in liver fibrosis	12
1.2.2. Regulation of MMP: different levels of control	12
1.2.2.1. Transcriptional regulation	12
1.2.2.2. Post-translational regulation	14
1.2.2.3. Extracellular inhibitors of MMP	15
1.3. TIMP1, key effector of liver fibrosis	18
1.3.1. Expression of TIMP1 during liver fibrosis	18
1.3.2. Promoter of <i>TIMP1</i> gene in HSC	19
1.3.2.1. Organisation of the minimal promoter	19
1.3.2.2. UTE-1 a novel regulator element	21
1.4. RUNX transcription factors	23
1.4.1. Biological function of RUNX	23
1.4.1.1. RUNX1, discovered as regulator of hematopoiesis	23
1.4.1.1.1. Chromosomal translocation of RUNX1	23
1.4.1.1.2. <i>Runx1</i> knock-out mice	25
1.4.1.1.3. RUNX1 involvement in cancer and autoimmune disease	25
1.4.1.2. RUNX2, key role in osteogenesis	26
1.4.1.3. RUNX3 tumor suppressor in gastric cancer	26
1.4.1.4. Expression pattern	27
1.4.2. Regulation of <i>RUNX</i> gene expression	29
1.4.2.1. Genomic organisation of RUNX	29
1.4.2.2. Alternative spliced variants	31
1.4.2.3. Transcriptional regulation	31
1.4.2.4. Signalling pathway regulating <i>RUNX</i> expression	34
1.4.3. RUNX activity and its regulation	35
1.4.3.1. RUNX gene target	35
1.4.3.2. Post translational regulations of RUNX	35
1.4.3.3. Regulation of RUNX activity by interaction with other factors	40
1.4.3.3.1. Functional domains of RUNX	40
1.4.3.3.2. Interaction of RUNX with co-repressors	42

1.4.3.3.3. Interaction of RUNX with co-activators	42
1.4.3.3.4. The model of enhanceosome	44
1.5. Conclusion	44
Chapter 2: Materials and Methods	46
2.1. Strains, cells and plasmids	47
2.1.1. Strains	47
2.1.1.1. Genotype	47
2.1.1.2. Culturing and media	47
2.1.1.3. Frozen stocks and recovering	48
2.1.2. Mammalian cells	48
2.1.2.1. Cell type	48
2.1.2.2. Culturing	48
2.1.3. Plasmids	49
2.1.3.1. Vectors used in the One-Hybrid System	49
2.1.3.2. Expression vector used in functional assay	50
2.2. DNA manipulation	51
2.2.1. Digestion of plasmid DNA	51
2.2.2. Ligation	52
2.2.3. Transformation of plasmid DNA into bacteria	52
2.2.4. PCR reaction	52
2.2.5. DNA purification	52
2.2.5.1. DNA purification from Bacteria	52
2.2.5.2. DNA purification from Yeast	53
2.2.5.3. Phenol/Chloroform extraction of DNA	53
2.2.5.4. DNA extraction from agarose gel	53
2.3. Screening of a cDNA library with the One-Hybrid System	54
2.3.1. Preparation of the target-reporter construct	54
2.3.1.1. Synthesis of the oligonucleotides	54
2.3.1.2. Digestion and ligation of plasmid DNA	55
2.3.1.3. Analysis of the transformed bacteria by PCR	55
2.3.2. Preparation of the plasmid DNA	56
2.3.2.1. Preparation of reporter plasmid DNA	56
2.3.2.2. Preparation of cDNA library plasmid	56
2.3.3. Transformation of plasmid DNA into yeast	56
2.3.3.1. Small-scale transformation procedure	56
2.3.3.2. Large scale transformation procedure	57
2.4. Gene expression determination	58
2.4.1. RT-PCR	58
2.4.1.1. RNA isolation	58
2.4.1.2. cDNA synthesis	58
2.4.1.3. PCR	59
2.4.1.4. TaqMan PCR	59
2.4.2. Western Blot	61
2.4.2.1. Preparation of cell protein extracts	62
2.4.2.2. Separation of proteins by electrophoresis	62
2.4.2.3. Protein transfer to Nitrocellulose	62
2.4.2.4. Immunolocalisation of proteins on nitrocellulose membranes	63
2.5. Studies of protein-DNA interaction	63
2.5.1. Electrophoretic mobility shift assay (EMSA)	63
2.5.1.1. Protein extraction	63
2.5.1.1.1. Yeast protein extraction for EMSA	63
2.5.1.1.2. Mammalian nuclear protein extraction	64
2.5.1.2. Labelling of the probe	64

2.5.1.3. DNA-protein binding reaction and electrophoresis of the complexes	65
2.5.2. Chromatin immunoprecipitation assay (ChIP)	66
2.6. Studies of proteins interactions: Immunoprecipitation assay	67
2.6.1 Cells extract preparation	67
2.6.2. FLAG-protein Immunoprecipitation	67
2.6.3. Elution of the FLAG-protein	68
2.7. Gene Overexpression: Reporter gene assay	68
2.7.1. Cloning DNA into reporter system	68
2.7.1.1. Cloning protein sequence from library's positive clones into an expression vector	68
2.7.1.2. Cloning of <i>TIMP1</i> promoter into pGL2 basic	68
2.7.2. Transfection	69
2.7.2.1. GeneJuice™ transfection	69
2.7.2.2. Effectene™ transfection	70
2.7.3. Chloramphenicol acetyl transferase (CAT) assay	70
2.7.3.1. Protein extraction	70
2.7.3.2. Enzymatic assay	71
2.7.4. Luciferase reporter gene assay	71
2.7.4.1. Protein extraction	71
2.7.4.2. Luciferase assay	72
2.7.5. β galactosidase assay	72
2.7.5.1. β galactosidase assay on Colonies	72
2.7.5.2. β -galactosidase assay on cell lysates	73
2.8. Gene silencing: baculovirus delivered shRNAi experiments	73
2.8.1. Construction of recombinant bacmid DNA	73
2.8.1.1. Cloning of oligonucleotide template into pFIGU plasmid donor	73
2.8.1.2. Transposition of the recombinant pFIGU plasmid into the bacmid	75
2.8.1.3. Isolation of recombinant Bacmid DNA	75
2.8.2. Production of baculovirus particles	76
2.8.2.1. Transfection of Sf9 cells with recombinant Bacmid: P0 viruses	76
2.8.2.2. Concentration and purification of amplified baculovirus (P1)	76
2.8.3. Determination of viral titre: Plaque assay	77
2.8.4. shRNAi delivery into cells: Infection of cells with recombinant viruses	77
2.9. Solutions and media	78
2.9.1. Bacteria and yeast culture	78
2.9.2. Cell culture	79
2.9.3. General buffers	79
2.9.4. Enzyme buffers	80
2.9.5. Yeast transformation media	80
2.9.6. TaqMan PCR	81
2.9.7. Sodium Dodecyl Sulphate Polyacrylamide Gel Electrophoresis and Western Blotting	81
2.9.8. EMSA	82
2.9.9. ChIP assay	84
2.9.10. β galactosidase assay	85
Chapter 3: Isolation of the UTE-1 binding protein	86
3.1. Construction of the reporter yeast	87
3.1.1. Cloning UTE-1 upstream of the reporter genes	87
3.1.2. Integration of the reporter constructs into the yeast	88
3.1.3. Testing the reporter yeast for background expression	90
3.2. Preparation of the library	91
3.2.1. Verification of the presence of a UTE-1 BP in the HeLa cell line	91
3.2.1.1. Presence of UTE-1 BP in HeLa confirmed by EMSA	92

3.2.1.2. Presence of a functional UTE-1 BP was determined by CAT assay	92
3.2.2. Amplification of the HeLa cDNA library	94
3.3. Screening of the library	94
3.3.1. Transformation and result of screening	94
3.3.2. Analysis of the positive clones	95
3.3.2.1. Determination of the insert size	95
3.3.2.2. Selection of the positive clones according to their capacity to bind to the UTE-1 sequence using EMSA	97
3.3.2.3. Selection of the positive clones according to their capacity to drive <i>lacZ</i> transcription using β -galactosidase assay	97
3.3.2.4. Selection of the positive clones according to their capacity to drive <i>TIMP1</i> transcription using reporter gene	100
3.3.3. Sequencing of the positive clones	102
3.3.4. RUNX1, the sought after UTE-1 Binding Protein?	102
3.4. Conclusion	103
Chapter 4: Expression of functional RUNX proteins in Hepatic Stellate Cells	105
4.1. RUNX RNA expression	106
4.1.1. Preparation of cDNA	106
4.1.2. RUNX RNA expression in Human activated HSC	107
4.1.2.1. RUNX1 and RUNX2	107
4.1.2.2. RUNX3	107
4.1.3. RUNX RNA expression in rat HSC	111
4.1.3.1. Assessment of PCR cycles conditions	111
4.1.3.2. RUNX amplification in rat HSC	113
4.2. RUNX proteins expression	113
4.2.1. RUNX1	115
4.2.2. RUNX2	115
4.2.3. RUNX3 and CBF β	117
4.3. Presence of functional RUNX protein in activated rat and human HSC	118
4.3.1. RUNX supershift EMSA	118
4.3.2. Binding of RUNX to <i>TIMP1</i> promoter <i>in situ</i>	120
4.3.2.1. Sonication optimisation	120
4.3.2.2. RUNX ChIP assay	122
4.4. Conclusion	122
Chapter 5: Role of RUNX proteins in <i>TIMP1</i> promoter activity	125
5.1. Set up of the reporter gene experiments	126
5.1.1. Cloning of the minimal <i>TIMP1</i> promoter in pGL2 reporter vector	126
5.1.2. Optimisation of transfection	127
5.1.3. Verification of the production of proteins by the related expression vectors	130
5.1.4. Selection of an appropriate transfection control	130
5.2. Regulation of <i>TIMP1</i> promoter by RUNX	133
5.2.1. Effect of RUNX on <i>TIMP1</i> promoter activity	133
5.2.1.1. Effect of RUNX1	135
5.2.1.2. Effect of RUNX2	135
5.2.2. Functional interaction between JunD and RUNX	138
5.2.2.1. Effect of RUNX on JunD-induced <i>TIMP1</i> promoter activation	138
5.2.2.2. Investigation of potential interaction between JunD and RUNX	141
5.2.3. Effect of the overexpression of RUNX and histone acetyltransferase	143
5.2.3.1. Effect of the overexpression of RUNX and MOZ on <i>TIMP1</i> activity	143
5.2.3.2. Effect of the overexpression of RUNX and CBP on <i>TIMP1</i> activity	145

5.3. Conclusion: Model of regulation of <i>TIMP1</i> promoter	145
Chapter 6: RUNX gene silencing: Development of a new technology	149
6.1. Delivering siRNA using baculovirus vector	150
6.1.1. Principles and theory of small interfering RNA and baculovirus	150
6.1.1.1. RNA interference	150
6.1.1.2. si RNAi expression vector	151
6.1.1.3. Advantage of the baculovirus system	151
6.1.1.4. Baculovirus expression system	153
6.1.2. Production of recombinant baculoviruses	153
6.1.2.1 Construction of the siRNAi vectors	153
6.1.2.2. Construction of the recombinant viruses	154
6.2. Silencing LMNA gene using baculovirus delivery system	158
6.2.1. Determination of the efficiency of TaqMan PCR	158
6.2.2. LMNA silencing in cell lines	160
6.2.2.1. Huh7 and Saos-2	160
6.2.2.2. LX2	160
6.2.3. LMNA silencing in primary HSC	164
6.3. RUNX silencing	167
6.4. Interferon response triggered by shRNAi	167
6.4.1 Aim of the study	167
6.4.2. Interferon response in Saos-2 and Huh7	169
6.4.3. Interferon response in primary HSC	171
6.4.4. Mechanism of the siRNA mediated effects	171
6.5. Conclusion	171
Chapter 7: General discussion	174
Appendices	180
Appendix 1: Plasmid maps	181
Appendix 2: Presence of RUNX in LX2	184
Appendix 3: Experimental data	185
List of references	200

List of Tables and Figures

Tables

1.1.	Molecular composition of the extracellular matrix molecules in the space of Dissé	4
1.2.	Matrix metalloproteinases involved in liver fibrosis and their domain structure	13
1.3.	Activities and characteristics of the different Tissue Inhibitors of Metalloproteinases (TIMP)	16
1.4.	Different RUNX nomenclatures	24
1.5.	Principal Runx expression sites and phenotype of knock out (KO) mice	28
1.6.	Characteristics of the different RUNX1 and RUNX2 spliced variants	32
1.7.	RUNX binding sites within promoter of RUNX regulated genes	36
1.8.	Target genes of RUNX proteins	37
2.1.	Primers used for amplification of <i>RUNX</i> genes by PCR from rat and Human cDNA	60
2.2.	Sequence of the oligonucleotides (ODN) cloned into pFIGU	75

Figures

1.1.	Features of HSC activation	6
1.2.	Cellular alterations in the hepatic sinusoid during chronic liver injury and fibrosis	8
1.3.	Balance between ECM deposition and degradation in liver	10
1.4.	Sequence comparison of the minimal <i>TIMP1</i> promoter (-102, +60) between species and localisation of the putative transcription factor binding sites	20
1.5.	Representation of translocation fusion proteins that disrupt RUNX	24
1.6.	Genomic organisation of the human <i>RUNX</i> genes	30
1.7.	mRNA and protein representation of the 2 main alternatively spliced forms of RUNX1	33
1.8.	Different pathways involved in the regulation of RUNX2 expression, phosphorylation and activity	39
1.9.	RUNX1 functional domain, sites of phosphorylation and acetylation and mapping of the interacting regions with coregulators	41
3.1.	Verification of the presence of 4x UTE-1 insert in pHISi, pHISi-1 and pLacZ by PCR amplification	89
3.2.	Presence of the UTE-1 BP in HeLa cell line	93
3.3.	Activation of CAT gene by UTE-1 element	93
3.4.	Amplification of the insert present in the his ⁺ lacZ ⁺ library clones	96
3.5.	Restriction digest of the plasmid A/1 and A/2	96
3.6.	Analysis of positive clone DNA binding activity	98
3.7.	βgalactosidase assay on different yeast reporter strain	99
3.8.	Effect of the overexpression of A/1 and A/2 on the activation of CAT by <i>TIMP1</i> promoter	101
4.1.	Amplification of ACTB sequence by PCR	108
4.2.	Representation of the different alternative splicing variants of RUNX1 and RUNX2 transcripts	109
4.3.	Amplification by PCR of the different RUNX1, RUNX2 and RUNX3 splicing variant cDNA in activated human HSC	110
4.4.	Representation of the amount of copies of amplicons per number of cycles during a PCR reaction Amplification of RUNX1, RUNX2 and ACTB sequence by semi-quantitative PCR	112
4.5.	Amplification of RUNX and ACTB sequences by PCR in rat HSC	114
4.6.	Expression of RUNX proteins in HSC	116

4.7.	Detection of RUNX1 and RUNX2 in UTE-1 DNA: protein complexes in activated rat and human HSC	119
4.8.	Optimisation of genomic DNA shearing by sonication	121
4.9.	Chromatin immunoprecipitation detection of RUNX1 binding to the <i>TIMP1</i> promoter (-102 to +60) in the human HSC cell line LX2	121
5.1.	Verification of the functionality of the new pTIMP1-Luc reporter plasmid	128
5.2.	Optimisation of effectene/DNA ratio in transfection experiment using different cell lines	129
5.3.	Verification of the overexpression of RUNX1B, RUNX1A, RUNX2, and JunD in Cos-1 cells by immunoblotting	131
5.4.	Induction of the β -galactosidase and Renilla reporter gene expression by RUNX proteins	132
5.5.	Activity of <i>TIMP1</i> minimal promoter containing a UTE-1 scrambled site compared to the WT promoter in HeLa cells and culture-activated rat HSC Cells	134
5.6.	Effect of overexpression of RUNX1 on <i>TIMP1</i> promoter activity in HeLa cells and culture-activated rat HSC	136
5.7.	Effect of overexpression of RUNX2 on <i>TIMP1</i> promoter activity in HeLa cells and culture-activated rat HSC	137
5.8.	Effect of co-overexpression of JunD and RUNX1B or RUNX1A on <i>TIMP1</i> promoter activity in HeLa cells and culture-activated rat HSC	139
5.9.	Effect of co-overexpression of JunD and RUNX2 on <i>TIMP1</i> promoter activity in HeLa cells and culture-activated rat HSC	140
5.10.	Interaction between JunD and RUNX detected by immunoprecipitation	142
5.11.	Effect of co-overexpression of MOZ and RUNX on <i>TIMP1</i> promoter activity in HeLa cells	144
5.12.	Effect of co-overexpression of CBP and RUNX on <i>TIMP1</i> promoter activity in HeLa cells	146
5.13.	Proposed model for the regulation of <i>TIMP1</i> promoter by RUNX1, JunD, MOZ and CBP	148
6.1.	Mechanism of RNA interference	152
6.2.	pFIGU plasmid map and shRNAi cloning strategy	155
6.3.	Generation of recombinant baculoviruses containing coding sequence for shRNA	156
6.4.	Determination of the efficiency of the real time PCR amplification of 3 target genes (LMNA, OAS1 and STAT1) and 3 references genes (18S, ACTB and GAPDH)	159
6.5.	LMNA gene expression in Huh7 and Saos-2 cells after 1 h incubation in media alone or containing recombinant virus	161
6.6.	LMNA expression level in Huh7 after infection with recombinant baculovirus	162
6.7.	LMNA expression level in Saos-2 after infection with recombinant baculovirus	163
6.8.	LMNA expression level in LX2 after infection with recombinant baculovirus	165
6.9.	LMNA expression level in primary human HSC after infection with recombinant baculovirus	166
6.10.	RUNX2 expression level in LX2 and Saos-2 cells after infection by recombinant baculovirus	168
6.11.	Induction of OAS1 and STAT1 gene expression by recombinant baculovirus on Saos-2 or Huh7	171
6.12.	Induction of OAS1 and STAT1 gene expression by recombinant baculovirus on primary human HSC	172

Declaration of Authorship

I, Marie-Anne BERTRAND, declare that the thesis entitled
**Molecular and Functional Characterisations of UTE-1 Binding Proteins
involved in the Regulation of the Human *TIMP1* Gene**
and the work presented in it are my own.

I confirm that:

- This work was done wholly or mainly while in candidature for a research degree at the University;
- Where any part of this thesis has previously been submitted for a degree or any other qualification at this University or any other institution, this has been clearly stated;
- Where I have consulted the published work of others, this is always clearly attributed;
- Where I have quoted from the work of others, the source is always given. With the exception of such quotations, this thesis is entirely my own work;
- I have acknowledged all main sources of help;
- Where the thesis is based on work by myself jointly with others, I have made clear exactly what was done by others and what I have contributed myself;
- Parts of this work has been published as:
Bertrand-Philippe, M., Ruddell, R.G., Arthur, M.J., Thomas, J., Mungalsingh, N., Mann, D.A. (2004). Regulation of tissue inhibitor of metalloproteinase 1 gene transcription by RUNX1 and RUNX2. *J.Biol.Chem.* 279, 24530-24539
Nicholson L., Philippe M., Paine A., Mann D.A. and Dolphin C. (2005). RNA interference mediated in human primary cells via recombinant baculoviral vectors. *Molecular Therapy*, in press.

Signed:



Date: December 2004

Acknowledgments

I would like to thank my supervisors, Professors Michael Arthur and Derek Mann for giving me the opportunity to do my PhD within the Liver group, and the British Liver Trust for funding the project.

I would also thank Dr Colin Dolphin, Dr Linda Nicholson and Professor Robert Hider for offering me the collaboration in London.

I would like to thank the members of the Liver group especially the Mann's Team, Dave, Fiona, Jelena, Karen, and Richard for their help and support during my PhD as well as for the improvement of my English vocabulary and song repertoires.

I would like to express my gratitude to Derek for his support and guidance. His constant enthusiasm and encouragements were very helpful during my PhD. I was very lucky to work with a supervisor with great human qualities and who always had "a last experiment idea".

During my 3 years in Southampton, I met very nice people who made Southampton an enjoyable place. Thanks to Ute, Roberto and Lisa for the great evenings and the numerous New Forest walks with unsuccessful mushroom picking. Thanks to Delphine and Katell for dragging me to the circuit training on a regular basis (i.e. every 4 months). A second thank to Delphine for her futon and her help with the submission of the thesis. Finally, thanks to Nane my fantastic flatemate.

I would also like to thank the Unilever band for their support and the brilliant time I have spent with them in Bedford, France, Switzerland, Scotland and Wales. Alex and Dave, Aurélia and Samuel, Bénédicte and Rob, Morgane and Graham, Sandra and Laurent, and Amar, thank you.

A big thank to my friend Geneviève for her constant encouragements and endless phone calls as well as her numerous visits to England to cheer me up.

I would like to thank my family, Jacqueline my mother, Agnès and Catherine my sisters and Eric my brother, their partners Claude, Hubert and Danielle, and my nieces and nephews for their support and encouragements over the past years. I should not forget to thank them for spending some of their holidays under the British rain.

Finally, I would like to express my deepest gratitude to my husband, Bastien for his help, support and patience during my PhD.

Abbreviations

aa	Amino acid
Ab	Antibody
ACTB	β actin
AEBSF	4-(2-Aminoethyl)benzenesulfonyl fluoride
ADH-1	Alcohol dehydrogenase-1
AML	Acute myeloid leukemia
AP-1/-2/-3	Activator protein-1/-2/-3
APS	Ammonium persulfate
BMP	Bone morphogenetic protein
bp	Base pairs
BSA	Bovine serum albumin
CAT	Chloramphenicol acetyl transferase
CBFβ	Core binding factor β
CCD	Cleidocranial dysplasia
C/EBP	CCAAT enhancer binding protein
cfu	Colony forming units
CMV	Cytomegalovirus
CRE	Cyclic AMP response element
CREB	CRE-binding protein
CSF	Colony stimulating factor
Ct	Cycles threshold
dIdC	Poly-deoxyinosinic-deoxycytidylic acid
DNA	Deoxyribose nucleic acid
DMEM	Dulbecco modified eagle medium
DMSO	Dimethyl sulfoxide
dsRNA	Double stranded RNA
DTT	Dithiothreitol
EAP	Glutamyl aminopeptidase
ECM	Extracellular matrix
EDTA	Ethylenediaminetetraacetic acid
EGFP	Enhanced green fluorescent protein
EGF	Epidermal growth factor
Egr-1	Early growth response protein-1
EMSA	Electrophoretic Mobility Shift Assay
ERK	Extracellular signal regulated kinase
ETO	Eight-twenty one
ETS	Transcription Factor, origin avian E26 erythroblastoma virus (v-ETS, E twenty-six)
EVI-1	Ecotropic virus integration 1 site protein
FAK	Focal adhesion kinase
FGF/bFGF	Fibroblast growth factor/basic fibroblast growth factor
FOS	Transcription factor, origin Finkel, Biskis, Jenkins\Reilly murine Osteosarcoma virus
FRA	Fos related antigen
GAPDH	Glyceraldehyde-3-phosphate dehydrogenase
GFAP	Glial fibrillary acidic protein
h	Hour
HAT	Histone acetyltransferase
HDAC	Histone deacetylase
HIS	Histidine
HSC	Hepatic stellate cell
HSV-TK	Herpes simplex virus thymidine kinase
ICAM-1	Intracellular adhesion molecule-1
IGF	Insulin-like growth factors
IL	Interleukin
IRES	Internal ribosome entry site

JNK	JUN N terminal kinase
JUN	Transcription factor, origin avian sarcoma virus 17 (v-Jun, Ju-nana, Japanese for 17)
kb	Kilo base
kDa	Kilo Dalton
KLF	Kruppel-like factor
Lac Z	β -Galactosidase
LBP-1	Leader binding protein-1
LEF/ALY	Lymphoid enhancer binding factor
LMNA	Lamin A/C
LTR	Long terminal repeat
MAPK	Mitogen activated protein kinase
MCP-1	Monocyte chemotactic protein-1
M-CSF-R	Macrophage colony-stimulating factor receptor
MEK	MAP/ERK kinase
MDR-1	Multi drug resistance-1
MMP	Matrix metalloproteinase
MOI	Multiplicity of infection
MPO	Myeloperoxidase
MTG	Myeloid translocation gene
MT-MMP	Membrane type matrix metalloproteinase
Myb	Transcription factor, origin Myeloblastoma (v-MYB avian E26 leukaemia virus)
mRNA	Messenger ribonucleic acid
NAD⁺	Nicotinamide adenine dinucleotide
NERF	New ETS related factor
NFκB	Nuclear factor κ B
nt	Nucleotide
OAS	Oligo adenylate synthetase
OD	Optical density
ODN	Oligonucleotide
ONPG	O nitrophenyl- β -D-galactopyranoside
PAGE	Poly-acrylamide gel electrophoresis
PAI-1	Plasminogen activator inhibitor-1
Pak	p21-activated protein kinase 1
PBS	Phosphate Buffered Saline
PCR	Polymerase chain reaction
PDGF	Platelet derived growth factor
PEA-3	Polyoma enhancer site 3
PEBP	Polyomavirus enhancer binding protein
pfu	Plaque forming units
PI3K	Phosphoinositide-3 kinase
PKA	Protein kinase A
PPAR	Peroxisome proliferative activated receptor
PTH	Parathyroid hormone
RISC	RNA-induced silencing complex
RHD	Runt homology domain
RNA	Ribonucleic acid
rpm	Rotation per minute
RT	Room temperature
RT PCR	Reverse transcriptase polymerase chain reaction
SBE	Smad binding element
SDS	Sodium dodecyl sulphate
SE	Standard Error
SFM	Serum free medium
siRNA	Small interfering RNA
shRNA	Short hairpin RNA
αSMA	α -Smooth muscle actin
SNP	Single nucleotide polymorphism
SP-1	Specificity Protein-1.

SRE	Serum response element
STAT	Signal transducer and activator of transcription
SV40	Simian papovavirus
TAE	Tris acetate EDTA
TBE	Tris boric acid EDTA buffer
TBS	Tris buffered saline
TCR	T-cell antigen receptor
TE	Tris EDTA buffer
TEL	Translocation-Ets-leukemia
TEMED	N,N,N',N'-Tetramethylethylenediamine
TGF	Transforming growth factor
TIE	TGF β inhibitory element
TIMP	Tissue inhibitor of metalloproteinase
TLE	Transducin-like enhancer of split
Tn	Transposon
TNFα	Tumour necrosis factor- α
tPA	Tissue plasminogen activator
uPA	Urokinase plasminogen activator
URA	Uracil
UTE-1	Upstream TIMP-1 element-1
UTE-1 BP	UTE-1 binding protein
UTR	Untranslated region
UV	Ultra Violet
VAR/VDR	Vitamin A receptor/Vitamin D receptor
VEGF	Vascular endothelial growth factor
VDRE	Vitamin D response element
v/v	Volume per volume
WT	Wild type
w/v	Weight per volume
YAP	Yes associated protein
3-AT	3-amino-1, 2, 4-triazole

Chapter 1

Introduction

Hepatic fibrosis is a disease process that represents a major medical problem with significant morbidity and mortality worldwide. In the western world it is one of the top ten causes of death, resulting in 6000 deaths every year in Britain alone. The major aetiological factor in the West is chronic ethanol consumption, whereas hepatitis viral infections B and C are the leading causes of liver fibrosis worldwide (Gabele *et al.*, 2003). With around 250 million people infected worldwide with hepatitis C, and 80 % of these going on to develop fibrosis, the public health burden of this disease process is clearly immense. This, along with the fact that there is no satisfactory medical treatment, warrants development of a greater understanding of hepatic fibrosis. Therefore, many researchers have been focusing on the molecular mechanism of liver fibrosis and this thesis reports 3 years of research carried out on the gene regulation of TIMP1, a protein upregulated during liver fibrosis.

1.1. The liver and liver fibrosis

1.1.1. Function of the liver

The liver is the largest internal organ and is situated under the diaphragm on the right side of the abdominal cavity. It is a large, lobed glandular organ. The blood containing the products of digestion from the capillary network of the gut is drained by the hepatic portal vein, whereas the hepatic artery supplies oxygen-rich blood to the liver. The two blood streams mingle in channels called sinusoids and are dispatched to the hepatic cells towards terminal hepatic venules which converge into the main hepatic veins for release to the general circulation (Lee, 2000).

The liver can be considered as a metabolic powerhouse. It destroys toxins and modifies molecules in order to enhance their water solubility which is indispensable for their transport through the body. In addition, a whole range of proteins involved in transport of molecules (albumin, transferrin) and the inflammatory response (α 1-anti-trypsin) are synthesised in the liver. Hepatic cells are also an important site for the storage and metabolism of vitamins and hormones (Lee, 2000).

1.1.2. Cell composition of the liver

1.1.2.1. Hepatocytes, the major cells of the liver and sinusoids

A majority of the functions described above take place within the hepatocytes which comprise 80 % of the liver. Hepatocytes are arranged in palissades along the sinusoids. The exchange of molecules between sinusoids and hepatocytes is optimized: the endothelium cells of the sinusoids possess many fenestrae which allow free passage of macromolecules and the hepatocytes have microvilli that increase the surface of contact. Also, the basement membrane-like extracellular matrix, which forms the space of Dissé (the subendothelial space between the endothelial cells and the hepatocytes), has a low density structure that minimally impedes sinusoid-hepatocytes exchange (Alcolado *et al.*, 1997).

1.1.2.2. Hepatic Stellate Cells, source of ECM and cytokines

While hepatocytes are the main cell component of the liver, hepatic stellate cells (HSC), located in the space of Dissé, represent less than 15 % of the total liver cells (Benyon and Arthur, 1998). They contain more than 75 % of the total body store of vitamin A in the form of retinyl esters in lipid droplets within the cytoplasm (Hendriks *et al.*, 1985). Furthermore, they are the major cellular source of extracellular matrix (ECM) present in the liver (Table 1.1.), and are also responsible for its degradation by producing a range of proteases and their respective regulators. Stellate cells have been recognized as an important source of cytokines and their circulating proteins, (IL-6, TNF α , EGF, TGF β 1, PDGF) (Friedman, 1996). They also synthesize several enzymes involved in intermediary metabolism and detoxification of ethanol such as glutathione-S-transferase or alcohol dehydrogenase (Yamauchi *et al.*, 1988; Lee *et al.*, 1994).

Collagens:	Types I, III, IV, V, VI, XIV
Proteoglycans:	Heparan, dermatan and chondroitin sulfates, perlecan, syndecan-1, biglycan, decorin
Glycoproteins:	Cellular fibronectin, laminin, merosin, tenascin, entactin undolin, hyaluronic acid

Table 1.1. **Molecular composition of the extracellular matrix molecules in the space of Dissé** . Adapted from Friedman, 1996.

1.1.3. Quiescent HSC : not that quiet

1.1.3.1. Change in HSC characteristics during activation

In response to specific stimuli, quiescent stellate cells undergo a process of activation towards a phenotype characterised by loss of retinoid droplets, an increase in proliferation, motility, contractility, and synthesis of ECM (Pinzani *et al.*, 1998). A key phenotypic feature of the activated HSC is the expression of α -smooth muscle actin and glial fibrillary acidic protein (GFAP) which defines the myofibroblastic nature of these cells (Rockey *et al.*, 1992) (Figure 1.1.).

1.1.3.2. Stimuli inducing HSC activation

Stimuli inducing HSC activation are soluble fibrogenic and proliferative factors released mainly by sinusoidal macrophages, Kupffer cells, (PDGF, TGF β 1) or by damaged hepatocytes (IGF-1, TGF- α , EGF) (Arthur *et al.*, 1998). Once activated, HSC also release TGF β 1 and PDGF, and therefore ensure a self-sustained phenotypic change (Pinzani *et al.*, 1994; Alcolado *et al.*, 1997). Besides, Collagen type I and III have also been shown to induce activation of HSC (Hellemans *et al.*, 1999). Finally, oxidative stress, such as lipid peroxide, can lead to activation of the HSC (Lee *et al.*, 1995). Lipid peroxides production is the result of the accumulation of ethanal in hepatocytes due to a shortage of the aldehyde dehydrogenase cofactor NAD⁺, thus preventing the conversion of toxic ethanal, itself converted from ethanol, to retinoic acid. Moreover, iron or copper overload can also result in lipid peroxidation (Houglum *et al.*, 1994; Chandrasoma *et al.*, 1995) (Figure 1.1.).

1.1.3.3. Transcription regulation associated with HSC activation

PDGF, IGF-1 and EGF activate the Ras-ERK pathway resulting in an increase in binding activity of the AP1 transcription factors which are involved in cell proliferation and growth control (Shaulian and Karin, 2001). The fibrogenic cytokine, TGF β , signals principally via the Smad family pathway where Smads regulate gene expression either directly or in association with other co-regulators

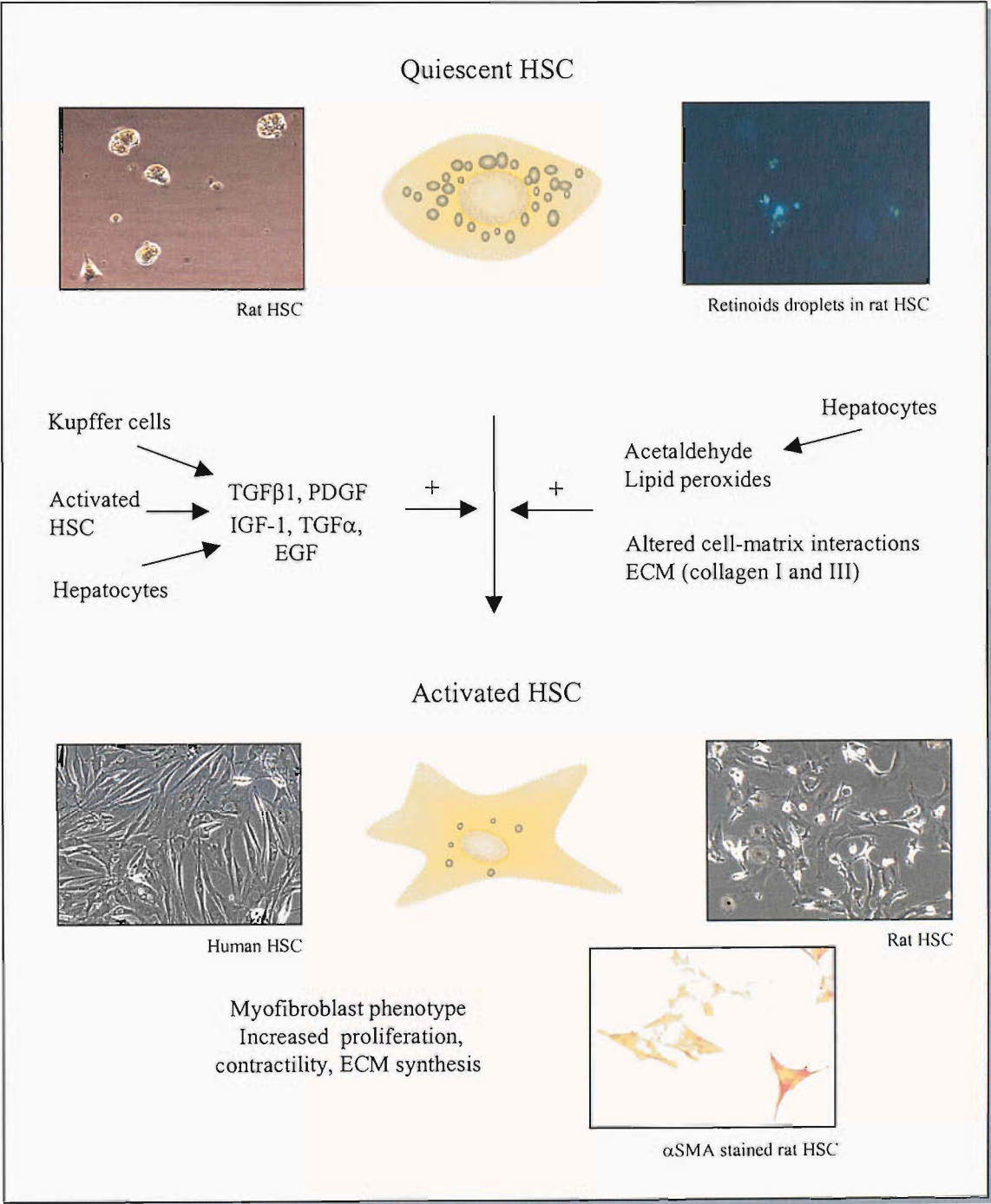


Figure 1.1. **Features of HSC activation.** Quiescent rat HSC (1 day post isolation) were viewed under an inverted bright filed microscope (left picture) or by fluorescent microscopy (right picture) which revealed the presence of retinoid droplets (328nm UV epifluorescence illumination at x200 magnification - Carl Zeiss). Activated rat HSC (7 days post isolation) and human HSC (21 days post isolation) were viewed under an inverted bright filed microscope (Carl Zeiss) at x160 magnification or x200 magnification (α SMA stained activated rat). Photographs were taken by Dr D. Smart, Dr R. Ruddell and author (Southampton).

such as AP1 factors. An AP1 binding site has been identified in the type I collagen promoter (Hui and Friedman, 2003).

The effect of oxidative stress is mediated by NF κ B, C/EBP β and c-Myb transcription factor pathways (Lee *et al.*, 1995). These factors are induced during activation and regulate different genes. For instance, c-Myb upregulates α -SMA expression whereas C/EBP β enhances type I collagen expression. NF κ B protects HSC against TNF α induced apoptosis (Mann and Smart, 2001). Another factor, which is induced during HSC activation, is Kruppel-like factor 6 (KLF6). Its putative targets include type I collagen, TGF β 1 and its receptors and urokinase-type plasminogen activators (uPA) (Hui and Friedman, 2003).

In contrast, some transcriptional factors are downregulated during the activation process such as PPAR γ which downregulates α -SMA and type I collagen expression. This suggests that the PPAR γ pathway is important in maintaining the quiescent phenotype of HSC. (Miyahara *et al.*, 2000).

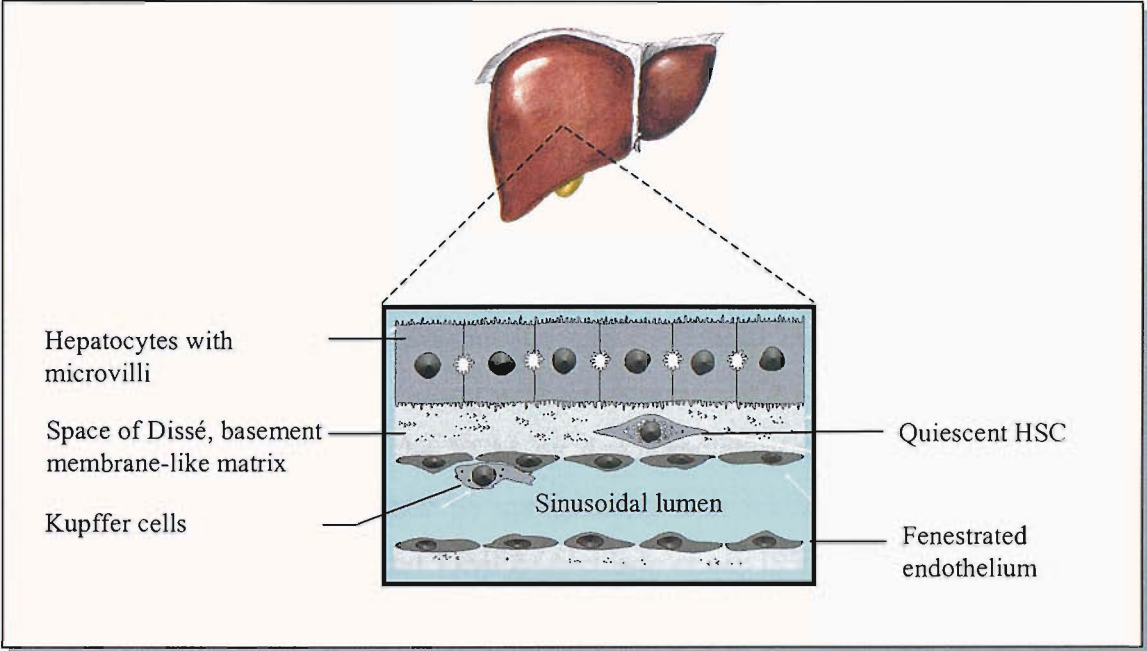
The activation of HSC is a complex process and has been shown to play a central role in the pathology of liver fibrosis.

1.1.4. Molecular changes during liver fibrosis

Liver fibrosis represents the final common pathological pathway leading to cirrhosis for a variety of chronic liver diseases, such as those arising from alcohol and drug abuse, viral infection (Hepatitis B or hepatitis C viruses), autoimmune and genetic disorders (Wilson's disease, toxic copper accumulation and haemochromatosis, iron toxic accumulation).

Liver fibrosis is characterized by an overall accumulation of extracellular matrix (ECM), but also by qualitative changes in the nature and distribution of collagenous and non collagenous ECM proteins within the liver (Williams and Iredale, 1998). These changes are initially concentrated in the space of Disse and lead to a change in the phenotype of the endothelial cells of the sinusoid as they lose their fenestrae, and also to a change in hepatocyte structure as the microvilli disappear (McGuire *et al.*, 1992). Therefore, the exchange of molecules between the sinusoid and hepatocytes is dramatically impaired leading to hepatic dysfunction (Figure 1.2.). However, the

Normal liver



Fibrotic liver

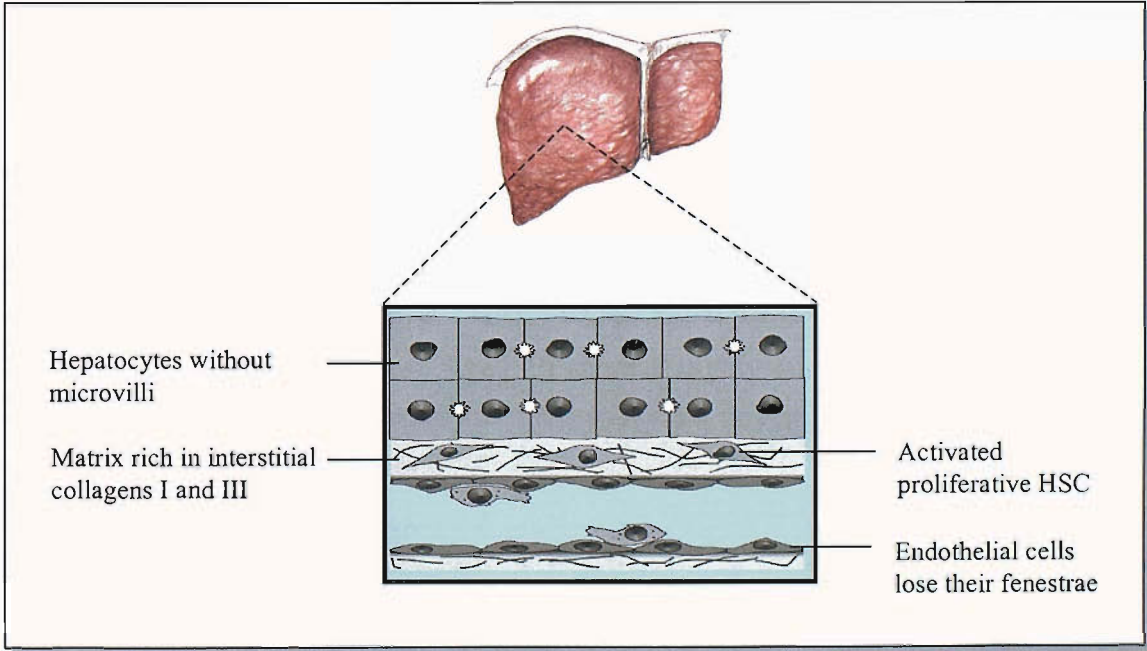


Figure 1.2. Cellular alterations in the hepatic sinusoid during chronic liver injury and fibrosis (adapted from Iredale, 1997).

gradual process of ECM accumulation is reversible upon removal of the primary injury (Benyon and Iredale, 2000; Hui and Friedman, 2003).

Hepatic stellate cells play a key role in the pathogenesis of liver fibrosis. In response to chronic injuries, the release of cytokines and ECM modification induce activation of HSC (phenomenon described in 1.1.3). HSC become the major source of ECM that is overexpressed in the space of Disse. Collagen type I, III and IV, undulin, elastin and laminin secretion is enhanced (Schuppan, 1990). However, the increase of collagen I synthesis is such that its ratio to type III and IV therefore increases (Benyon and Arthur, 1998). Along with an increased ECM synthesis, activated HSC control the degradation of the ECM by downregulating the expression of several metalloproteinases (MMP) and by upregulating their inhibitors, tissue inhibitors of metalloproteinase, TIMP1 and TIMP2 (Alcolado *et al.*, 1997). As a consequence, the level between ECM deposition and degradation, which in normal liver is finely balanced, is shifted toward ECM accumulation in the fibrotic liver (Figure 1.3.).

Therefore, the regulation of MMP and their inhibitors is one of the critical point in the control of liver fibrosis as the restoration of MMP expression and/or activity could enhance the degradation of ECM excess in the liver.

1.2. Matrix metalloproteinases, ECM degrading enzymes

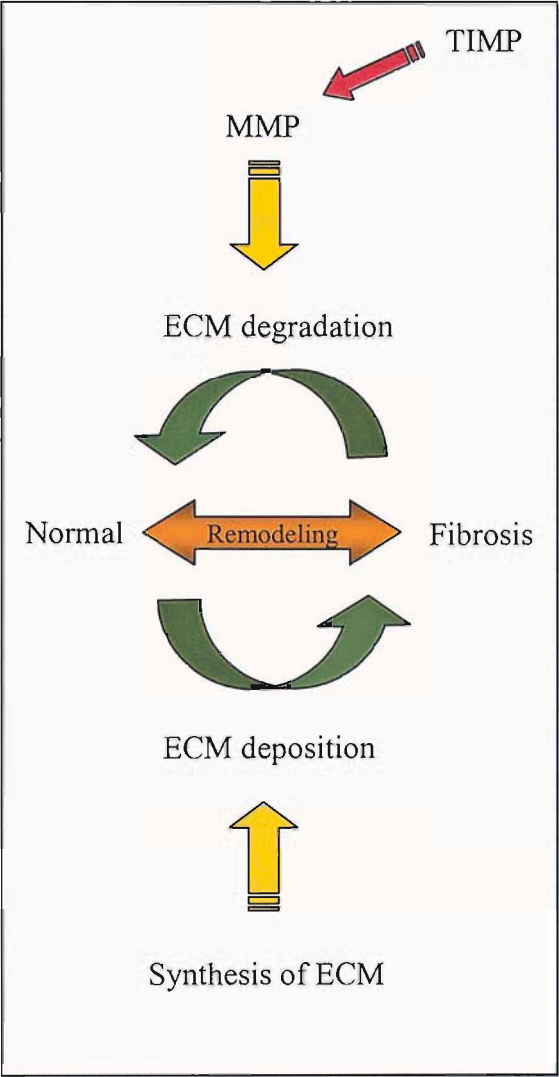
MMP or matrix metalloproteinases are part of the Metzincin superfamily of zinc dependent proteases which also includes serralyisin, astacins and the ADAMS/ADAMTS proteases. They all share a highly conserved catalytic domain containing 3 histidines that bind Zn^{2+} (Stocker *et al.*, 1995).

1.2.1. Characteristics of MMP

1.2.1.1. Nomenclature, substrate and structure of MMP

To date, 22 human MMP have been characterised, 16 of which are secreted and 6 are located at the surface of the plasma membrane (Nagase and Woessner, 1999; Sternlicht and Bergers, 2000). Although they used to be classified according to their main substrate (i.e. collagenases, gelatinases, stromelysins and membranes-types metalloproteinases), the overlapping substrate specificities justify the use of a

Normal liver



Fibrotic liver

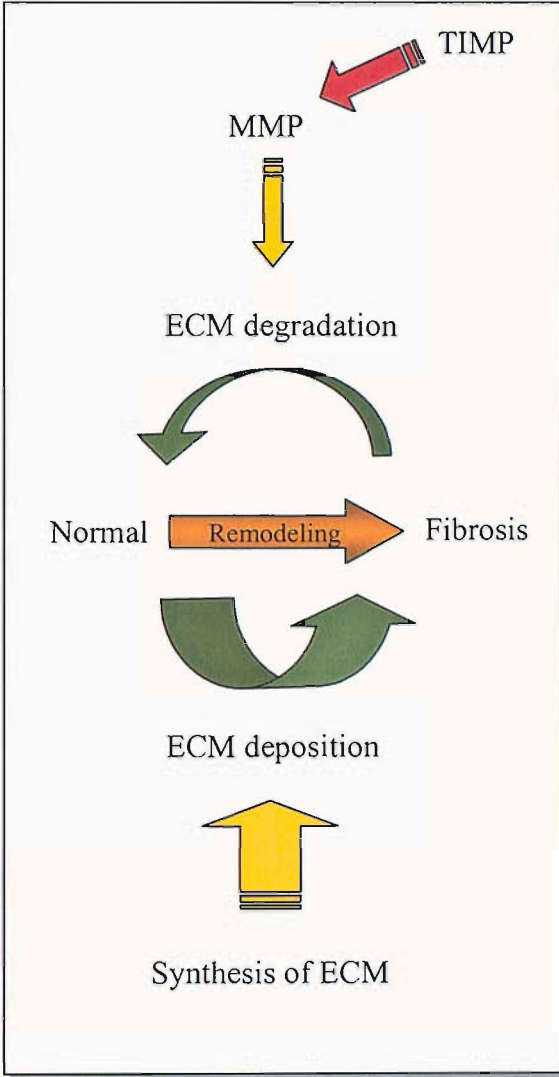


Figure 1.3. **Balance between ECM deposition and degradation in the liver.** In the fibrotic liver, the equilibrium is shifted towards ECM accumulation.

sequential numeric nomenclature (i.e. MMP1 to MMP28 including all vertebrate MMP) (Sternlicht and Werb, 2001). They can cleave numerous extracellular substrates, (other proteineases, clotting factors, latent growth factors, cell surface receptors) and between them virtually all ECM proteins (Sternlicht and Werb, 2001). All MMP have a N-terminal predomain that is removed after it has directed their synthesis to the endoplasmic reticulum, followed by a prodomain that maintains the enzymes in an inactive state until it is removed. The catalytic domain is situated between the propeptide and a hinge structure that links it to a hemopexin domain. The latter is present in all but a few MMP, and influences TIMP binding, the binding of certain substrates and some proteolytic activities (Sternlicht and Werb, 2001). MMP2 and MMP9 are further distinguished by the insertion of 3 cysteine-rich repeats within the catalytic domain which are required to bind and cleave collagen and elastin (Murphy *et al.*, 1994, Sternlicht and Werb, 2001). In addition, the transmembrane MMP contain a propeptide cleavage site recognised by the furin family of serine proteinases, along with a transmembrane domain and a short cytoplasmic C-terminal tail (Sternlicht and Werb, 2001).

1.2.1.2. Role of MMP: ECM digestion...and more

Not only are MMP important for ECM remodelling, but they also play a key role in the regulation of cellular signals. By degrading the ECM they release various growth factors and cytokines that were sequestered within the ECM such as TGF β 1 (Imai *et al.*, 1997). They also disturb cell-matrix interactions leading to apoptosis in anchorage-dependent cells (Alexander *et al.*, 1996). MMP influence cell behaviour by cleaving cell-cell adhesion proteins, by releasing bioactive cell surface molecules or by cleaving cell surface molecules that transduce signals from the extracellular environment (Fas ligand, TNF α , FGF receptor 1). In addition, they inactivate bioactive molecules by cleaving them and generating breakdown products with a new biological activity; for example, plasminogen is cleaved by MMP2 or MMP9 generating the angiogenesis inhibitor angiostatin (O'Reilly *et al.*, 1999).

The regulation of ECM degradation by MMP is important in various development and pathological processes such as bone formation, cancer (tumor metastasis, angiogenesis) and fibrosis (Sternlicht and Werb, 2001). For example, during cancer

progression, the breakdown of the ECM allows migration of the tumor cells, and as mentioned earlier, the impaired degradation of the ECM in the liver leads to fibrosis.

1.2.1.3. MMP in liver fibrosis

In human liver fibrosis, MMP1, 2, 3 and 9 are responsible for the degradation of the matrix during ECM remodelling (Arthur *et al.*, 1998). They degrade an array extracellular proteins (Table 1.2.). Expression of MMP1, which degrades collagen I, is downregulated in *in vitro* models of fibrosis but does not significantly change in animal and human models of chronic liver fibrosis. This difference can be due to an initial early acute-phase response to HSC isolation *in vitro*. In contrast, the activity of MMP2, 3 and 9, which degrade collagen IV and the components of the normal-basement-like membrane, have been shown to increase in all models (Rescan *et al.*, 1993; Arthur, 2000; Benyon and Arthur, 2001). MMP14, a membrane-bound MMP, is important for proMMP2 activation and its gene expression is induced during liver fibrosis (Takahara *et al.*, 1997). MMP3 is also a key proactivator of MMP (Schuppan *et al.*, 2001).

The constant remodelling of the ECM is important in normal tissue and is dependant on MMP activities. Therefore, MMP are subject to complex regulation to ensure that tissues are not damaged by abnormal activities of MMP.

1.2.2. Regulation of MMP: different levels of control

MMP are mainly regulated at the transcriptional and post-translational levels as well as at the protein level, via extracellular inhibitors.

1.2.2.1. Transcriptional regulation

MMP are regulated at the level of transcription by various effectors. *MMP* gene expression is regulated by growth factors, cytokines (interleukins, EGF, bFGF, PDGF, TGF β 1), chemical agents (phorbol ester, retinoic acid, glucocorticoids) and by matrix-cell and cell-cell interactions (type-1 collagen, integrin-dependent pathways) (Nagase and Woessner, 1999; Benyon and Arthur, 2001; Sternlicht and

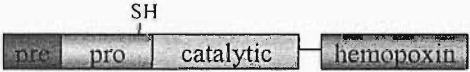
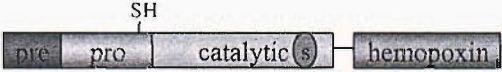

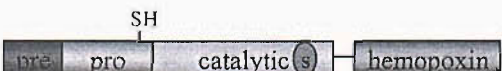

MMP number	Alternative name	Cellular origin in the liver	Substrate (non exhaustive)	Structure
MMP1	Interstitial collagenase	HSC, Kupffer cells	Collagen I, III, VII, VIII, X, gelatin, aggrecan, tenascin	
MMP2	Gelatinase-A	HSC	Gelatin, collagen I, IV, V, VII, X, XI	
MMP3	Stromelysin-1	HSC, Kupffer cells	Collagen I, III, IV, V, VIII, XI, Aggrecan tenascin; decorin	
MMP9	Gelatinase-B	Kupffer cells	Gelatin, collagen I, IV, V, VII, X, XI, elastin, aggrecan	
MMP14	MT1-MMP	HSC, Hepatocytes	Collagen I, III, aggrecan, Pro-MMP2	

Table 1.2. **Matrix metalloproteinases involved in liver fibrosis and their domain structures.** Pre, prepeptide; pro, propeptide; F, cleaving site for Furin enzyme; S, cysteine rich region; TM, transmembrane domain; C, cytoplasmic tail. Adapted from Arthur *et al.*, (1998) and Sternlicht and Werb (2001).

Werb, 2001). Many of these stimuli induce the expression of *MMP* via JNK or ERK activation of c-fos/c-jun transcriptional factors that bind to the AP-1 site within the *MMP* promoters, such as *MMP1*, 3 and 13 (Mann and Smart, 2001; Sternlicht and Werb, 2001). Others transcriptional factors have been shown to be important for the regulation of the transcription such as Ets (*MMP1*), RUNX2 (*MMP13*, main collagenase in rat liver fibrosis) (Pendas *et al.*, 1997; Jimenez *et al.*, 1999). Moreover, AP-2, Sp1, NFκB, C/EBPβ and the retinoic acid response element have also been found in several *MMP* promoters (Sternlicht and Werb, 2001). In addition, basal and inducible levels of *MMP* gene expression can also be influenced by genetic variations such as SNP (Ye, 2000).

In the liver, the most important factor is TGFβ1, which downregulates *MMP1* and *MMP3* expression. *MMP1* repression mediated by TGFβ, is Smad/AP1 dependent and does not involve the TGFβ–inhibitory element (TIE) located upstream of the AP1 site within the *MMP1* promoter (Hall *et al.*, 2003). Retinoic acid, which is generated from the metabolism of the stored retinyl ester by activated HSC, inhibits the expression of *MMP1*. In contrary, PDGF, TNFα and bFGF upregulate *MMP1* (Benyon and Arthur, 2001).

On the other hand, *MMP2* expression is not modulated by the effectors of *MMP1* expression. *MMP2* is known to be often constitutively expressed and is regulated, along with other MMP, at a post-translational level (Benyon and Arthur, 2001; Sternlicht and Werb, 2001).

1.2.2.2. Post-translational regulation

MMP are secreted as inactive proenzymes. The sulfhydryl group of a cysteine near the C-terminal of the prodomain is a fourth ligand for the zinc ion in the active site. The removal of the propeptide results in the replacement of the thiol group by a water molecule that can then hydrolyse the peptide bond of the MMP targets.

The extracellular activation of the latent MMP can be initiated by active MMP or by serine proteinases. For example, MMP1, MMP9 and MMP3 are activated by the serine protease, plasmin, upon its activation by urokinase plasminogen activator/tissue-plasminogen activator/plasminogen activator inhibitor-1 (uPA/tPA/PAI-1) system (Carmeliet *et al.*, 1997; Irigoyen *et al.*, 1999). MMP1 and MMP9, once modified by plasmin, still require other modifications performed this time by MMP3

(Suzuki *et al.*, 1990). TGF β 1 inhibits the conversion of proMMP1/3 into MMP1/3 by upregulating the expression of PAI-1.

MMP2 is activated by MMP14 and TIMP2 at the cell surface through a unique multistep process. TIMP2, which is normally an inhibitor of MMP, acts as bridging molecule between MMP14 and proMMP2 forming a ternary complex. The proMMP2 is then cleaved by a free MMP14. However, when present in excess, TIMP2 also inhibits the activity of MMP14 and MMP2, newly released (Sato *et al.*, 1994;Butler *et al.*, 1998;Benyon and Arthur, 2001).

A third activation process concerns mainly the Membrane-Type MMP such as MMP14, which can be activated before they reach the cell surface. The prodomain is cleaved by intracellular serine proteases that recognise the furin-like enzyme recognition motif situated in the N-terminal region of the prodomain (Pei and Weiss 1995).

Once activated the MMP are still subject to extracellular regulation of their activity by endogenous protease inhibitors.

1.2.2.3. Extracellular inhibitors of MMP

α 2-macroglobulin is an abundant plasma protein and a major endogenous inhibitor of the MMP and other proteases. This large glycoprotein (725 kDa) is also expressed in the liver, mainly by hepatocytes (Benyon and Arthur, 2001). The inhibition of MMP is an irreversible process because after α 2-macroglobulin binds to MMP, this complex is removed by endocytosis (Sternlicht and Werb, 2001).

Tissue Inhibitor of metalloproteinases (TIMP) are also endogenous regulators of MMP activity and include 4 different TIMP proteins (TIMP1-4) that share 37-51 % overall sequence identity. They are expressed from separate genes and their characteristics are listed in Table 1.3. (Crocker *et al.*, 2004). The TIMP are low molecular weight proteins (approximately 20 kDa), and a number are glycosylated (TIMP1 and TIMP3). TIMP1 and TIMP2 are secreted into the intracellular milieu whilst TIMP3 is detected in association with the extracellular matrix (Denhardt *et al.*, 1993). They can either inhibit the active form of MMP via their N-terminal domain or block the conversion of the proenzyme via their C-terminus (Murphy and Willenbrock, 1995).

	TIMP1	TIMP2	TIMP3	TIMP4
MMP inhibition	all but MMP14	all	MMP1, 2, 3, 7, 9, 14 ADAM	MMP1, 2, 3, 7, 9
Protein size (kDa)	28	21	23-36	23
Glycosylation	yes	no	yes	no
Localisation	diffusible	diffusible	ECM bound	diffusible
Expression	inducible	constitutive	inducible	?
Binding to proMMP	MMP9	MMP2	?	?
Major tissue sites	bone, ovary	brain, heart, lung, placenta, ovary, testis	heart, kidney, thymus	brain

Table 1.3. Activities and characteristics of the different Tissue Inhibitors of Metalloproteinases (TIMP). Adapted from Croker *et al.*, 2004.

For instance, TIMP1 binds to proMMP-9, and TIMP2 to proMMP-2, inhibiting their activation by MMP3 and MMP14 respectively (Howard and Banda, 1991;Goldberg *et al.*, 1992). TIMP block the active site of active MMP by binding in a stoichiometric manner and inhibit irreversibly MMP activity (Murphy and Docherty, 1992). Although different TIMP bind tightly to most MMP, some differences in affinity have been reported. Thus, TIMP3 is a more potent inhibitor of MMP9 than other TIMP and TIMP1 is the only one that does not inhibit MMP14 (Brew *et al.*, 2000;Sternlicht and Werb, 2001).

TIMP1 and TIMP3 are inducible by serum, phorbol ester and a variety of cytokines and growth factors that also regulate *MMP* expression. Whereas TNF α induces *TIMP1* in the same manner as *MMP1* and *MMP3*, TGF β 1 upregulates *TIMP1* but reduces *MMP1* expression. In contrast, *TIMP2* is generally constitutively expressed in cells, although it has been shown to be repressed by TGF β 1 (Benyon and Arthur, 2001).

Whereas the function of TIMP4 is still under investigation, the other TIMP have been shown to be multifunctional molecules with additional biological functions which are independent of MMP-inhibitory activities. For example, TIMP1 has mitogenic activities on a number of cell types, and can protect several cells from apoptosis, including B cells and mammary epithelium cells (Hayakawa *et al.*, 1992; Hayakawa *et al.*, 1994;Guedez *et al.*, 1998;Li and Fridman, 1999). In contrast, TIMP3 was shown to induce apoptosis of human colon carcinoma cells (Smith *et al.*, 1997). On the other hand, TIMP2 has been associated with pro and anti apoptotic effects, as well as mitogenic properties (Gomez *et al.*, 1997). A recent review underlined the importance of the MMP-inhibition independent TIMP properties in the development and pathology of the central nervous system (Crocker *et al.*, 2004).

As for MMP, the abnormal expression of TIMP, which as a consequence modifies MMP activities, results in alterations in the remodelling of the ECM that are implicated in many pathologies such as artherosclerosis, tumor metastasis and angiogenesis (Sternlicht *et al.*, 1999). Therefore, there is great interest in understanding the cellular mechanisms that control TIMP expression. In the scope of liver fibrosis, a particular interest was focused on the prototypic member of the TIMP family, TIMP1.

1.3. TIMP1, key effector of liver fibrosis

1.3.1. Expression of TIMP1 during liver fibrosis

There is a growing consensus of opinion that the development and progression of liver fibrosis is due to a combined effect of increased matrix synthesis in response to liver injury, and a decreased matrix degradation mediated by the inhibition of MMP activities by TIMP1. Several studies uncovered the role of TIMP1 in liver fibrosis.

Iredale *et al.* (1992) showed that *in vitro*, in early culture, quiescent HSC do not express TIMP1. With culture activation of HSC, there is an increase in TIMP1 mRNA and protein expression. When TIMP1 is withdrawn from the HSC culture supernatants, the detectable MMP activity increases by more than 20-fold (Iredale *et al.*, 1992). In addition, elevated *TIMP1* expression by HSC has been associated with the fibrotic human liver (Iredale *et al.*, 1995; Benyon *et al.*, 1996). Expression of *TIMP1* has been studied in a rat model of reversible liver fibrosis and the results show that the resolution of liver fibrosis is accompanied by a reduction in the expression of *TIMP1*. Moreover, the level of MMP1 protein expression remains constant although its activity increases (Iredale *et al.*, 1998).

A study using transgenic mice which overexpress TIMP1, showed that these mice develop more severe liver fibrosis and more rapidly than wild type mice, following CCl₄ liver injury (Yoshiji *et al.*, 2000). Another study using the same transgenic mice showed that overexpression of TIMP1 attenuates spontaneous resolution of liver fibrosis in the transgenic mice (Yoshiji *et al.*, 2002).

Another aspect implicating TIMP1 in liver fibrosis is its ability to inhibit HSC apoptosis thereby preventing the reduction of activated HSC, which are the major source of the ECM (Murphy *et al.*, 2002).

As overexpression of TIMP1 by HSC results in a decrease in MMP activation and activity, TIMP1 plays a key role in the net accumulation of the ECM in the fibrotic liver. Therefore, understanding the molecular regulation of its expression is important and may lead to the identification of potential therapeutic targets.

1.3.2. Promoter of *TIMP1* gene in HSC

TIMP1 gene transcription can be stimulated by a wide variety of agents including all-*trans* retinoic acid, phorbol esters, growth factors and cytokines (TGF β 1, PDGF, EGF, IL-6, IL-11, bFGF) and viruses (Campbell *et al.*, 1991; Logan *et al.*, 1996; Edwards *et al.*, 1987). All-*trans* retinoic acid interacts in a synergistic manner with different growth factors (TGF β 1, PDGF, EGF, bFGF) to induce expression of TIMP1 protein (Bigg *et al.*, 1999; Bigg *et al.*, 2000).

1.3.2.1. Organisation of the minimal promoter

The study of regulation of *TIMP1* expression at the transcriptional level arises from the observation that HSC activation is accompanied by transactivation of the *TIMP1* promoter (Bahr *et al.*, 1999). Hence, TIMP1 reporter activity is increased when transfected into activated HSC compared to the basal level of activity observed after the same reporter into quiescent HSC. This suggests an important role for the transcription factors that regulate the activity of the *TIMP1* promoter.

Analysis by truncation mutagenesis demonstrated that the minimum active *TIMP1* promoter in human fibroblasts and HSC included a 162 bp region (from -102 to +60 bp, with reference to the transcription starting point) (Clark *et al.*, 1997; Bahr *et al.*, 1999) (Figure 1.4.). The promoter does not contain a canonical TATA-box (TATA^{A/T} A^{A/T}) but a related sequence (ATTTAT), has been found about 20 bases upstream of the main transcription start point (Clark *et al.*, 1997). The translation start site is located on exon 2. As a result, the first exon of *TIMP1* gene is transcribed, but not translated (Dean *et al.*, 2000).

Within the minimal promoter, several DNA recognition sequences for specific transcription factors have been identified. The 3' end contains a LBP-1 binding site (between +25 and +60) that appears to be essential for promoter activity, although EMSA data suggest that the protein binding this sequence is not LBP-1 (Clark *et al.*, 1997). The 5' extremity includes non canonical AP-1 site (5'-TGAGTAA-3' instead of 5'-TGAGTCA-3') which is particularly important for the function of the minimal active *TIMP1* promoter in human and culture-activated rat HSC, as its mutation decreases promoter activity by more than 90 % (Clark *et al.*, 1997; Bahr *et al.*, 1999).

AP-1 is essential for the TGF β 1 induced expression of *TIMP1* although it does not involve the Smad pathway (Hall *et al.*, 2003). Although the classical AP-1 dependent transactivators of the *TIMP1* gene are c-Jun/c-Fos heterodimers, Smart *et al.* (2001) demonstrated that in activated HSC, JunD homodimers are responsible in part for the activation of the promoter.

Computer sequence analysis of the *TIMP1* promoter identified putative PEA-3, STAT-1 and SP1 sites. AP-1 PEA-3 and STAT-1 form the Serum Response Element (SRE). However, classical regulation of *TIMP1* which involves cooperative activation by AP-1 and PEA-3 binding proteins (Jun/Fos and ETS respectively) does not occur in HSC as the mutation of the PEA-3 site only slightly affects *TIMP1* promoter activity (30 % less active) and ETS 1/2 protein expression is downregulated upon activation of HSC (Logan *et al.*, 1996; Bahr *et al.*, 1999).

Another binding site, within the minimal promoter, which was not unveiled by computer analysis but by DNase footprinting was called the Upstream TIMP Element-1 (UTE-1) (Trim *et al.*, 2000). This site is also important for transcriptional regulation as the presence of a mutated UTE-1 sequence within the *TIMP1* promoter reduced its transcriptional activity by 30 fold in activated HSC (Trim *et al.*, 2000).

Finally, outside the minimal promoter, two negative regulatory regions have been identified, in position -1718/-1458 and within the intron 1 (+648/+748). Although the upstream repression effector is unknown, the intron 1 repression might be induced by SP1/SP3 (Dean *et al.*, 2000).

The high level of conservation of the *TIMP1* promoter across Human, Rat and Mouse species, especially within the AP-1, PEA3 and UTE-1 binding sites, emphasize the importance of these domains for the *TIMP1* gene regulation

1.3.2.2. UTE-1 a novel regulator element

UTE-1 was first identified as an 11 nucleotide element (5'-TGTGGTTTCCG-3') located downstream of the AP-1 site (-62/-52) (Trim *et al.*, 2000) and was essential for *TIMP1* promoter activity. Computer analysis available at the time of the research, did not match UTE-1 with any known transcription factor binding sites, although there was some sequence homology with the AP3 site and AP3-like site. EMSA and

southwestern blotting experiments showed the existence in activated HSC of a 30 kDa UTE-1 binding protein (UTE-1 BP) that does not bind to the AP3 or AP3-like sequences. Interestingly, 2 UTE-1 binding proteins of 35 kDa and 47 kDa, have been detected in quiescent HSC but not in activated cells (Trim *et al.*, 2000).

However, another study demonstrated that the UTE-1 DNA binding activity, as well as *TIMP1* expression, is induced over activation of the HSC. Moreover, culture of freshly isolated HSC on Matrigel, a basement membrane like ECM gel which prevents the cells from becoming activated, suppressed induction of UTE-1 DNA binding activity and *TIMP1* expression (Bertrand-Philippe *et al.*, 2004). Therefore, there is a close association between the activated phenotype of HSC, and UTE-1 activity. Using reporter gene assays, the UTE-1 site was shown to be unable to function in isolation, and therefore probably operates in cooperation with multiple *cis*-acting regulatory elements. This hypothesis corroborates with the detection of cooperative activation of the reporter gene transcription by UTE-1 and SRE. The loss of this effect when UTE-1 was distal to the SRE suggested that the UTE-1 BP may interact with a member of the AP-1 and ETS family of transcription factors (Bertrand-Philippe *et al.*, 2004).

Hence, identification of the UTE-1 factor is crucial for a better understanding of the *TIMP1* gene regulation.

As a consequence, the isolation of the UTE-1 BP, described in chapter 3, was the starting point of the research described in this thesis. The identification of the UTE-1 BP as RUNX transcription factors opens an entirely new field of research, which was never associated with neither *TIMP1* gene regulation nor liver fibrosis. Therefore, the second part of the introduction covers the current knowledge on this complex family of transcription factors.

1.4. RUNX transcription factors

The RUNX transcription factors include 3 proteins, RUNX1, RUNX2 and RUNX3 and were formerly called AML1, AML3 and AML2 (Table 1.4.). Although they bind to the same DNA sequence via an identical DNA binding domain, called the runt domain, they present specific biological functions.

1.4.1. Biological function of RUNX

1.4.1.1. RUNX1, discovered as regulator of hematopoiesis

1.4.1.1.1. Chromosomal translocation of RUNX1

The first evidence of a biological function of RUNX1 came from the observation that the *RUNX1* gene is the most frequent target of chromosomal translocation associated with leukemia (Miyoshi *et al.*, 1991). The t(8;21) translocation is a frequent abnormality associated with acute myeloid leukemia (AML) and results in the fusion of the 5' end of the *RUNX1* gene (containing the runt domain) with a nuclear protein *ETO* gene (Nucifora and Rowley, 1995). The t(16;21) translocation fuses *RUNX1* to an ETO-related gene called *MTG16* (Gamou *et al.*, 1998). The t(3;21) translocation associated with AML, myelodysplastic syndrome (MDS) or chronic myelogenous leukemia (CML) leads to the fusion of *RUNX1* with *EAP*, *MDS1* or *EVI-1* (Nucifora and Rowley, 1994; Nucifora and Rowley, 1995). A fourth translocation t(12;21) is responsible of the fusion of the N-terminal domain of *TEL* to nearly all of *RUNX1* and is present in 30 % of pediatric B-cell acute lymphoblastic leukemia case (Golub *et al.*, 1995; Romana *et al.*, 1995).

These translocations lead to the synthesis of chimeric proteins which may act as dominant inhibitors of RUNX-dependent transcriptional activation such as RUNX1/EVI-1 (Tanaka *et al.*, 1995a), RUNX1/ETO (Meyers *et al.*, 1995; Melnick *et al.*, 2000) and TEL/RUNX1 (Fears *et al.*, 1997). In other cases, chimeric proteins are dysfunctional (RUNX1/EAP) (Nucifora *et al.*, 1993) (Figure 1.5.).

In addition, several point mutations in the *RUNX1* gene, inactivating RUNX1 DNA binding properties, have been associated with various types of leukemias (Osato *et al.*, 2001).

Official name	Acute myloid leukemia	Core binding factor	Polyomavirus enhancer binding protein 2	Other
RUNX1	AML1	CBF α -2	PEBP2 α -B	
RUNX2	AML3	CBF α -3	PEBP2 α -C	OSF2 NMP2
RUNX3	AML2	CBF α -1	PEBP2 α -A	

Table 1.4. **Different RUNX nomenclatures.** OSF-2 is osteoblast stimulating factor 2 and NMP2 is nuclear matrix protein 2.

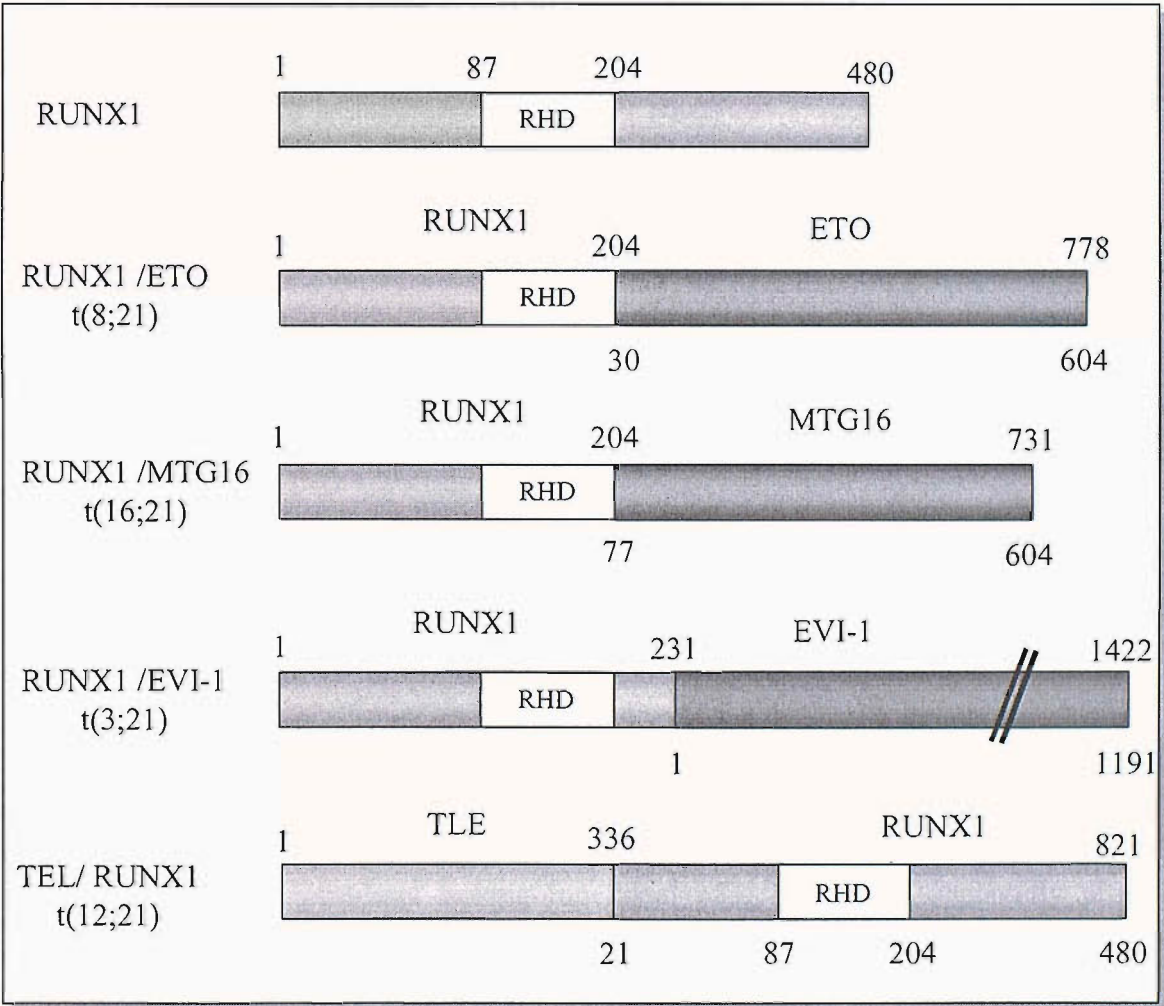


Figure 1.5. **Representation of translocation fusion proteins that disrupt RUNX.** RHD is the runt domain. Adapted from Lutterbach and Hiebert, 2000.

These observations highlight the importance of RUNX1 in hematopoiesis as structural alterations of RUNX1 trigger leukemia transformation. This was confirmed by studies using knock-out mice.

1.4.1.1.2. *Runx1* knock-out mice

Runx1-deficient embryos lack definitive hematopoietic progenitors and fail to develop foetal liver hematopoiesis. The embryos died around E12.5 (Okuda *et al.*, 1996). The absence of a more widespread phenotype in these mice can be due to the fact that *Runx1* plays a less critical role in other tissues or that its function is complemented by *Runx2* or *Runx3*. This work has been confirmed by a knock-in strategy using murine embryonic stem cell. These cells containing the *Runx1*-knock-in allele showed a restored ability to differentiate into all lineages of definitive hematopoiesis (Okuda *et al.*, 2000). Finally *Runx1* heterozygous animals have reduced numbers of myeloid and erythroid progenitors (Wang *et al.*, 1996).

In conclusion, studies by Okuda and Wang demonstrated that *Runx1* played a pivotal role in regulating the transcription of genes that were essential for definitive hematopoiesis.

1.4.1.1.3. RUNX1 involvement in cancer and autoimmune disease

Although the oncogenic properties of RUNX1 involved in leukemia are the consequence of an alteration of RUNX1, there is some evidence showing that intact RUNX1 might also have intrinsic oncogenic potential. Recently, an extra copy of functional RUNX1 has been implicated in a Down syndrome-related acute leukemia (Ito, 2004). Using an *in vitro* model, RUNX1 has been shown to induce morphological transformation and tumorigenic conversion in 3T3 fibroblasts as well as accelerating the progression of the cells into the S phase of the cell cycle in 32Dcl3 myeloid cells (Strom *et al.*, 2000; Cameron and Neil, 2004). Finally, in murine embryonic fibroblasts lacking functional p53, *Runx1* has apparently pro-oncogenic effects on cell growth that include cytoskeletal reorganization, reduced contact inhibition at confluence and accelerated tumour expansion *in vivo* (Wotton *et al.*, 2004).

Cancer is not the only field where RUNX1 has been identified as a key player. Interestingly, RUNX1 has also been shown to play a central role in the development of autoimmune disease. For instance, one of the identified psoriasis-associated

regulatory SNP (single nucleotide polymorphism) affected the binding of RUNX1 (Alarcon-Riquelme, 2003).

1.4.1.2. RUNX2, key role in osteogenesis

RUNX2 is believed to play a role in osteoblast differentiation and bone ossification as inactivating mutations of the human RUNX2 are the cause of cleidocranial dysplasia (CCD), which is abnormal skeletal genesis and arrest of osteoblast development (Mundlos *et al.*, 1997). Moreover, disruption of one *Runx2* allele in mice is sufficient to produce skeletal defects that consist of failure of endochondral and membranous bone formation and the *Runx2* +/- mice present the typical features of human CCD (Otto *et al.*, 1997). Konori *et al.* (1997) deleted the *Runx2* gene in mice and the *Runx2*-/- mice died at birth from respiratory failure due to a total lack of bone.

Although *RUNX2* has not yet been implicated in human cancers, *Runx2* oncogenic activity has been demonstrated in mice. *Runx2* cooperates with *Myc* to induce murine T-cell lymphoma formation. However, *Runx2* overexpression alone is insufficient for lymphoma development (Cameron and Neil, 2004). Other recent studies have demonstrated that metastatic breast cancer cells express RUNX2 which is responsible for the formation of bone osteolytic lesions (Barnes *et al.*, 2003; Barnes *et al.*, 2004)

1.4.1.3. RUNX3 tumor suppressor in gastric cancer

Although RUNX1 and RUNX2 have been studied for more than a decade, few studies focused on the third member of the RUNX family. The role of RUNX3 was unravelled only in the past 3 years, and interest in RUNX3 is growing as it has been implicated in gastric cancer, the second largest cause of cancer-related mortality worldwide (Bae and Choi, 2004). A major study has been carried out by Li *et al.* (2002) where they showed that RUNX3 is expressed in the glandular stomach epithelium cell and that *Runx3*-/- mouse gastric mucosa exhibits hyperplasia due to the stimulated proliferation and suppressed apoptosis in the cells. Therefore, the stomach mucosa of the knock out mice is twice as thick as that of wild type mice. *Runx3*-/- mice died soon after birth probably due to starvation. RUNX3 has a potent

antioncogenic activity and is frequently inactivated in gastric cancer (60 % of gastric cancer specimens examined) by hemizygous deletion and hypermethylation of its promoter region (Li *et al.*, 2002). Furthermore, loss of RUNX3 expression by DNA hypermethylation is frequently associated with the evolution of lung cancer, whereas RUNX3 overexpression is detected in pancreatic tumor cells (Li *et al.*, 2004a; Li *et al.*, 2004b)

RUNX3 is also involved in neurogenesis and thymopoiesis. A study using another strain of *Runx3*^{-/-} mice (which showed 10-20 % survival rate) demonstrates that RUNX3 is also critical in the regulation of the axonal projections of a specific subpopulation of dorsal root ganglions (Inoue *et al.*, 2002) as the knock out mice displayed several motor discoordination. Moreover, RUNX3, along with RUNX1 is responsible for epigenetic silencing at the CD4 locus during T-cell differentiation (Woolf *et al.*, 2003; Taniuchi and Littman, 2004).

In conclusion, the RUNX proteins have been identified as key regulators of hematopoiesis (RUNX1), osteogenesis (RUNX2) or as a tumor suppressor in gastric cancer (RUNX3), although there is a growing body of evidence regarding their contribution in other biological pathways.

The regulation of such different biological processes by related transcription factors that bind to the same DNA binding site can be explained, to some extent, by their highly distinct tissue-specific expression.

1.4.1.4. Expression pattern

RUNX proteins are not ubiquitously expressed but have distinct tissue-specific expression patterns which correlate with the phenotypes of the respective knock-out mice (Table 1.5.). There is, however, few spatial or temporal expression overlapping. In the mouse embryo, *Runx1* is mainly expressed in hematopoietic progenitor, in endothelial cells in regions from which hematopoietic cells appear to emerge and in the liver (North *et al.*, 1999). In the adult hematopoietic system, *Runx1* is highly expressed in myeloid, B- and T-lymphoid cells, whereas *Runx3* is expressed in mature dendritic cells and T cells (Levanon and Groner, 2004). All 3 *Runx* proteins are expressed in the thymus, although there is a spatial reorganization of the different pattern of expression upon embryonic development. In adults, expression of the

Tissue/cell type	Runx1	Runx2	Runx3	KO phenotype
<i>Dorsal root ganglia</i>				<i>Runx3</i> KO:
TrkA	+			impaired development of TRkC neurons
TrkC			+	
<i>Hematopoiesis</i>				<i>Runx1</i> KO:
AGM	+			lack of definitive hematopoiesis
Fetal liver	+		+	
Fetal thymus	+	+	+	
Thymus cortex	+			<i>Runx1 and Runx3</i> KO: impaired T-cell development
Thymus medulla			+	
Spleen	+		+	
<i>Skeleton</i>				
Immature and permanent cartilage	+			<i>Runx2</i> KO: impaired development of osteoblast
Hypertrophic cartilage		+	+	
Osteoblasts	+	+		
Membranous bone	+	+		

Table 1.5. **Principal Runx expression sites and phenotype of knock out (KO) mice.**
AGM stands for aorta-gonad-mesonephros. Adapted from Levanon and Groner (2004).

Runx proteins are located where immature thymocytes reside correlating with their roles as regulators in T-cell development during thymopoiesis (Woolf *et al.*, 2003).

Both Runx1 and Runx3 are highly expressed in cranial and dorsal root ganglia (DRG), but in different neuronal populations (Inoue *et al.*, 2002). RUNX3 is also expressed in the glandular stomach epithelium cells (Li *et al.*, 2002).

Finally, all Runx proteins are expressed in cartilage although only biological functions of Runx2 has been identified in bone development so far (Levanon and Groner, 2004).

The tissue-specific expression of the RUNX proteins, which also varies with the different phases of development, highlight the importance of tightly regulated *RUNX* gene expression at the transcriptional and post transcriptional level.

1.4.2. Regulation of *RUNX* gene expression

1.4.2.1. Genomic organisation of RUNX

RUNX1, RUNX2 and RUNX3 are encoded by 3 different single genes which are highly similar in respect to their genomic organisation.

RUNX1 (260 kb), *RUNX2* (120 kb), and *RUNX3* (67 kb) genes are located on chromosome 21 (21q22), 6 (6p21) and 1 (1p36) respectively (Levanon *et al.*, 1994). The *RUNX1* gene contains 11 exons whereas the *RUNX2* gene includes 9 exons (Geoffroy *et al.*, 1998;Xiao *et al.*, 1998b;Terry *et al.*, 2004). *RUNX3* contains the smallest number of exons (i. e. 6), all of which are conserved among the 3 *RUNX* genes (Bangsow *et al.*, 2001). The runt domain is encoded by exons 2 (partially), 3 and 4 (Levanon *et al.*, 2001). A recent study has identified a *RUNX2* specific C-terminal exon (6.1) (Terry *et al.*, 2004) (Figure 1.6.). Gene expression is regulated by 2 widely spaced promoters, P1 (distal) and P2 (proximal) (Ghozi *et al.*, 1996;Drissi *et al.*, 2000;Bangsow *et al.*, 2001). The promoters, except RUNX2 P2, do not contain a classic TATA box, but an initiator (Inr) consensus sequence that is important for the assembly of transcription complexes in TATA-less promoter. The P2 promoter contains an IRES and is nested within a large CpG island which might be involved in tissue-specific expression of the gene (Levanon and Groner, 2004). The two promoters generate a large number of different mRNA.

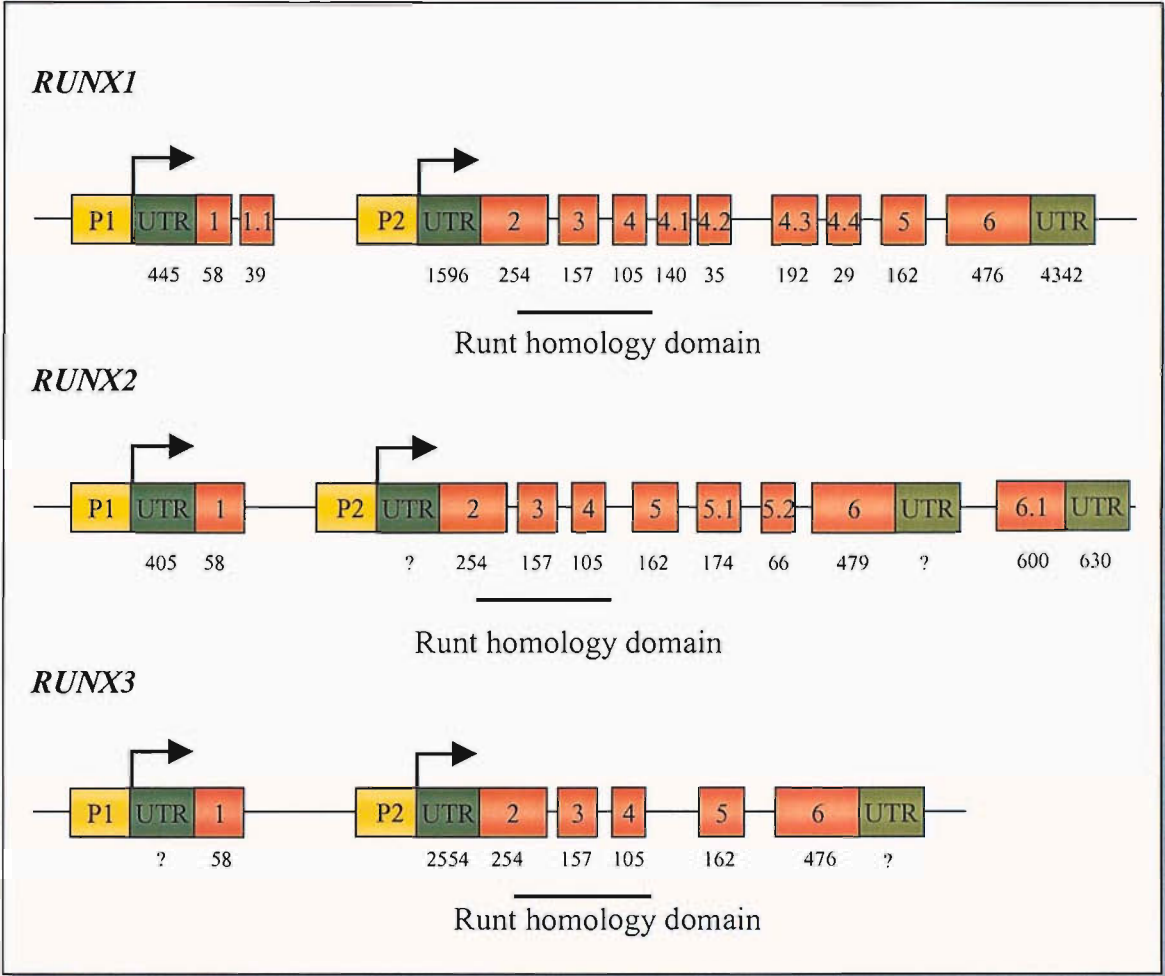


Figure 1.6. **Genomic organisation of the human *RUNX* genes.** Orange boxes represent coding exons. P1 and P2 correspond to the two promoters and UTR to the untranslated regions. The number under the exon boxes indicate the number of bases when known. The nomenclature of the exons is based on the principle that exons common to all three *RUNX* are designated with a major number (1-6) while the exons specific to each *RUNX* are denoted by a second number (e.g. 5.1). Adapted from Levanon and Groner (2004), Terry *et al.* (2004) and AceView Database.

1.4.2.2. Alternative spliced variants

Several mRNA are generated due to the alternative slicing process, differential usage of polyadenylation signals and stop codon containing exons (Levanon *et al.*, 1994; Miyoshi *et al.*, 1995; Levanon *et al.*, 2001). The main transcripts for RUNX1, RUNX2 and RUNX3 encode a 480, 513 and 415 aa protein respectively (Drissi *et al.*, 2000; Bangsow *et al.*, 2001; Levanon *et al.*, 2001). However, different proteins, ranging in size between 7-56 kDa can be expressed depending on the cell type and the stage of development. RUNX proteins have their amino acid sequence starting with MASNS when expressed from the P1 promoter or MRIPV when expressed from the P2 promoter (Banerjee *et al.*, 1997; Bangsow *et al.*, 2001). The mRNA and protein characteristics of the alternately spliced forms of RUNX1 and RUNX2, identified in the Aceview Database at the time of the research, are listed Table 1.6. The frequency of expression, and the significance of the various isoforms to RUNX biology remain unclear, although some studies have identified differential properties of some isoforms. For instance, the two main forms of RUNX1, represented in Figure 1.7., and called RUNX1B (the main form expressed from P1) and RUNX1A (a truncated form of RUNX expressed from P2, containing the Runt domain but lacking the C-terminal domain of RUNX1B) have the opposite effect on the regulation of the TCR β enhancer promoter (Bae *et al.*, 1994; Kim *et al.*, 1999). The expression of the isoforms can be cell-specific. For instance, the MASNS isoform of RUNX2 is predominately expressed in T cells and in osteoblast (Ogawa *et al.*, 1993b; Banerjee *et al.*, 1997).

1.4.2.3. Transcriptional regulation

Both promoters contain several RUNX-binding sites suggesting the possibility of auto and/or cross regulation of the gene by RUNX proteins (Ghozi *et al.*, 1996; Drissi *et al.*, 2000; Bangsow *et al.*, 2001). Interestingly, two of the RUNX binding sites have a highly conserved position at the beginning of the P1 5' UTR in all three human and mouse genes (Drissi *et al.*, 2000; Bangsow *et al.*, 2001). Although Drissi *et al.* (2000) showed that *RUNX2* expression was inhibited by RUNX2 *in vitro*, their role in the

Name	Protein size		Gene			
	Amino acid	kDa	CDS length	Nb of exons	5'UTR	3'UTR
RUNX1						
a (RUNX1B)	480	51.8	6230	8	445	4342
b	453	48.7	7285	6	1596	4327
c	389	41.4	3089	5	1596	323
d	348	37.7	1710	5	283	380
f (RUNX1A)	250	27.4	2724	5	1578	393
g	238	25.6	905	4	191	?
h	188	20.4	2287	4	1596	124
i	144	15.6	2268	2	1499	343
j	118	13.3	1226	1	292	577
k	77	8.3	908	1	480	194
m	62	6.9	1131	1	205	942
n	?	?	346	2	249	?
RUNX2						
a (RUNX2)	507	57	1860	8	405	?
b	450	51	1698	7	405	?
c	440	55	1347	7	?	?

Table 1.6. **Characteristics of the different RUNX1 and RUNX2 spliced variants.**

Adapted from AceView Database (April 2003) and Terry *et al.*, 2004.

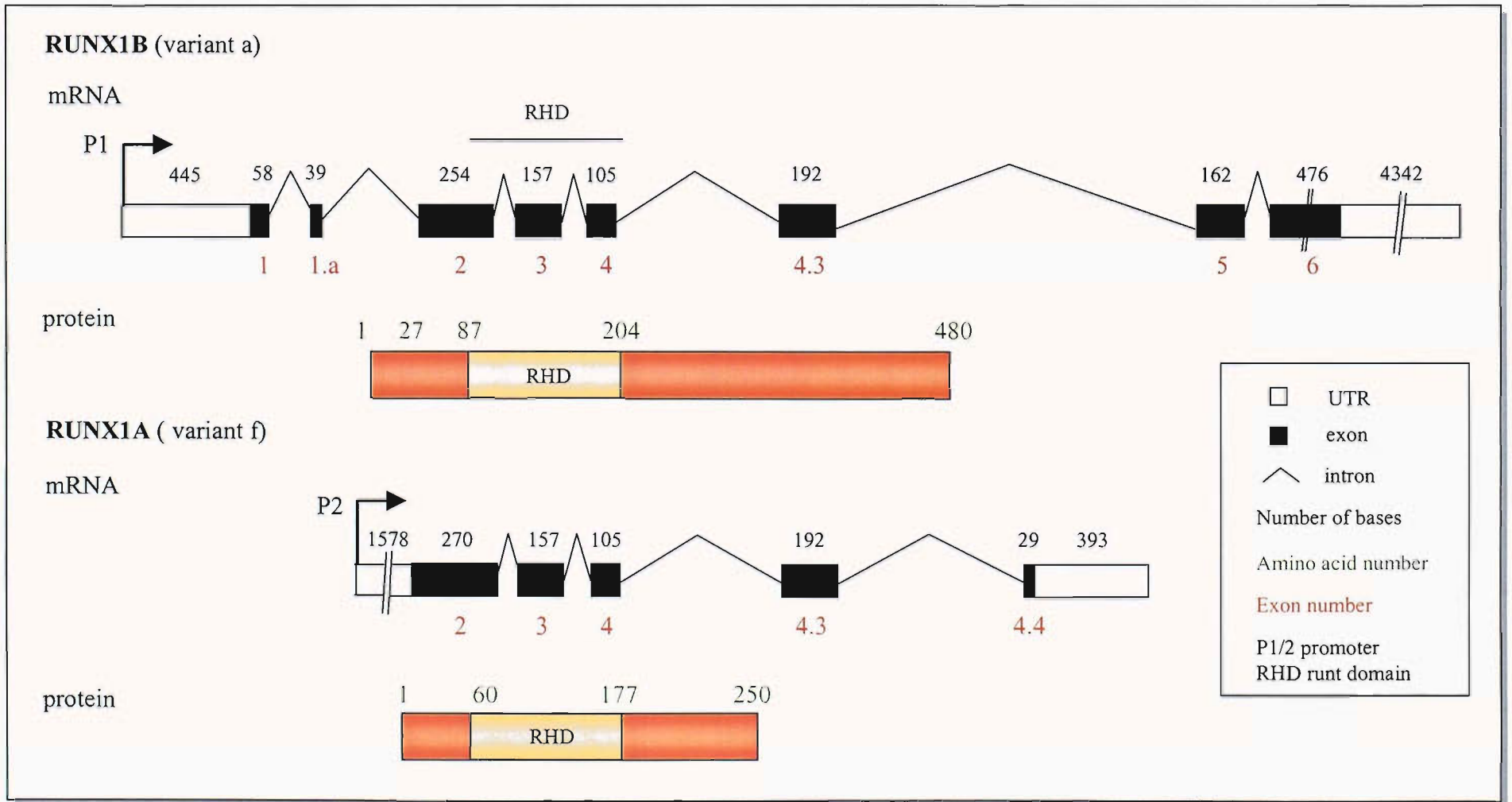


Figure 1.7. mRNA and protein representation of the 2 main alternatively spliced forms of RUNX1. RUNX1A is identical to RUNX1B within the region spanning amino acid 5 to 242.

regulation of *RUNX* transcription remains unclear (Levanon and Groner, 2004). Several other regulatory elements have been identified within the promoter regions. *RUNX1* promoters contain binding site for transcription factors such as PU-1, CRE (distal promoter) SP1, PU-1/ETS-like (proximal promoter) (Ghozi *et al.*, 1996). *RUNX2* promoters include c-Myb, NFκB, AP-1 and a vitamin D response element (VDRE) within P1, as well as a C/EBP and CREB binding site within P2 (Drissi *et al.*, 2000). In osteoblastic cells, AP1 site preferably binds FosB to induce *RUNX2* expression, whereas VDRE mediate vitamin-D dependent inhibition of *RUNX2* transcription (Zambotti *et al.*, 2002; Drissi *et al.*, 2002).

In the case of *RUNX3*, the distal promoter contains binding sites for ETS, CREB, E-box, whereas the proximal promoter includes SP1, Egr-1 and E-box binding sites (Bangsow *et al.*, 2001).

Although several functional analyses by reporter gene assay systems showed that the activity of the regulatory elements are cell-specific, detailed evidence about the regulation of *RUNX* gene expression are still missing (Bangsow *et al.*, 2001; Otto *et al.*, 2003; Levanon and Groner, 2004).

1.4.2.4. Signalling pathway regulating *RUNX* expression

Expression of *RUNX* proteins are influenced by retinoids, vitamin D, TGFβ, BMP, FGF (Otto *et al.*, 2003). Whereas retinoids and vitamin D upregulated *RUNX1* and *RUNX3* expression, they downregulated *RUNX2* expression (Le *et al.*, 1999). TGFβ has opposite effects on *RUNX2* transcription depending on the cell and its developmental stage, which correlates with the stimulatory and inhibitory effects of TGFβ on early and terminal osteoblast differentiation respectively (Levanon and Groner, 2004). BMP were shown to increase *RUNX2* expression (Lee *et al.*, 2000; Barnajee *et al.*, 2001). TGFβ and BMP are members of the TGFβ superfamily and induced transcription through different receptors and Smad proteins. (Yamaguchi *et al.*, 2004). Furthermore, FGF has been shown to regulate *RUNX* expression in several cell lines, although the positive or negative effects were cell dependant (Levanon and Groner, 2004).

1.4.3. RUNX activity and its regulation

1.4.3.1. RUNX gene target

RUNX proteins regulate the activity of their target genes by binding to a specific sequence within their promoter. The consensus sequence is 5'-TG^T/cGGT-3', or in reverse orientation, 5'-^A/cACC^A/gCA-3'. However, analysis of the different known RUNX binding sites reveal that the sequence 5'-AACCACA-3' occurs more frequently than the other binding sequences (Table 1.7.) (Otto *et al.*, 2003).

A large number of putative or proven RUNX target have been identified and are listed in Table 1.8. RUNX1 regulates most of the genes involved in hematopoiesis, whereas RUNX2 activate the ones related to bone formation. The transient overexpression of RUNX demonstrated that RUNX could act as an activator or repressor of gene expression depending on the promoter and the cell type. For instance, RUNX activated osteocalcin gene transcription but repressed the bone sialoprotein one (Banerjee *et al.*, 1997;Javed *et al.*, 2001). RUNX1 represses transcription of p21^{waf-1/Cip1} in NIH 3T3 cells and activated the same promoter in K562 myeloid cells line (Lutterbach *et al.*, 2000). Furthermore, cross activation of promoter activity by the three RUNX proteins have been observed, suggesting that these *in vitro* experiments do not utterly reflect the physiological context (Javed *et al.*, 2001).

Of interest regarding liver fibrosis, RUNX2 has been shown to regulate MMP13 and $\alpha 1(I)$ collagen (Ducy *et al.*, 1997;Jimenez *et al.*, 1999). In addition, the TGF- β type I receptor promoter contains 6 RUNX binding sites (Chang *et al.*, 1998).

1.4.3.2. Post translational regulations of RUNX

Another level of RUNX regulation is by posttranslational modification of the protein, such as phosphorylation or acetylation of specific residues. Tanaka *et al.*, (1996) demonstrated that RUNX1 show an enhanced gene transactivation when the serines S-249 and S-266 are phosphorylated *in vivo* by ERK. However, these phosphorylations do not affect RUNX DNA binding affinity suggesting that the modifications may have an effect on RUNX1 interaction with other factors instead. Indeed, Imai *et al.*, (2004) showed that the phosphorylation of RUNX1 disrupts the

Gene	Sequence	Position	References
Human RUNX1 (P1)	TTGTGGAA	-69	Ghozi <i>et al.</i> , 1996
Murine Runx2 (P1)	CACCACA	-1024	Xiao <i>et al.</i> , 2001
	TACCACA	-33	
	AGTGGTA	-119	
	AACCACA	-74	
	AACCACA	+29	
	AACCACA	+37	
	TGCGGTG	+47	
Human RUNX3 (P1)	AACCACA	-4	Bangsow <i>et al.</i> , 2001
	AACCACA	+5	
Human IL-3	TGTGGT	-139	Uchida <i>et al.</i> , 1997
	TGTGGG	-52	
Murine myeloperoxidase	AACCACA	Enhancer	Nuchprayoon <i>et al.</i> , 1994
Neutrophil elastase	GGCCACA	-72	Nuchprayoon <i>et al.</i> , 1994
M-CSF receptor	TGTGGTT	-73	Fears <i>et al.</i> , 1997
Human granzyme B	CACCACA	-92	Wargnier <i>et al.</i> , 1995
TCRa	TCCCGCA	Enhancer	Giese <i>et al.</i> , 1995
Complement receptor 1	TGTGGT	-42	Kim <i>et al.</i> , 1999
Rat collagenase 3	AACCACA	-132	D'Alonzo <i>et al.</i> , 2002; Jimenez <i>et al.</i> , 1999
Rat TGF- β receptor type I	TTCCGCA	-1101	Ji <i>et al.</i> , 1998
	GGCCGCA	-1077	
	AACCGCG	-546	
	AGCCACA	-313	
	AACCACG	-251	
	GGCCGCG	-81	
Murine osteopontin	AACCACA	-136	Sato <i>et al.</i> , 1998
Murine osteocalcin	AACCACA	-136	Ducy <i>et al.</i> , 1996
Chicken BSP	TGTGGAG	-1204	Javed <i>et al.</i> , 2001
	AACCACA	-813	
	AGTGGTC	-514	
	TGTGGTG	-444	
	TGTGGTT	-414	
	TGTGGTG	-318	
C/EBP δ	AACCGCA	-165	McCarthy <i>et al.</i> , 2000

Table 1.7. **RUNX binding sites within promoter of RUNX regulated genes.** Otto *et al.*, 2003.

Hematopoietic genes

B-cell specific tyrosine kinase (BLK)¹, cell surface glycoprotein (CD36, CD11a, CD4)², granulocyte-macrophage colony-stimulating factor (GM-CSF)³, Immunoglobulin μ heavy chain⁴, IgA1⁵, IgC α ⁶, Macrophage colony-stimulating factor (M-CSF) receptor⁷, macrophage inflammatory protein-1 α ⁸, interleukin-3 (IL-3)⁹, neutrophil proteins-3 (NP-3)¹⁰, myeloperoxidase (MPO)¹¹, neutrophil elastase¹², T cells receptor (TCR) α , β enhancer¹³, TCR α , β , γ , δ , chains¹⁴

Bone-related genes

Alkaline phosphatase (ALP)¹⁵, *bone sialoprotein (BSP)*¹⁶, C/EBP δ ¹⁷, dentin sialoprotein (DSP)¹⁸, Estrogen receptor α ¹⁹, galectin-3²⁰, human vitamin D receptor (hVDR)²¹, MMP13²², Osteocalcin (OC)²³, osteopontin (OP)²⁴, osteoprotegerin (OPG)²⁵, prolactin²⁶, *RUNX2*²⁷, sclerostin (SOST)²⁸, TGF- β receptor-1 (TGF β R1)²⁹, α 1(I) collagen³⁰, VEGF³¹

Others

Bcl2³², latent membrane protein (LMP-1)³³, *multidrug resistance gene 1 (MRD1)*³⁴, p14^{ARF}³⁵, *p21^{waf-1/Cip1}*³⁶, p21^{waf-1/Cip1}³⁷, *Rous sarcoma virus long terminal repeat (LTR)*³⁸, sex limited protein (SLP)³⁹

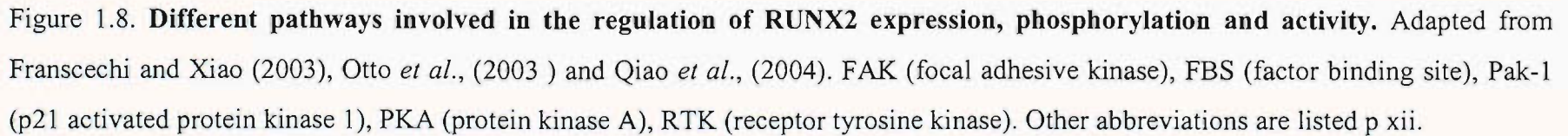
Table 1.8. **Target genes of RUNX proteins.** Gene names in regular are upregulated and gene names in italic are downregulated by RUNX.

1. Libermann *et al.* (1999) 2. Armesilla *et al.* (1996), Stein *et al.* (2004) 3. Kanno *et al.* (1998), Petrovick *et al.* (1998) 4. Stein *et al.* (2004) 5. Pardali *et al.* (2000) (6) Hanai *et al.* (1999) 7. Zhang *et al.* (1994) 8. Bristow and Shore (2003) 9. Uchidi *et al.* (1997) 10. Westendorf *et al.* (1998) 11. Kitabayashi *et al.* (1998) 12. Nuchprayoon *et al.* (1994) 13. Bae *et al.* (1994), Kim *et al.* (1999), Levanon *et al.* (1998), Meyers *et al.* (1995) 14. Meyers *et al.* (1995), Giese *et al.* (1995), 15. Stein *et al.* (2004) 16. Javed *et al.* (2000), Javed *et al.* (2001) 17. McCarthy *et al.* (2000) 18, 19, 21. Stein *et al.* (2004) 20. Stock *et al.* (2003) 22. Mengshol *et al.* (2001), Jimenez *et al.* (1999) 23. Barnajee *et al.* (1997), Ducy *et al.* (1997), Javed *et al.* (1999), Javed *et al.* (2000) 24. Ducy *et al.* (1997), Innam and Shore (2003) 25-26. Stein *et al.* (2004) 27. Drissi *et al.* (2000) 28. Severson *et al.* (2004) 29. Chang *et al.* (1998) 30. Ducy *et al.* (1997) 31. Sun *et al.* (2004) 32-33. Stein *et al.* (2004) 34. Lutterbach *et al.* (1998), Nisson *et al.* (1993), Javed *et al.* (2000) 35. Linggi *et al.* (2002) 36-37. Lutterbach *et al.* (2000) 38. Javed *et al.* (2000) 39. Stein *et al.* (2004) .

interaction between RUNX1 and the corepressor, mSin3A. As these phosphorylation sites are conserved in RUNX2, but not RUNX3, it is possible that RUNX2 is also positively regulated by ERK. Moreover, p300-mediated acetylation significantly enhances RUNX1 DNA binding affinity. Two lysines located in the N-terminal region of RUNX1 (Y-24 and Y-43) are acetylated by p300 *in vitro* and *in vivo* (Yamaguchi *et al.*, 2004).

On the other hand, RUNX2 is negatively regulated by the phosphorylation of two other conserved serines (S-104 and S-451) (Wee *et al.*, 2002). While the phosphorylated S-104 reduced the DNA binding affinity of RUNX2 by preventing it from interacting with CBF β (interaction which is normally required for DNA binding- see 1.4.3.3.3.), phosphorylated S-451 downregulated the RUNX2-dependent transactivation. These modifications do not involve any of the MAPK family members (Wee *et al.*, 2002). In contrast, other studies have demonstrated a positive regulation of RUNX2 activity via ERK-dependent phosphorylation, without however, identifying the residues involved (Xiao *et al.*, 2000). The MEK/ERK branch of the MAP kinase pathway can be activated by different stimuli such as ECM modification, or by FGF2 or IGF-1, which have been shown to enhance RUNX2 activity (Xiao *et al.*, 1998a; Franceschi and Xiao, 2003; Qiao *et al.*, 2004). ECM binding to integrins on the cell surface activates focal adhesion kinase (FAK), and FGF2 activates the receptor tyrosine kinase. Both kinases induce ras activity and subsequently activate the ERK pathway. IGF-1 stimulated PI3K which activated p21-activated protein kinase 1 (Pak) leading to activation of the ERK pathway (Qiao *et al.*, 2004). Another stimuli involved in the phosphorylation of RUNX2 is the parathyroid hormone (PTH) which activates the Protein Kinase A (PKA), that not only phosphorylates RUNX2, but also regulates transcription factors such as AP-1 family members that cooperatively activate RUNX target genes (Selvamurugan *et al.*, 1998; Hess *et al.*, 2001; D'Alonso *et al.*, 2002).

Transcriptional regulation and posttranslational modification of RUNX involve a complex network of signal pathways which influence RUNX functionality and are summarized Figure 1.8. Furthermore, RUNX activity is also modulated by other transcription factors and cofactors via specific interactions.



1.4.3.3. Regulation of RUNX activity by interaction with other factors

The 3 RUNX factors are highly conserved. They share 50-60 % homology in their C-terminal sequence and more than 90 % in the runt domain. RUNX1 activation/repression domains have been mapped in different studies and are represented along with the different transcriptional factors and co-factors that bind to them in Figure 1.9.

1.4.3.3.1. Functional domains of RUNX

The runt domain is highly conserved between the 3 RUNX proteins and is the region of the protein that binds to the DNA sequence. The DNA affinity of RUNX is increased by its interaction with CBF β within the runt domain (Meyers *et al.*, 1993; Ogawa *et al.*, 1993a).

The N-terminal region prevents the runt domain from interacting with either CBF β or DNA as the deletion of this region significantly increases the frequency of RUNX/CBF β dimerisation and the DNA binding ability of the runt domain (Kim *et al.*, 1999).

In early studies, the C-terminal region was assigned as the transactivation domain of RUNX (Bae *et al.*, 1994; Tanaka *et al.*, 1995b). These studies were supported by the fact that the fused RUNX-ETO, and RUNX-EVI-1 that lacked the RUNX C-terminal domain, suppressed the promoter transactivation by RUNX (Meyers *et al.*, 1995; Tanaka *et al.*, 1995a). However, in an extended study using a gene reporter assay, Kanno *et al.* (1998) identified transcriptional activation and inhibitory domains within the C-terminal region. The transactivation domain can be divided into 3 activation domains according to their cell-specific activity. The last 5 amino acids (VWRPY) were identified by Arosen *et al.* (1997) as another inhibitory domain which is present in all RUNX factors. Kanno's EMSA experiments (1998) also showed that the interaction of RUNX1 with CBF β is blocked by the region including aa 411 to 451 and that the DNA-binding activity is inhibited by the region spanning aa 183 to 291, called a negative regulatory domain for DNA binding (NRDB).

Several proteins have been shown to interact within these domains and to modulate RUNX activity.

NRDBn/c: negative regulatory domain for DNA binding in Nt/Ct

NRHn/c: negative regulatory domain for heterodimerization in Nt/Ct

NMTS: nuclear matrix targeting signal

NLS: nuclear localisation signal

AD: transcription activation domain

TE1,2,3 subelements within AD

ID: transcription inhibition domain

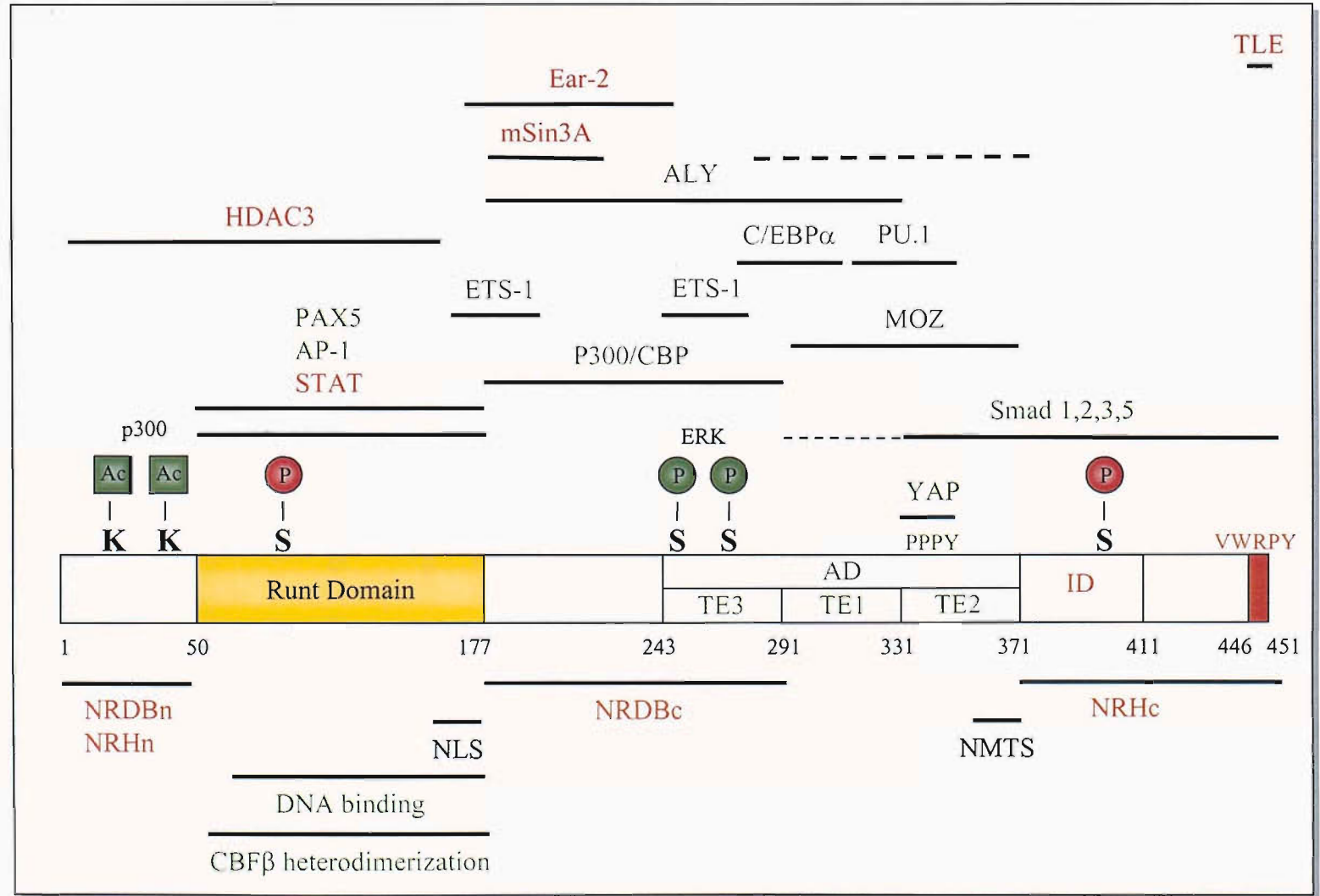


Figure 1.9. **RUNX1** functional domains, sites of phosphorylation and acetylation and mapping of the interacting regions with coregulators. Adapted from Ito, 2004.

1.4.3.3.2. Interaction of RUNX with co-repressors

The Groucho/TLE class of proteins have been shown to interact with the C-terminal of RUNX (VWRPY) (Aronson *et al.*, 1997; Levanon *et al.*, 1998; Javed *et al.*, 2000). Although these interactions are responsible for the transcriptional repression of several RUNX-regulated genes, such as MDR-1, T-cell receptor enhancer α and β , the mechanism for the repression of other genes (p21^{waf-1/Cip1}, LTR) is independent of these interactions (Levanon *et al.*, 1998; Javed *et al.*, 2000; Lutterbach *et al.*, 2000). These observations led to the identification of another repressor, mSin3 which has been shown to interact with all three RUNX proteins (Lutterbach *et al.*, 2000). This repression is not only dependent on the interaction between RUNX and mSin3, but required the presence of a C-terminal region spanning aa 290-387 (Lutterbach *et al.*, 2000). In addition, Ear-2 is a member of the nuclear hormone receptor superfamily which interacts with RUNX1 in the C-terminal region adjacent to the runt domain. Although Ear-2 does not affect the transactivation of transcription by RUNX1 on its own it inhibits the cooperative activation of the M-CSF-R1 promoter by RUNX1 and C/EBP (Ahn *et al.*, 1998). The latent form of STAT-1 has been shown to bind RUNX2 retaining it in the cytoplasm (Kim *et al.*, 2003). Finally, transcription can be repressed by the interaction of RUNX with histone deacetylases (HDAC) (Schroeder *et al.*, 2004). HDAC are enzymatic components of multi-protein complexes, recruited by transcription factors, that remove acetyl residues from nucleosomal histones and other substrates leading to chromatin condensation and gene repression.

1.4.3.3.3. Interaction of RUNX with co-activators

The main cofactor of RUNX activity is CBF β (Core-binding factor β), also called PEBP2 β , which forms a constitutive heterodimer with RUNX (Ogawa *et al.*, 1993a). CBF β binds to the runt domain of RUNX and enhances RUNX DNA binding by inducing a conformational change in the Runt domain (Tang *et al.*, 2000). The heterodimerization of CBF β with RUNX prevents this latter from being degraded by the ubiquitin-proteasome pathway (Huang *et al.*, 2001). Interestingly, a chromosomal inversion, identified in some case of leukemia, involves the fusion *CBF β* gene to a smooth muscle myosin heavy chain gene (Lutterbach and Hiebert, 2000). *Cbf β* ^{-/-} knock-out mice present similarities with the *Runx1*^{-/-} and *Runx2*^{-/-} knock-out mice:

they are not viable due to a lack of definitive hematopoiesis and present a delay in intramembranous ossification and chondrocyte differentiation (Sasaki *et al.*, 1996; Kundu *et al.*, 2002).

In many reporter gene experiments the degree of transcriptional activation by the forced expression of RUNX was not elevated, highlighting the weak intrinsic activational properties of RUNX. However, synergistic promoter transactivation was observed in experiments where RUNX was cotransfected with other transcription factors, suggesting another level of regulation of RUNX activity by co-regulators. These latter include transcription factors such as ETS-1 (Giese *et al.*, 1995; Kim *et al.*, 1999), NERF-2 (Cho *et al.*, 2004), C/EBP α , PU-1 (Petrovick *et al.*, 1998), Smads (Hanai *et al.*, 1999) AP-1 (Hess *et al.*, 2001), PAX5 (Libermann *et al.*, 1999) or cofactors such as MOZ (Kitabayashi *et al.*, 2001), p300/CBP (Kitabayashi *et al.*, 1998), YAP (Yagi *et al.*, 1999) or ALY/LEF (Bruhn *et al.*, 1997) (Figure 1.9.).

Different mechanisms of activation have been reported depending on the different coactivators recruited within the promoter. M-CSF promoter activation involves the interaction between several factors (RUNX/C/EBP α /PU-1) while TCR β enhancer promoter involves the interaction of RUNX and ETS-1 between their respective negative regulatory domains for DNA binding. This interaction synergistically enhances the binding of the two proteins on their respective DNA binding sites (Zhang *et al.*, 1994; Zhang *et al.*, 1996; Petrovick *et al.*, 1998; Kim *et al.*, 1999).

Histone acetyltransferases such as MOZ or p300/CBP are proteins that increase transcription by acetylating the histones associated with DNA and recruiting basal transcription factors (Sterner and Berger, 2000). p300 stimulates RUNX1-dependent transcription, depending on the promoter context, as it activates the MPO promoter, but not the TCR β enhancer promoter (Kitabayashi *et al.*, 1998) In another study, Kitabayashi *et al.* (2001) showed that MOZ and RUNX1 activate transcription in a synergistic manner and that the RUNX proteins interact with 2 domains of MOZ. Interestingly, CBP/p300 is found to be disrupted and fused in frame with MOZ by chromosomal translocation in acute myeloid leukemia and myelodysplastic syndrome (Borrow *et al.*, 1996).

1.4.3.3.4. The model of enhanceosome

Synergistical activation of promoters by RUNX and c-Myb transcriptional factors, without involvement of physical interactions, has also been described (Hernandez-Munain and Krangel, 1994; Hernandez-Munain and Krangel, 1995; Britos-Bray and Friedman, 1997). Since several studies have demonstrated the interaction of p300/CBP with c-Myb (Oelgeschlager *et al.*, 1996; Mink *et al.*, 1997), these observations suggest that the formation of an enhanceosome complex, containing RUNX, cMyb and p300, is responsible for the promoter transactivation.

An enhanceosome includes several transcription factors and co-factors that form a network of protein-protein and protein-DNA interaction specific to each promoter (Ito, 1999). The composition of the complex, containing repressors or activators, determines the positive or negative regulation of transcription. In addition, the nature of the enhanceosome is not only dependent upon the promoter sequence which dictates the recruitment of specific transcription factors, but also on the availability of the different co-factors within the cell. While RUNX is a weak activator/inhibitor of transcription on its own, its emerging role is to act as an organizing factor that facilitates chromatin remodelling and assembly of the transcriptional enhanceosome, as shown by the TCR α and the osteocalcin model of promoter activation (Ito, 1999; Gutierrez *et al.*, 2004).

1.5. Conclusion

TIMP1 is an inhibitor of metalloproteinases involved in ECM homeostasis and its deregulation is associated with several pathological conditions such as cancer and cirrhosis. In the liver, its enhanced expression is responsible in part for the formation of fibrotic bands which impairs liver functions.

On the other hand, RUNX proteins are transcription factors regulating several important biological pathways, such as hematopoiesis, osteogenesis and neurogenesis, by organizing the formation of transcriptional complexes that drive the transcription of key protein genes involved in these pathways.

These proteins have never been linked ... so far ...

The aims of the work described in this thesis were to:

- Identify the RUNX transcription factors as the UTE-1 binding protein using the One-Hybrid System
- Establish the presence and the functionality of RUNX proteins in Hepatic Stellate cells
- Investigate the mechanisms by which the RUNX proteins regulate the *TIMP1* promoter by
 - overexpressing RUNX proteins in *TIMP1*-reporter gene assays
 - silencing *RUNX* gene expression using shRNAi technologies and baculovirus gene delivery system

Chapter 2

Materials and Methods

2.1. Strains, cells and plasmids

2.1.1. Strains

2.1.1.1. Genotype

E. coli DH5 α : ϕ 80*lacZ* Δ M15, *rec A1*, *end A1*, *gyr A96*, *thi-1*, *hsd R17* (r_K^- , m_K^+), *sup E44*, *rel A1*, *deo R*, Δ (*lacZYA-argF*) U169

E. coli HB101: *thi-1*, *hsd S20* (r_B^- , m_B^+), *sup E44*, *rec A13*, *ara-14*, *leu B6*, *pro A2*, *lacY1*, *rps L20* (str^r), *xyl-5*, *mtl-1*

E. coli BNN132: *end A1*, *gyr96*, *thi*, *hsd R17*, *sup E44*, *rel A1*, Δ (*lac-proAB*), (F', *traD36*, *proAB*⁺ *lacI*^q*Z* Δ M15), (λ , Kan, Cre)

E. coli DH10BacTM: F⁻*mcrA* Δ (*mmr-hsdRMS-mrcBC*) ϕ 80*lacZ* Δ M15 Δ *lacX74* *recA1* *endA1* *araD139* Δ (*ara*, *leu*)7697 *galU* *galK* λ -*rpsL* *nupG*/bMON14272/pMON7124

S. cerevisiae YM4271: MAT α , *ura3-52*, *his3-200*, *ade2-201*, *lys2-801*, *leu2-3*, 112, *trp1-901*, *tyr1-501*, *gal4- Δ 512*, *gal80- Δ 538*, *ade5::hisG*.

2.1.1.2. Culturing and media

Media are listed in 2.9.1.

Bacteria were grown in LB/amp i.e. LB containing 50 μ g/mL ampicillin (Sigma). Ampicillin was used as an agent of selection for the different plasmids as they conferred to the bacteria a resistance to ampicillin. Overnight cultures of bacteria were incubated at 37°C with shaking (200 rpm).

Yeast were grown in normal medium YPDA (Clontech) or in selective medium (SDA) (Clontech) lacking one or two amino acids allowing nutritive selection. Addition of 3-amino-1, 2, 4-triazole (3AT) (Sigma) into the media allowed nutritive selection. Overnight liquid cultures of yeast were incubated at 30°C with vigorous shaking (230-270 rpm). The inoculum, one to several large colonies, had to be vortexed first into a small volume of medium in order to avoid clumps that would slower the growth. After 16-18 h the culture reached the stationary phase.

2.1.1.3. Frozen stocks and recovering

Bacteria were stored for 2 years in LB/amp containing 15 % (v/v) glycerol (Sigma) at -70°C. The yeast strains were also stored indefinitely in YPDA medium with 25 % (v/v) glycerol at -70°C.

To recover frozen strains, a small portion of the frozen glycerol stock was streaked out onto either LB/amp or YPDA agar plate and the plate was incubated at 37°C overnight (bacteria) or 30°C for 3-5 days (yeast) until the colonies reached 2 mm in diameter.

2.1.2. Mammalian cells

2.1.2.1. Cell type

Cos-1: Fibroblast-like cells growing as monolayers. They originated from African green monkey kidney derived from CV-1, a simian cell line (*cercopithecus aethiops*), by transformation with an origin-defective mutant of SV-40.

HeLa : Human epithelial-like cells growing as monolayers. They were purified from a cervix carcinoma tumor.

Saos-2: Human epithelial-like cell line growing as monolayers. They were established from a primary osteogenic sarcoma.

Huh7: Differentiated human hepatoma cell line cells growing as monolayers.

LX2: Spontaneously immortalized Human Stellate Cell line.

Rat Hepatic Stellate Cell: The primary cells were purified from Sprague-Dawley rat liver.

Human Hepatic Stellate Cell: They were obtained from patients undergoing liver surgery.

2.1.2.2. Culturing

Media are listed in 2.9.2.

All cells were incubated at 5 % CO₂ atmosphere at 37°C. and were cultivated in complete media. Cell lines were routinely cultivated in T75 flask and passaged before confluence every 4-5 days. Cells were detached from the flask by

trypsinizing. Briefly, cells were washed in HBSS-Ca²⁺ and incubated with 1 mL of trypsin at 37°C for 1 min. Trypsin was then inhibited by addition of 9 mL complete media and 1 mL was transferred into a new T75 flask containing fresh complete media.

Primary Hepatic Stellate cells were routinely cultivated in 10 cm dishes (rat HSC) or T25 flask (human HSC). They were passaged once (rat HSC) or up to 4 times (human HSC) before confluence using citric saline solution. Cells were washed with PBS and incubated with citric saline solution at 37°C for 5 min before being harvested by centrifugation at 1,000 x g for 5 min, resuspended in fresh complete media and transferred into new flask.

2.1.3. Plasmids

Each plasmid contained the resistance gene to ampicillin. Maps of plasmids are listed in appendix 1.

2.1.3.1. Vectors used in the One-Hybrid System (Clontech)

Reporter vectors

pHISi and pHISi-1: These 6.8 kb and 5.4 kb vectors were designed to be integrated into the *HIS3* locus of the yeast genome by homologous recombination. They carried the *HIS3* reporter gene upstream of a multiple cloning site. pHISi also carried *URA3* gene.

placZi: this was a 6.9 kb vector designed to integrate into the yeast genome at the *URA3* locus. It carried the *lacZ* reporter gene upstream of a multiple cloning site and the *URA3* gene for nutritional selection

Control plasmids

p53HIS (6.6 kb) and p53BLUE (6.7 kb) contained three tandem copies of the consensus p53 binding site downstream of the *HIS3* reporter gene in pHISi and downstream of *lacZ* reporter gene in placZi respectively. They also contained the *URA3* gene for nutritional selection.

pGAD424 (6.6 kb) expressed a truncated GAL4 protein containing only the activation domain of the protein.

pGAD53m (7.8 kb) contained the mouse p53 cDNA in frame with the GAL4 activation domain gene. It also contained the *LEU2* gene for nutritional selection.

Library plasmid

pACT₂ (8.1 kb + cDNA insert) generated a fusion of the GAL4 activation domain, an HA epitope and the protein encoded by a cDNA in the HeLa library. The hybrid protein was expressed at high levels in yeast host cells from the constitutive ADHI promoter. The protein was targeted to the nucleus by the nuclear localisation sequence from SV40 T-antigen. pACT₂ was a shuttle vector that replicated autonomously in both *E. coli* and *S. cerevisiae*. The plasmid contains the *LEU2* gene.

2.1.3.2. Expression vector used in functional assay

pBLCAT2 (4.5 kb) and pBLCAT3 (4.3 kb) (ATCC) derived from pUC18. They contained the coding region of the bacterial chloramphenicol acetyltransferase (CAT) gene, the small t intron and polyadenylation signal from SV40. While pBLCAT3 did not contain any promoter region, pBLCAT2 contained the Herpes simplex virus Thymidine Kinase (TK) promoter for studying the effect of putative regulatory elements on a heterologous eukaryotic promoter.

pCMV2 (4.7 kb) and pCMV5 (4.7 kb) (pCMV2-JunD-D. Smart, Southampton; pCMV5-RUNX1B-S. Hiebert, Nashville; pCMV5-RUNX2-P. Shore, Manchester) These eukaryotic expression vectors contained the immediate-early region of the human cytomegalovirus promoter (Pcmv), the transcription termination and polyadenylation region of the human growth hormone gene. They also contained the SV40 virus DNA replication origin.

pFIGU (C. Dolphin, London) (7.1 kb) derived from the pFastBac1 baculoviral shuttle vector (Bac-to-Bac; Invitrogen) and contained the CMV promoter (Pcmv), internal ribosome entry site (IRES) and enhanced green fluorescent protein gene (EGFP). The sequence of the human U6 RNA Pol III promoter, including the distal and proximal sequence elements and TATA box was cloned into the vector in an opposite orientation to the Pcmv-driven IRES2-EGFP cassette. Presence of tn7 element in the plasmid allowed transposition to a bacmid which contained the mini-*att*TN7 attachment site.

pGL2-basic (5.6 kb) and pGL2-control (6.0 kb) (Promega) carried the coding region for firefly luciferase (*Photinus pyralis*), the polyadenylation signal from SV40. pGL2-basic lacked eucaryotic promoter and enhancer sequences whereas pGL2-control contained a SV40 promoter and enhancer sequences.

pLNCX (Clontech) (6.6 kb) (pLNCX-FLAG-RUNX1A/-RUNX1B/-CBP/-MOZ - I. Kitabayashi, Tokyo). It contained the human cytomegalovirus immediate early promoter (Pcmv) and the multiple cloning site immediately downstream of the promoter.

pRK5 (BD PharMingen) (4.7 kb) (pRK5-FLAG-RUNX2 - P. Shore, Manchester). This eukaryotic expression vector contained the immediate-early region of the human cytomegalovirus promoter (Pcmv). It also contained a polyadenylation signal from SV40 for RNA processing in mammalian cells and a SV40 origin for episomal plasmid amplification in COS cells.

pRL-TK (4.0 kb) (Promega) contained the cDNA encoding *Renilla* luciferase cloned from the anthozoan coelenterate *Renilla reniformis*. The reporter gene was under control of the herpes simplex virus thymidine kinase promoter which provided low levels of renilla luciferase expression.

pSG5 (Stratagene) (4.1 kb) (pSG5-clone A1/-clone A2). This eukaryotic expression vector contained the early SV40 promoter and also the T7 bacteriophage promoter and a polyadenylation signal. The presence of the rabbit β -globulin intron II downstream of the SV40 promoter allow the splicing of expressed transcript.

pSV- β -Galactosidase (Promega) (6.8 kb): The SV40 early promoter and enhancer drove transcription of the bacterial *lacZ* gene, which in turn, is translated into the β -galactosidase enzyme.

2.2. DNA manipulation

2.2.1. Digestion of plasmid DNA

1 μ g of DNA was digested in a total volume of 20 μ L containing 0.1 mg/mL acetylated BSA, 1x multicore or appropriate enzyme buffer (2.9.4.) and 500 U of appropriate restriction enzymes (Promega). The digestion was performed at 37°C for 2 h. The products of the digest were resolved by electrophoresis on an 1 % (w/v)

agarose gel and visualised by UV detection of incorporated ethidium bromide (Sigma).

2.2.2. Ligation

0.025 μg of digested plasmid was mixed with 0.02 μg of DNA insert, 1x ligation buffer (2.9.4.) and 0.8 U of T4 DNA ligase (Promega) in a total volume of 10 μL H_2O . The reaction was performed at RT for 4 h or at 4°C overnight. 1 μL of the ligation mixture was used for transformation into bacteria.

2.2.3. Transformation of plasmid DNA into bacteria

100 μL of competent bacteria DH5 α or HB101 (Promega) were mixed with 0.5 μg of DNA into a prechilled eppendorf. After 10 min incubation on ice, the cells were heat-shocked at 42°C for 45 sec and placed on ice for 2 min. The mixture was plated out onto LB plates containing 50 $\mu\text{g}/\text{mL}$ ampicillin. The plates were incubated at 37°C overnight.

2.2.4. PCR reaction

Typically, 100 ng DNA was used for PCR reaction along with 1x PCR buffer (2.9.4.), 1 U Taq polymerase (Sigma), 10 pmol of appropriate primers and 10 mM dATP, dTTP, dCTP, dGTP into a final volume of 50 μL .

When performing a large number of PCR reactions, 100ng DNA was mixed with 10 pmol of appropriate primers and 1x PCR master mix (Promega) that contained Taq DNA polymerase, dNTPs, MgCl_2 and reaction buffers at optimal concentration.

The products of the PCR were resolved by electrophoresis on a 1 to 2 % (w/v) agarose gel and stained with ethidium bromide and viewed under UV light.

2.2.5. DNA purification

2.2.5.1. DNA purification from Bacteria

Bacteria that contained the plasmid of interest were inoculated into 3 mL of LB/amp and incubated at 37°C for 8 h. 200 µL of the start-up culture were used to inoculate 100 mL LB/amp. After 18 h incubation at 37°C, the cells were collected by centrifugation at 3000 x g for 15 min and the plasmids were purified using Hispeed DNA purification kit (Qiagen) according to the manufacture's protocol. DNA concentrations were determined by spectrophotometry at a wavelength of 260nm.

2.2.5.2. DNA purification from Yeast

The yeast colony that contained the plasmid of interest was plated out on selective medium in order to form a thick patch of cells after 3-day incubation at 30°C. The cells were scraped and resuspended into 50 µL 67 mM KH₂PO₄, pH 7.5. The cell walls were disrupted by 50 U of lyticase (Sigma) and the solution was mixed by pipetting up and down several times. After 1 h incubation at 37°C, 10 µL 20 % (v/v) SDS (Sigma) was added to the mix and the latter was vortexed for 1 min. Samples were freeze-thawed once. The mix was applied on a chromaspin-1000 column (Clontech) from which storage buffer had been previously discarded by centrifugation (5 min, 700 x g). The columns were centrifuged 5 min at 700 x g and the DNA was collected in the eluate. DNA samples were stored at -20°C.

5 µL of the eluate was transformed into *E. coli* HB101 as described in 2.2.3. The plasmid was extracted from the bacteria (2.2.5.1.) and stored at -20°C until further use.

2.2.5.3. Phenol/Chloroform extraction of DNA

Phenol/chloroform extraction was used to separate DNA from proteins.

1 volume of phenol:chloroform:isoamyl alcohol (25:24:1) (Sigma) was added to the DNA sample and the latter was vortexed for 1 min. After centrifugation for 5 min at 16,000 x g, the upper phase was collected and mixed with one volume of chlorophorm:isoamyl alcohol (24:1). After vortexing for 30 sec the sample was

centrifuged for 2 min at 16,000 x g and the upper phase was transferred into a sepharose column from a gel extraction kit (Qiagen) following the manufacture's protocol. (2.2.5.4.)

2.2.5.4. DNA extraction from agarose gel

Qiaquick gel extraction kit (Qiagen) was used to extract and purify DNA from standard agarose gel when DNA fragments had been separated by electrophoresis. Briefly, DNA was excised from the agarose gel and the gel slice was weighted. The sample was dissolved in 3 volumes of buffer QG (using the estimation 100 mg = 100 μ L) and heated for 10 min at 50 °C. 1 volume of isopropanol was added to the DNA and the mix was applied to a Qiaquick column before being centrifuged for 1 min at 16,000 x g. The column was washed with 0.5 mL of buffer QG and 0.75 mL of buffer PE and the column was dried out with an additional centrifugation step at 16,000 x g for 1 min. DNA was then eluted with 50 μ L of H₂O and centrifugation at 16,000 x g for 1 min.

2.3. Screening of a cDNA library with the One-Hybrid System

2.3.1. Preparation of the target-reporter construct

The aim of this experiment was to clone a target element downstream of *HIS3* or *LACZ* gene of the reporter plasmid (pHISi, pHISi-1 or pLacZi)

2.3.1.1. Synthesis of the oligonucleotides

Three sets of two antiparallel oligonucleotides were chemically synthesised by Sigma-Genosys. The oligonucleotides contained 4 tandem copies of the wild type or mutated UTE-1 binding site, flanking by different restriction sites on each end. These later were compatible with the restriction sites of the multiple cloning sites (MCS) of the reporter plasmid (pHISi, pHISi1 or pLacZi).

The oligonucleotides were as followed

Oligonucleotide		Restriction site	Reporter plasmid	Assay
S	5'-AATTC(TGTGGTTTCCG) ₄ T-3'	5' <i>Eco</i> RI and 3' <i>Xba</i> I	pHISi or pHISi-1	1 st screening nutritive selection
AS	5'-CTAGA(CGGAAACCACA) ₄ G-3'			
S	5'-AATTC(TGTGGTTTCCG) ₄ -3'	5' <i>Eco</i> RI and 3' <i>Sal</i> I	pLacZi	2 nd screening β gal activity
AS	5'-TCGA(CGGAAACCACA) ₄ G-3'			
S	5'-AATTC(TGTTAGTTCCG) ₄ -3'	5' <i>Eco</i> RI and 3' <i>Sal</i> I	pLacZi	3 rd screening β gal activity
AS	5'-TCGA(CGGAACTAACA) ₄ G-3'			

Each oligonucleotide was phosphorylated at the 5' end prior to annealisation: 20 pmol of oligonucleotide were incubated with 100 pmol of ATP, 1x buffer “one-phor-all” (Promega) (2.9.4), 5-10 U of T4 polynucleotide Kinase (Promega) to a final volume of 10 μ L. After 45 min at 37°C the sense and antisense strand were mixed together and heated at 90°C for 2 min, following by a slow cooling to RT.

2.3.1.2. Digestion and ligation of plasmid DNA

pHISi and pHISi-1 were digested by *Eco*RI and *Xba* I. pLacZi was digested by *Eco*RI and *Sal* I as described in 2.2.1. The integration of the annealed oligonucleotides within the plasmid were performed by ligation as described in 2.2.2.

2.3.1.3. Analysis of the transformed bacteria by PCR

The presence of the 4xUTE1 oligonucleotide within the target reporter plasmid was tested by PCR. The forward primer was complementary to the 4xUTE1 oligonucleotide and the reverse primers were specific to each reporter vector.

The forward primer was common to the three reporter plasmids and its sequence was 5'-CCGTGTGGTTTCCGTGTGGTTTCCGTGTGG-3'

The reverse primer differed depending on the reporter plasmid used. Their sequence were

5'-GCACTCAACGATTAGCGACCAGCCGGAATG-3' (for pHISi and pHISi) and 5'-AAGGGGGATGTGCTGCAAGGCGATTAAGTC-3' (for pLacZi).

The three primers were dissolved in H₂O at a concentration of 10 pmol/ μ L.

Colonies that had been transformed with the reporter vector, were dissolved in 10 μ L H₂O. 5 μ L was used for PCR reaction as described in 2.2.3. The program used for amplification was as followed:

95°C-5 min, 30 cycles at 95°C-30 sec/59.6°C-1 min/72°C-2 min and a final step at 72°C for 10 min

The positive clones were then sent for sequencing to confirm the presence of insert (Lark Technologies). The primers used for sequencing were as follow:

pHISi: 5'-TTCCCAGTCACGACGTTG-3'

pHISi-1: 5'-ATTATCATGACATTAACC-3'

pLacZi: 5'-GCTACAAAGGACCTAATG-3'

2.3.2. Preparation of the plasmid DNA

2.3.2.1. Preparation of reporter plasmid DNA

The target reporter plasmids of interest were purified as described in 2.2.5.1. Prior to integration into the yeast genome, the target reporter plasmid were digested by *Xho* I (pHISi and pHISi-1) and by *Nco* I (pLacZi) for linearisation using the same condition as described in 2.2.1.2.

2.3.2.2. Preparation of cDNA library plasmid

A premade matchmaker cDNA library from HeLa cells (Clontech #HL4048AH) was purchased. The library composed of cDNA cloned into pACT₂ was initially transformed into *E. coli* BNN132. The library required amplification to provide a sufficient quantity of plasmids for the yeast transformation. The number of clones was determined by spreading serial dilutions of the library onto LB/amp plates. Enough DNA from the library was then diluted into a LB/amp and spread onto LB/amp plates in order to have an even growth of 10.5×10^6 clones, which is the number of clones needed to have a representation of the cDNA library. The growing colonies were collected by scraping the plates into LB/amp containing 25 % (v/v) glycerol (Sigma). Bacteria culture were harvested by centrifugation (3000xg, 15 min) and the plasmid DNA was purified using giga kit (Qiagen) according to the manufacture's protocol.

2.3.3. Transformation of plasmid DNA into yeast

2.3.3.1. Small-scale transformation procedure

The small-scale transformation was used to transform yeast with the target reporter construct that would be integrated into the yeast genome at a specific locus by homologous recombination. It is also used to transform yeast with vector that expressed protein to be tested in the β -galactosidase assay.

A fresh (one to three-week-old) yeast colony was used to inoculate 1 mL of YPDA or appropriate SD medium. The clumps were dispersed by vigorous vortexing for 1 min before transferring the medium into 50 mL YPDA or SDA medium. The culture grows at 30°C for 16-18 h with shaking (250 rpm) to stationary phase ($OD_{600} > 1.5$). The overnight culture was diluted into 300 mL of YPDA or SDA medium to give an OD_{600} of 0.2-0.3. After 3 h incubation at 30°C with shaking (230 rpm) the culture reaches a mid-log phase ($OD_{600} = 0.4-0.6$). Cells were harvested by centrifugation at 1,000 x g for 5 min at RT and the pellet was washed once in sterile TE. After centrifugation (1,000 x g, 5 min, RT) the cell pellet was resuspended in 1.5 mL of freshly prepared, sterile 1xTE/1xLiAc (Sigma). These competent cells should be used within 1 h. 0.1 μ g of DNA (or 1 μ g when doing transformation to integrate a reporter vector into the yeast genome) was mixed with 0.1 mg of herring testes carrier DNA (Clontech). 0.1 mL of yeast competent cells was added to the DNA mix and was mixed by vortexing. 0.6 mL of sterile PEG/LiAc solution (2.9.5.) was added to the mix and the solution was vortexed at high speed for 10 sec. The solution was incubated at 30°C for 30 min with shaking at 200 rpm. 70 μ L DMSO (Sigma) was added to it and mixed by gentle inversion. The cells were then heat-shocked for 15 min at 42°C and were immediately placed on ice for 1-2 min. The cells were collected by centrifugation for 5 sec at 10,000 x g at RT and resuspended in 0.5 mL of sterile TE. 100 μ L of the transformation mix were plated onto appropriate SD media that selected for the desired transformant. In the case of vector integration experiment, the pellet was resuspended in 150 μ L TE and the entire volume was plated out onto one plate. The plates were incubated up side down at 30°C until colonies appeared (2-4 days).

2.3.3.2. Large scale transformation procedure

The large scale transformation procedure was used for the transformation of the cDNA library into yeasts.

The volume of the mid-log phase culture stays the same (300 mL) as for a small-scale transformation. 20 µg of cDNA library plasmid and 2 mg of carrier DNA were added to 1.5 mL competent cells. 6 mL PEG/LiAc was added to the mix and after the incubation period at 37°C, 700 µL of DMSO was gently mix with the solution. The final pellet was resuspend into 7 mL TE and the mix was plated out onto 150 mm petri dishes with appropriate selective media.

2.4. Gene expression determination

RT-PCR and western blot were used in order to determine whether a specific gene mRNA was transcript and translated into protein in different cells.

2.4.1. RT-PCR

2.4.1.1. RNA isolation

Total RNA was isolated from cells using the Rneasy mini kit (Qiagen) according to the manufacturers instruction. Cells were scraped into cold PBS and pelleted down by centrifugation (1,000 x g, 3 min). The pellet was resuspended in 350 µL RLT buffer containing 1 % (v/v) βmercaptoethanol. The lysate was loaded onto a QIAshredder spin column (Qiagen) and centrifuged for 2 min a 1,000 x g. 1 volume of 70 % ethanol was added to the homogenized lysate. The sample was applied to a silica-gel-based minicolumn and centrifuged at 8,000 x g for 15 s. The column was then washed consecutively once with 700 µl buffer RW1 and twice with 500 µL buffer RPE by centrifugation (8,000 x g, 15 s). Total RNA was eluted from the column by centrifugation at 8,000 x g for 1 min with 30 µL H₂O. The concentration of RNA was determined by measuring the absorbance at 260 nm in a spectrophotometer.

2.4.1.2. cDNA synthesis

RNA was first treated for genomic DNA contamination. The reaction consisted of 1 µg RNA in a 10 µL reaction containing 1U DNase (Promega) and 1 µL of DNase buffer. After 30 min incubation at 37°C, the reaction was stopped by addition of 1 µL stop buffer (Promega). The synthesis of cDNA from total RNA was completed using a RNA-dependent DNA polymerase, the Moloney Murine Leukemia Virus reverse transcriptase (M-MLV RT) (Promega). First RNA was mixed with 500nM of random hexamers and heated at 70°C for 5 min and then put on ice for 2 min. 200 U of M-MLV RT, 20 U RNasin (Promega), 250 nM dNTP mix (Promega) 1x reaction buffer (Promega) and H₂O to a final volume of 20 µL was added to the sample. cDNA synthesis occurred for 1h at 42°C. The reaction was stopped by storing the samples at -20°C. cDNA samples for TaqMan experiments were diluted into 80 µL of RNase-free water to give a final concentration of 10 ng/µL.

2.4.1.3. PCR

PCR were performed on cDNA as described in 2.2.3. using the RUNX primers and specific annealing temperature listed Table 2.1.

The program used was as followed:

94°C-5 min, 1 cycle

94°C-30 sec/AT-30 sec/72°C-30 sec, 30 to 35 cycles

72°C for 10 min, 1 cycle

The products of the PCR were resolved by electrophoresis on an 1 % (w/v) agarose gel and visualised by UV detection of incorporated ethidium bromide (Sigma). The DNA products were checked by sequencing (Lark Technologies) using the forward primer of each PCR reaction.

2.4.1.4. TaqMan PCR

Real time PCR (TaqMan) was used in the study of the effect of shRNAi mediated by Baculovirus on RNA level of several genes (LMNA, STAT1, OAS1). Buffer are listed in 2.9.6.

Rat gene	primers		AT	Amplicon size
<i>RUNX1</i>	F	5'-AGGCAAGATGAGCGAGGCGTTG-3'	58.9°C	657 bp
	R	5'-TGAGGGTTAAAGGCAGTGGAGT-3'		
<i>RUNX2</i>	F	5'-GCTCCGGAATGCCTCTGCTGTTAT-3'	59.2°C	590 bp
	R	5'-CACCTGCCTGGCTCTTCTTACTGA-3'		
<i>RUNX3</i>	F	5'-CAGCCAGGCCAGACCCCAATCCA-3'	66.6°C	535 bp
	R	5'-GTCCATGCGGCCCGGTGTGCTCAG-3'		
<i>ACTB</i>	F	5'-AGAGGGAAATCGTGCGTGACA-3'	57°C	453 bp
	R	5'-ACATCTGCTGGAAGGTGGACA-3'		
Human gene	primers			
<i>RUNX1a</i>	F	5'-AGATGTAGGGCTAGAGGGGTGAGG-3'	59.7°C	674 bp
	R	5'-TTGCGGTGGGTTTGTGAAGA-3'		
<i>RUNX1b,c</i>	F	5'-CGCCCCTGTCGCCGTCTGGTA-3'	63.9°C	1079,887 bp
	R	5'-CGATGCCGATGCCCGAGGTGA-3'		
<i>RUNX1d</i>	F	5'-TCGCAGCGTGGTAAAAGAAATCAT -3'	58.5°C	450 bp
	R	5'-AGCCGCTCGGAAAAGGACAAG-3'		
<i>RUNX1f</i>	F	5'-CACTGGCGCTGCAACAAGACC -3'	60.1°C	687 bp
	R	5'-GGGGGAGAAGGGACACGGAGGAAT-3'		
<i>RUNX1g</i>	F	5'-AAGAGGGTGCATTTTCAGGAG-3'	59°C	631 bp
	R	5'-GGTGTACCAGCCCCAAGTG-3'		
<i>RUNX1h</i>	F	5'-ATGCGTATCCCCGTAGATGCCAG-3'	58C	560 bp
	R	5'-TTAAATGTGAGGATACCGAGGCCAG-3'		
<i>RUNX1i</i>	F	5'-CCTTGGCCTGCGTTGGACCTT-3'	59.7°C	2100 bp
	R	5'-GCTTTACGGGGGCCTGACATC-3'		
<i>RUNX1j</i>	F	5'-TTGTTATTCTATTCCAGAATCTCTTCC-3'	58°C	357 bp
	R	5'-TTACGACGGTTTGCAGAGGGG-3'		
<i>RUNX1k</i>	F	5'-ATGGATCCCGGTACACTTTCAATACT-3'	58°C	234 bp
	R	5'-TTGTTATTCTATTCCAGAATCTCTTCC-3'		
<i>RUNX1m</i>	F	5'-TCCAAACCCAGTCAACATCTAATC-3'	58°C	816 bp
	R	5'-CAAGCCCTGCAGTGAATCTCT-3'		
<i>RUNX1n</i>	F	5'-TCAGCAGGCAGGACGAATCA-3'	58°C	248 bp
	R	5'-AGCACTGTGGGTACGAAGGAAATG-3'		
<i>RUNX2*</i>	F	5'-ACCCCAGGCAGGCACAGTCTTC-3'	61.3°C	424,358 bp
	R	5'-CCGGGGTAGGGTGGTGGCAGGTA-3'		
<i>RUNX2**</i>	F	5'-GCTCCGGAATGCCTCTGCTGTTAT-3'	59.2°C	590,417 bp
	R	5'-CACCTGCCTGGCTCTTCTTACTGA-3'		
<i>RUNX3</i>	F	5'- TCCCAGGCCAGAGAAGATGAGTC -3'	58.2°C	563 bp
	R	5'- AGAGGGGGCGGGGATGTTGCTTAT -3'		

Table 2.1. Primers used for amplification of *RUNX* genes by PCR from rat and Human cDNA. F and R: Forward and Reverse primers and AT: Annealing Temperature.

20 ng of cDNA were used per PCR reaction containing 1.25 μ L TaqMan Universal Master Mix (Applied Biosystems) and 0.125 μ L Target Assay Mix or Endogenous Control Assay Mix (Assays-on-Demand, Applied Biosystems) in a total volume of 25 μ L. The reactions were set up into a 96-well Optical Reaction plate which was then covered with ABI Prism Optical Caps (Applied Biosystems). The thermal cycling and the quantifying were performed on the TaqMan ABI Prism 7700 Sequence Detector (Applied Biosystems). The PCR thermal cycling conditions were:

50°C-2 min, 95°C-10 min 1 cycle; 95°C-15 sec, 60°C-1 min, 40 cycles

Reactions were performed in triplicate for each target gene (LMNA, OAS1, STAT1) or endogenous control (18S RNA, GAPDH or ACTB). Amplification of the endogenous control were performed in separated well as the target assay and control assay mixes contained the same TaqMan MGB probes (6-FAM, $\lambda_{\text{max}} = 518\text{nm}$) except for ACTB which contains a VIC probe ($\lambda_{\text{max}} = 546\text{nm}$).

The relative gene expression of a given gene was calculated using a excel program, REST-XL version 2 downloaded from the website www.wzw.tum.de/gene-quantification.

The calculation was based upon the equation:

$$R = E_{\text{Target}}^{(\Delta CT_{\text{Target}})} / E_{\text{Ref}}^{(\Delta CT_{\text{Ref}})}$$

where E_{Target} was the efficiency of target amplification (example :LMNA)

E_{Ref} was the efficiency of reference amplification (i.e. endogenous control, ACTB)

$\Delta CT_{\text{Target}}$ was the difference of CT between the control condition (Example: no treatment) and the treated sample (example: virus treatment) of the target gene (LMNA)

$\Delta CT_{\text{Reference}}$ was the difference of CT between the control condition (Example: no treatment) and the treated sample (example: virus treatment) of the reference gene (ACTB)

CT was the threshold cycle number, *i.e.*, when the fluorescence signal crossed a preset detection threshold.

To determine the efficiency of a given amplification, several TaqMan PCR were performed on samples containing serial dilution of starting cDNA. A standard curve

was constructed by plotting log input cDNA against CT value. The slope of the standard curve gave the efficiency of the reaction using the formula $E=10^{-1/\text{slope}}$

2.4.2. Western Blot

SDS-Polyacrylamide gel electrophoresis (PAGE) was used to separate whole cells or nuclear protein extracts by size, prior to western blotting onto nitrocellulose membranes. The presence of the proteins was detected by immunoblotting with antibodies raised against these proteins. Gel and buffer composition are listed in 2.9.7.

2.4.2.1. Preparation of cell protein extracts

For nuclear cell extract, cells were prepared as described in 2.5.1.1.2. An aliquot of nuclear extract was kept aside for protein determination and the remaining sample was mixed with a 1/3 volume of 4x Loading Buffer and heated for 10 min at 70°C.

For whole cell extracts, cells were resuspended in 2-pellet volumes of RIPA buffer and leave on ice for 10 min. The samples were then centrifuged for 2 min at 16,000 x g. A 5 µL supernatant aliquot was taken for protein assay using BioRad protein assay kit. The remaining supernatant was mixed with a 1/3 volume of 4x Loading Buffer and heated for 10 min at 70°C.

2.4.2.2. Separation of proteins by electrophoresis

Electrophoresis was performed using discontinuous SDS polyacrylamide gel system using the BioRad apparatus. The 10 % (v/v) polyacrylamide resolving gel was first poured up to approximately 1cm below the bottom of the comb. The level of the gel was maintained horizontal with the addition of 100 µL propan-2-ol on the surface of the gel until the gel had set. Propan-2-ol was washed off with water and the gel interface was blotted dry before the addition of the 4 % (v/v) stacking gel layer with a comb to form the wells. Once the gel set, the comb was removed and the wells washed with dH₂O. The gels were fitted in the electrophoresis apparatus and submerged with running buffer. The protein size markers (broad range, New England

Biolabs) and samples were loaded onto the wells. Electrophoresis was performed at 100 V until sufficient separation of the protein marker bands.

2.4.2.3. Protein transfer to Nitrocellulose

The gels were removed from the electrophoresis apparatus and the stacking gel layer was removed. The gels were allowed to equilibrate in transfer buffer for 10 min. Transfer was performed using a wet blotting method according to the Biorad manual's protocol. Proteins were transferred to nitro-cellulose (NC Blotting membrane Protran, Schleicher and Schuell) by horizontal electrophoresis in transfer buffer at 100 V, at 4°C for 1 h.

2.4.2.4. Immunolocalisation of proteins on nitrocellulose membranes

Following transfer, the nitrocellulose membranes were placed in a blocking buffer 30 min at RT. The membranes were washed for 10 min in TBS/T (1x Tris Buffered Saline (TBS) containing 0.1 % (v/v) Monolaurate Polyoxyethylenesorbitan or Tween 20). The membrane were incubated with the antibody raised against the protein of interest at a concentration of 0.1 to 1 µg/mL diluted in antibody binding buffer. The incubation was performed at 4°C overnight. The next day, the membrane was washed for at least 1 h with repeated changes of TBS/T. A species-IgG-specific Horseradish peroxidase (HRP) conjugate antibody (Sigma), specific to the species in which the initial antibody was raised, was then incubated with the membrane for 1h. This antibody was diluted in the same buffer as the first antibody at a concentration of 1:2000. Following incubation the membrane was washed for at least 1 h with repeated changes of TBS/T. The complex protein-primary antibody-HRP conjugated antibody was visualised by autoradiography using ECL Western Blotting Reagent (Amersham). The antibodies used were ACTB (Sigma), FLAG (Sigma), GAPDH (Abcam), JunD (Sigma), LMNA (Serotec), RUNX1 (Active Motif), RUNX2 (Oncogene).

2.5. Studies of protein-DNA interaction

2.5.1. Electrophoretic mobility shift assay (EMSA)

Compositions of buffers are listed in 2.9.8.

2.5.1.1 Protein extraction

2.5.1.1.1 Yeast protein extraction for EMSA

A single colony was incubated in 25 mL of selective medium for 45-50 h at 30°C with vigorous shaking (250 rpm). Cells were harvested by centrifugation (5 min, 1000 x g, 4°C) and the pellet was washed in 15 mL ice cold H₂O. The cell walls were disrupted with 10 U/mL lyticase (Sigma) in 15 mL 67 mM KH₂PO₄, pH 7.4 (Sigma) for 90 min at RT. The cells were collected by centrifugation (5 min, 1000 x g) and they were resuspended in buffer A before being frozen in liquid nitrogen for 5-10 min. Upon thawing at 4°C with shaking, the cells were homogenised using a T25 ultraturax homogeniser with 8 mm shaft diameter (Fisher) (4x20 sec-strokes at 11000 rpm). Cell debris were collected by centrifugation (30 sec, 800 x g, 4°C). The remaining supernatant was centrifuged at 3200 x g for 8 min at 4°C and the pellet, which contained the nuclei, was resuspended in 200-500 µL of Dignam C buffer. The solution was applied to a Qiashredder column (Qiagen) and the column was centrifuged for 2 min at 16,000 x g. The eluate was collected and frozen in aliquot in liquid nitrogen and then stored at -70°C.

2.5.1.1.2. Mammalian nuclear protein extraction

Nuclear extracts were prepared from cells by a protocol modified from Dignam's original protocol (Dignam *et al.*, 1983). Cells were washed twice in 1xPBS and harvested by scrapping into 1xPBS. Cells were centrifuged at 10,000 x g for 45 sec and the pellet was resuspended in 2x pellet volume of Dignam A buffer containing protease and phosphatase inhibitors. The sample was centrifuged (10,000 x g, 30 s) and resuspended into Dignam A buffer and then centrifuged again. The pellet was resuspended into 1x pellet volume of Dignam C buffer containing protease and phosphatase inhibitors and applied on the centre of a QIAshredder column (Qiagen).

The column was centrifuged at 16,000 x g for 30 sec and the eluate containing the nuclear extracts was aliquoted and stored at -70°C.

2.5.1.2. Labelling of the probe

2.5 pmol sense oligonucleotide was radiolabelled at its 5' end with 50 μ Ci [γ -³²]ATP (Amersham) in presence of 10 U T4 polynucleotide kinase (USB) and 1x enzyme buffer in a total volume of 20 μ L. The reaction was carried out at 37°C for 30 min and was ended by addition of 50 μ L TE. The oligonucleotide was separated from the enzyme by phenol extraction: 60 μ L phenol: chloroform: isoamyl alcohol (25: 24:1) (Sigma) was added to the reaction and the sample was centrifuged 2 min at 10,000 x g. The upper phase was collected and mixed with 60 μ L chloroform: isoamyl alcohol (24:1) (Sigma). After centrifugation at 10,000 x g for 2 min, the aqueous phase was applied in the centre of a G25 sepharose column (Amersham), which had been prepared according to the manufacture's protocol, to eliminate the remained unincorporated [γ -³²]ATP. 5 pmol of unlabelled antisense oligonucleotide was added to the eluate (60 μ L) and the oligonucleotides were annealed by incubation at 90°C for 5 min following by cooling down to RT. The probe, which was at a final concentration of 0.04 pmol/ μ L, was stored at -20°C until further use.

The sequence of the oligonucleotides used for the synthesis of the UTE-1 probe was

sense 5'-GGCCTGTGGTTTCCGC-3'

antisense 5'-GCGGAAACCACAGGCC-3'

2.5.1.3. DNA-protein binding reaction and electrophoresis of the complexes

Nuclear extracts (5 to 20 μ g) were mixed with 1 μ g polyIdC (Sigma) to a total volume of 18 μ L. The presence of polyIdC would prevent any non specific DNA binding. The mix was incubated on ice for 10 min and 2 μ L of radiolabelled probe was added. The sample was incubated for a further 20 min on ice to allow oligonucleotide/protein binding to occur. Following the addition of 4 μ L of 6x gel loading buffer, the samples were loaded onto an 8 % (w/v) polyacrylamide gel containing 0.5 % (v/v) TBE. Electrophoresis was carried out at a constant current of 18 mA for 2-3 h in 0.5 % (v/v) TBE. The gel was then dried on 3MM Whatman paper under vacuum for 1 h at 80°C. The radioactive labelled DNA was visualised by

autoradiography at -70°C for varying period of time depending on the activity of the probe using a autoradiography blue sensitive film (Kodak).

Competition EMSA were performed by incubating the nuclear extracts with various excess concentration of non-radiolabelled doublestranded UTE-1 oligonucleotides during the first incubation step. The oligonucleotides used for non specific competition were

AP-1 sense 5'-CGCTTGATGAGTCAGCCGGAA-3'

antisense 5'-TTCCGGCTGACTCATCAAGCG-3'

C/EBP sense 5'-TCCCTTTGTAGTGTTTCCCAACTCA-3'

antisense 5'-TGAGTTGGGAAACACTACAAAGGGA-3'

Supershift EMSA were performed by incubating the nuclear extracts and the probe with 2 µL of antibodies at 4°C 12 h before loading onto the gel.

The antibodies used were RUNX1 C19, SP1 (Santa Cruz Biotechnologies), RUNX2 and RUNX3 (Active Motif).

2.5.2. Chromatin immunoprecipitation assay (ChIP)

The protocol was optimised from the Upstate ChIP assay kit. Buffers compositions are listed in 2.9.9.

1x10⁶ cells were seeded on a 10 cm dish in 10 mL complete medium. 24 h later, 270 µL 37 % (v/v) formaldehyde (Sigma) was added to the medium (final concentration of 1 % (v/v)) and the plates were incubated for 2 to 5 min at 37°C to allow crosslinking between proteins and DNA. Cells were first washed twice with ice cold PBS and then they were scraped in cold PBS containing 1 % (v/v) protease inhibitors cocktail (Sigma) and pelleted by centrifugation at 1,000 x g for 4 min at 4°C. The cells pellet was resuspended in 200 µL of SDS Lysis Buffer and incubated for 10 min on ice. The lysate was sonicated in a sonicated waterbath (U50, Ultrawave Limited) for 3 min, 2 to 5 times. Between each sonication the sample was kept on ice for 1 min. To visualize DNA shearing efficiency, 8 µL 5 M NaCl and 1 µL of RNase cocktail (Ambion) was added to the sample and the crosslinks reverted for 4 h at 65°C. DNA was recovered by phenol/chloroform extraction, as previously described in 2.2.5.3., and 20 µL was run on an 1% (w/v) agarose gel. Otherwise, the sonicated lysate was centrifuged for 10 min at 16,000 x g at 4°C and the cells debris was

discarded. The supernatant was diluted 10 fold in ChIP dilution buffer to a final volume of 2 mL and precleared with 80 μ L of salmon sperm DNA/Protein A agarose for 30 min at 4°C with agitation. The agarose pellet was discarded by brief centrifugation and 3 μ L of appropriate antibody (RUNX1-Active Motif, RUNX2-Oncogene, Notch2-Sigma) was added to the supernatant for an overnight incubation at 4°C. 60 μ L of salmon sperm DNA/Protein A agarose was added to the mix for 1 h at 4°C with rotation. The agarose complex was pelleted by gentle centrifugation (700 x g, 1min) and washed for 4 min on a rotating platform subsequently with 1 mL of buffer LS, HS, LC and finally 2 times with 1x TE. The protein-DNA complexes were eluted from the antibody by addition of 250 μ L elution buffer to the agarose complex. After vortexing briefly and incubating at RT for 15 min with rotation the sample was centrifugated at 16,000 x g. The supernatant was kept and the elution step was repeated. The two eluates were combined and 20 μ L NaCl and 2 μ L RNase cocktail were added before a 4 h incubation step at 65°C. DNA was recovered by phenol chloroform extraction and then purified using a QiaQuick spin column according to manufacture's protocol (Qiagen gel purification kit). DNA was eluted in 30 μ L H₂O and 5 μ L was used for PCR with primers designed to amplify the *TIMP1* minimal promoter:

5'-GTAGGTCTCGAGGGTGGGTGGATGAGTAATGCA-3'

5'-CAAGAAAGCTTCCCAGCTCCGGTCCCTGCTG-3'

The PCR conditions were 94°C 2 min following by 40 cycles at 94°C 30 sec, 58°C 30 sec and 72°C 30 sec and a final extension at 72°C for 7 min.

2.6. Studies of proteins interactions: Immunoprecipitation assay

Immunoprecipitation experiments using FLAG IP kit (Sigma) were carried out in order to investigate potential interaction between RUNX1 or RUNX2 with JunD.

2.6.1 Cells extract preparation

1x10⁶ cos-1 cells were seeded onto 10cm dishes in complete medium the day prior to transfection. A total of 9 μ g of pLNCX-RUNX1-FLAG, pLNCX-RUNX2-FLAG or pCMV2-JunD expression plasmids were transfected into the cells using GeneJuice as

described in 2.7.2.1. After 2 days of incubation at 37°C, cells were washed twice in cold PBS and then scraped into 1 mL IP Lysis Buffer (50 mM Tris-HCl, pH 7.4, 150 mM NaCl, 1 mM EDTA, 1 % (v/v) Triton X-100). The samples were incubated on ice 15 min before recovering the cell lysate by centrifugation at 16,000xg for 10 min at 4°C.

2.6.2. FLAG-protein Immunoprecipitation

40 µL ANTI-FLAG M2 (Sigma) affinity gel per mL of cell lysate, were washed with 10 volumes of wash buffer (0.05M Tris-HCl, pH 7.4, 150 mM NaCl) and centrifugated (10,600 x g, 5 sec). The washes were repeated 3 times. The cell lysate was then added to the washed resin and the samples were incubated overnight at 4°C on a roller shaker. The next day, non specific bound proteins were eliminated with 3 washes (resuspension of the resin in 500 µL wash buffer following by centrifugation at 10,600 x g-5 sec).

2.6.3. Elution of the FLAG-protein

The proteins bound to the resin were eluted with 100 µL elution buffer (0.1 M glycine, pH 3.5) at RT with gentle shaking for 5 min. The supernatant was recovered by centrifugation at 10,600 x g for 5 sec, diluted in SDS sample buffer and heated for 10 min at 70°C. The samples were ready for loading on SDS-PAGE and immunoblotting using specific antibodies against the proteins of interest.

2.7. Gene Overexpression: Reporter gene assay

2.7.1. Cloning DNA into reporter system

2.7.1.1. Cloning protein sequence from library's positive clones into an expression vector

The insert coding for the protein of interest was extracted from the pACT₂ plasmid by digestion with *Bam*HI and *Bgl*II as described in 2.2.1. The expression vector pSG5

was digested under the same conditions. After 2 h incubation at 37°C, the insert and the linearized pSG5 were viewed on a 1 % (w/v) agarose gel and extracted from the gel using the gel extraction kit (Qiagen) (2.2.5.4). The insert was ligated into the plasmid as described in 2.2.2. The recombinated plasmids were extracted from the bacteria using Hispeed maxiprep (Qiagen) (2.2.5.1.) and used for CAT assay.

2.7.1.2. Cloning of *TIMP1* promoter into pGL2 basic

The minimal human WT or mutated *TIMP1* promoter (-102/+60) DNA fragment was amplified by PCR. 0.3 µg of *TIMP1*-pBLCAT₃ plasmid (WT or Mut) used for CAT reporter gene assay was used as DNA template for PCR reaction (2.2.4.) (Gift from D. Smart, Southampton). Specific primers were designed in order to both recognise the region of interest and insert 2 restriction sites at the end of the amplicon (*Xho*I and *Hind*III in 5' and 3' end respectively). The forward and reverse primer were 5'-GTAGGTCTCGAGGGTGGGTGGATGAGTAATGCA-3' and 5'-CAAGAAGCTTCCCAGCTCCGGTCCCTGCTG-3'

The program for amplification was as followed : 94°C-2 min, 35 cycles at 94°C-1 min/55°C-1 min/72°C-1min and a final step at 72°C for 5 min.

1 µg pGL2 basic plasmid was digested with *Xho*I and *Hind*III as described in 2.2.1. The products of the PCR and the linearized plasmid separated by electrophoresis on a 1 % (w/v) agarose gel, stained with ethidium bromide and visualised under UV light. They were then extracted from the gel using the Qiagen gel extraction kit following the manufacture's protocol (2.2.5.4.)

The PCR product was inserted into the linearised pGL2 basic plasmid by ligation and transformed into *E. coli* HB101 (Promega) as described in 2.2.3. Plasmids were extracted from transformed bacteria as described in 2.2.4. The presence of the insert was checked by *Xho*I/*Hind* III DNA digestion and sequencing (Lark Technologies) using GLprimer1 (Promega).

2.7.2. Transfection

Two different transfection reagents were used depending on the type of cells to be transfected. Effectene (Qiagen) was mainly used to transfect primary cells while

GeneJuice (Novagen) was used to transfect cell lines. Basically, DNA was shuttled into the cells as it formed a positive lipophile complex with polyamines (GeneJuice) or liposaccharide (Effectene)

2.7.2.1. GeneJuice™ transfection

24 h prior transfection 2×10^5 HeLa cells were seeded per 35mm well (6well plate) or 1×10^5 in 17.5 mm well (12 well plate) in 2 mL of complete media in order to have 40-60 % confluency for transfection. 3 μ l of GeneJuice and 100 μ L of serum free medium per μ g of transfected plasmidic DNA were combined and mixed thoroughly by vortexing. After 5 min of incubation at RT, DNA was added to the mix and left for 5-10 min at RT. The solution was then added dropwise to the cells.

2.7.2.2. Effectene™ transfection

5×10^5 rat or human Hepatic Stellate Cells were seeded per 35 mm well in 2 mL complete medium. Cells were incubated for 6-8 days at 37°C, 5 % CO₂ and were transfected with the appropriate expression vector. At this stage cells were 60-80 % confluent.

The day of the transfection, DNA was diluted with buffer EC to a total volume of 150 μ L. 8 μ L Enhancer per μ g of DNA was added to the mix and vortexed for 1 sec. The ratio of DNA to Enhancer had to be constant (1:8). After 2-5 min of incubation at RT 10 μ L Effectene was added to the solution and mixed by 10 sec vortexing. The DNA-effectene complex formation took place during a 10 min incubation at RT. Meanwhile the media in the wells were replaced by 1.5 mL of fresh complete media. 600 μ L complete media was added to the transfection complexes and mixed by pipetting up and down. The solution is then added dropwise to the cells and the dish was gently swirled to ensure uniform distribution of the transfection complexes. In the case of transfection with HeLa or cos 7 cell lines, the cells were plated out the day before at a density of 2×10^5 cells per 35 mm well.

2.7.3. Chloramphenicol acetyl transferase (CAT) assay

2.7.3.1. Protein extraction

48 h post-transfection, cells were washed twice in 1xPBS and scraped into 0.7 mL 1xPBS and collected into an eppendorf. The wells were rinsed with 0.7 mL 1xPBS which was pooled in the previous eppendorf. The cells were collected by centrifugation (10,000 x g, 2 min) and resuspended in 50 μ L 0.25 M Tris buffer pH 7.4 (Sigma). Proteins were extracted by snap freezing the pellet in liquid nitrogen for 1 min, followed by heat shocking at 37°C for 5 min and vortexing for 10 sec. This cycle was repeated three times. The treatment led to a disruption of the cell membranes. The cytoplasmic extract was separated from the cells debris by centrifugation (10,000 x g, 5min) and recovered into a fresh tube. 5 μ L of the extract was removed for protein concentration determination using a Biorad protein determination kit.

2.7.3.2. Enzymatic assay

10 to 20 μ g of proteins were diluted into 50 μ L 0.25 M Tris buffer. The enzymatic activity of the chloramphenicol acetyl transferase present in the 50 μ L protein extract was assessed by adding the substrates, 20 μ L AcetylcoA (Sigma) and 1 μ L 14 C-chloramphenicol, and the buffer, 70 μ L 1M Tris, pH 7.4. The reaction occurred at 37°C for 2 h. After the incubation, 400 μ L ethyl acetate (Sigma) was added to sample, which was vortexed for 30 sec prior to centrifugation at 16,000 x g for 2 min. The ethyl acetate phase was transferred into a new tube. The solvent was evaporated by drying in a vacuum centrifuge for 30 min. The dried pellet was redissolved in 10 μ L ethyl acetate and spotted onto a silica gel 60 F₂₅₄ TLC plate (Merck). Separation of the different radioactive compounds was achieved by immersing the bottom of the TLC plate in a chromatography tank containing 100 mL chloroform:methanol (95:5) (Sigma). The solvent migrated towards the top of the plate by capilarity. The compounds comigrated with the solvent but each one at a different speed due to a difference in molecular weight. The TLC plate was dried at 37°C for a few min and then exposed to a phosphoimager screen overnight. Quantification of the activity of the CAT was achieved by analysing the screen using

a phosphoimager (STORM) and then using an Image Quantifier program to calculate percentage conversion of ^{14}C -chloramphenicol to its acetylated products.

2.7.4. Luciferase reporter gene assay

2.7.4.1. Protein extraction

24-48 h post-transfection, the cells were washed once with PBS and scraped in 800 μL PBS. The cells were collected by centrifugation at 1,000 x g for 5 min and the pellet resuspended in 50-100 μL of passive lysis buffer (Promega) and incubated for 10 min at RT. 5 μL was used to determine protein concentration using Biorad kit and the samples were stored at -20°C until further use.

2.7.4.2. Luciferase assay

The luciferase reporter gene assay was performed according to the manufacturer's protocol (Promega). Briefly, 20 μL of cell lysate was mixed with 100 μL luciferase assay reagent II (Promega) in a luminometer tube by pipetting 2-3 times. The tube was placed into the luminometer (Turner Design Model TD-20/20) which was programmed to perform a 2-sec premeasurement delay following by a 10 sec measurement period. The firefly luciferase activity was then recorded. When measuring the renilla luciferase activity, 100 μL of Stop and Glo reagent was added to the tube and mixed by vortexing rapidly before recording the renilla luciferase activity with the luminometer.

2.7.5. β galactosidase assay

Buffers are listed in 2.9.10.

2.7.5.1 . β galactosidase assay on Colonies

A β -galactosidase assay called colony lift filter assay was performed as a second screening on yeast colonies transformed with the library plasmids, and also on yeast colonies transformed with plasmids extracted from the positive clones of the library.

The fresh colonies (2-4 day growth) were filter lifted with a sterile whatman #5 filter (Fisher). The filter was transferred to a pool of liquid nitrogen, colonies facing up. After the filter had frozen completely, it was removed from the liquid nitrogen and it was allowed to thaw at room temperature. This freeze-thaw cycle lyses the yeast cell wall. The filter was placed, colonies facing up, onto another filter that had been presoaked in buffer Z/X-gal solution. The filters were incubated at RT until colonies turned blue due to the activity of the β -galactosidase, which degraded X-gal into a coloured product.

2.7.5.2. β -galactosidase assay on cell lysates

This method was used for assaying β -galactosidase activity in lysate prepared from cells transfected with β -galactosidase reporter vectors (pSV- β -Galactosidase) and was adapted from the protocol “ β -galactosidase Enzyme Assay System” (Promega). Proteins extraction was performed as described in 2.7.4.1 exempt that the pellet was resuspended in 50 μ L Reporter Lysis Buffer (Promega). After an 15 min incubation at RT, the samples were vortexed for 10-15 sec and centrifuged at 16,000 x g for 2 min at 4°C. The supernatant was transferred into a well of a 96-well plate. 50 μ L of assay buffer was added to the sample, which was then mixed by pipetting. The plate was covered and put in a 37°C incubator for 30 min. The reaction was stopped by addition of 150 μ L 1 M sodium carbonate and the absorbance of the sample was read at 420 nm in a plate reader.

2.8. Gene silencing: baculovirus delivered shRNAi experiments

2.8.1. Construction of recombinant bacmid DNA

2.8.1.1. Cloning of oligonucleotide template into pFIGU plasmid donor

pFIGU was developed by Dr Colin Dolphin (King's College London). It contained an U6 promoter upstream of an *Age*I / *Spe*I cloning site.

65 to 67 nt DNA template oligonucleotides (ODN) were designed to produce short hairpin RNA targeting a 22 nt unique region within the gene of interest. The 22-nt

sequences were BLAST searched using NCBI program against all human sequence deposited in the GenBank databases to confirm that there was no significant homology to genes other than the targets. ODN sequences are listed Table 2.2. DNA was flanking by *Age*I (5'end) and *Spe*I (3'end) (NEB) restriction site and contained an 8 nt loop between two 22 nt complementary sequence. Sense and antisense DNA was chemically synthesized and FPLC purified (Oswell). Equimolar amounts of the two strands were mixed together and annealed by heating for 3 min at 95°C, then cooled to RT in ligase buffer (Promega). pFIGU was digested with *Age*I and *Spe*I at 37°C for 2 h in appropriate buffer (NEB) and gel purified using a gel extraction kit (Qiagen). The double stranded oligonucleodite was integrated into pFIGU by ligation and the new plasmid was transformed into competent DH5 α as previously described in 2.2.2. and 2.2.3 Bacteria were then plated out on selective media containing 50 μ g/mL ampicillin. After amplification of selected bacteria, plasmid was purified by maxiprep (Qiagen) (2.2.5.4.) and the presence of the insert checked by *Msc*I/*Cla*I digestion (NEB) and by sequencing (Lark technologies).

2.8.1.2. Transposition of the recombinant pFIGU plasmid into the bacmid

Containing-bacmid competent *E. Coli* cells, DH10Bac™ (Invitrogen) were thaw on ice. 100 μ L of which were gently mixed with 1 ng recombinant pFIGU and the mix was incubated on ice for 30 min. The mixture was heat-shocked for 45 sec at 42°C and immediately chilled on ice for 2 min. Cells were allowed to recovered in 900 μ L S.O.C for 4 hours at 37°C with gentle shaking. Cells were then plated onto LB plates containing 50 μ g/mL kanamycin, 7 μ g/mL gentamicin, 10 μ g/mL tetracycline, 100 μ g/mL X-gal and 40 μ L/mL IPTG. Plates were then incubated at 37°C for 24 h. Positive white colonies were restreaked on new plates containing 50 μ g/mL kanamycin, 7 μ g/mL gentamicin, 100 μ g/mL X-gal and 40 μ L/mL IPTG and were allowed to grow for another 48 h.

2.8.1.3. Isolation of recombinant Bacmid DNA

A single positive white colony of DH10Bac was inoculated into 2 mL LB medium supplemented with 50 μ g/mL kanamycin and 7 μ g/mL gentamicin. After 12h-growth at 37°C with shaking (250 rpm) cells were harvested by centrifugation at 14,000 x g

LMNA (nt 824-845)
5'-CCGGACTTCCAGAAGAACATCTACCATCGATAGTAGATGTTCTTCTGGAAGTCCTTTTT-3'
5'-CTAGAAAAAGGACTTCCAGAAGAACATCTACTATCGATGGTAGATGTTCTTCTGGAAGT-3'
LMNA mismatch
5'-CCGGACTTgCAGAAGAtCATCTACCATCGATAGTAGATGaTCTTCTGcAAGTCCTTTTT-3'
5'-CTAGAAAAAGGACTTgCAGAAGAtCATCTACTATCGATGGTAGATGaTCTTCTGGAAGT-3'
RUNX2 (nt 857-877) variant a
5'-CCGGACCCTTCCAGACCAGCAGCACATCGATATGCTGCTGGTCTGGAAGGGTCCTTTTT-3'
5'-CTAGAAAAAGGACCCTTCCAGACCAGCAGCATATCGATGTGCTGCTGGTCTGGAAGGT-3'
RUNT (nt 347-368)
5'-CCGGCGCTGCAACAAGACCCTGCCATCGATAGGCAGGGTCTTGTTGCAGCGCCTTTTT-3'
5'-CTAGAAAAAGGCGCTGCAACAAGACCCTGCCTATCGATGGGCAGGGTCTTGTTGCAGCG-3'

Table 2.2. **Sequence of the oligonucleotides (ODN) cloned into pFIGU.** They were designed to produce short hairpin RNA targeting a 21 nucleotide region (nt) within *LMNA*, *RUNX2* or *RUNT* genes (runt homologous domain common to the 3 *RUNX* genes). The underlined sequence corresponded to the *ClaI* site within the loop of the hairpin.

for 1 min. the pellet was resuspended in 0.3 mL solution I (15 mM Tris-HCl pH 8, 10 mM EDTA, 100 µg/mL RNase). The cells were lysed by adding 0.3 mL solution II (0.2 N NaOH, 1 % (v/v) SDS) and incubated at RT for 5 min. The addition of 0.3 mL 3 M potassium acetate precipitated *E. Coli* protein and genomic DNA and the bacmid DNA was separated from the precipitate by centrifugation (10 min, 16,000 x g). Bacmid DNA was precipitated by addition of 0.8 mL absolute isopropanol and centrifugation at 16,000 x g for 15 min. the pellet was washed with 0.5 mL 70% ethanol and centrifuged for 5 min at 16,000 x g. After 10 min air-drying, the pellet was resuspended in 40 µL TE and stored at -20°C. The presence of the bacmid was checked by visualisation on a 0.8 % (w/v) agarose gel by UV detection of incorporated ethidium bromide.

2.8.2. Production of baculovirus particules

2.8.2.1. Transfection of Sf9 cells with recombinant Bacmid: P0 viruses

9×10^5 Sf9 cells were seeded per 35 mm-well in 2 mL of Sf-900 II SFM (Invitrogen) containing antibiotics (50 U/mL penicillin, 50 µg/mL streptomycin) and left for a 1 h at 27°C. 5 µL bacmid DNA and 6 µL CellFECTIN (Invitrogen) reagent were diluted separately into 100 µL Sf-900 II SFM without antibiotics before being mixed together and incubating for 15 to 45 min at RT. 0.8 mL of Sf-900 II SFM without antibiotics was then added to the complex and the mixture was overlaid onto the cells which were previously washed with Sf-900 II SFM without antibiotics. The cells were incubated for 5 h at 27°C before the transfection mixture was removed and replaced with 2 mL Sf-900 SFM (Invitrogen) containing antibiotics. After 72 h, viruses were separated from cell debris by centrifuging the cell supernatant for 5 min at 500 x g. The clarified supernatant containing the viruses (P0) was stored at 4°C and protected from light until further use.

2.8.2.2. Concentration and purification of amplified baculovirus (P1)

5×10^8 Sf 9 were infected with 5×10^6 particules of baculovirus from P0 and cultivated in 500 mL of Sf-900 II medium in a spinner flask. After 5 days of incubation at 27°C the cells were discarded by centrifugation at 5,000 x g for 30 min. The clarified

supernatant was filtered through 0.45 μm filter membrane (Millipore) and 20 mL aliquots were dispatched into 30 mL ultracentrifuge tubes. The supernatant was underlayered with 3 mL of a sucrose cushion (25% (w/w) sucrose dissolved in 5 mM NaCl, 10 mM EDTA) and the tubes were topped up with PBS. After ultracentrifugation at 80,000 \times g for 90 min at 4°C, the supernatant was decanted and the pellet resuspended in 1 mL PBS/FCS (PBS containing 1% (v/v) FCS) and centrifuged for 5 min at 20,800 \times g. The pellet was then resuspended in PBS/FCS and 500 μL aliquots were stored in the dark at 4 °C.

2.8.3. Determination of viral titre: Plaque assay

8×10^5 Sf9 cells were seeded per 35 mm-well in 2 mL of Sf-900 II SFM. Once the cells had attached (1 hour at RT), the supernatant was removed and replaced with 1 mL of 10^{-4} , 10^{-6} , 10^{-8} diluted virus in Sf-900 II SFM. The infection occurred for 1 h at RT in the dark. Meanwhile autoclaved 5% (w/v) low melting point agarose (Novagen) and SF900 II medium were incubated in a 50°C water bath. When the infection period was complete, agarose was diluted 1:5 with the Sf900 media and cooled down to 35°C. The inoculum was completely removed and carefully replaced with 2.5mL diluted agarose, which was allowed to harden for 10 min. The plates were then placed in a box containing wet sterile tissue to ensure a humid environment and incubated for 4-6 days at 27°C.

To stain the cells, 1% agarose (w/v) was dissolved in PBS containing 1 mg/mL MMT (Sigma) and poured onto the overlay.

2.8.4. shRNAi delivery into cells: Infection of cells with recombinant viruses

2×10^5 cells were seeded into 6-well plates in 2 mL complete media. The following day, cells were washed 2 times with serum free media prior to infection. Then, the cells were covered with 400 μL of serum free media containing the recombinant virus for an 1 h at 37°C. The viruses were then discarded by 3 washes with complete media. After 2 to 4 days of incubation at 37 °C the cells were washed 2 times with cold PBS and scraped into 1 mL cold PBS. The samples were halved for protein and RNA extraction and cells were collected by centrifugation at 2,000 \times g at 4°C for 2 min. RNA and protein extraction were performed as described in 2.4.1.1 and

2.4.2.1.respectively. Proteins samples were run on a western blot as described in 2.4.2.2. and RNA samples were used to synthesise cDNA, which was analysed by TaqMan PCR as described in 2.4.1.2 and 2.4.1.4.

2.9. Solutions and media

All chemicals were obtained from Sigma unless otherwise stated

2.9.1. Bacteria and yeast culture

LB (Luria bertani) medium

Tryptone	1 % (w/v)
Bactopeptone	0.5 % (w/v)
Sodium chloride	1 % (w/v)
Adjust to pH 7.0	

1.5 % (w/v) agar was added to the medium for LB agar plates.

Autoclaved.

YPDA

YPDA is YPD containing 0.003 % (w/v) adenine hemisulfate.

YPD Difco peptone	20 g/L
Yeast extract	10 g/L

26.5 g of premade YPD (Clontech) were dissolved per liter of H₂O. 20 g/L agar were added when preparing plates.

After autoclaved medium had cooled to 55°C, 15 mL of a 0.2 % (w/v) adenine hemisulfate solution was added per liter of medium.

SDA

SDA is SD containing 0.003 % (w/v) adenine hemisulfate.

SD

Minimal SD base	6.7 g/L
Dropout solution	0.77 g/L

5 different dropout solutions were used, each one containing all essential amino acid except either leucine, uracile, histidine, leucine and histidine, or uracile and histidine, depending on the selective media wanted.

Adjust to pH 5.8

After autoclaved medium has cooled to 55°C, 15 mL of a 0.2 % (w/v) adenine hemisulfate solution was added per liter of medium.

Adenine hemisulfate

200 mg per 100 mL of dH₂O for a 0.2 %(w/v) solution

2.9.2. Cell culture

Complete medium

Dulbecco Modified Eagle Medium (Gibco)	500 mL
Glutamine (200mM) (Gibco)	50 mL
Sodium Bicarbonate (7.5 %)	250 mL
Fetal Calf Serum (Gibco)	10 % (v/v) (cell line) or 16 % (v/v) (primary HSC)
Penicillin and Streptomycin (Gibco)	2.5x 10 ⁵ U

Hank's Buffered Saline (- or + Ca²⁺) (HBSS)

Obtained as a 10x stock (Gibco)	
HBSS 10x	100 mL
Sodium bicarbonate (7.5%)	4.6 mL
Hepes (1M)	5 mL
Made up to 1 L with sterile water.	

Citric saline (x10)

Potassium chloride	1.35 M
Sodium citrate	0.15M
Autoclave	

2.9.3. General buffers

Agarose gel sample buffer 6x (Promega)

TE	1x
Sucrose	40 % (w/v)
Bromophenol Blue	0.025 % (w/v)

Phosphate buffered saline (PBS)

Sodium chloride	137 mM
Potassium chloride	2.7 mM
Disodium phosphate (Na ₂ HPO ₄)	4.3 mM
Monopotassium phosphate (KH ₂ PO ₄)	1.47 mM

TAE 50x (tris acetate EDTA) electrophoresis buffer

Tris-acetate pH 7.2	2 M
EDTA (ethyl ene diamine tetra acetic acid pH 8.0	0.1 M

TE (tris EDTA)

Tris-HCl pH 8.0	10 mM
EDTA pH 8.0	1 mM

2.9.4. Enzyme buffers

Ligase buffer (10x) (Promega)

Tris-HCl pH 7.8	300 mM
Magnesium chloride	100 mM
DTT	100 mM
ATP	10 mM

Restriction enzyme buffer (Promega)

Multicore buffer (x10)	
tris-acetate pH 7.5	250 mM
potassuim acetate	1 M
magnesium acetate	100 mM
DTT	10 mM

Buffer B (x10)

Tris-HCl	60 mM
MgCl ₂	60 mM
NaCl	500 mM
DTT	10 mM

Taq polymerase buffer x10

Tris-HCl pH8.3	100 mM
KCl	500 mM
MgCl ₂	15 mM
Gelatin	0.01 % (v/v)

2.9.5. Yeast transformation media

PEG/LiAc solution (polyethylene glycol/lithium acetate):

PEG 4000	40 % (w/v)
TE	1x
LiAc	0.1 M

Lithium Acetate

1 M solution	102 g/L in H ₂ O
adjust to pH 7.5 with dilute acetic acid and autoclave	

2.9.6. TaqMan PCR

TaqMan PCR master mix (x2) (Applied Biosystem)

MgCl ₂	5 mM
dATP, dCTP, dGTP, dUTP	200 µM each
AmpliTaq Gold DNA polymerase	0.05 U/µL
AmpErase UNG	0.01 U/µL
Passive reference dye ROX	

Assays-on-Demand (x20) (Applied Biosystem)

TaqMan MGB probe	5 µM
Forward primers	18 µM
Reverse primers	18 µM

2.9.7. Sodium Dodecyl Sulphate Polyacrylamide Gel Electrophoresis and Western Blotting

RIPA buffer

Tris-HCl pH 7.4	50 mM
Tergitol (NP-40)	1 % (v/v)
Na-deoxycholate	0.25 % (v/v)
NaCl	150 mM
EDTA	1 mM

SDS Sample Buffer

Tris-HCl 0.5M pH 6.8	12.5 % (v/v)
Glycerol	10 % (v/v)
Sodium Lauryl Sulphate (SDS)	2 % (w/v)
Bromo Phenol Blue	0.004 % (w/v)
DTT	10 mM

SDS PAGE 5X Electrophoresis Buffer

Tris Base	124 mM
Glycine	1 M
SDS	173 mM

Volume adjusted with distilled water, pH 8.3 do not adjust

SDS PAGE 4 % Stacking Gel

Tris-HCl pH 6.8	375 mM
SDS	3.5 mM
Acrylamide-Bis 37:1(Promega)	4.0 % (w/v)
APS	0.1 % (w/v)
TEMED	0.1 % (v/v)

SDS PAGE 10 % Resolving Gel

Tris-HCl pH 8.8	375 mM
SDS	3.5 mM
Acrylamide-Bis 37:1 (Promega)	7.5 % (w/v)
APS	0.05 % (w/v)
TEMED	0.1% (v/v)

Transfer Buffer (Western)

Tris-Base	25 mM
Glycine	192 mM
Methanol (BDH)	20 % (v/v)

Adjust volume with distilled water, pH 8.3 do not adjust

Tris Buffer Saline (TBS) X 20

NaCl	4 M
Tris-HCl pH 7.4	0.4 mM

Membrane Blocking Buffer

TBS	1x
Tween 20	0.3 % (v/v)
Skimmed Milk protein (Marvel)	3 % (w/v)

Antibody Binding Buffer

TBS	1x
Tween 20	0.15 % (v/v)
Skimmed Milk protein (Marvel)	0.6 % (w/v)
Bovine Serum Albumin (BSA)	0.6 % (w/v)

2.9.8. EMSA**Buffer A**

NaCl	150 mM
HEPES pH 7.9	10 mM
EDTA	1 mM
AEBSF	1 mM
Tergitol (NP40)	6 % (v/v)

Dignam A

Hepes pH 7.9	10 mM
Magnesium Chloride	1.5 mM
Potassium Chloride	10 mM
DTT	0.5 mM
Tergitol (NP-40)	0.2 % (v/v)

Add 1x Proteinase and phosphatase inhibitors mix just prior to use

Dignam C

Hepes pH 7.9	20 mM
Glycerol	25 % (v/v)
Sodium chloride	0.42 M
Magnesium chloride	1.5 mM
DTT	0.5 mM
EDTA	0.2 mM

Add 1x Proteinase and phosphatase inhibitors mix just prior to use

Proteinase and phosphatase inhibitors mix

Sodium orthovanadate (Na_3VO_4)	1 mM
Sodium fluoride	1 mM
4-(2-aminoethyl)benzenesulfonyl fluoride (AEBSF)	1 mM
aprotinin	2 $\mu\text{g/mL}$

Acrylamide gel non denaturing

Acrylamide-bis 37:1 (Promega)	8 % (w/v)
TBE	0.5x
APS 10 % (w/v)	0.8 % (v/v)
TEMED	0.16 % (w/v)

EMSA gel loading buffer 6x

Tris-HCl	10 mM
Ficol 400	10 % (w/v)
EDTA pH 8.0	50 mM
Xylene Cyanol	0.2 % (w/v)
Orange G	0.2 % (w/v)
Bromophenol Blue	0.2 % (w/v)
Adjust to pH 7.5. Sterilized by filtration	

TBE 5x

Tris-base pH 8.3	0.5 M
Boric acid	0.4 M
EDTA (pH 8)	10 mM

2.9.9. ChIP assay

SDS lysis buffer

SDS	1 % (v/v)
EDTA	10 mM
Tris-HCl pH 8.1	50 mM

ChIP dilution buffer

SDS	0.01 % (v/v)
Triton X-100	1.1 % (v/v)
EDTA	1.2 mM
Tris-HCl pH 8.1	16.7 mM
NaCl	167 mM

Buffer LS (low salt Immune complex wash buffer)

SDS	0.1 % (v/v)
Triton X-100	1 % (v/v)
EDTA	2 mM
Tris-HCl pH 8.1	20 mM
NaCl	150 mM

Buffer HS (High salt Immune complex wash buffer)

SDS	0.1 % (v/v)
Triton X-100	1 % (v/v)
EDTA	2 mM
Tris-HCl pH 8.1	20 mM
NaCl	500 mM

Buffer LC (LiCl Immune complex wash buffer)

LiCl	0.25 M
NP40	1 % (v/v)
deoxycholate	1 % (w/v)
EDTA	1 mM
Tris-HCl pH 8.1	10 mM

Salmon Sperm DNA/Protein A agarose

Protein A agarose (Santa Cruz Biotechnology)	500 μ L
prewashed 5x with TE	
BSA	500 μ g
Salmon Sperm (Stratagene)	20 μ g
TE	up to 1 mL

2.9.10. β galactosidase assay**Z buffer**

Na ₂ HPO ₄ ·7H ₂ O	60 mM
NaH ₂ PO ₄ ·H ₂ O	40 mM
KCl	10 mM
MgSO ₄ ·7H ₂ O	0.1 mM

Adjust to pH 7.0 and autoclave

Z buffer/X-gal solution

Z buffer	100 mL
X-gal solution 50 mg/mL (Promega)	0.668 mL
β -mercaptoethanol	0.27 mL

2x Assay buffer

Na_2HPO_4 pH 7.3	200 mM
MgCl_2	2 mM
β mercaptoethanol	100 mM
ONPG	1.33 mg/ μL

Chapter 3

Isolation of the UTE-1 binding protein

The expression of the *TIMP1* gene is regulated by several proteins (Clark *et al.*, 1997, Smart *et al.*, 2001). Among the factors that bind to the promoter region, an unknown 30 kDa protein had been identified (Trim *et al.*, 2000). This protein binds to a specific sequence upstream of the starting point of transcription (-63 to -53) called UTE-1. The isolation of the UTE-1 binding protein (UTE-1 BP) was carried out using the MATCHMAKER One-Hybrid System (Clontech). The system involved a strain of yeast, called the reporter strain, which was genetically modified as its genome contains a mutated gene conferring auxotrophy for histidine. The wild type gene (*HIS3*), under the control of the UTE-1 element, was introduced into the genome by homologous recombination and the yeast lost its auxotrophy for histidine only when the UTE-1 BP had activated the transcription of the *HIS3* gene. Considering the fact that the yeast did not synthesise an endogenous UTE-1 BP, the activation factor was introduced to the yeast via a cDNA library. The proteins coded in the library were fused with a target-independent activation domain that was recognised by the yeast transcription machinery. The clone that synthesised the UTE-1 BP was selected by growing the transformed yeast on medium lacking histidine.

To conduct the assay, the UTE-1 sequence had to be cloned upstream of the reporter gene *HIS3* in a plasmid that would be integrated into the genome of the reporter yeast. The latter was transformed with a cDNA library and plated on selective medium. The positive clones were tested using a LacZ reporter system to eliminate any false positive colonies. Finally, DNA binding was confirmed by independent methods, i.e. EMSA and CAT assay.

3.1. Construction of the reporter yeast

3.1.1. Cloning UTE-1 upstream of the reporter genes

pHISi and pHISi-1 contained the *HIS3* gene downstream of a minimal promoter constituted of 2 TATA boxes, and a multiple cloning site where the UTE-1 sequence could be inserted. The two plasmids were constructed using two different backbones and they presented different levels of *HIS3* background expression due to the TATA boxes. Although the UTE-1 sequence was cloned into both vectors and integrated into the yeast genome, only the plasmid that would provide the more stringent condition for the library screening was used.

pLacZi contained the gene encoding for the β -galactosidase enzyme from *E. coli*. The 4xUTE-1 element was inserted upstream of the minimal promoter of the *lacZ* gene and integrated into the yeast along with the HIS3 reporter gene in order to create a dual reporter strain. The latter allowed a double screening of the library as the colonies grown on selective medium were also tested for β -galactosidase activity.

Two antisense oligonucleotides corresponding to 4 tandem copies of the UTE-1 element and flanked by the appropriated restriction sites was synthesised and annealed. They were cloned into the pHISi, pHISi-1 and pLacZi vectors. The presence of the inserts in the plasmids was checked by PCR. One of the PCR primers was specific to the UTE-1 sequence allowing the amplification of a fragment, (374 bp in pHISi and pHISi-1 and 350 bp in pLacZi) only when the insert was cloned (Figure 3.1.). 3 positive clones (one for each plasmid) were sent for sequencing to confirm the presence of the 4x UTE-1 copies.

3.1.2. Integration of the reporter constructs into the yeast

The modified plasmids, containing 4 copies of the UTE-1 element, and called 4UTE1pHISi, 4UTE1pHISi-1, 4UTE1pLacZi were linearized by digestion in the 3' untranslated region immediately following the HIS3 marker (in pHISi and pHISi-1) or within the URA3 marker (of pLacZi). The linearization in these regions increased the efficiency of the homologous recombination at the corresponding locus in the yeast. Furthermore, integration into the mutated *his3* or *ura3* locus of the yeast conferred a *his*⁺ or *ura*⁺ phenotype on the transformants so that they could be selected on the appropriate medium. The background expression of the HIS3 gene was high enough to allow the strain to grow on a medium lacking histidine (SD-his) even if the HIS3 was under control of the 4UTE element. The non-integration of the plasmids into the yeast genome resulted in their lost, as the plasmids did not carry a yeast replication of origin. To create a double reporter strain, 4UTE1pLacZi had to be integrated first into the yeast genome. The transformed strain, which grew on medium lacking uracil (SD-ura), was subsequently transformed with 4UTE1pHISi and the dual strain was selected on SD-his. The sequence of the transformation was critical as the 4UTE1pHISi also carried the selective marker URA3. The yeast strain that had integrated 4UTE1pHISi into its genome already had an *ura*⁺ phenotype preventing the selection of the integrated 4UTE1pLacZi on SD-ura.

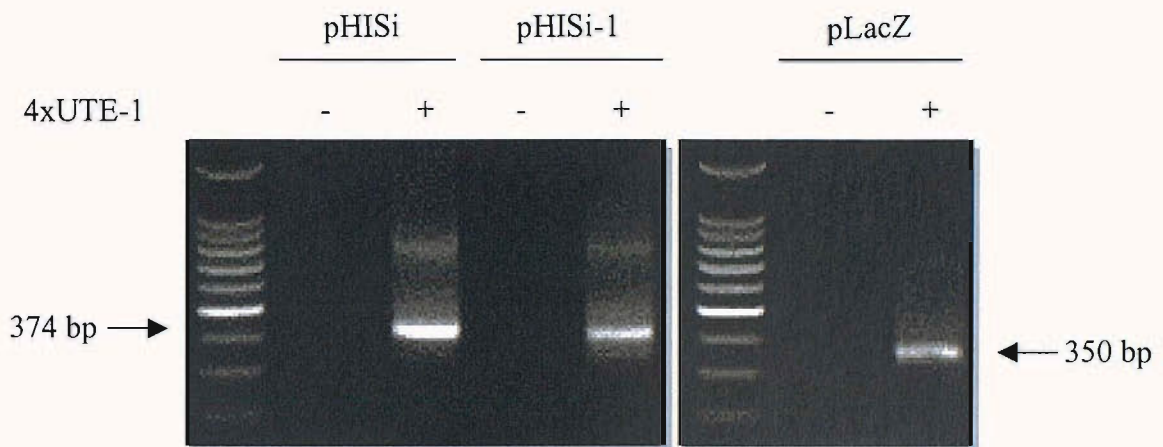


Figure 3.1. **Verification of the presence of 4xUTE-1 insert in pHISi, pHISi-1 and pLacZ by PCR amplification.** *E. coli* DH5 α colonies containing reporter plasmids with (+) or without (-) the 4xUTE-1 element cloned upstream of the reporter gene, were dissolved in 5 μ L H₂O and PCR was performed using one primer complementary to UTE-1 sequence and the other specific to the plasmid (pHISi/pHISi-1 or pLacZi) as described in 2.3.1.3. DNA was separated on a 2 % (w/v) agarose gel at 50 mA and visualised by ethidium bromide staining.

As a negative control, parallel transformation with the related uncut vector was carried out.

The yeast YM4271 was transformed with 4UTE1pLACZ according to the protocol described in 2.3.3.1. After 3-4 day incubation at 30°C, approximately 100 colonies grew on SD-ura plates. One of the colonies was resuspended in SD-ura and grown overnight to be transformed either with 4UTE1pHISi or 4UTE1pHISi-1. After the transformation with linearized 4UTE1pHISi, approximately 200 colonies grew on SD-his plates compared with 7 colonies of the other reporter construct. Interestingly, not only did fewer 4UTE1pHISi-1⁺ colonies develop, but their growth rate was also slower than the other dual strain.

3.1.3. Testing the reporter yeast for background expression

Once the dual reporter strain had been selected, the background expression of the two reporter genes (*HIS3* and *LacZ*) was evaluated in order to see whether the basal and inducible expression would interfere during the screening.

When testing the yeast for expression of the *lacZ* gene using the β -galactosidase assay described in 2.7.5.1., the colonies lift turned blue after several hours. This reflects the activity of the β -galactosidase resulting from a constitutive synthesis of the enzyme. Nevertheless, this could be considered as a low background expression since a high level of background would have resulted in the colonies turning blue within 15 min.

As mentioned earlier, there was a significant amount of constitutive leaky expression of *HIS3*. This was driven by one of the TATA boxes present in the minimal promoter of *HIS3* gene while the other TATA box may have been deactivated by the insertion of the 4x-UTE-1 element.

Although this leaky expression was useful for the selection of the yeast on SD-his, for the construction of the reporter strain, it had to be reduced for the screening of the library. To do so, 3-amino-1, 2, 4-triazole (3-AT), a competitive inhibitor of the *HIS3* gene product (his3p), was incorporated into the medium, at a concentration that inhibited all constitutive his3p. The minimum concentration needed was determined by plating 5 μ L of the dissolved reporter strain in TE, on SD-his plates containing an increasing amount of 3-AT. The condition where no growth was observed was used for the screening of the library.

The growth of 4 dual strains, which had integrated 4UTE1pHISi and 4UTE1pLacZi were tested on SD-his containing 0, 15, 45, 60 mM 3-AT. After 3 days of incubation at 30°C, many colonies appeared in plates with no, or 15 mM 3-AT, and only a few (5-10) appeared on the two highest 3-AT concentrations.

Under the same conditions of growth, the dual strain, which had integrated 4UTE1pHISi-1 and 4UTE1pLacZi, was only growing in the absence of 3-AT.

According to these results, the reporter strain with the pHISi-1 construct had the lower background level of HIS3 expression, and therefore was used for the transformation of the library. Nevertheless, the very slow growth rate of this strain could have resulted from an unhealthy state of the culture and one colony of the other dual strain was preferably chosen for the subsequent experiment even though a higher concentration of 3-AT (at least 45 mM) had to be added to the medium.

The reporter strain that had integrated 4UTE1pHISi and 4UTE1pLacZi into its genome was transformed with a cDNA library. We assumed that the library included cDNA encoding for the putative UTE-1 BP. Before the transformation was performed, preliminary experiments were carried out in order to determine the titre and the quality of the cDNA library.

3.2. Preparation of the library

3.2.1. Verification of the presence of a UTE-1 BP in the HeLa cell line

A HeLa cDNA library compatible with the One-Hybrid System was purchased. A commercial library was selected instead of making a library from HSC since TIMP1 is expressed in various human cell types including HeLa.

Before purchasing the library, the expression of UTE-1 BP in this cell line was verified by EMSA and CAT assay.

3.2.1.1. Presence of UTE-1 BP in HeLa confirmed by EMSA

A nuclear extract of HeLa cells was incubated with a UTE-1 radioactive probe and the mix was run on a non-denaturing polyacrylamide gel. The autoradiogram of the gel in Figure 3.2., showed a slow migration band corresponding to a complex DNA-protein. The UTE-1 specificity of the complex was shown by a competitive reaction as the radioactive complex was competed only by the presence, in the mix of cold UTE-1 probe, but not AP-1 probe. Therefore these results suggested that an UTE-1 BP was present in HeLa nuclear extracts.

3.2.1.2. Presence of a functional UTE-1 BP was determined by CAT assay

The HeLa cells were also transfected with a plasmid containing a reporter gene under the control of the UTE-1 sequence. One, two or four copies of the UTE-1 element had been previously cloned upstream of the gene encoding for the chloramphenicol acetyl transferase (CAT) by Dr J. Trim, Southampton. CAT protein catalysed the transfer of the acetyl group from acetyl coA to the substrate, chloramphenicol. The enzyme reaction could be quantified by incubating cell lysates with [^{14}C] chloramphenicol and following the product formation by physical separation with thin layer chromatography. Figure 3.3. showed that the promoter was not functional when one or two copies of UTE-1 element were present within the regulatory region as the enzymatic activity in the cell extract reflected the level of activity of the promoter. In contrast, 4 copies of the element strongly induced the synthesis of the enzyme shown by a high enzymatic activity of the extract. This experiment suggested that the HeLa cells produced a protein that bound to the UTE-1 sequence and induced the transcription of the reporter gene. Nevertheless, the activational properties of the UTE-1 BP were dependent on the presence of several proteins, as the activity of the reporter gene was only detectable with 4 copies of the element, which allowed the gathering of several proteins within the promoter region. Interestingly, comparable results were previously obtained in similar experiments carried out in rat HSC and 3T3 cells.

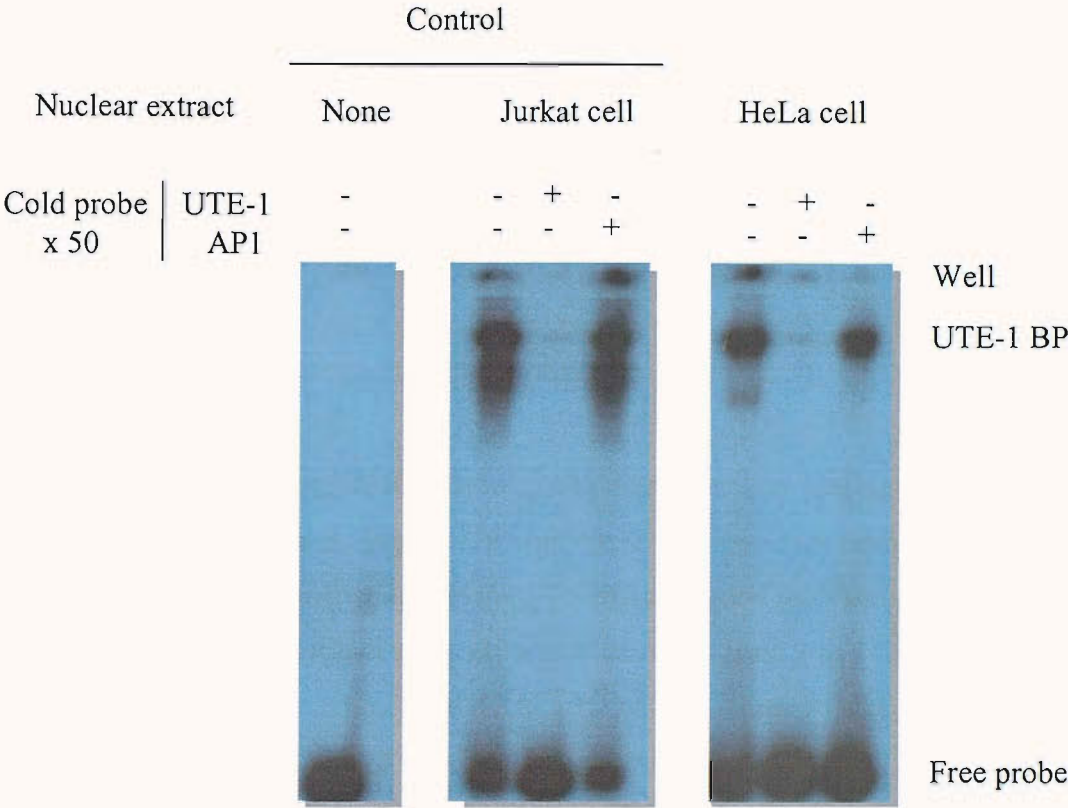


Figure 3.2. **Presence of the UTE-1 BP in HeLa cell line.** 30 µg Hela nuclear extract or 10 µg Jurkat nuclear extract were incubated with UTE-1 radioactive probe in the absence or presence of an 50-fold excess of unlabelled probe (UTE-1) or oligonucleotide that matched the AP-1 binding site. The mix was run on an 8 % (v/v) non denaturing polyacrylamide gel at 18 mA.

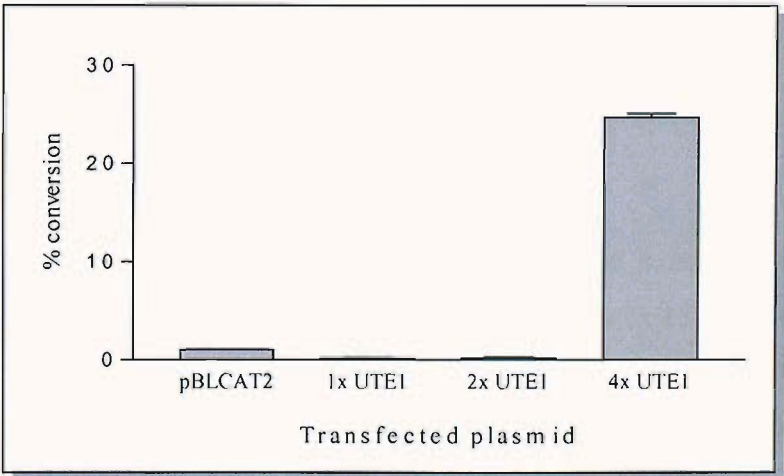


Figure 3.3. **Activation of CAT gene by UTE-1 element.** HeLa cells were transfected with a plasmid containing the CAT gene under control of 1, 2 or 4xUTE-1. CAT activity was mesured as described in 2.7.3.2. The results are expressed as a percentage of substrate conversion relative to the control (pBLCAT2).

The results of the EMSA and CAT assay experiments led to the conclusion that the HeLa cDNA library was suitable for the screening as the cells expressed a UTE-1 BP.

3.2.2. Amplification of the HeLa cDNA library

The HeLa cDNA library had to be amplified to obtain a sufficient amount of plasmid for library screening.

The titre of the library, 2×10^8 cfu/mL, was determined by plating out serial dilution of 10 μ L of the stock library. According to the product certificate, the library contained 3.5×10^6 independent clones. To ensure a good representation of the library during the screening, it had been advised to screen at least 2 to 3 times the number of independent clones. Therefore 52.5 μ L of the library had to be amplified ($3 \times 3.5 \times 10^6 / 2 \times 10^8$). As 15,000 colonies could grow on a 10cm petri dish, $10.5 \times 10^6 / 1.5 \times 10^4 = 700$ LB/amp plates were poured. To ensure that 100 μ L of media was plated out per petri dish 52.5 μ L was diluted in 70 mL of LB. After plating out the library, the 700 plates were incubated at 37°C overnight, and the growing colonies were collected by scraping the plates into LB/amp media containing 25 % (v/v) glycerol. One third of the bacteria culture were harvested and 380 μ g of plasmid DNA was obtained by purification using a Qiagen purification kit.

3.3. Screening of the library

3.3.1. Transformation and result of screening

20 μ g of the DNA library was transformed into the reporter strain according to the protocol described in 2.3.3.2. The cells were plated out onto 15 SD-his-leu plates (150 mm diameter) containing 45 mM 3-AT and incubated for 4 days at 30°C. The efficiency of the transformation was determined by plating out a 1:500 dilution of the cell mix onto a SD-leu plate, that was 4.1×10^4 cfu per μ g DNA.

More than 1,000 clones grew on SD-his-leu medium. The biggest colonies were restreaked on the same medium in order to be tested in the β -galactosidase colony-lift assay. As described in 2.7.5.1., 2 colonies showed a clear positive blue signal,

one within 20 min and one after 8 h, resulting from the activation of the β -galactosidase gene under control of the 4xUTE-1 element. This second screening allowed differentiation of colonies that grew on SD-his-leu due to the background expression of HIS3, from the ones that grew following the activation of the reporter gene via the inducible promoter. This second step was indispensable considering the excessive background growth on the library screening medium. Retrospectively, a higher 3-AT concentration in the medium would have been more suitable for the screening. The plasmids from the two positives clones, called A and B, were extracted and transformed into *E. coli* HB101 as described in 2.2.5.2. for plasmid amplification and extraction.

3.3.2. Analysis of the positive clones

3.3.2.1. Determination of the insert size

E. coli HB101 that had incorporated the plasmid from the positive clones (plasmid A and B) grew on LB/amp plates. Colonies from the two plasmid transformations were resuspended into water and PCR was performed using these aliquots as a source of DNA template. The primers (Clontech) were designed to amplify the region where the cDNA was inserted during the creation of the library. Therefore the amplified fragment contained the insert and the size of the latter could be estimated.

Figure 3.4. showed the results of the PCR reaction on an agarose gel. All the colonies transformed with plasmid B generated an amplified fragment of 1.5 kb (only one is shown here), whereas colonies transformed with plasmid A generated 2 different profiles of amplification. Some colonies had a 2 kb amplified fragment (A/1 and A/3) and some did not show any amplified product (A/2). One explanation was that the PCR reaction did not work properly in every sample. However, extraction of the plasmids from bacterial colonies A/1 and A/2, and digestion with *Bgl*/II, revealed the presence of two plasmids with different sized insert. The original yeast colonies A were not pure but contained 2 clones. Therefore, the DNA mix resulting from the plasmid purification of the yeast clone A contained 2 kind of plasmids. The digestion showed that A/1 contained an insert of 2.5 kb and A/2 a 1.5 kb insert (Figure 3.5.).

These three plasmids may have contained the cDNA sequence of 3 different proteins and further experiments were carried out to check for any false positives.

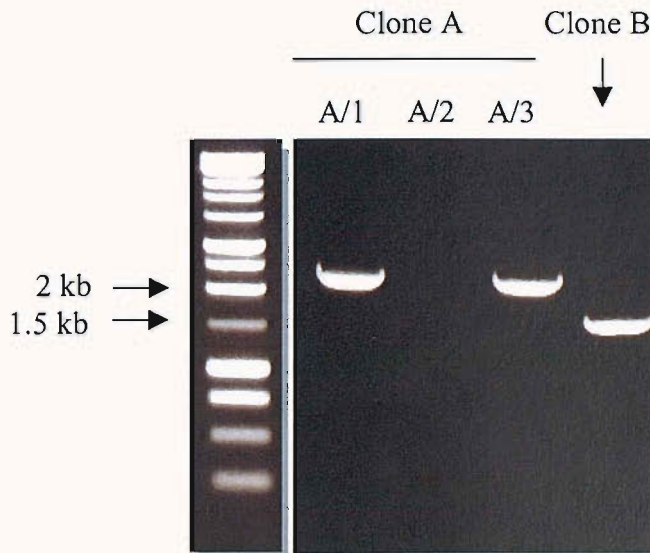


Figure 3.4. **Amplification of the insert present in the his^+ $lacZ^+$ library clones.** Plasmids from the 2 positive clones were extracted and transformed into *E. coli* HB101. PCR was performed directly with bacteria resuspended in H_2O and primers that amplified the region containing the cDNA insert (Clontech). Amplified fragment were visualised on a 1 % (w/v) agarose gel at 50 mA and stained with ethidium bromide.

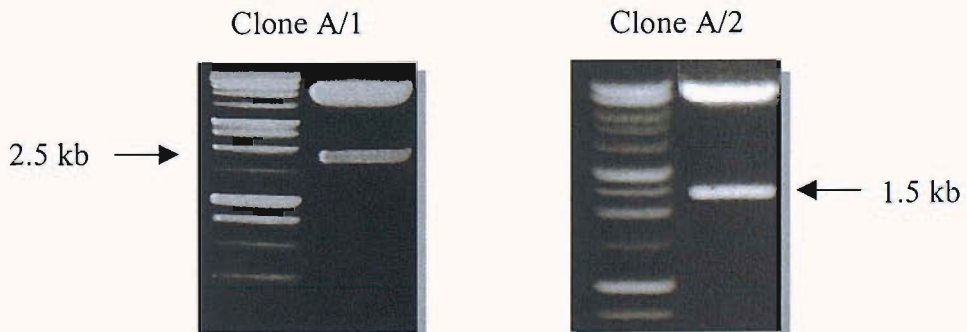


Figure 3.5. **Restriction digest of the plasmid A/1 and A/2.** 1 μg of plasmid was incubated with *Bgl*/II at 37°C for two hours. DNA was separated on a 1% (w/v) agarose gel at 50 mA and visualised by ethidium bromide staining.

3.3.2.2. Selection of the positive clones according to their capacity to bind to the UTE-1 sequence using EMSA

Firstly, the binding properties to UTE-1 sequence were checked by EMSA.

The original yeast YM4271 was transformed with plasmids A/1, A/2 or B. After several days of growth, a protein extract of each transformed yeast was prepared and incubated with a radioactive UTE-1 probe. The mix was run on a non-denaturing polyacrylamide gel and any formation of complex protein-DNA was visualised by autoradiograph (Figure 3.6.).

A protein-DNA complex was formed only with the protein extract of the yeast which synthesised the protein encoded by plasmid A/2. This complex was specific to the UTE-1 sequence as it was not competed by the presence, in excess, of a non specific sequence (C/EBP). These results suggested that the plasmid A/2 was coding for a protein that bound to UTE-1 sequence.

3.3.2.3. Selection of the positive clones according to their capacity to drive *lacZ* transcription using β -galactosidase assay

β -galactosidase assay was also carried out to identify the plasmid that encoded for the UTE-1 BP. Three different yeast reporter strains were transformed with one of the three plasmids A/1, A/2, and B. The strains contained within their genome the *lacZ* gene under the control of either 4 copies of UTE-1, 4 copies of a mutated UTE-1 element, or 3 copies of the p53 binding sequence. The latter was also transformed with a plasmid encoding for the p53 protein as a positive control (pGAD53m) or with the same empty plasmid (pGAD424, encoding only for the GAL4 activation domain) as a negative control. The transformed colonies grew on SD-leu plates for 3 days, to allow the yeast to synthesis the protein encoded for the plasmids, before assaying the activity of the β -galactosidase enzyme. The higher the enzymatic activity was, the stronger the gene activation by regulatory elements.

Figure 3.7. showed the results of the assays. The strongest signal was given by the positive control, and the yeast which had been transformed with the plasmid A/2.

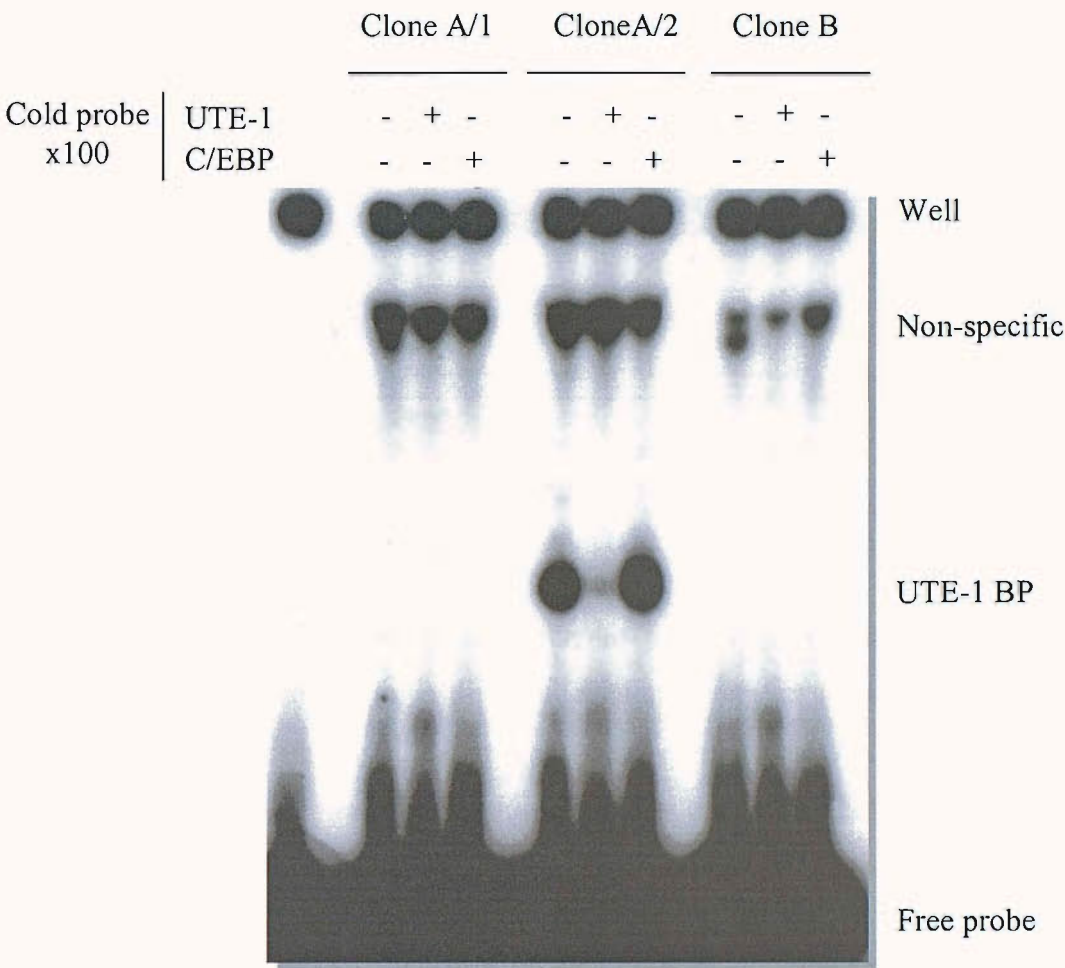


Figure 3.6. **Analysis of positive clone DNA binding activity.** EMSA was performed using 5 μ L protein extract from yeast that were preliminary transformed with plasmid pACT₂ A/1, A/2 or B. The extracts were incubated with UTE-1 radioactive probe in absence or presence of an 100-fold excess of unlabelled probe or oligonucleotide that corresponded to C/EBP binding site. The mix was run on a 8 % (v/v) non denaturing polyacrylamide gel at 18 mA.


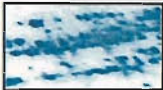

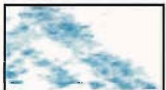







Regulatory sequence	Clone A/1	Clone A/2	Clone B
4xUTE-1			
4xUTE-1 mutated			
3x p53 binding sequence			
Positive control			
Negative control			

Figure 3.7. **β galactosidase assay on different yeast reporter strains.** The *lacZ* gene was under the control of a different regulatory sequence and the yeast was transformed with plasmid pACT2 purified from either clone A/1, A/2 or B. The enzymatic activity was measured by the lift colony assay: The colonies were lifted onto a Whatman paper and soaked with Xgal which was degraded into a blue product by the β -galactosidase.

The two other transformed yeasts gave only a weak signal indicative of background enzymatic activity. The same leaky expression of the enzyme was observed when the *lacZ* gene was under control of the mutated UTE-1 site whatever the plasmid present in the yeast.

This showed that the 3 base pair mutation introduced into the UTE-1 binding site inhibits the binding of the UTE-1 BP and that the enhanced activity observed with the A/2 clone was specific to the UTE-1 sequence. The specificity of the assay was also shown by the fact that no blue signal was observed when the *lacZ* gene was under control of the p53 binding sequence and when the yeast produced any protein but p53.

These assays supported the fact that the protein encoded for the plasmid A/2 was likely to be the UTE1 BP. Two of the three clones were also tested in an *in vitro* reporter gene assay to determine if overexpression of the proteins from the clones would enhanced the activity of the *TIMP1* promoter.

3.3.2.4. Selection of the positive clones according to their capacity to drive *TIMP1* transcription using reporter gene

The inserts A/1 and A/2 were extracted from the pACT₂ plasmid by the appropriate restriction enzymes and cloned into a mammalian expression vector (pSG5) as described in 2.7.1.1. The Cos-1 cell line and rat activated Hepatic Stellate Cells were cotransfected with 0.5µg of the CAT reporter gene, under the control of the *TIMP1* gene, and 1.5 µg expression vector coding for A/1 or A/2 protein. The enzymatic activity of the CAT, which was an indication of the ability of the promoter to induce transcription, was determined following the protocol described in 2.7.5 (Figure 3.8.).

The *TIMP1* promoter was active in both cell types. When the plasmid A/1 was overexpressed, the expression of CAT was not altered relative to the control cells (*TIMP1*). On the other hand, the transfection of plasmid A/2 led to a reduction in CAT expression in Cos-1 cells and activated rat stellate cells. Protein A/2 had a negative effect on the regulation of CAT by the *TIMP1* promoter. An explanation of this surprising result was that the activation of the promoter required the interaction of the UTE-1 BP with other transcription factors, and therefore these partners were a limitant factor in the assay as they had been diluted among the large quantity of the protein A/2.

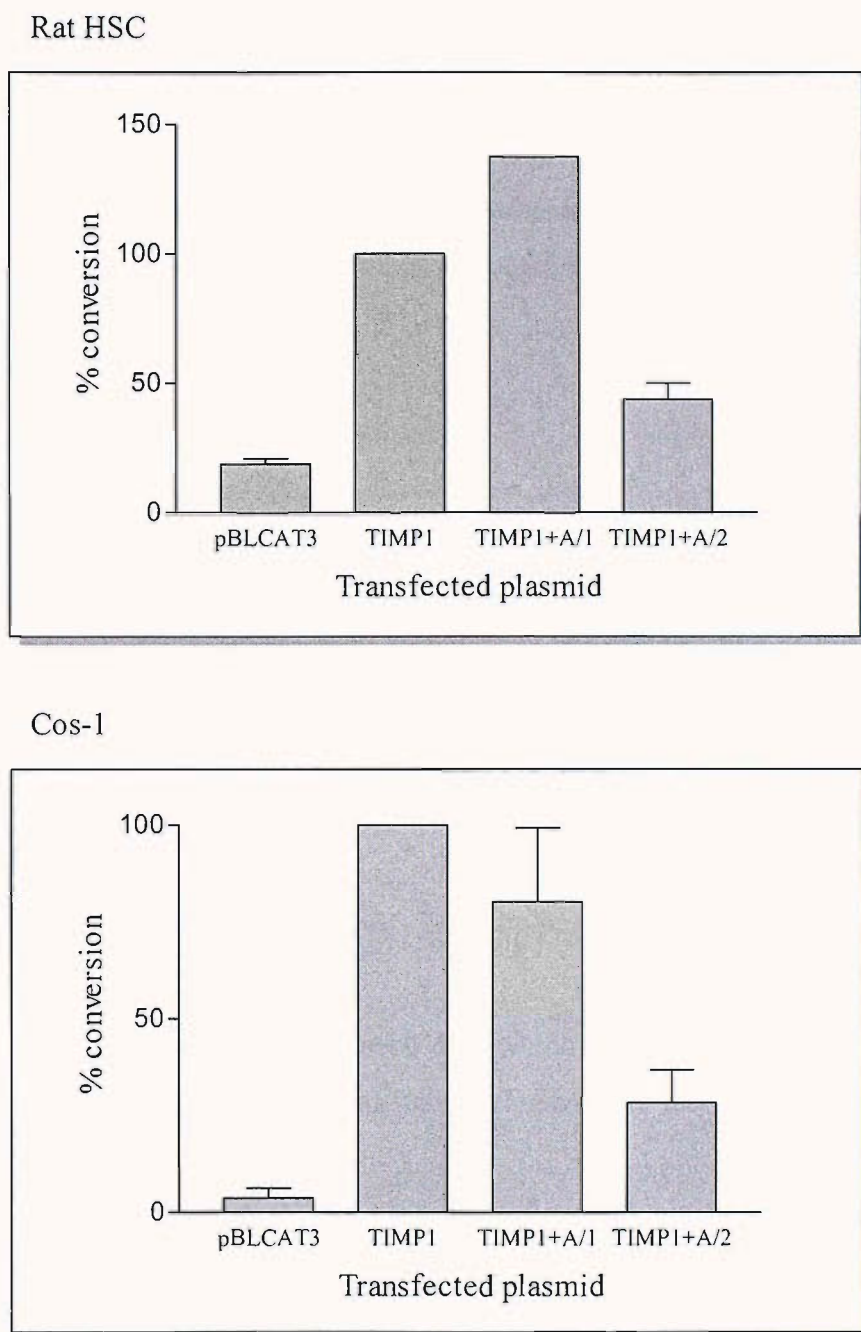


Figure 3.8. **Effect of the overexpression of A/1 and A/2 on the activation of CAT by *TIMP1* promoter.** Rat activated HSC and Cos-1 cells were cotransfected with a plasmid containing the CAT gene under control of *TIMP1* promoter and a plasmid encoding for A/1 or A/2 proteins. CAT activity was measured as described in 2.7.3.2. The results are expressed as a percentage of substrate conversion relative to the control (*TIMP1* alone).

In conclusion, these results confirmed that the protein A/1 was not a protein involved in the activation of the *TIMP1* promoter, but raised the question of the ability of the protein A/2 to activate the *TIMP1* promoter. Although the negative effect on the CAT expression seen with the presence of the protein A/2 did not exclude the latter from being a regulator element of the *TIMP1* promoter. The sequencing of the clone to identify the protein A/2 would give further information that might help to understand this phenomenon.

3.3.3. Sequencing of the positive clones

Whilst the experiments described above were carried out, the 3 clones A/1, A/2 and B were sent for sequencing. The sequences were analysed using an alignment program, BLAST. According to the highest percentage of similarity, clone A/1 coded for a Homo sapiens hypothetical protein FLJ11583 (XM_015726.1), clone A/2 coded for Homo sapiens runt-related transcription factor 1 or RUNX1 (NM_001754) and clone B for Homo sapiens cDNA FLJ11842 (AK_021904).

3.3.4. RUNX1, the sought after UTE-1 Binding Protein?

Along with the experimental approach data which suggested that clone A/2 was the UTE-1 BP, the sequencing data indicated that the clone A/2 encoded for a transcription factor called RUNX1.

According to the literature, RUNX1 is a 52 kDa protein, but several spliced forms are also expressed, among them, a 30 kDa protein, corresponding to the size of UTE-1BP (Levanon *et al.*, 2001). Moreover, the consensus DNA binding sequence of RUNX1 is TGT/CGGT which matches part of the UTE-1 binding site within the *TIMP1* promoter (Meyers *et al.*, 1993). As the UTE-1 binding site was initially identified as an 11 bp element, the shorter RUNX consensus sequence (5-6 bases) might unfortunately have been disregarded during the UTE-1 identification attempt using the bioinformatics tools available at the time of the search.

RUNX1 is considered to be a weak regulator of transcription, but cooperatively activates or represses gene expression with other transcription factors or co-factors (Ito, 1999). This correlates with previous finding in our laboratory suggesting that the UTE-1 BP is unable to function in isolation (Bertrand-Philippe *et al.*, 2004).

Interestingly, with regard to *TIMP1* promoter organisation, which includes adjacent AP-1, ETS and UTE-1 element, RUNX binding sites have also been located next to AP-1 and/or ETS-1 binding site, in several promoters such as the *T cell receptor beta* (TCR β) enhancer as well as the *granulocyte macrophage colony-stimulating factor* (GM-CSF), the *MMP13* and the *B cell-specific tyrosine kinase* (BLK) promoters (Jimenez *et al.*, 1999; Kim *et al.*, 1999; Liu *et al.*, 2004; Cho *et al.*, 2004). Furthermore, cooperation of transcriptional activation of these factors has been reported concurring yet again with our preliminary findings which identified cooperative functionality between UTE-1 and the SRE elements within the *TIMP1* promoter (Kim *et al.*, 1999; Hess *et al.*, 2001; Bertrand-Philippe *et al.*, 2004).

Taken together, these results strongly suggest that the UTE-1 binding protein is RUNX1.

3.4. Conclusion

Within the *TIMP1* promoter region a novel regulatory element was discovered, called UTE-1 which was the binding site for an unknown 30 kDa protein. The characterisation of the UTE-1 binding protein (UTE-1 BP) is an important step towards the understanding of the transcriptional mechanisms responsible for controlling *TIMP1* expression.

The strategy of purification of the UTE-1 BP chosen was the screening of a cDNA library using the One-Hybrid System. The positive clone that was selected after the screening and several verification experiments, encoded for the RUNX1 protein. RUNX1 is part of a family of 3 transcriptional factors, RUNX1, RUNX2, and RUNX3, that regulate different gene involved in hematopoiesis, osteogenesis and neurogenesis respectively (Westendorf and Hiebert, 1999; Ito, 2004).

Although RUNX1 was identified as the UTE-1 binding protein by the One-Hybrid System, RUNX2 and RUNX3 are also potential candidate as they share similar properties (i.e. binding to the same DNA sequence, cooperative functionality with other regulators). Interestingly, although no link between RUNX proteins and *TIMP1* has been identified so far, RUNX2 has already been associated with matrix remodelling accordingly to its key role in bone formation (Stein *et al.*, 2004). For

instance, RUNX2 had been shown to induce MMP13 and type I collagen expression (Ducy *et al.*, 1997; Jimenez *et al.*, 1999).

To further confirm the role of RUNX in *TIMP1* gene regulation in liver fibrosis, the presence and functionality of the RUNX proteins in Hepatic Stellate Cells have to be assessed. This following study might define more precisely which RUNX protein is involved in the regulation of *TIMP1* gene in HSC, as RUNX proteins show a tissue-specific expression pattern in relation with their gene expression regulation specificity (Levanon and Groner, 2004).

Chapter 4

Expression of functional RUNX proteins in Hepatic Stellate Cells

In the first part of this work, the UTE-1 element within the *TIMP1* promoter was identified as a potential RUNX binding site. Consequently, we were interested in the UTE-1 binding factors in Hepatic Stellate Cells. Previous studies revealed the presence of a 30 kDa protein, UTE-1 binding protein, which binds to UTE-1 and which was induced during the activation of the HSC during liver injury (Trim *et al.*, 2000). The hypothesis tested in this chapter was that the UTE-1BP was part of the RUNX family. Therefore, to confirm this idea, the expression of the RUNX protein in HSC was investigated by RT-PCR and Western blot. In addition, their ability to bind to the UTE-1 sequence was studied *in vitro* by EMSA supershift experiments and *in vivo* by ChIP assay.

4.1. RUNX RNA expression

The existing literature mentioned several spliced forms of RUNX1 and RUNX2 (Miyoshi *et al.*, 1995;Levanon *et al.*, 2001;Xiao *et al.*, 1998). The aim of these experiments was to determine which RUNX spliced variant RNA were expressed in human activated HSC. Furthermore, in order to detect any changes in the expression of the RUNX proteins upon activation, as it would be expected for the UTE-1 binding protein, RUNX RNA expression was compared in quiescent and activated rat HSC extracts. Indeed, the relative RNA levels in freshly isolated and activated human HSC could not be compared as the purity of the HSC population after isolation was not as high as that for rat HSC owing to scarcity of starting material.

4.1.1. Preparation of cDNA

Total RNA was extracted as described in 2.4.1.1. To avoid any contamination of genomic DNA, which might have been carried over during the extraction of RNA, RNA was treated with DNase prior to the reverse transcription reaction. DNase is an enzyme that degrades DNA but leaves RNA intact. The elimination of the genomic DNA contamination was checked by PCR using primers specific to *β actin* (*ACTB*) gene, a housekeeping gene present in every cell type. To ensure the integrity of the cDNA synthesised, another PCR was carried out using the same primers but using cDNA as a template in the reaction.

Figure 4.1. showed an example of PCR on a non treated RNA which amplified an ACTB fragment. As the DNA polymerase used in the PCR only amplified the DNA fragment from a DNA template, this attested that genomic DNA was present in RNA samples after the extraction (A.). Following DNase treatment, PCR did not show any amplification of the ACTB fragment suggesting the absence of DNA (B.). Finally, the PCR amplification of the ACTB sequence from the cDNA samples (C.) indicated that the RT-PCR was successful and cDNA could be used for further PCR experiments.

4.1.2. RUNX RNA expression in Human activated HSC

cDNA was generated from total RNA extracted from passaged and several week-cultured (activated) human HSC. PCR was performed on 2 different batches of cDNA using specific primers for *RUNX1*, *RUNX2*, and *RUNX3*.

4.1.2.1. RUNX1 and RUNX2

According to AceView database (NCBI, April 2003), and as listed in Table 1.6., 12 spliced variants of RUNX1, and 3 of RUNX2 had been identified, and are represented in Figure 4.2. PCR primers (*) were designed in order to amplify specifically each variant. As shown in Figure 4.3., 8 RUNX1 mRNA were present in activated human HSC, among them, the main forms RUNX1B (variant a) and RUNX1A (variant f). Only variant d, g, i and j were not expressed in activated human HSC. Some of the other variants expressed do not contain the Runt domain (k, m, n) which suggests an impaired functionality of the potential proteins.

In the case of RUNX2, 2 alternative forms of cDNA, which only differed by one exon of 162 bp (exon 5), were detectable in human HSC. In contrast, the variant that missed the 66 bp exon (exon 5.2) was not detected (Figure 4.3.).

The sequence identities of the cDNA products were confirmed by sequencing.

4.1.2.2. RUNX3

Although 5 types of RUNX3 transcripts have been identified (Bangsow *et al.*, 2001), one pair of PCR primers were initially designed to amplify cDNA corresponding to the 4 main variants. Figure 4.3. showed that RUNX3 cDNA was not expressed at a

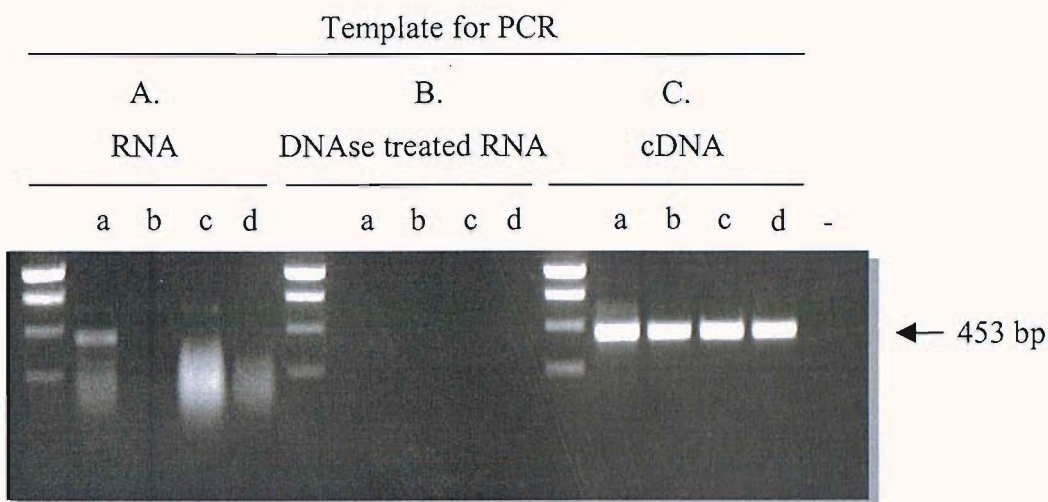


Figure 4.1. **Amplification of ACTB sequence by PCR** on different cDNA (C.) and RNA preincubated (B.) or not (A.) with DNase. PCR products were run on an 1 % (w/v) agarose gel and visualized by ethidium bromide staining. (-) was the PCR negative control (no template). The RNA was extracted from (a) human activated HSC (b) quiescent or (c)/(d) activated rat HSC. PCR was set up for 40 cycles.

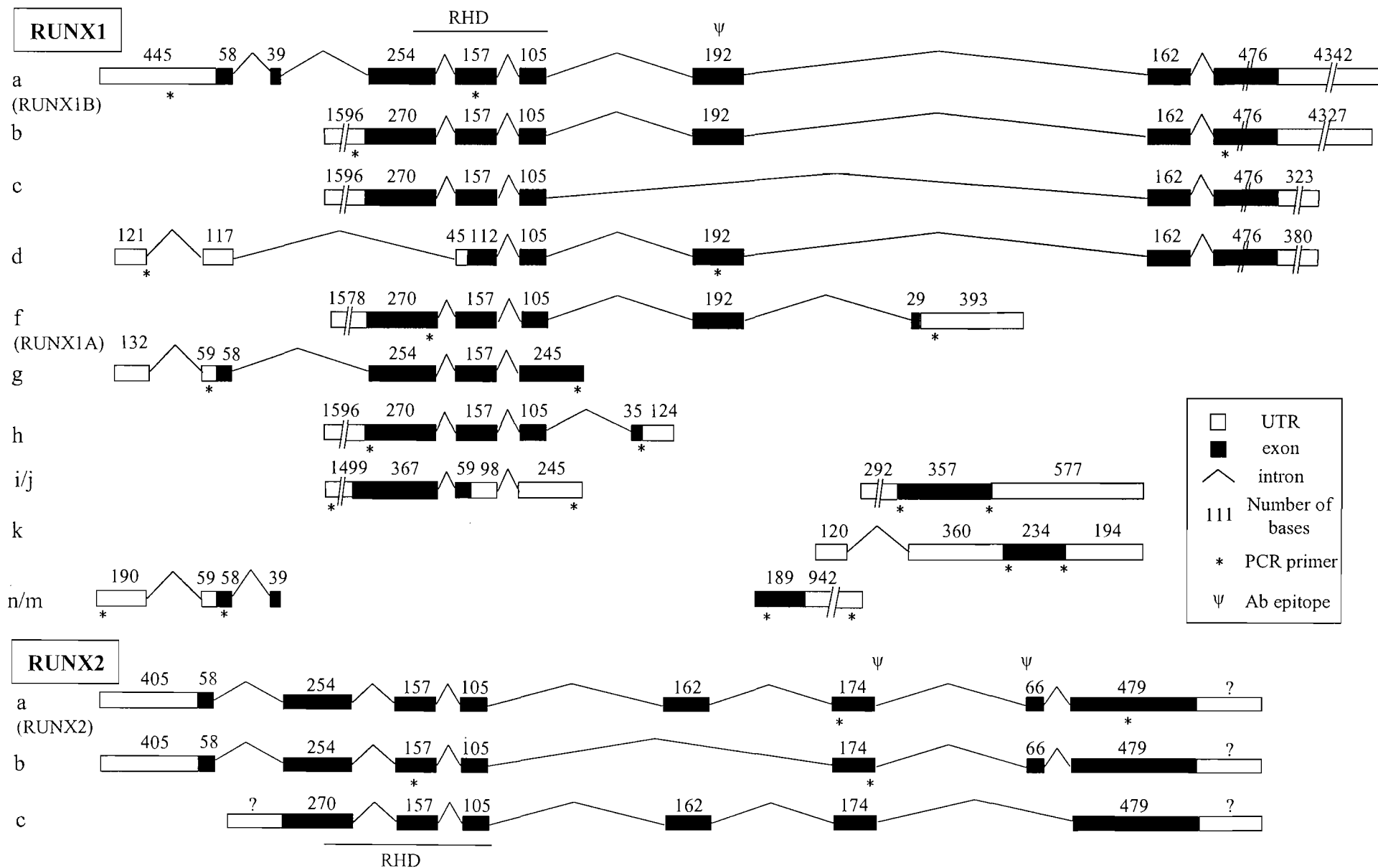


Fig 4.2. Representation of the different alternative splicing variants of RUNX1 and RUNX2 transcripts. Adapted from Aceview Database.

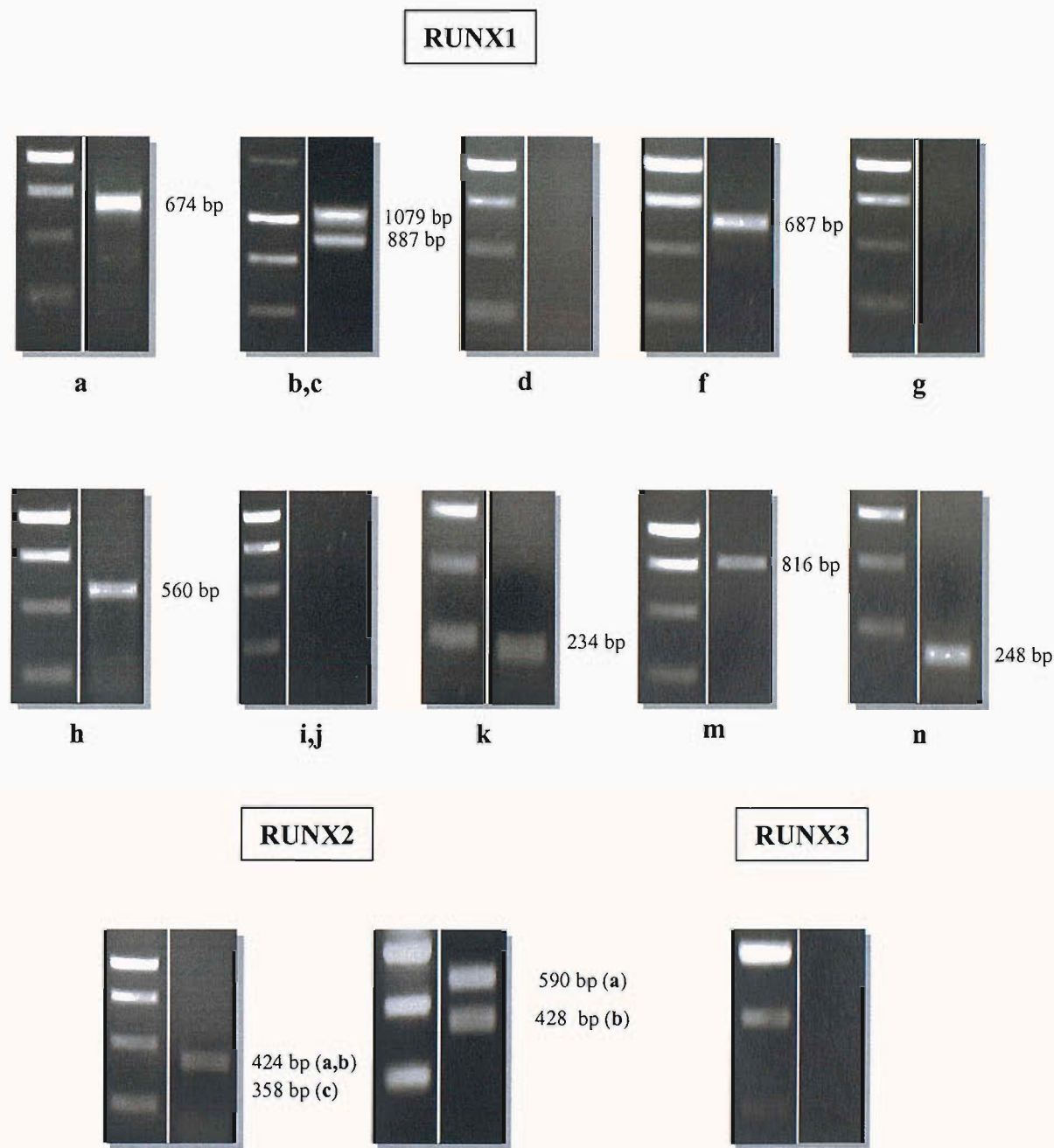


Figure 4.3. **Amplification by PCR of the different RUNX1, RUNX2 and RUNX3 splicing variant cDNA in activated human HSC.** cDNA was synthesised from RNA extracted from activated human HSC and PCR were performed using specific primers for *RUNX1*, *RUNX2* or *RUNX3* genes. Location of the different primers (*) were shown in Figure 4.2. PCR were run for 40 cycles at annealing temperatures listed in Table 2.1. PCR products were run on an 1 % (w/v) agarose gel and visualized by ethidium bromide staining. Gels were representative of PCR performed on 2 different batches of human HSC.

level detectable by PCR in human HSC. No additional investigation was carried out as it was decided it would not have added further critical information.

In conclusion, the main variant forms of RUNX1 and RUNX2 mRNA were expressed in culture-activated human HSC whereas RUNX3 mRNA was not detectable.

4.1.3. RUNX RNA expression in rat HSC

The studies on the regulation of RUNX RNA were possible in rat HSC using the well-established *in vitro* model where freshly isolated cells were plated out onto plastic and cultivated until they become activated. After a week of culture, HSC presented the characteristics of activated myofibroblast-like HSC similar to those observed in fibrotic liver (Friedman, 2000). This model was validated by proteomics analysis which compared the protein alteration profiles of cultured-activated HSC and cells purified from the livers of rats that had undergone an 8 week CCl₄ liver injury study (Kristensen *et al.*, 2000). Therefore, RNA extracted from quiescent (1 day cultured) and activated HSC (7 day cultured) mimic the wound healing process that occurred in fibrotic event. RT-PCR performed on these RNA samples, under the right cycles conditions, monitor the changes that occurred upon activation.

4.1.3.1. Assessment of PCR cycles conditions

Initially, the number of PCR cycles required to amplify sufficient DNA without reaching the plateau of the PCR, i.e. where the difference in the amount of starting cDNA of two samples could not be distinguished as shown on Figure 4.4.a., was established. To do so, PCR with different cycles numbers were run for each gene of interest. Figure 4.4.b. showed that the number of amplification steps needed to remain in the exponential phase was dependent upon the target gene, reflecting not only the variability of amount of each cDNA represented in the extract but also the efficiency of each PCR. 30, 40 and 20 PCR cycles were sufficient to detect RUNX1, RUNX2 and ACTB cDNA respectively without reaching the plateau of the PCR in both quiescent and activated HSC cDNA extracts. Therefore, these conditions were used for the subsequent PCR.

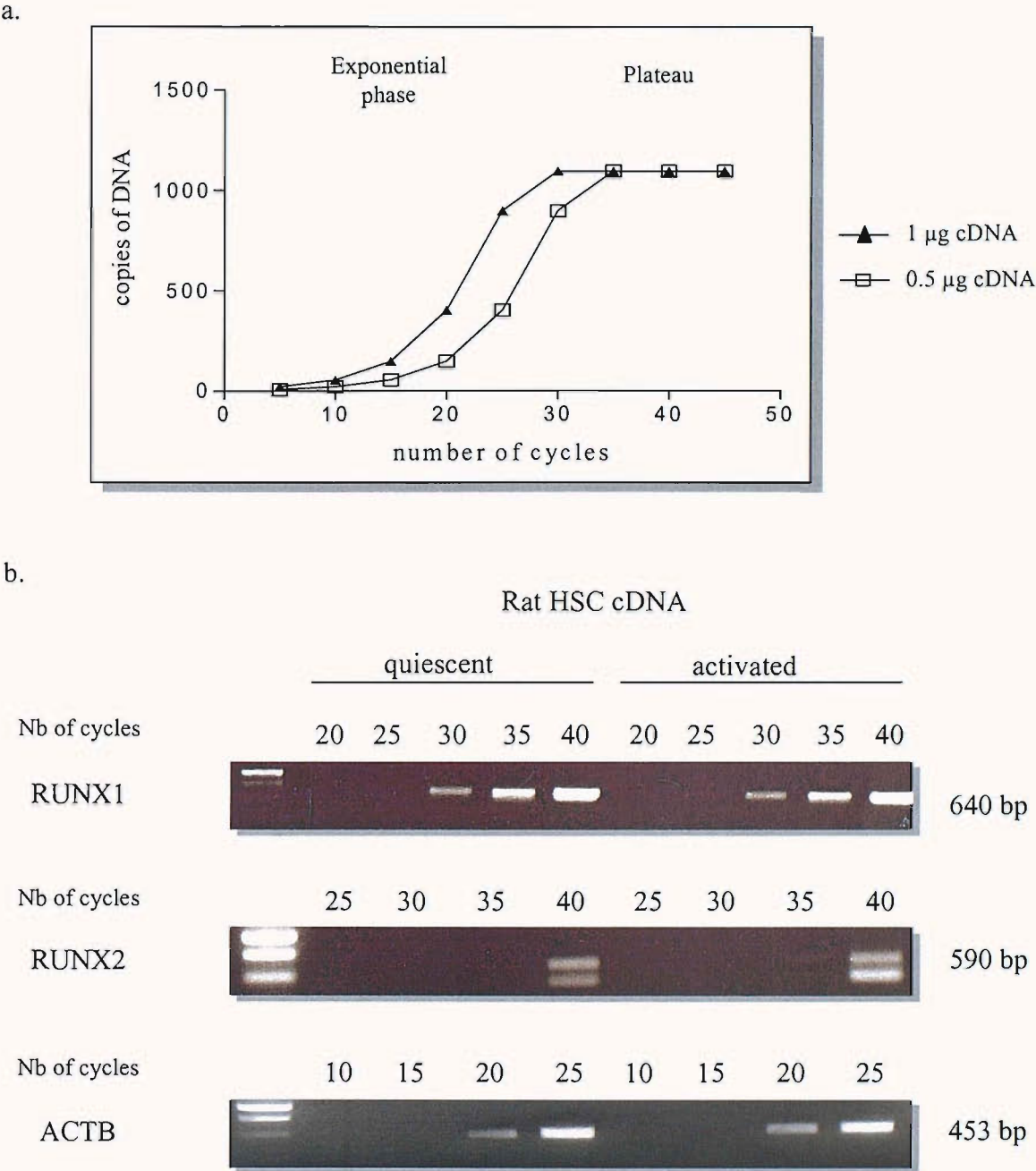


Figure 4.4. a. **Representation of the amount of copies of amplicons per number of cycles during a PCR reaction.** Simulation using 2 different amounts of starting cDNA. b. **Amplification of RUNX1, RUNX2 and ACTB sequence by semi-quantitative PCR.** cDNA was made from RNA extracted from quiescent and activated rat HSC and PCR were performed using specific primers for RUNX1, RUNX2 and ACTB. PCR was stopped at different cycles. Products of the PCR were run on an 1 % (w/v) agarose gel and visualised by ethidium bromide staining.

4.1.3.2. RUNX amplification in rat HSC

PCR was performed on cDNA generated from quiescent and activated HSC RNA using primers specific for *RUNX1*, *RUNX2* and *RUNX3*. PCR products were separated by electrophoresis on an 1 % (w/v) agarose gel stained with ethidium bromide and visualised under UV light. Figure 4.5. showed that the *RUNX1* 640 bp cDNA fragment was amplified by PCR at an identical level in quiescent and activated HSC. The same amplification pattern occurred for *RUNX2* cDNA (590 and 428 bp). These results suggest that the major forms of *RUNX1* and *RUNX2* RNA were consistently expressed in quiescent and activated HSC.

In contrast, a downregulation of *RUNX3* gene expression occurred during *in vitro* activation of HSC. As shown in Figure 4.5. *RUNX3* mRNA was present in quiescent HSC but underwent a drastic decrease upon activation of HSC such that the transcript was undetectable by PCR in activated HSC. These results concurred with the absence of *RUNX3* RNA observed in activated human HSC. The sequence identity of the cDNA products was confirmed by sequencing.

In conclusion, the RT-PCR experiments showed that the main isoforms of *RUNX1* and *RUNX2* mRNA were expressed in rat HSC. Although *RUNX3* mRNA was present in quiescent HSC, its expression was downregulated during culture activation of rat HSC, whereas *RUNX1* and *RUNX2* mRNA expression did not significantly change upon culture induced activation of rat HSC.

RT-PCR experiments were performed on activated human and rat HSC in order to determine the presence and the change in the expression level of RUNX transcripts. The next part of the study was to investigate the presence of RUNX protein in HSC and investigate any post transcriptional regulation.

4.2. RUNX proteins expression

Whole proteins were extracted from quiescent rat HSC and activated rat and human HSC as described in 2.4.2.1. The presence and the regulation of RUNX proteins were studied by immunoblot analysis.

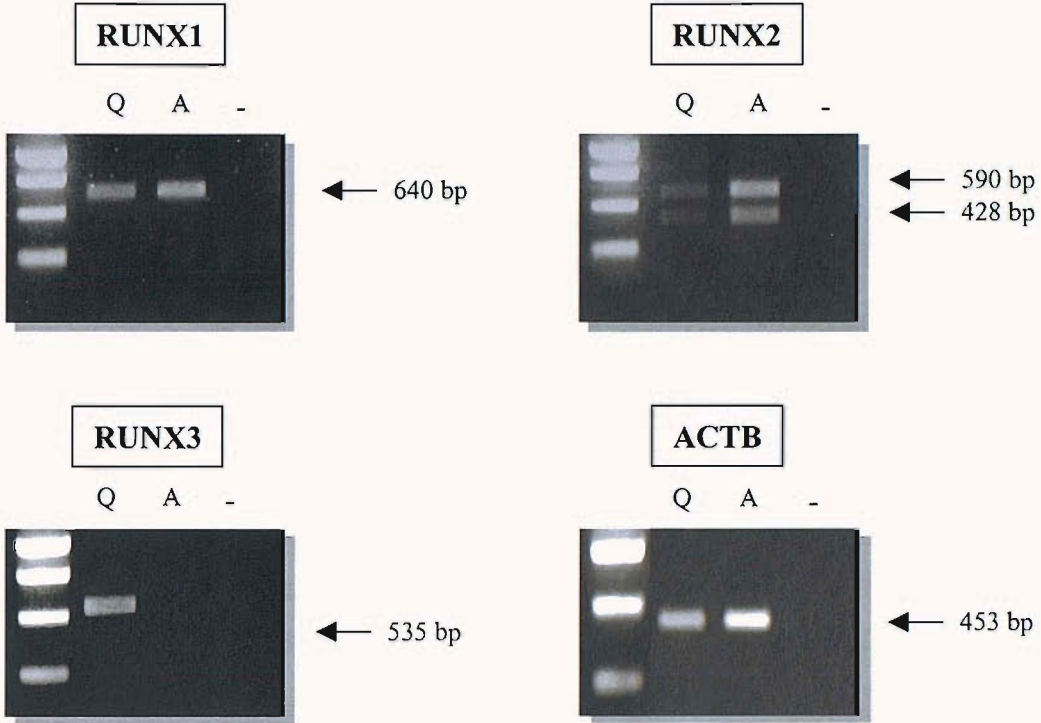


Figure 4.5. **Amplification of RUNX and ACTB sequences by PCR in rat HSC.** cDNA was reversed transcribed from total RNA isolated from quiescent (Q) and activated (A) rat HSC. PCR were performed using specific primers for rat *RUNX1*, *RUNX2* or *RUNX3* genes at annealing temperatures listed in Table 2.1. PCR products were run on an 1 % (w/v) agarose gel and visualized by ethidium bromide staining. (-) represented the reaction negative control (no cDNA template). PCR were run for 30 cycles for RUNX1, 40 cycles for RUNX2 and RUNX3 and 20 cycles for ACTB. The gel was representative of PCR performed on cDNA samples prepared from 2 different rat HSC batches.

4.2.1.RUNX1

The RUNX1 antibody used for the experiment was raised against the amino acids 231-245 which corresponded to the 192 bp exon (ψ on Figure 4.2.). Therefore, only variants a, b, d and f could be detected with this antibody. As shown on Figure 4.6.a., several proteins, in human activated extracts reacted to the anti-RUNX1 antibody. Only the main isoforms of RUNX1, variant a/RUNX1B (52 kDa) and variant b (49 kDa) were expressed. Variant d (38 kDa) and f/RUNX1A (27 kDa) were not detectable although RUNX1A RNA was expressed, suggesting posttranscriptional regulation. In addition, a 64 kDa protein appeared although with a very weak signal, on the immunoblot which did not correspond to any listed variant of RUNX1. However, the high molecular weight of this protein was also observed in Cos-1 cells transfected with a RUNX1B expression vector (Figure 4.6.). This could be explained by posttranslational modifications that might have occurred on RUNX1B such as glycosylation, phosphorylation or acetylation, phenomenon very common in Eukaryotes (Comer and Hart, 2000). As a matter of fact, several studies showed that RUNX1 is subject to phosphorylation and acetylation (Yamaguchi *et al.*, 2004).

In contrast to the mRNA studies, changes in the expression of the RUNX1 proteins were observed upon culture activation of rat HSC. Freshly isolated rat HSC lacked significant RUNX1 protein expression whereas activated HSC expressed three anti-RUNX1 reactive proteins which corresponded to the ones observed in the activated human extract (Figure 4.6.a.).

4.2.2.RUNX2

The RUNX2 antibody was raised against a synthetic peptide matching the amino acid 318-334 of the protein. This corresponds to a region spanned between the 162 bp and 66 bp exons (ψ on Figure 4.2.). Therefore, this antibody would recognise the 2 main variants, a and b, which were the only ones expressed in activated HSC at the RNA level. Human HSC expressed a 30kDa and a 65 kDa protein, recognised by anti-RUNX2, that was also expressed in rat activated HSC (Figure 4.6.b.). The higher molecular weight protein was likely to correspond to full length RUNX2 (variant a), in comparison with RUNX2 transfected Cos-1 cells and according to

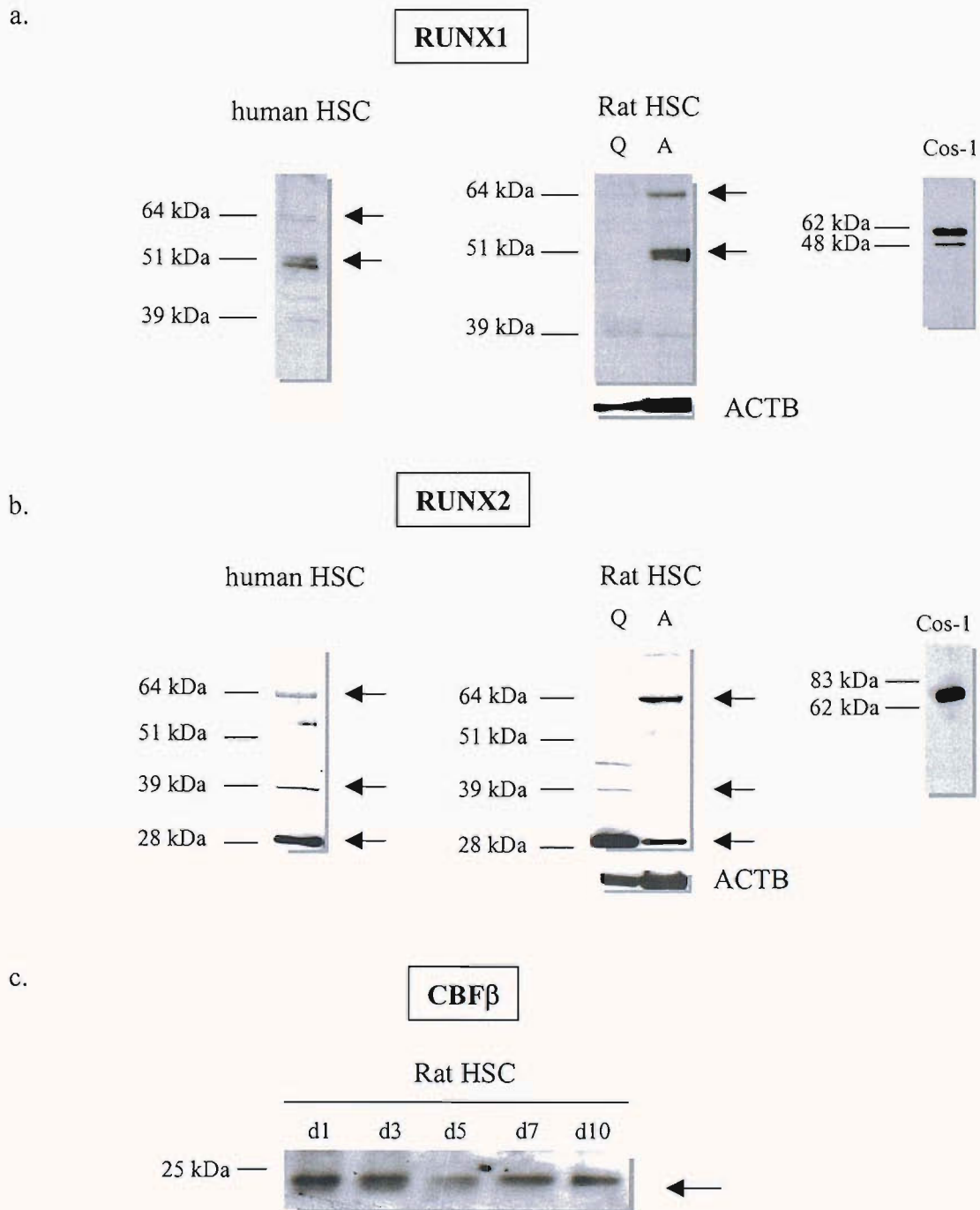


Figure 4.6. **Expression of RUNX proteins in HSC.** Whole cell protein extracts (20 μ g) prepared from freshly isolated quiescent (Q) and activated (A) rat HSC and activated human HSC were used for SDS-PAGE and immunoblot detection of RUNX1 using an anti-RUNX1 antisera (a.) and RUNX2 using an anti-RUNX2 antisera (b.). To control for observed differences between quiescent and activated rat HSC protein extracts were also probed for expression of ACTB. The gels shown were representative of 3 independent experiments.

c. Expression of CBF β in rat HSC nuclear extract over activation of HSC.

previous reports (Prince *et al.*, 2001). Another 40 kDa protein was detected in human HSC, and only weakly in quiescent rat HSC. Strangely, none of the proteins detected by immunoblotting corresponded in size to the predicted spliced forms of RUNX2 listed in Table 1.6. (51 to 57 kDa), although the detection of a 40 kDa protein was mentioned in the antibody datasheet. The presence of a 65 kDa RUNX2 can be explained by posttranslational modifications such as phosphorylation which have also been observed in RUNX2 (Wee *et al.*, 2002; Qiao *et al.*, 2004). In contrast, the 2 other proteins may correspond to new alternative spliced products as new studies have revealed the presence of a new alternative 3'exon in the *Runx2* gene (Terry *et al.*, 2004). As for RUNX1, changes in the RUNX2 expression were observed upon activation in rat HSC. The 65 kDa protein was upregulated whereas the 30 kDa protein was significantly downregulated in activated rat HSC.

4.2.3. RUNX3 and CBF β

As activated HSC did not express RUNX3 mRNA, the protein expression was not investigated. However, the presence of CBF β , protein which enhances RUNX DNA binding affinity by dimerisation with RUNX, was examined during the activation of the rat HSC. Figure 4.6.c. showed that the protein was present in HSC and the level of expression did not change upon activation.

From these data we concluded that HSC express the main isoforms of RUNX1, (RUNX1B) and RUNX2 proteins and that post-transcriptional events occur during HSC activation. However, the DNA binding capacities of RUNX to interact with the UTE-1 sequence still needed to be confirmed. This was achieved using a supershift EMSA experiment and ChIP assay.

4.3. Presence of functional RUNX protein in activated rat and human HSC

4.3.1 RUNX supershift EMSA

Activated rat or human HSC nuclear extracts were incubated with $\gamma^{32}\text{P}$ labelled UTE-1 oligonucleotide probe and antibodies specific for RUNX1, RUNX2 or a non related antibody, as described in 2.5.1. When the antibody interacted with the protein that bound to the UTE-1 probe, it formed a complex that would migrate at a slower rate than the protein-probe complex in a non-denaturing polyacrylamide gel. Figure 4.7. showed that RUNX1 formed a supershift complex with the protein that interacted with the UTE-1 probe in both rat and human activated HSC nuclear extracts. The supershift observed was probably due to the formation of large multimeric complexes that were unable to enter the gel or could result from the disruption of the DNA-interaction by the antibody.

In Contrast a supershift of the UTE-1 DNA-protein complex in the presence of RUNX2 antiserum was only observed in rat HSC. Either RUNX2 did not bind to the UTE-1 element in Human HSC or the antibody was not suitable for supershift experiments as suggested by the weak supershift observed in the rat HSC extract. Another hypothesis was that competition for the binding of the UTE-1 site occurred between RUNX1 and RUNX2, and that in the conditions of the experiment, RUNX1-UTE-1 complexes diluted out RUNX2-UTE-1 complexes to a level undetectable in the supershift assay.

These experiments suggest that rat activated HSC expressed RUNX1 and RUNX2 which were able to interact with the UTE-1 binding site whereas RUNX1 was the only functional protein detectable in the UTE-1 DNA-protein in human activated HSC.

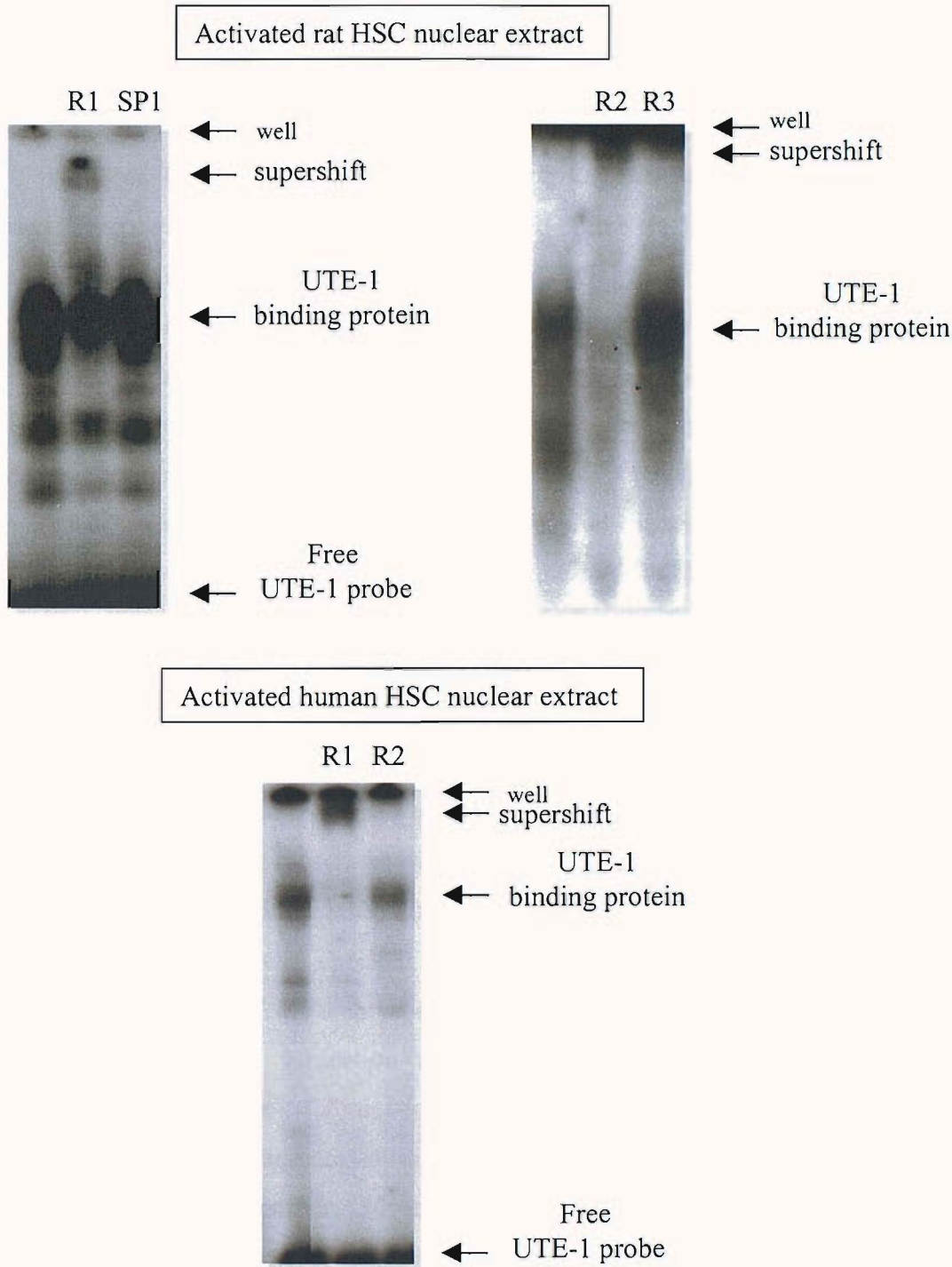


Figure 4.7. **Detection of RUNX1 and RUNX2 in UTE-1 DNA: protein complexes in activated rat and human HSC.** 10 μ g of nuclear extracts of activated rat or human HSC were incubated with 0.2 ng of γ^{32} P labelled UTE-1 oligonucleotide probe. 4 μ g RUNX1 (R1), RUNX2 (R2), RUNX3 (R3) or SP1 supershift antibodies were added to the mix 12 h prior to loading the sample on an 8 % (v/v) non denaturing polyacrylamide gel. The gel was run at 15 mA for approximately 2 hours. The gels were representative of at least two independent experiments.

4.3.2. Binding of RUNX to *TIMP1* promoter *in situ*

We next employed ChIP assays to determine *in situ* binding of RUNX proteins to the *TIMP1* promoter. For these studies a well-characterised human HSC cell line LX2 was used, which we previously confirmed expressed both RUNX1 and RUNX2 main variants (Appendix 2) (Taimr *et al.*, 2003). The cells were first incubated with formaldehyde. This treatment creates covalent links within DNA-protein complexes. Genomic DNA was then sheared by sonication into small fragments (500 bp) and then incubated with the antibody of interest. The antibody-protein-DNA complex was immunoprecipitated and analysed by PCR to identify the DNA fragment which was pulled down with the antibody. Before performing the assay, the sonification conditions were optimised in order to obtain sheared DNA of 500 bp fragment.

4.3.2.1. Sonication optimisation

In this experiment, a consistent number of cells were first treated with formaldehyde for 3 different incubation period (5, 10 or 30 min). Each sample was then sonicated for 2 to 4 sets of 3 min. The crosslinks were reversed prior to recovering the DNA by phenol/chloroform extraction. The size of the sonicated DNA, which was characterized by a smear, was checked by gel electrophoresis as shown on Figure 4.8. When comparing the different conditions tested, we noticed that the DNA became more resistant to sonication with increasing time of crosslinking. For instance, for the same time of sonication (2 x 3 min) the DNA was sheared into mostly 2000 to 1000 bp fragments after 10 min of crosslinking and 500 bp after 5 min of crosslinking. Moreover, 30 min crosslinked DNA was unaffected by sonication treatment. On the other hand, for a given formaldehyde incubation period, expanding the time of sonication did not expand the pool of small range fragments as expected.

According to this experiment the best conditions for preparing LX2 sheared DNA, which were used for the main experiment, was 5 min cross linking followed by 2 x 3 min sonication.

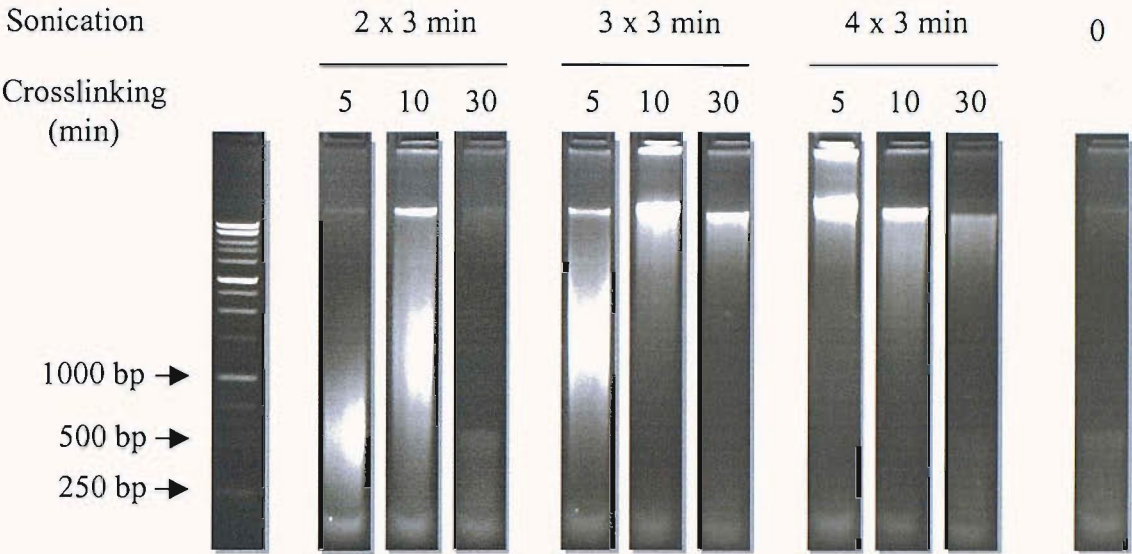


Figure 4.8. **Optimisation of genomic DNA shearing by sonication.** 1×10^6 cells were incubated for 5, 10 or 30 min with 1 % (v/v) formaldehyde which crosslinked protein to DNA. Cells were lysed and genomic DNA sheared with 2, 3 or 4 incubations of 3 min each in a sonicator waterbath. Crosslinks were reversed and DNA recovered by phenol/chloroform extraction. Shearing efficiency was visualized by running DNA on a 1 % (w/v) agarose gel and bromide ethidium staining.

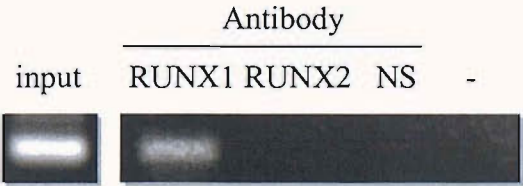


Figure 4.9. **Chromatin immunoprecipitation detection of RUNX1 binding to the *TIMP1* promoter (-102 to +60) in the human HSC cell line LX2.** Input represented PCR carried out on chromatin prior to immunoprecipitation. RUNX1, RUNX2 and NS corresponded to PCR carried out on chromatin following immunoprecipitation with anti-RUNX1, anti-RUNX2 or non-specific antisera (anti-Notch2). The negative control (-) represented a chromatin immunoprecipitation assay carried out in the absence of antibody. The gel shown was representative of 3 independent chromatin immunoprecipitation experiments .

4.3.2.2. RUNX ChIP assay

Three antisera were used to pulldown DNA-protein complexes that were sheared as mentioned above; Anti-RUNX1, anti-RUNX2 and anti-Notch2 sera. The latter was used for a specificity control as Notch2 was known not to bind to the *TIMP1* promoter. PCR was carried out on DNA following immunoprecipitation with the different anti sera using primers which recognised the *TIMP1* minimal promoter. Therefore, the *TIMP1* promoter region was amplified only if the protein that was pulled down with the related antiserum, was initially associated with it.

The results of the PCR demonstrated that RUNX1 was consistently found to be associated with the *TIMP1* promoter (Figure 4.9.). RUNX2 ChIP assays failed to demonstrate any interaction between RUNX2 and the promoter. This was probably due to technical problems related to RUNX2 antibodies, as confirmed by the manufacture's datasheet. Indeed the antibody is not recommended for ChIP assays but this information was not available at the time of the experiment.

4.4. Conclusion

Screening a HeLa library for UTE-1 binding protein revealed that RUNX was a potential candidate. In this study, we assessed the expression of the different spliced variants of RUNX RNA and proteins in human HSC, and monitored the changes of expression of the main variants in cultured rat HSC using RT-PCR and western blots.

RT-PCR analysis identified, in human activated HSC, the expression of the two RUNX1 main spliced variant mRNAs, which are processed from either the P1 (RUNX1B) or the P2 promoter (RUNX1A). In contrast, the two RUNX2 variant mRNAs detected were transcribed exclusively from the P1 promoter, demonstrating a P1 cell-specific activity, as *in vitro* both promoters show transcriptional activity (Ghozi *et al.*, 1996; Drissi *et al.*, 2000). Tissue-specific expression of RUNX2 P1 isoforms have already been identified in osteoblasts and osteosarcoma cell lines (Xiao *et al.*, 1998). This can be explained by the fact that the P2 promoter is specifically nested within a large CpG island, and therefore prone to silencing by hypermethylation (Levanon and Groner, 2004).

Regarding RUNX3 expression, its mRNA was downregulated when rat HSC become activated. This correlates with the absence of RUNX3 mRNA in activated human cells. This tissue and developmental specific expression of RUNX3 was already identified in other tissues. For instance, cortex expression of RUNX3 is downregulated during the development of the thymus, and subsequently its expression in the adult is confined to the medulla (Levanon and Groner, 2004).

In contrast, RUNX1 and RUNX2 mRNA expression did not change upon activation, although immunoblot detection of the proteins revealed quantitative variations, suggesting the occurrence of posttranscriptional and posttranslation regulations. Of interest, a 39 kDa RUNX2 is detected in quiescent HSC, which may coincide with the 35 kDa protein that binds to the UTE-1 oligonucleotide in quiescent HSC (Trim *et al.*, 2000).

The role of the different RUNX isoforms in the regulation of *TIMP1* expression in HSC remains to be elucidated. Several studies have described the expression of different RUNX isoforms with opposite effects on promoter activity. RUNX1B and RUNX1A activates and inhibits the TCR β enhancer promoter respectively (Bae *et al.*, 1994; Kim *et al.*, 1999). More recently, Sun *et al.*, (2004) demonstrated that RUNX2 inhibits p21^{CIP1} transcription while its spliced variant, missing exon 5.2., has no effect on the cdk inhibitor expression. Therefore, one tempting hypothesis is that the ratio between RUNX activator/repressor isoforms expressed in HSC dictates the *TIMP1* expression level.

Supershift EMSA experiments confirmed that rat and human activated HSC expressed endogenous RUNX1 that bound to the UTE-1 binding site, whereas functional endogenous RUNX2 was only detectable in rat activated HSC. In addition, ChIP experiments confirmed that RUNX1, but not RUNX2, was associated with the *TIMP1* promoter. These results suggested that, although both RUNX1 and RUNX2 were expressed in HSC, RUNX1 was more likely to bind to the *TIMP1* promoter. However, the role of RUNX2 in *TIMP1* gene regulation could not be utterly excluded as the analysis of RUNX2 functionality was limited by the availability of appropriate antibody. This was confirmed by recent studies that used a new RUNX2 antibody to achieve successful ChIP experiments (Gutierrez *et al.*, 2004; Schroeder *et al.*, 2004).

The level of expression of RUNX proteins is generally low, making their detection difficult in the experiments described above (Ito, 2004). RUNX expression is regulated by different factors including TGF β , FGF and retinoids (Otto *et al.*, 2003). Interestingly, these factors have been implicated in the progression of liver fibrosis (Alcolado *et al.*, 1997). Amongst them, TGF β plays a key role in the pathology of the disease as it upregulates type I collagen and TIMP1 expression while downregulates MMP1 expression leading to an overall accumulation of collagen (Hui and Friedman, 2003). A RUNX binding site has been identified in the *type I collagen* and in the *TIMP1* promoter (Ducy *et al.*, 1997; Bertrand-Philippe *et al.*, 2004). As TGF β regulation on *RUNX* gene expression has been shown to be cell-dependent, it would be interesting to determine whether it enhances the level of RUNX proteins in HSC (Levanon and Groner, 2004).

First of all, the role of RUNX on the *TIMP1* promoter activity needs to be determined in order to characterise which of the RUNX proteins is involved in the upregulation of TIMP1 upon activation of HSC.

Chapter 5

Role of RUNX proteins in *TIMP1* promoter activity

In the previous chapter, we showed that RUNX proteins were expressed in rat and human HSC and that they bound the UTE-1 binding site within the *TIMP1* promoter. However, their role in *TIMP1* gene regulation still had to be assessed. In this study, we wanted to monitor the effects of RUNX1 and RUNX2 on the activity of the *TIMP1* promoter using CAT or luciferase reporter gene assays. Once the experimental conditions were set up and validated, the effect of overexpression of RUNX proteins on *TIMP1* transcription activity was monitored, as well as the influence of RUNX on another activator of the *TIMP1* promoter in HSC, JunD.

5.1. Set up of the reporter gene experiments

Reporter gene assays are regularly used as indicators of transcriptional activity in cells and, for our experiments, we aimed to use a reporter vector containing a reporter gene (CAT or luciferase) under control of the *TIMP1* promoter sequence. This construct would be transferred to the cells along with the expression vectors for specific proteins (RUNX) using chemical transfection reagents. Then, the enzymatic activity of the reporter protein, which was directly related to the activation of the promoter by the overexpressed proteins, would be measured. Therefore, preliminary experiments were carried out which included the cloning of the *TIMP1* minimal promoter into the reporter vector, the optimisation of the transfection conditions, the validation of the expression vectors for RUNX and finally the selection of a valid control for transfection efficiency.

5.1.1. Cloning of the minimal *TIMP1* promoter in pGL2 reporter vector

The human *TIMP1* minimal promoter (-102, +60) had already been cloned upstream of the CAT reporter gene assay (pTIMP1-CAT) and was used in previous experiments (Smart *et al.*, 2001). In addition, the same sequence was then cloned into the pGL2 basic vector, upstream of the Firefly luciferase gene (referred as luciferase gene), as described in 2.7.1.2., in order to carry out luciferase reporter gene assays which are quicker and safer to use, compared to the CAT reporter gene assay.

The presence of the promoter upstream of the luciferase gene was confirmed by sequencing, and the activity of the reporter gene was checked by transfecting increasing amounts of the TIMP1-luciferase reporter gene (pTIMP1-Luc) into HeLa

cells and activated rat HSC (Figure 5.1.). The activity of the luciferase, which was related to the amount of luciferase produced, was monitored according to the manufacture's protocol 24 h post transfection. The transcription of the reporter gene under control of the *TIMP1* promoter increased by 20 fold compared to the basal level of transcription in pGL2 basic. In addition, transfections increasing the amount of pTIMP1-Luc led to an increase in luciferase activity (Figure 5.1.a). These data proved the successful cloning of the *TIMP1* promoter into the reporter vector.

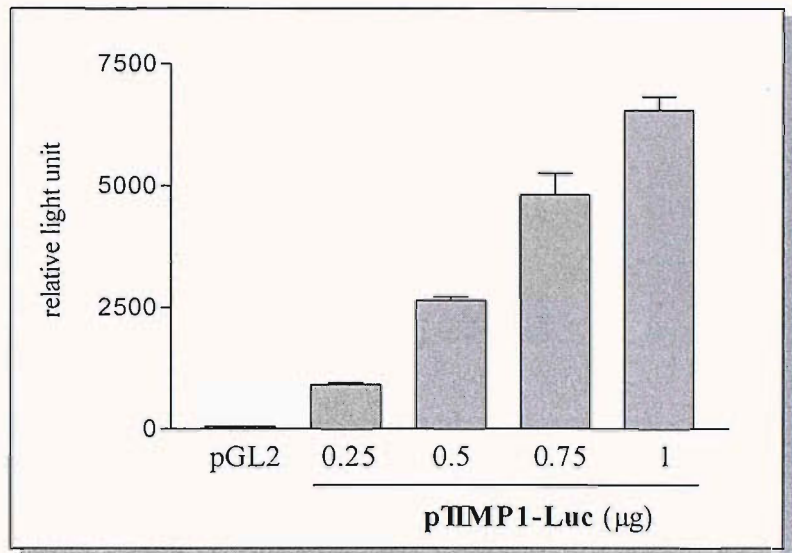
In contrast, the low level of transcription in activated rat HSC, of both pGL2 control, which contained the luciferase gene under control of the strong constitutive promoter SV40, and pTIMP1-Luc, confirmed the poor transfection rate in primary cells already mentioned in previous studies (Gao *et al.* 2001) (Figure 5.1.b.). In the view of these data, it had been chosen to preferably use the CAT reporter gene assay for transfection in HSC. Indeed, the low transfection rate could be overcome by the fact that chloramphenicol acetyl transferase is more stable than luciferase, and therefore the accumulation of the enzyme in the cells would allow the amplification of the enzymatic signal, and consequently offered a better measurement of the enzyme activity.

Nevertheless, the pTIMP1-Luc could be used for reporter gene assay in HeLa, as it was more convenient when doing high numbers of transfections.

5.1.2. Optimisation of transfection

The main reagent used for the transfection of pTIMP1-CAT and expression vectors into cells was effecteneTM. The optimal conditions of use of effectene were determined in 3 different cell types: HeLa, Cos-1 and activated rat HSC. Four concentrations of the pTIMP1-CAT reporter gene were tested (0.25 µg, 0.5 µg and 1 µg) in combination with 3 different ratio DNA:effectene (µg:µL) 1:10, 1:25, and 1:50. The results are shown in Figure 5.2. Among the 3 cells types, activated HSC showed the lowest activity of CAT confirming the difficulty of transfection of these primary cells. Whatever the concentration of the reporter gene transfected the conversion rate was approximately the same, and was never higher than 10 %, whereas this latter could reach 65 % in HeLa or Cos-1. In contrast, the level of activity of the reporter gene in HeLa and Cos-1 increased with increasing amount of

a.

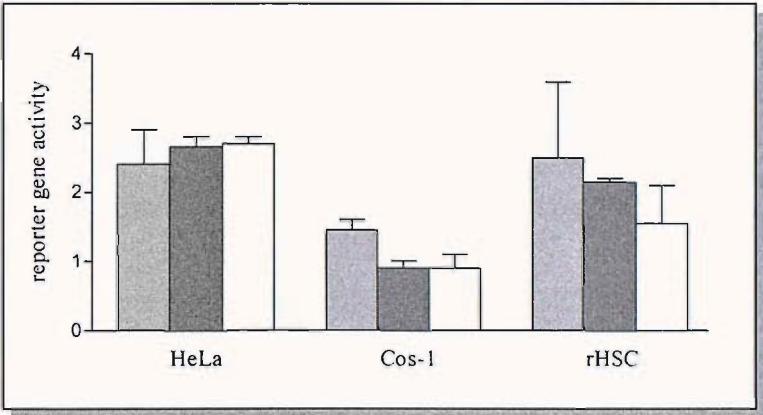


b.

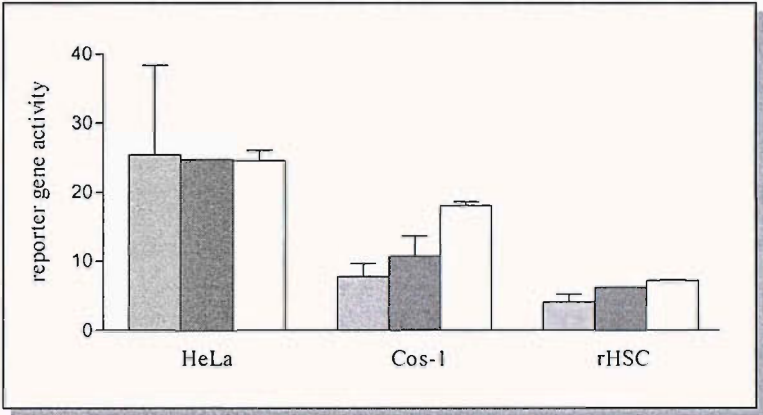
Reporter gene	Luciferase activity	
	HeLa cells	Activated rat HSC
0.25 µg pTIMP1-Luc	911.1	0.2
0.5 µg pTIMP1-Luc	2633.4	0.2
1 µg pTIMP1-Luc	6544.7	0.6
1 µg pGL2 control	>9,999	7.1
2 µg pGL2 control	>9,999	6.3

Figure 5.1. **Verification of the functionality of the new pTIMP1-Luc reporter plasmid.** The *TIMP1* minimal promoter was cloned upstream of the Firefly luciferase reporter gene in pGL2 basic vector (pTIMP1-Luc). Increasing amounts of pTIMP1-Luc were transfected into 10⁵ HeLa cells (a. and b.) and in activated rat HSC (b). As a reference, pGL2 under control of SV40 promoter (pGL2 control), was also transfected into Hela and rHSC (b.). The activity of the reporter gene was monitored as described in 2.7.4.

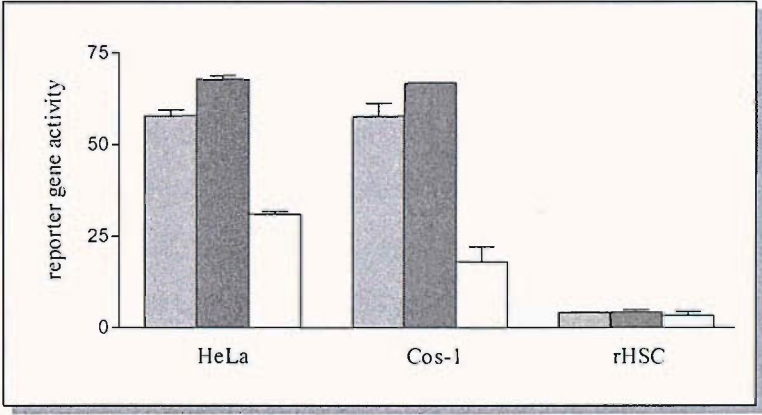
0.25 µg pTIMP1-CAT



0.5 µg pTIMP1-CAT



1 µg pTIMP1-CAT



Ratio effectene:DNA
1:10 1:25 1:50

Figure 5.2. **Optimisation of effectene/DNA ratio in transfection experiment using different cell lines.** 0.25 µg, 0.5 µg or 1µg of pTIMP1-CAT were transfected into cells using 3 different ratio DNA:effectene (µg:µL) 1:10, 1:25 and 1:50 as described in 2.7.2.2. Cells were harvested 48 h after transfection and CAT activity was monitored as described in 2.7.3.

the reporter vector transfected. Among the different DNA:effectene ratios tested, 1:10 and 1:25 gave similar results and therefore 1:10 was chosen in the subsequent experiments.

5.1.3. Verification of the production of proteins by the related expression vectors

In order to verify that the vectors, pCMV5-RUNX1B, pLNCX-FLAG-RUNX1A, pCMV5-RUNX2 and pCMV2-JunD translated the correct protein, each plasmid was transfected into Cos-1 cells. Whole protein extracts were run on a SDS-PAGE, and the presence of the protein of interest was detected by immunoblotting using specific antisera. Figure 5.3. showed that the vectors encoding for RUNX1A or RUNX1B, expressed respectively a 30 kDa and 50 kDa protein that interacted with anti-RUNX1 antisera as expected. Furthermore, pCMV5-RUNX2 produced a 60 kDa protein that reacted with anti-RUNX2 antisera, and the JunD expression vector expressed 2 isoforms of JunD of the expected sizes (a long and a short form) resulting from post-translational modifications.

The experiment confirmed that these expression vectors were suitable for the overexpression of RUNX and JunD in the reporter gene assays.

5.1.4. Selection of an appropriate transfection control

A control gene vector could be used to normalize for transfection efficiency or cell lysate recovery between transfection experiments. The control vector, cotransfected with the other plasmids, typically contained a reporter gene driven by a constitutive promoter. The 2 most common control reporter genes, β -Galactosidase and Renilla luciferase (referred as Renilla reporter), under control of SV40 early promoter and HSV-TK respectively, were cotransfected with pTIMP1-Luc and RUNX expression plasmids. The activity of the different reporter genes were monitored and Figure 5.4. represents examples of 2 experiments. It reveals the effect of RUNX expression on the level of transcription, not only of the luciferase gene, but also of the control reporter genes. Luciferase and β -galactosidase transcription were downregulated by RUNX1 whereas Luciferase and Renilla expression were upregulated by RUNX2. These results clearly indicated that these assumed constitutive promoters driving the control reporter gene were responsive to the overexpression of RUNX proteins and

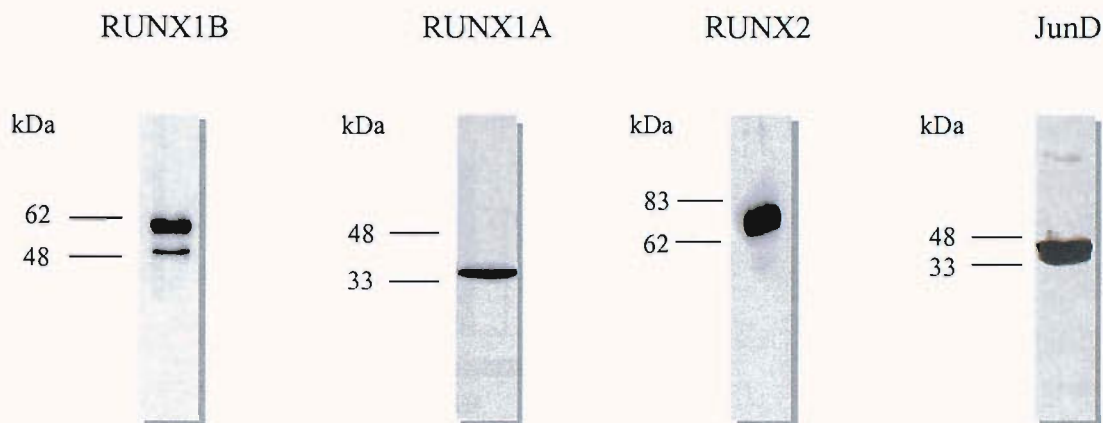


Figure 5.3. Verification of the overexpression of RUNX1B, RUNX1A, RUNX2, and JunD in Cos-1 cells by immunoblotting. 1 μ g of expression plasmid carrying cDNA cassettes for RUNX1B, RUNX1A, RUNX2 or JunD were transfected in Cos-1 cells. 48 h post transfection, cell whole extracts were prepared and used for SDS-PAGE and immunoblot detection of RUNX1 using anti-RUNX1 antisera (Active Motif for RUNX1B and Sigma for RUNX1A), RUNX2 using an anti-RUNX2 antisera (Oncogene) or JunD using an anti-JunD antisera (Sigma).

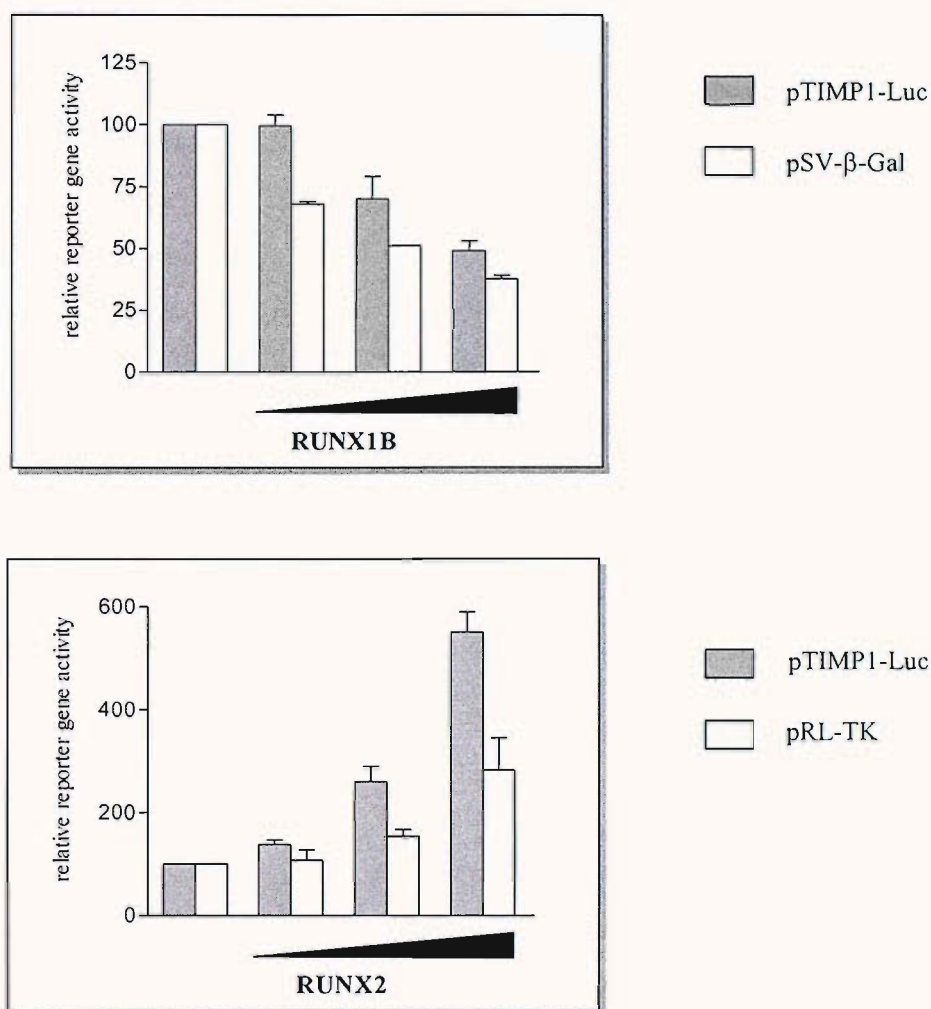


Figure 5.4. **Induction of the β -galactosidase and Renilla reporter gene expression by RUNX proteins.** 10^5 cells HeLa cells were transfected with $0.05 \mu\text{g}$ pTIMP1-Luc and either $0.01 \mu\text{g}$ pSV- β -Gal (β -galactosidase reporter vector) with increasing amount of RUNX1B expression vector or $0.01 \mu\text{g}$ pRL-TK (Renilla reporter vector) with increasing amount of RUNX2 expression vector. After 48 h, cells were harvested and the different reporter gene activities were monitored according to manufacture's protocols. The results were expressed as the mean percentage (\pm SE) activity relative to the control (reporter vector alone) of 2 independent experiments done in triplicate.

therefore were not suitable for controlling our experiments. The inducible expression of Renilla was also supported by the fact that in 2003, Promega launched a new synthetic Renilla control plasmid in which most of the potential transcription factors site within the plasmid were mutated.

While nowadays, the difference in the rate of transfection efficiency between samples is low due to the use of well optimised reagents and kits such as transfection reagents or plasmid purification kits, the control for cell viability after treatment is still important. In our experiments, this was achieved by monitoring the protein concentration of each sample, which would give an indication of the state of the cells and at least revealed any important variation of cell lysate recovery between the samples.

Although the efficiency of transfection could not be controlled using typical control reporter genes due to the influence of RUNX on transcription of these gene, normalising the samples according to their protein concentration was the compromised option chosen.

The parameters of the reporter gene assay were set up and controlled and the assay was ready to be used for the investigation of the role of RUNX in the *TIMP1* promoter activity and their potential interplay with other co-regulators of the promoter.

5.2. Regulation of *TIMP1* promoter by RUNX

5.2.1. Effect of RUNX on *TIMP1* promoter activity

The pTIMP1-Luc and pTIMP1-CAT (pTIMP1 WT) vectors were transfected into HeLa cells and culture-activated rat HSC respectively, together with increasing concentrations of the RUNX expression vectors for RUNX1A (C-terminal truncated RUNX1 protein), RUNX1B (full length RUNX protein) and RUNX2. In addition, pTIMP1-Luc or pTIMP1-CAT containing a scrambled UTE-1 site (mutated pTIMP1) were also transfected into these cells with the highest concentration of the different RUNX expression vectors. In Figure 5.5., the impaired activity of the mutated pTIMP1 compared to the WT (50 % decrease) is demonstrated. The resulting activities of the reporter gene products are shown in Figures 5.6. and 5.7.

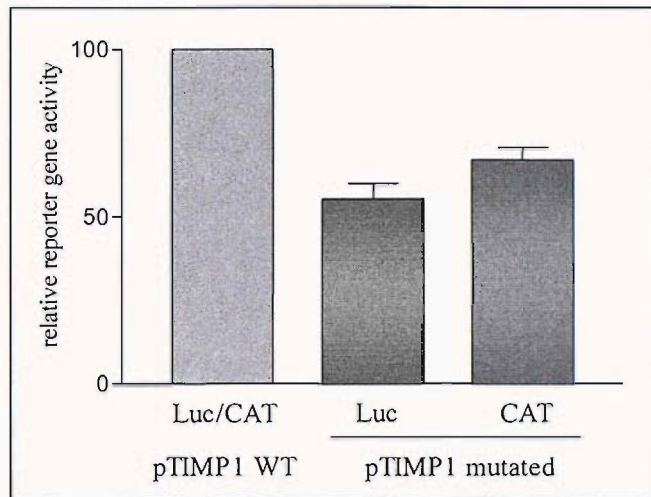


Figure 5.5. Activity of the *TIMP1* minimal promoter containing a UTE-1 scrambled site compared to the WT promoter in HeLa cells and culture-activated rat HSC Cells. Cells were transfected with 0.05 μ g luciferase reporter (HeLa) or 1 μ g CAT reporter (activated rat HSC) gene under control of the human *TIMP1* minimal promoter (-102,+60) containing the original UTE-1 binding site (pTIMP1 WT) or a scrambled UTE-1 sequence (pTIMP1 mutated). After 48 h, cells were harvested and reporter gene activities monitored according to the manufacture's protocols. The results were expressed as the mean percentage (\pm SE) of activity relative to the control (pTIMP1 WT alone) of 3 independent experiments done in triplicate.

5.2.1.1. Effect of RUNX1

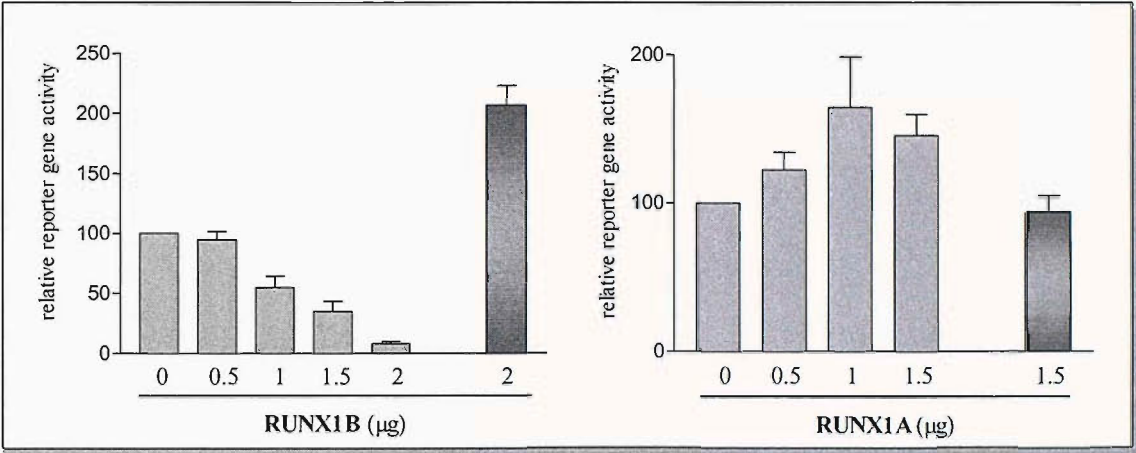
In both HeLa and activated rat HSC cells, overexpression of RUNX1B resulted in a dose-dependent repression of *TIMP1* promoter activity. This effect was reverted when the UTE-1 binding site within the promoter was mutated. In contrast, co-transfection of the 250 aa RUNX1 short isoform, RUNX1A, led to a moderate activation of the WT, but not the mutated pTIMP1 (Figure 5.6.). These results suggested that in the context of the *TIMP1* promoter, the domain responsible for the inhibitory effect of RUNX1 was situated within the C-terminal domain of the protein. The activation of the reporter by RUNX1A concurred with previous studies that demonstrated its positive regulation properties (Kim *et al.*, 1999, Petrovick *et al.*, 1998), even though it was first considered as an inhibitor of transcription (Meyer *et al.*, 1995; Javed *et al.*, 2000).

While RUNX1B had been shown previously to have either stimulatory or inhibitory effects on transcription depending on the factors recruited in the enhanceosome (Ito, 1999), our data suggested that in the context of the *TIMP1* promoter, RUNX1B recruits, via its C-terminal domain, transcriptional repressors which results in an inhibition of the transcription of the promoter.

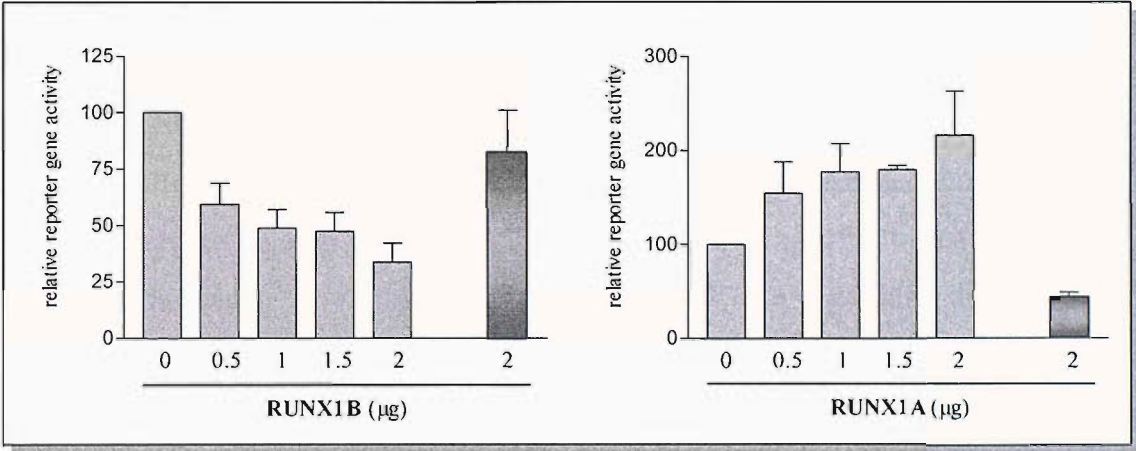
5.2.1.2. Effect of RUNX2

In contrast, the overexpression of RUNX2 induced an increase in the transcriptional level of the reporter gene in HeLa cells but had a more modest positive effect in activated rat HSC. In addition, the *TIMP1* promoter with a scrambled UTE-1 binding site did not respond to the presence of RUNX2, confirming the specificity of the activation of the *TIMP1* promoter by RUNX2 (Figure 5.7.). The difference in RUNX2 activation of the reporter gene between HeLa and HSC could be explained by a cell-specificity effect of RUNX2, as already described for RUNX1 (Lutterbach *et al.*, 2000). Moreover, the modest RUNX2-mediated promoter induction can be explained by the impaired phosphorylation of the protein, which has been shown to be critical for the transcriptional activity of RUNX2 (Francheschi *et al.*, 2003).

HeLa cells



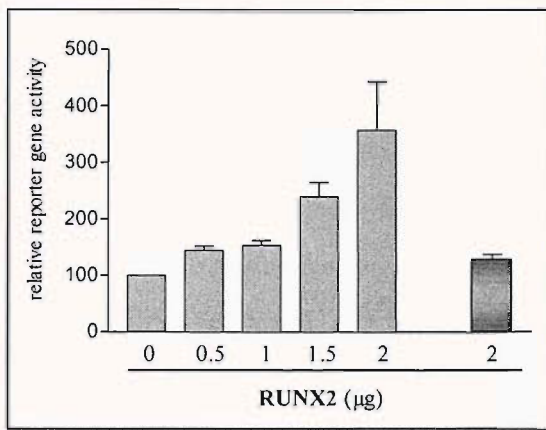
Activated rat HSC



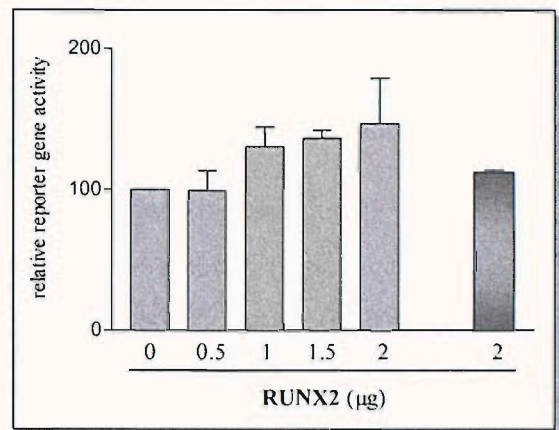
■ pTIMP1 WT ■ pTIMP1 mutated

Figure 5.6. Effect of overexpression of RUNX1 on the *TIMP1* promoter activity in HeLa cells and culture-activated rat HSC. Cells were transfected with 0.05 μ g luciferase reporter (HeLa) or 1 μ g CAT reporter (activated rat HSC) gene under the control of the human *TIMP1* minimal promoter (-102,+60) containing the original UTE-1 binding site (pTIMP1 WT) or a scrambled UTE-1 sequence (pTIMP1 mutated) in the presence of increasing amounts of expression vector carrying cDNA cassettes for RUNX1B and RUNX1A. For each transfection, the amount of DNA was equalized to 2 μ g with pCMV5. After 48 h, cells were harvested and reporter gene activities monitored according to the manufacture's protocols. The results were expressed as the mean percentage (+/- SE) of activity relative to the control (pTIMP1 WT or pTIMP1 mutated alone) of at least 2 independent experiments done in triplicate.

HeLa cells



Activated rat HSC



■ pTIMP1 WT ■ pTIMP1 mutated

Figure 5.7. Effect of overexpression of RUNX2 on the *TIMP1* promoter activity in HeLa cells and culture-activated rat HSC. Cells were transfected with 0.05 µg luciferase reporter (HeLa) or 1 µg CAT reporter (activated rat HSC) gene under the control of the human *TIMP1* minimal promoter (-102,+60) containing the original UTE-1 binding site (pTIMP1 WT) or a scrambled UTE-1 sequence (pTIMP1 mutated) in the presence of increasing amounts of expression vector carrying cDNA cassettes for RUNX2. For each transfection, the amount of DNA was equalized to 2 µg with pCMV5. After 48 h, cells were harvested and reporter gene activities monitored according to the manufacture's protocols. The results were expressed as the mean percentage (+/- SE) of activity relative to the control (pTIMP1 WT or pTIMP1 mutated alone) of at least 2 independent experiments done in triplicate.

These experiments suggested that RUNX2 and RUNX1A functioned as positive regulators of *TIMP1* gene transcription whereas RUNX1B repressed *TIMP1* promoter activity. As both RUNX proteins were expressed in activated rat HSC, a hypothesis would be that the balance between RUNX factors recruited to the promoter would dictate the level of transcription.

Another important determinant of the positive or negative effects of RUNX on *TIMP1* gene regulation was the promoter context as mentioned in other studies (Bae *et al.*, 1994; Meyers *et al.*, 1995; Kitabayashi *et al.*, 1998; Javed *et al.*, 2000; Lutterbach *et al.*, 2000). Therefore, it was relevant to consider the role of transcription factors binding to sites adjacent to RUNX sites.

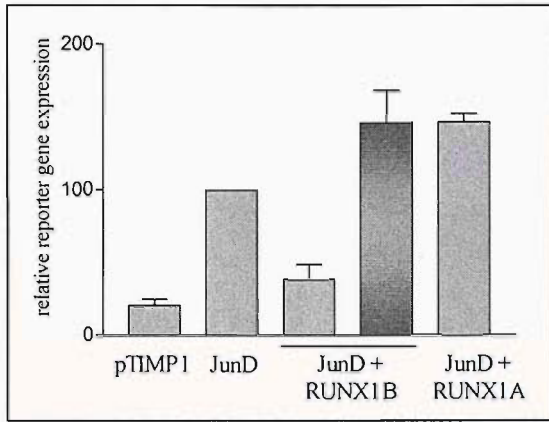
5.2.2. Functional interaction between JunD and RUNX

RUNX binding sites are often found in proximity to Ets or AP-1 sites, and RUNX factors can interact directly with transcription factors binding at these adjacent sites (Giese *et al.*, 1995; Hess *et al.*, 2001; D'Alonzo *et al.*, 2002). The UTE-1 site is in close proximity to an SRE. The two elements cooperate in a synergistic fashion to stimulate transcription of a heterologous minimal active promoter providing they are in close proximity (Bertrand-Philippe *et al.*, 2004). These findings indicate that the UTE-1 BP, i.e. RUNX, may functionally interact with factors that bind to the SRE. This latter consists of overlapping AP-1, STAT and ETS binding motifs of which the AP-1 site is functionally the most important in HSC (Bahr *et al.* 1999). As JunD is the critical component of transcriptionally active AP-1 dimers in activated HSC (Bahr *et al.*, 1999; Smart *et al.*, 2001), the effects of RUNX on JunD-induced transcription of *TIMP1* as well as potential physical interaction between JunD and RUNX were investigated.

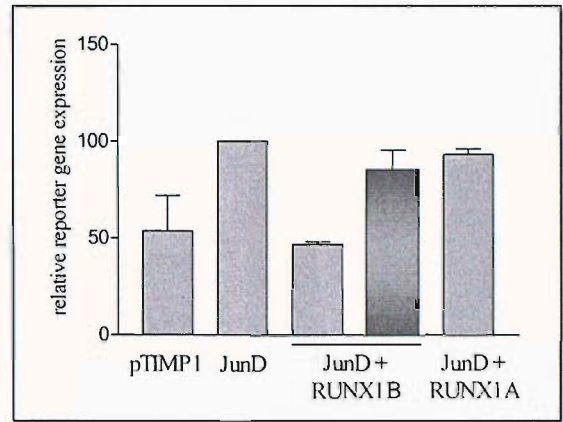
5.2.2.1. Effect of RUNX on JunD-induced *TIMP1* promoter activation

JunD was overexpressed in HeLa or activated rat HSC, together with pTIMP1-Luc or pTIMP1-CAT, respectively (pTIMP1 WT), in the presence or absence of RUNX1B, RUNX1A or RUNX2. 48 h post infection, reporter gene activities were monitored and the results are shown Figures 5.8. and 5.9.

HeLa cells

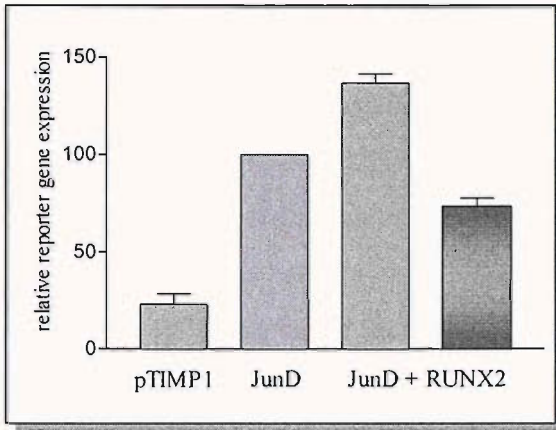
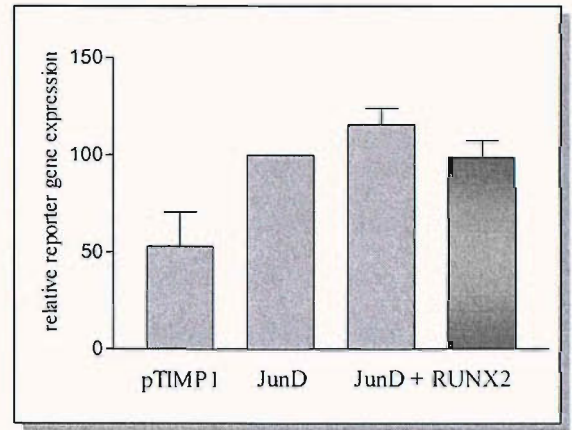


Activated rat HSC



 pTIMP1 WT
  pTIMP1 mutated

Figure 5.8. Effect of co-overexpression of JunD and RUNX1B or RUNX1A on the *TIMP1* promoter activity in HeLa cells and culture-activated rat HSC. Cells were transfected with 0.05 μ g luciferase reporter (HeLa) or 1 μ g CAT reporter (activated rat HSC) gene under control of the human *TIMP1* minimal promoter (-102,+60) containing the original UTE-1 binding site (pTIMP1 WT) or a scrambled UTE-1 sequence (pTIMP1 mutated) in the presence of 1 μ g of expression vector for JunD alone or in combination with 0.5 μ g of RUNX1B or RUNX1A expression vector. For each transfection, the amount of DNA was equalized to 1.5 μ g with pCMV2. 48 h post transfection, cells were harvested and the reporter gene activities measured according to the manufacture's protocols. Results were expressed as the mean percentage (\pm SE) of the reporter gene activity relative to the promoter activity (pTIMP1 WT or pTIMP1 mutated) in presence of JunD alone of at least 3 independent experiments done in triplicate.

HeLa cells**Activated rat HSC**



 pTIMP1 WT
  pTIMP1 mutated

Figure 5.9. Effect of co-overexpression of JunD and RUNX2 on the *TIMP1* promoter activity in HeLa cells and culture-activated rat HSC. Cells were transfected with 0.05 μ g luciferase reporter (HeLa) or 1 μ g CAT reporter (activated rat HSC) gene under control of the human *TIMP1* minimal promoter (-102,+60) containing the original UTE-1 binding site (pTIMP1 WT) or a scrambled UTE-1 sequence (pTIMP1 mutated) in the presence of 1 μ g of expression vector for JunD alone or in combination with 0.5 μ g of RUNX2 expression vector. For each transfection, the amount of DNA was equalized to 1.5 μ g with pCMV2. After 48 h, cells were harvested and the reporter gene activity measured according to the manufacture's protocol. Results were expressed as the mean percentage (\pm SE) of the reporter gene activity relative to the promoter activity (pTIMP1 WT or pTIMP1 mutated) in presence of JunD alone of at least 2 independent experiments done in triplicate.

JunD activated the *TIMP1* promoter as previously shown (Smart *et al.*, 2001), but in presence of RUNX1B, JunD-induced transcription was reduced to basal level. In contrast, RUNX1A did not repress JunD activation, neither did RUNX1B when the UTE-1 binding site was mutated (Figure 5.8.). These results suggested that the C-terminal domain of RUNX1B prevented JunD from activating the promoter. In contrast, the overexpression of RUNX2 did not significantly increase JunD-induced *TIMP1* promoter activity in both HeLa cells and activated rat HSC (Figure 5.9.).

In order to have a better understanding of the interplay between RUNX and JunD, we next determined whether RUNX1 and RUNX2 could interact with JunD by carrying out immunoprecipitation experiments.

5.2.2.2. Investigation of potential interaction between JunD and RUNX

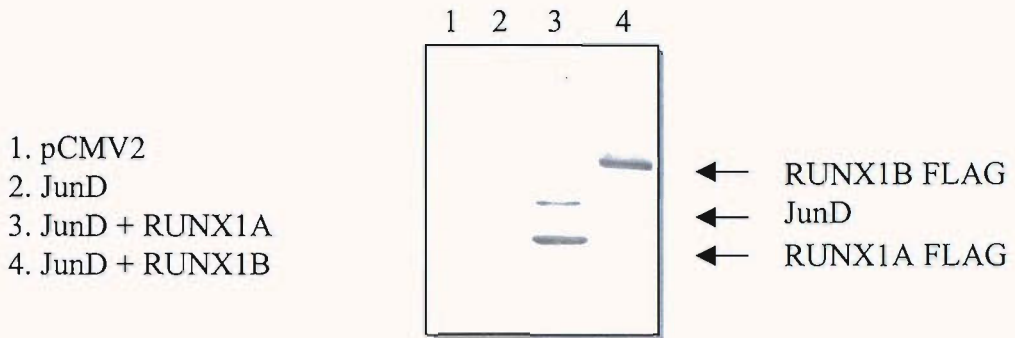
JunD was overexpressed with pLNCX-FLAG-RUNX1B, pLNCX-FLAG-RUNX1A or pRK5-RUNX2-FLAG in Cos-1 cells. Then, RUNX proteins were immunoprecipitated and the presence of JunD was detected by immunoblot.

As shown in Figure 5.10.a., JunD was co-immunoprecipitated with RUNX1A, but not with RUNX1B. Hence, these results suggest that the repressive effect of RUNX1B on the *TIMP1* promoter was associated with loss of interaction of RUNX1B with JunD, which resulted from properties of the C-terminal regions of RUNX1B. Since this region has been shown to contain binding sites for a variety of proteins including transcriptional co-repressors, it is possible that these interactions may prevent the interaction with JunD (Aronson *et al.*, 1997; Levanon *et al.*, 1998; Huang *et al.*, 2001). Occupancy of the UTE-1 binding site by RUNX1B might have brought about repression of *TIMP1* promoter activity by both recruiting transcriptional repressor and destabilizing the association of JunD on the promoter.

In addition, JunD failed to be co-immunoprecipitated with RUNX2 (Figure 5.10.b.) suggesting that the lack of synergistic activation of the *TIMP1* promoter by RUNX2 and JunD could be related to a deficient interaction between the two factors.

Although these experiments gave some indications on how the interplay between RUNX and JunD may influence the *TIMP1* promoter activity, it was important to note that additional experiments needed to be carried out to strengthen these hypotheses, such as the immunoprecipitation of JunD followed by immunodetection of RUNX proteins or immunoprecipitation of endogenous RUNX in HSC.

a.



b.

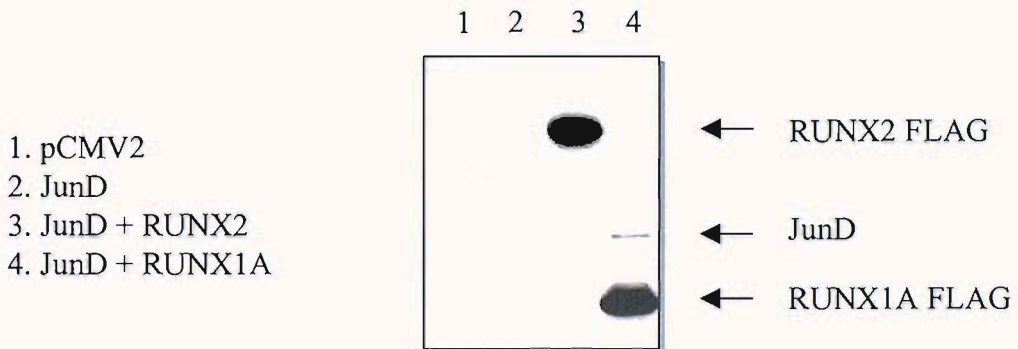


Figure 5.10. **Interaction between JunD and RUNX detected by immunoprecipitation.** Cos-1 cells were transfected with expression vectors for JunD either alone or with FLAG-tagged RUNX1A (a. and b.), RUNX1B (a.) or RUNX2 (b.) expression vectors. 48 h after transfection, cells were harvested, and lysates were used for immunoprecipitation with anti-FLAG antibody which was monitored by immunoblotting of immunoprecipitates with anti-FLAG antisera. Coimmunoprecipitation of JunD was detected by immunoblotting using an anti-JunD antisera. The gels shown were representative of two independent experiments.

Within a promoter, the regulators of transcription can be divided into two categories: transcription factors (JunD, RUNX) that bound directly to the DNA and coactivators of transcription that regulate the transcription via their interaction with the transcription factors. In parallel to the studies on the effects of RUNX and JunD on *TIMP1* promoter activity, the influence of the overexpression of RUNX with coactivators of transcription on *TIMP1* expression was also briefly investigated.

5.2.3. Effect of the overexpression of RUNX and histone acetyltransferase

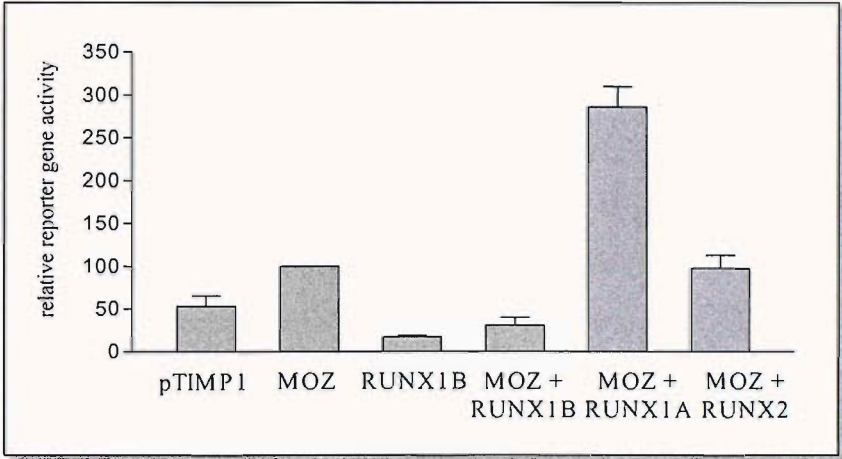
Histone acetyltransferases (HAT) are cofactors that regulate the transcription by modifying chromatin proteins resulting in the destabilisation of nucleosome structure and giving other transcription factors more access to a genetic locus (Sterner and Berger, 2000). MOZ and CBP are of particular interest as they have been identified in chromosomal translocation associated with leukaemia. One of them involves the fusion of the two proteins resulting in aberrant chromatin acetylation and leukaemia. Furthermore, interaction between RUNX and MOZ or CBP have been reported (Kitabayashi *et al.* 1998, 2001). We decided to investigate the influence of these 2 co-factors on the RUNX-mediated regulation of *TIMP1* promoter.

5.2.3.1. Effect of the overexpression of RUNX and MOZ on *TIMP1* activity

MOZ (pLNCX-MOZ) was overexpressed in HeLa cells together with pTIMP-Luc in the presence or absence of RUNX1B, RUNX1A or RUNX2. 48h post transfection, reporter gene activity was monitored.

MOZ enhanced the activity of the *TIMP1* promoter, but in presence of RUNX1B, MOZ-induced transcription was reduced below the basal level. In contrast, RUNX1A and MOZ strongly activate the promoter suggesting that the C-terminal domain of RUNX1B is responsible for RUNX1 inhibition of MOZ activity. On the other hand, the expression of RUNX2 did not affect MOZ-induced transcription (Figure 5.11.a.). The cooperative effect of MOZ and RUNX1A is all the more surprising since RUNX1A (250 aa) lacks the domain that interacts with MOZ (aa 295-363). A third factor might be involved in the induction of the transcription by MOZ and RUNX1A. Since MOZ have been previously shown to interact with RUNX1B resulting in a stimulation of the RUNX1-mediated transcription (Kitabayashi *et al.*, 2001), it is

a.



b.

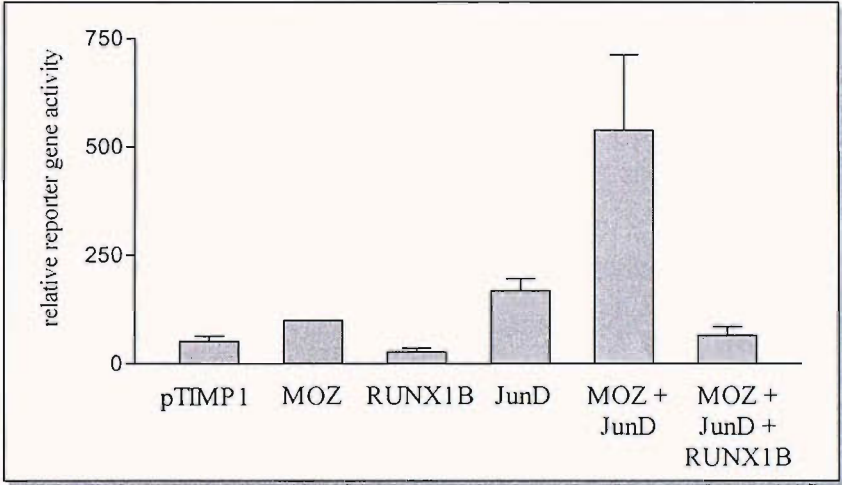


Figure 5.11. **Effect of co-overexpression of MOZ and RUNX on the *TIMP1* promoter activity in HeLa cells.** Cells were transfected with 0.1 μ g luciferase reporter gene under the control of the human *TIMP1* minimal promoter (-102,+60) in the presence of (a.) 1 μ g of expression vector for MOZ alone or in combination with 0.5 μ g of RUNX expression vectors (b.) 0.5 μ g of expression vector for MOZ, JunD and RUNX1B. For each transfection, the amount of DNA was equalized to 1.5 μ g with pCMV5. After 48 h, cells were harvested and the reporter gene activity measured according to the manufacture's protocol. Data were represented as the mean percentage (+/- SE) of activity relative to the promoter activity in presence of MOZ alone of at least 2 independent experiments done in triplicate.

probable that in the context of the *TIMP1* promoter, RUNX1B does not interact with MOZ and therefore, the MOZ-induced transcription is mediated through another factor whose activity is inhibited by RUNX1B, such as JunD.

To test this hypothesis, we next determined the effect of JunD and MOZ on the transcription in absence or presence of RUNX1B. As expected, JunD and MOZ synergistically upregulated the promoter activity but this strong induction was, once again, lost in the presence of RUNX1B (Figure 5.11.b.). RUNX1B not only inhibits JunD activity (5.2.2.1) but also counteracts the influence of MOZ on JunD-induced transcription suggesting that MOZ interacts with JunD and the RUNX1B-mediated inhibition of MOZ activation is a consequence of the inhibition of JunD activity by RUNX1B.

Since RUNX1A interacts with JunD, but not MOZ, we can further suggest that RUNX1A influence on MOZ-induced transcription occurred via JunD.

5.2.3.2. Effect of the overexpression of RUNX and CBP on *TIMP1* activity

CBP (pLNCX-CBP) was overexpressed in HeLa together with pTIMP-Luc in the presence or absence of RUNX1B. 48h post transfection, the reporter gene activity was monitored.

A clear synergistic activation of *TIMP1* expression by RUNX1B and CBP was detected (Figure 5.12.). This effect has already been reported by Kitabayashi team (1998) although not in the context of the *TIMP1* promoter.

This data suggest that RUNX1B forms an enhanceosome with CBP which positively regulates transcription of *TIMP1*.

5.3. Conclusion: Model of regulation of *TIMP1* promoter

We demonstrated that overexpression of RUNX1A increased *TIMP1* promoter activity, whereas RUNX1B acted as an inhibitor of transcription, probably by recruiting via its C-terminal domain, transcriptional corepressor. In addition, JunD has been shown to interact with RUNX1A but not RUNX1B and this loss of interaction correlated with the specific inhibitory effect of RUNX1B on JunD-induced transcription. Hence, these data suggest that the C-terminal region of RUNX1B is responsible for the inhibition of both transcription and interaction with

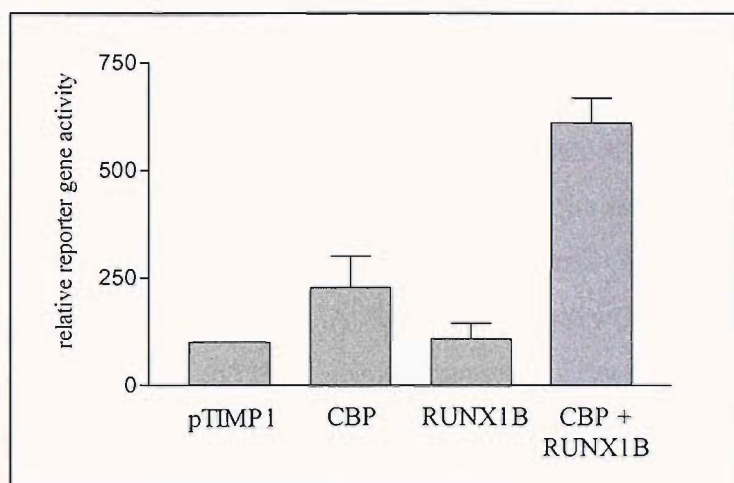


Figure 5.12. **Effect of co-overexpression of CBP and RUNX on the *TIMP1* promoter activity in HeLa cells.** Cells were transfected with 0.1 μ g luciferase reporter gene under the control of the human *TIMP1* minimal promoter (-102,+60) in the presence of 1 μ g of expression vector for CBP alone or in combination with 0.5 μ g of RUNX1B expression vector. For each transfection, the amount of DNA was equalized to 1.5 μ g with pCMV5. After 48 h, cells were harvested and the reporter gene activity measured according to the manufacture's protocol. Data were represented as the mean percentage (\pm SE) of activity relative to the control (pTIMP alone) of at least 2 independent experiments done in triplicate.

JunD. As a result, RUNX1B also inhibited MOZ influence on JunD-induced transcription activation.

Concurring with our data, a recent study demonstrated that RUNX1B binds to the corepressor mSin3A and this interaction is released when RUNX1B is phosphorylated by ERK (Imai *et al.*, 2004). As mSin3 interacts with HDACs, its recruitment by RUNX1B within the promoter results in an inactivation of *TIMP1* transcription through deacetylation of histone proteins and chromatin remodelling.

They also demonstrated that RUNX1A does not interact with mSin3. Therefore it is tempting to suggest that mSin3 prevents the interaction between RUNX1B and JunD. This is supported by the fact that the AP-1 and mSin3 interaction domain are located in close proximity, which could result in steric obstruction.

The ERK-dependant phosphorylation of RUNX1 is mediated by several factors such as BMP, FGF, IGF, PTH or collagen. These factors may enhance the transcription of *TIMP1* by phosphorylating RUNX1B, releasing the corepressor and thus allowing coregulator such as CBP to interact with RUNX1B. The synergistical activation of *TIMP1* by RUNX1B and CBP can also results from a direct shift from RUNX1/mSin3 complex towards RUNX1B/CBP association.

Figure 5.13. represents a model of *TIMP1* activation by RUNX1, JunD, MOZ and CBP that concurred with our finding and the current knowledge on RUNX1 activity. Some aspects of the model still remains to be elucidated such as the effect of RUNX1A, JunD and MOZ on *TIMP1* promoter or MOZ and JunD physical interaction.

In contrast, RUNX2 shows some transcriptional activation, but does not influence JunD-induced activation of *TIMP1* nor interact with JunD. This suggests that RUNX2 recruits other factors that are associated with RUNX1 enhanceosome. This hypothesis needs further investigation.

In conclusion, reporter gene assays gave some insight about the mechanisms that regulate *TIMP1* promoter activity. The results suggest a complex regulation of *TIMP1* expression by RUNX1 and RUNX2 whose effects are dependent upon extracellular signals and interactions with other factors forming in repressive or activating enhanceosomes.

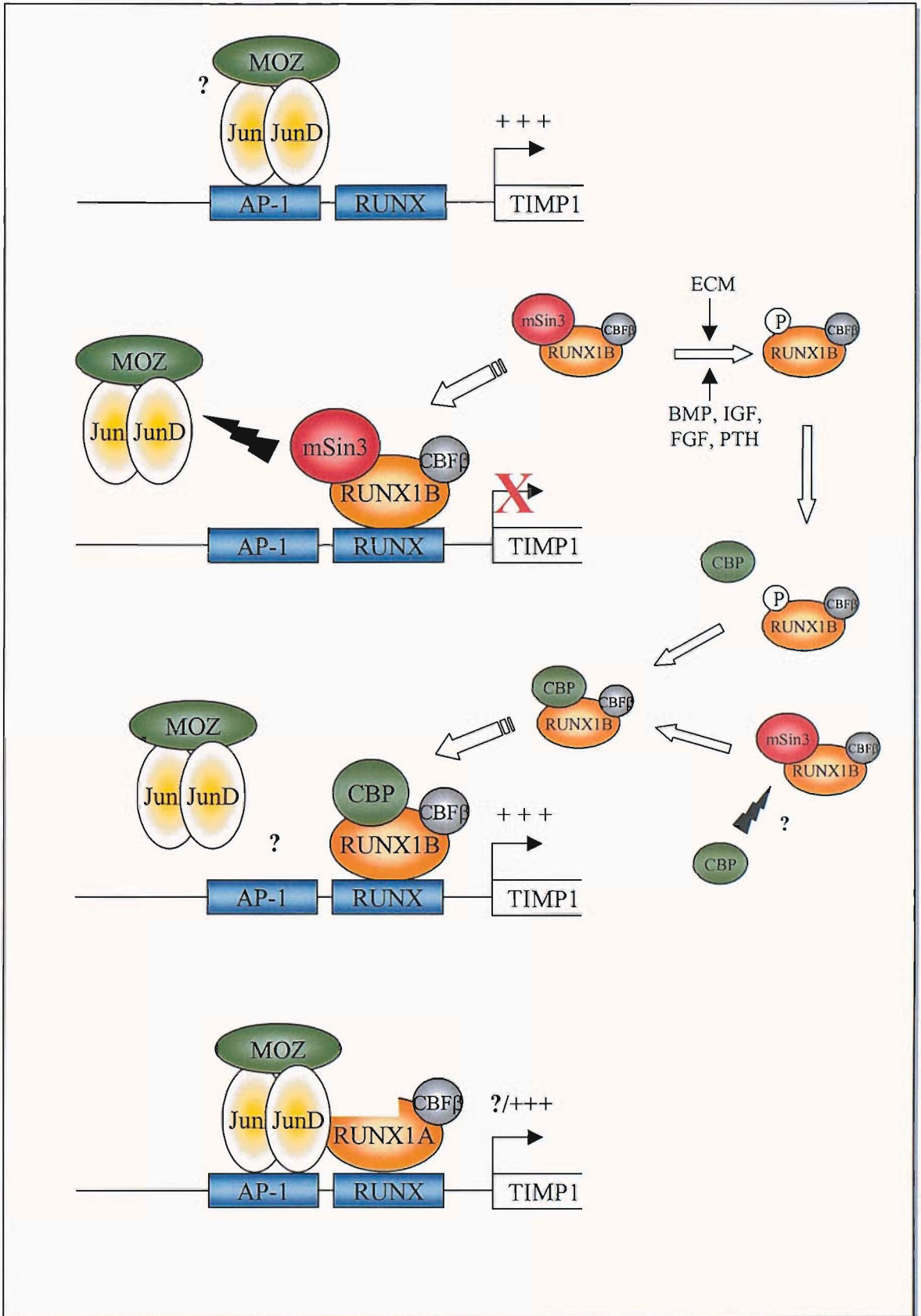


Figure 5.13. **Proposed model for the regulation of *TIMP1* promoter by RUNX1, JunD, MOZ and CBP.** (P) represents phosphorylation of RUNX1B and (?) details of the model that needs further investigation.

Chapter 6

RUNX gene silencing: Development of a new technology

The role of RUNX1 and RUNX2 in *TIMP1* promoter regulation was initially investigated using the classical approach of reporter gene assay. This assay involved a reporter gene under control of the *TIMP1* promoter in an expression vector that was co-transferred into cells along with expression vectors for RUNX1 or RUNX2. The regulation of expression of the reporter gene was assayed by measuring its enzymatic activity. Although this assay offered some advantages (no time consuming allowing the investigation of different overexpression conditions), it had its limitations (limiting level of coregulators), and complementary studies needed to be carried out in order to have a better understanding of the role of RUNX in *TIMP1* gene regulation. An opposite approach to the overexpression of proteins was to experimentally inhibit RUNX gene expression, and monitor any change in cell functions occurring as a consequence of the absence of RUNX protein (i.e. *TIMP1* expression). Small interfering RNA (siRNA), a powerful growing tool to achieve gene silencing, has been selected for our studies. In addition, siRNA were produced using baculoviral vectors in order to tackle the problem of transfection efficiency, especially in primary HSC. This chapter described the principle of the system, its optimisation using a siRNA silencing a gene coding for a ubiquitous protein, Lamin (LMNA) and a preliminary experiment regarding RUNX2 gene silencing.

6.1. Delivering siRNA using baculovirus vector

6.1.1. Principles and theory of small interfering RNA and baculovirus

6.1.1.1. RNA interference

siRNA technologies are based on the phenomenon called RNA interference in which the introduction of double stranded RNA (dsRNA) in cells results in the degradation of the complementary mRNA. Once entering the cells, the long dsRNA are processed into short 21-25 nucleotide RNA by the ribonuclease enzyme Dicer. Then, these small interfering RNA (siRNA) associate with numerous proteins to form the RNA-induced silencing complex (RISC). In an ATP dependent manner, RISC unwinds the siRNA duplex and the antisense strand interacts with the targeted mRNA. The bound mRNA is cleaved and sequence specific degradation of mRNA

results in gene silencing (Figure 6.1.) (McManus and Sharp, 2002; Dillin, 2003). The aim of the siRNA technologies is to trigger the RNA interference response by introducing into the cells a small RNA duplex matching a specific region of the gene of interest in order to degrade the mRNA of this gene.

Different methods are available for generating siRNA: *in vitro* preparation of siRNA including chemical synthesis, *in vitro* transcription of siRNA and long dsRNA, which are then digested *in vitro* with Rnase III to create an siRNA cocktail, or *in vivo* expression of siRNA including siRNA expression vectors or siRNA expression cassettes. The *in vitro* preparation involves the introduction of the *siRNA* directly into cells by classical transfection methods (lipofection, electroporation), while the *in vivo* expression relies on the introduction of DNA-based vectors and cassettes that expressed siRNA within the cells.

6.1.1.2. si RNAi expression vector

For our experiment, the siRNA expression vector system was selected. In general, this system contains the U6 or H1 promoter to drive the expression of a small hairpin siRNA (shRNA) by the RNA polymerase III. The transcription of the template is terminated upon incorporation of several uridines. The transcript, lacking a Poly(A) tail, folds back on itself to form a short hairpin with a loop that is removed in the cell by endoribonucleases, forming the siRNA. To construct a siRNAi expression vector, two oligodeoxynucleotides encoding the desired shRNA sequence were ordered, annealed and cloned into the vector downstream of the promoter. The backbone vector employed could be mammalian expression vectors or viral vectors (adenoviral or retroviral). In addition, viral vectors offered the possibility of incorporating siRNA vectors into the cells by transduction.

6.1.1.3. Advantage of the baculovirus system

Efficient delivery of siRNA expression constructs represents a critical step in siRNA technology. Primary cells which are transfected with a very low efficiency would not incorporate a sufficient amount of the siRNA expression vectors to allow detection of any gene silencing. Therefore, viral delivery was a solution to overcome this problem as virus efficiently transduced many primary and differentiated cells.

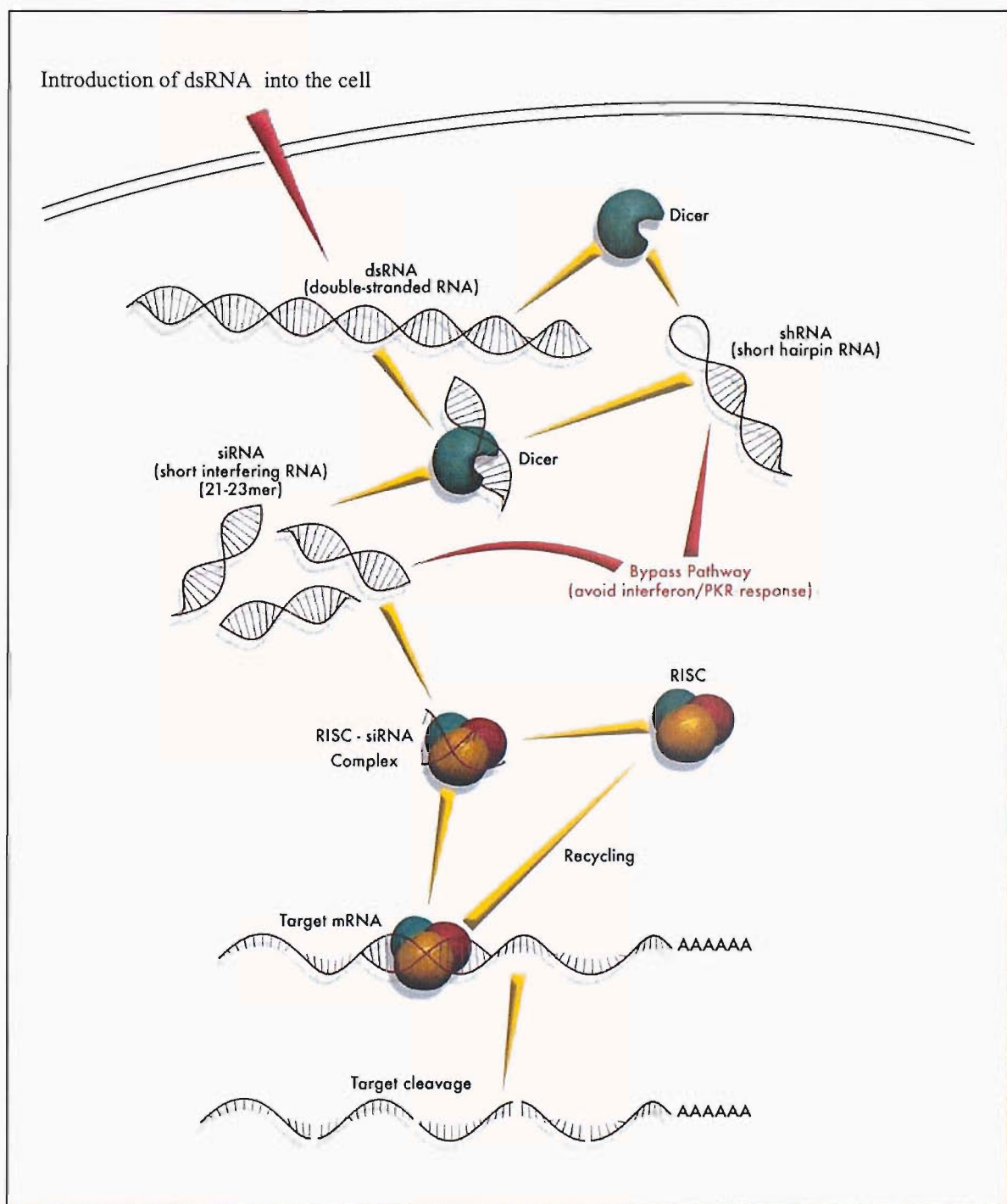


Figure 6.1. **Mechanism of RNA interference.** Adapted from siRNA technology and applications (Uspstate).

However, although siRNA adenovirus vectors had already been developed (Xia *et al.*, 2002), the novelty was to develop siRNA baculovirus vector: Baculoviruses are indeed able to deliver genes into mammalian cells, and these genes are expressed when controlled by a promoter active in mammalian cells (Boyce and Bucher, 1996). Moreover, baculovirus vectors offer several advantages compared to the other virus systems: Baculoviruses transduces efficiently activated HSC without showing any cytotoxicity (Gao *et al.*, 2002). In addition, baculovirus vectors do not replicate or produce viral gene products in mammalian cells making this system very safe to work with (biosafety level 1) (Tjia *et al.*, 1983). Finally, unlike adenoviruses and retroviruses, the baculoviruses vectors are relatively easy to construct and propagate as replication-competent viruses in Sf9 insect cells.

6.1.1.4. Baculovirus expression system

The baculovirus *Autographa californica* nuclear polyhedrosis virus (AcNPV) has a large (130 kb) circular double stranded DNA genome. The majority of the genome was integrated into a large plasmid called bacmid which was able to propagate in *E. coli* as it contained the low-copy-number mini-F replicon and a kanamycin resistance marker for selection. It also included a segment of DNA encoding the lacZ α peptide and, within this sequence, a short segment containing the attachment site for the bacterial transposon Tn7 (mini-attTn7) where the transposition of the mini-Tn7 element from the donor plasmid, containing the siRNAi expression cassette, occurred as long as the Tn7 transposition functions were provided in *trans* by a helper plasmid.

6.1.2. Production of recombinant baculoviruses

6.1.2.1 Construction of the siRNAi vectors

The siRNA expression vector used in the experiment was pFIGU (Figure 6.2.) and derived from pFastBac1 (Invitrogen), a plasmid which was initially designed for the production of recombinant proteins in insect cells. The baculovirus specific promoter (i.e. the polyhedrin promoter from AcNPV) was replaced with the U6 and pCMV promoters orientated in an opposite way. pCMV drove the transcription of EGFP,

which would serve as a control for transduction efficiency, whereas U6 promoter controlled the siRNA transcription.

The oligonucleotides corresponding to the shRNA were designed by Dr Dolphin following empirical rules established by previous work (Elbashir *et al.*, 2001). A 22 nt sequence specific to LMNA, RUNX2 or RUNT domain was selected in a region away from the 3' and 5' UTR region and the start codon. The sequence contained 30 to 70 % G/C and started with 2 G in order to correspond simultaneously to the *AgeI* restriction site and to the first G of the transcriptional start of the U6 promoter. As a result, the ODN contained the 22 nt sequence and its complementary sequence separated by the *Clal* restriction site which would become the loop of the shRNA. This sequence was also flanked at the 5' end by a couple of CC to complete the *AgeI* restriction and at the 3' end by a *SpeI* restriction site preceding by a series of T for the transcription termination and the 3'UU-overhang of the shRNA (Figure 6.2.). The ODNs were cloned upstream of the U6 promoter as described in 2.8.1.1. and shown in Figure 6.2. The integration of the ODN into pFIGU was checked by *MscI/Clal* digestion. The latter generated 3 fragments, instead of 2, as it introduced a *Clal* restriction site within the plasmid (Figure 6.2.). In addition, the expression of EGFP was also checked by transfecting directly pFIGU in Huh7 and LX2 where the presence of green cells were checked using a fluorescent microscope. Unfortunately, no green cells were detectable after transfection indicating that the pCMV promoter did not work as expected. Therefore, the control for transduction efficiency was not available for the time of the experiments meanwhile improvement over this matter was considered.

6.1.2.2. Construction of the recombinant viruses

The siRNA expression cassette of pFIGU containing the pCMV and U6 promoters was located within a region flanked by 2 mini-Tn7 elements which were inserted into the mini-*att*TN7 of the bacmid once pFIGU was transformed into competent *E. coli* cells (Figure 6.3.). Transposition of the cassette into the bacmid disrupted expression of the lacZ α peptide, therefore colonies containing the recombinant bacmid were white when growing on a medium containing X-gal and IPTG. The recombinant bacmid was purified from small scale cultures by miniprep and was then used to infect insect cells to produce viral particules. A few days after the infection, the

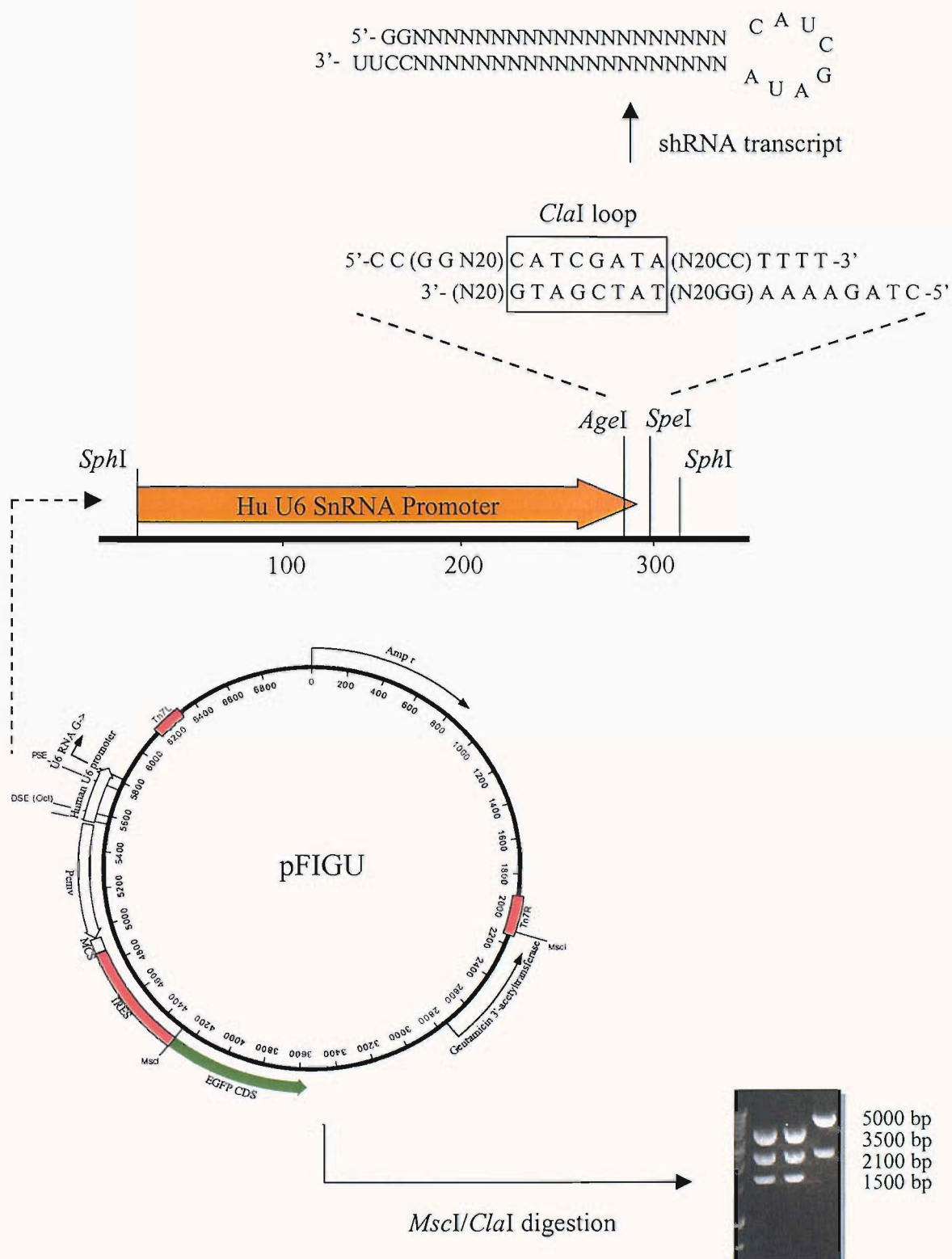


Figure 6.2. **pFIGU plasmid map and shRNAi cloning strategy.** ODN corresponding to the shRNA was cloned upstream of the U6 promoter and the presence of the insert was confirmed *MscI/ClaI* digestion of pFIGU as described in 2.8.1.1.

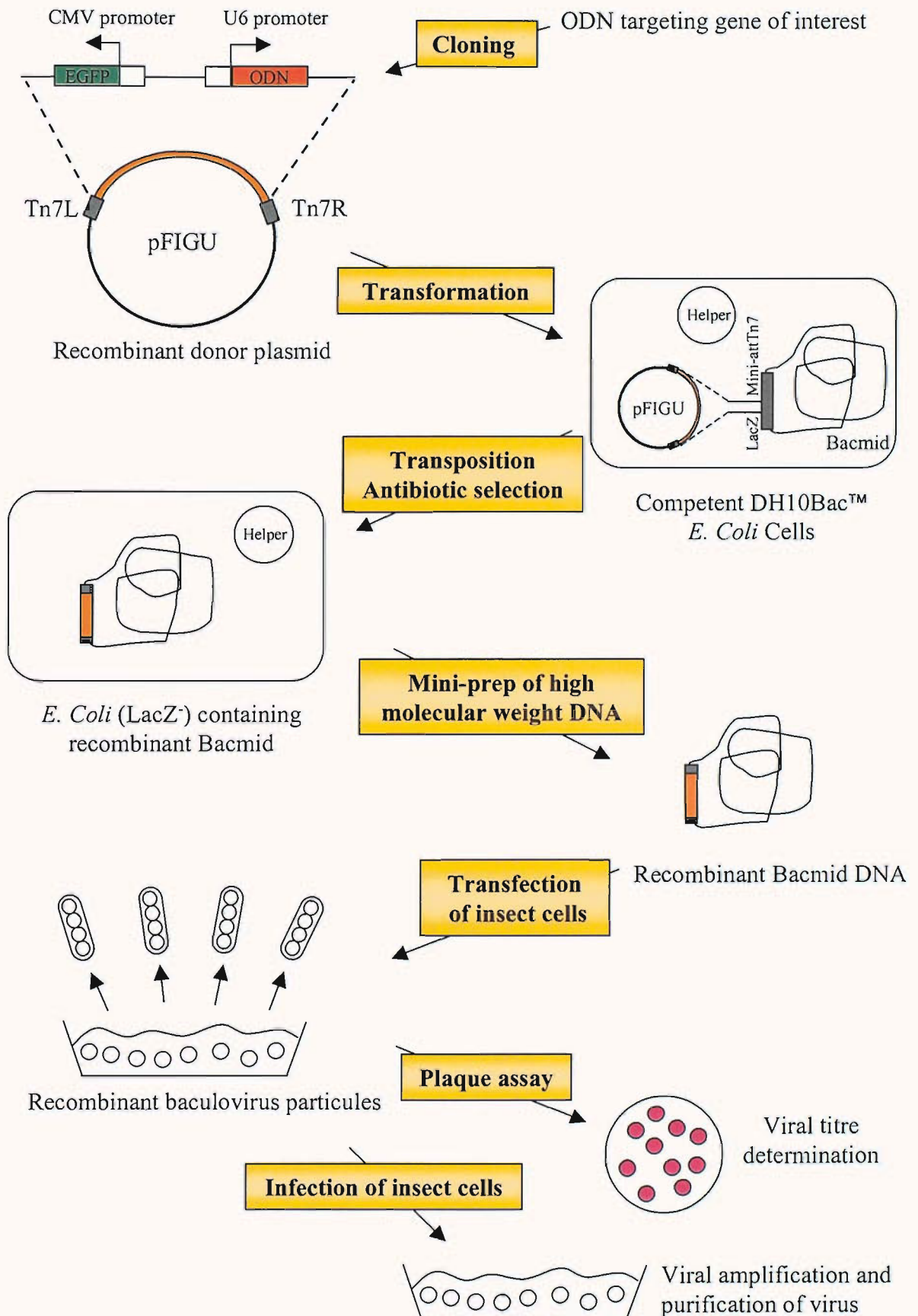


Figure 6.3. **Generation of recombinant baculoviruses containing coding sequence for shRNA.** Adapted from Bac-to-Bac® Baculovirus expression system manual (Invitrogen).

supernatant of the culture was centrifuged to separate the viruses from the cell debris which were discarded. Then, the titre of the virus solution, i.e. clarified supernatant called P0 recombinant virus, was determined by the plaque assay as described in 2.8.3. In addition, an aliquot of this preparation was used to infect a new bigger batch of insect cells in order to amplify the viruses. To purify and concentrate the viruses, they were pelleted down by ultracentrifugation through a sucrose cushion. The pellet was resuspended in a small volume of PBS and the titre of this preparation, called concentrated P1 recombinant virus, was also determined by plaque assay.

Four sets of baculoviruses containing expression cassettes for shRNA targeting LMNA (wild type or mismatch), RUNX2 or RUNT domain were constructed. The titres of the different batches were as follow:

Target gene	Batch	titre (pfu/mL)
LMNA Wild Type	P0	4×10^7
	P1	6×10^8
LMNA Mismatch	P0	4×10^7
	P1	4×10^8
RUNX2	P0	5×10^7
	P1	4×10^8
RUNT	P0	4×10^7
	P1	4×10^8

The concentration of virus was approximately identical for all the different P0 preparations, around 5×10^7 pfu/mL. In addition, the amplification and concentration of the viruses increased the titre by one log which gave a P1 batch of 5×10^8 pfu/mL.

Following the construction of the recombinant baculoviruses, the next step of the experiment was to test whether the viruses were able to infect cells and express the shRNA. As a proof of principles LMNA siRNA baculoviruses were first assessed in 3 cells line, Huh7, Saos-2 and LX2 before being tested in primary human HSC and also before evaluating the RUNX siRNA baculoviruses.

6.2. Silencing LMNA gene using baculovirus delivery system

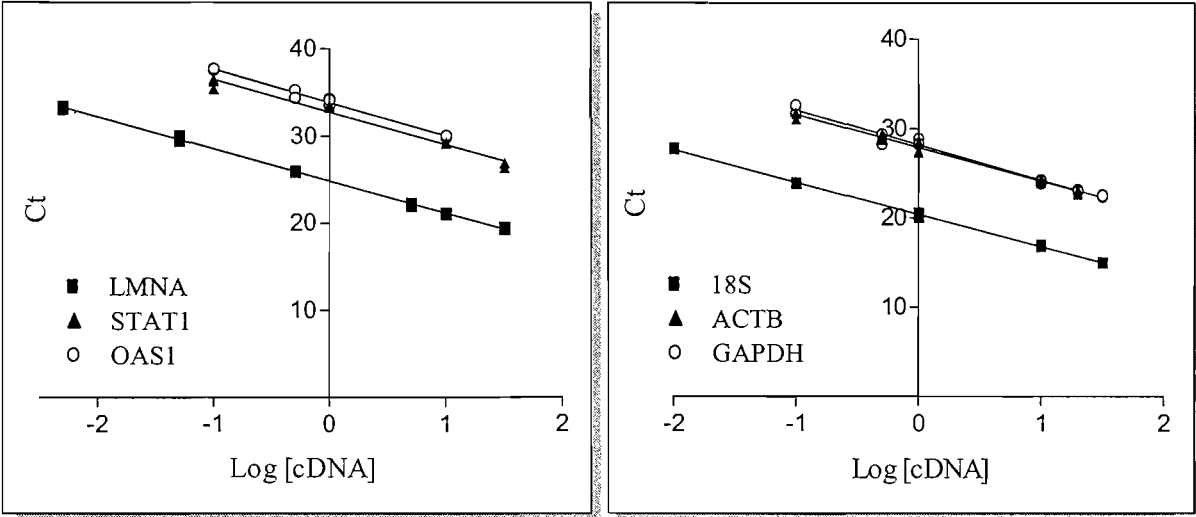
LMNA is a non-essential gene ubiquitously expressed in many different cell types and is a well established siRNA positive control. This gene was then ideal for testing the baculovirus system as failing to knock down LMNA expression, would mainly be the consequence of an ineffective baculovirus siRNA vector or due to poor transduction rate.

Gene silencing was assessed by investigating both mRNA and protein levels of the LMNA. While the protein level were analysed by western blot, mRNA expression was determine by real-time TaqMan PCR. This technique involved preliminary optimisation procedures.

6.2.1. Determination of the efficiency of TaqMan PCR

The expression of 3 different genes (LMNA, OAS1, STAT1) were analysed by TaqMan PCR. LMNA was the gene targeted by the shRNA whereas OAS1 and STAT1 were two genes whose expression was induced by the interferon/PKR response and therefore were used to control for non specific effects triggered by shRNA. In addition, amplification of an endogenous control was performed to standardize the amount of DNA in each sample. The most appropriate endogenous control was first selected among 3 different housekeeping genes (ACTB, GAPDH, 18S) depending on their amplification efficiency, as it should be approximately the same as the target genes one. To determine the efficiency of a reaction, PCR were performed on different amounts of LX2 cDNA and the Ct (cycles threshold) for each reaction was plotted against the log of cDNA concentration (Figure 6.4.a.). The slope of the curve gave the efficiency of the reaction according to the formula $10^{-1/\text{slope}}$. The efficiencies of the different reactions were listed in Figure 6.4.b. Whereas the 3 target gene PCR had comparable efficiency (around 1.84), the 3 reference gene amplification efficiencies were more disparate (between 1.79 and 1.89). According to the results, ACTB was the endogenous gene with the closest efficiency of reaction to the target genes and therefore was chosen as the reference gene for the subsequent experiments.

a.



b.

	slope	Y-intercept	1/slope	efficiency
<i>Target gene</i>				
LMNA	-3.68 ± 0.03	24.85 ± 0.04	-0.272	1.84
OAS1	-3.82 ± 0.18	33.86 ± 0.12	-0.262	1.83
STAT1	-3.72 ± 0.22	32.76 ± 0.21	-0.269	1.86
<i>Reference gene</i>				
18S	-3.62 ± 0.04	20.41 ± 0.05	-0.276	1.89
ACTB	-3.76 ± 0.11	27.88 ± 0.10	-0.266	1.85
GAPDH	-3.94 ± 0.11	28.23 ± 0.11	-0.254	1.79

Figure 6.4. **Determination of the efficiency of the real time PCR amplification of 3 target genes (LMNA, OAS1 and STAT1) and 3 references genes (18S, ACTB and GAPDH).** (a) The standard curves for the amplification of the different genes represented cycle threshold versus Log of LX2 cDNA concentration. (b) parameters of the standard curves allowed to calculate the efficiency of the reaction using the formula $10^{-1/\text{slope}}$.

6.2.2. LMNA silencing in cell lines

LMNA knockdown was first investigated in cell lines which were known to be transduced efficiently by baculovirus, the hepatoma line Huh7 (Condreay *et al.*, 1999) and the osteogenic sarcoma line Saos-2 (Song *et al.*, 2003).

6.2.2.1. Huh7 and Saos-2

Both cell lines were transduced by 1 h incubation with P0 recombinant virus generating shRNA targeting either LMNA at different MOI (0.4, 4, 40) or LMNA containing 2 mismatches at a MOI of 40. 2 or 4 days post infection, LMNA proteins and RNA levels were determined by western blot and TaqMan PCR respectively. The knockdown mediated by LMNA shRNA was compared to the one generated by LMNA mismatch shRNA as a preliminary experiments demonstrated that there was no effect on LMNA gene expression by the mismatch shRNA relative to the untreated samples (Figure 6.5.). Besides, equal loading was controlled with the expression of GAPDH for western blot and gene expression was standardized with the amplification of an endogenous control (ACTB).

Figures 6.6. and 6.7. showed that LMNA expression was depleted relative to the control at both the protein and the RNA levels in Huh7 and Saos-2 cells extracts that were incubated with LMNA recombinant virus. RNA expression was down regulated by 85 % (Huh7) and 95 % (Saos-2) compared to the control, at a MOI of 40. In addition, a clear dose response effect was observable as the knockdown of LMNA increased with the MOI and 4 was the minimum MOI at which LMNA gene expression significantly decreased. Moreover, the gene knock down could still be detectable 4 day post infection.

In conclusion, these experiments demonstrated that the recombinant baculovirus expressed a functional shRNA as proven by the LMNA gene silencing achieved after incubation of the cells with the virus.

6.2.2.2. LX2

Before assessing the effect of the recombinant baculovirus on primary HSC, the HSC cell line LX2 was also transduced with the viruses expressing shRNA targeting the

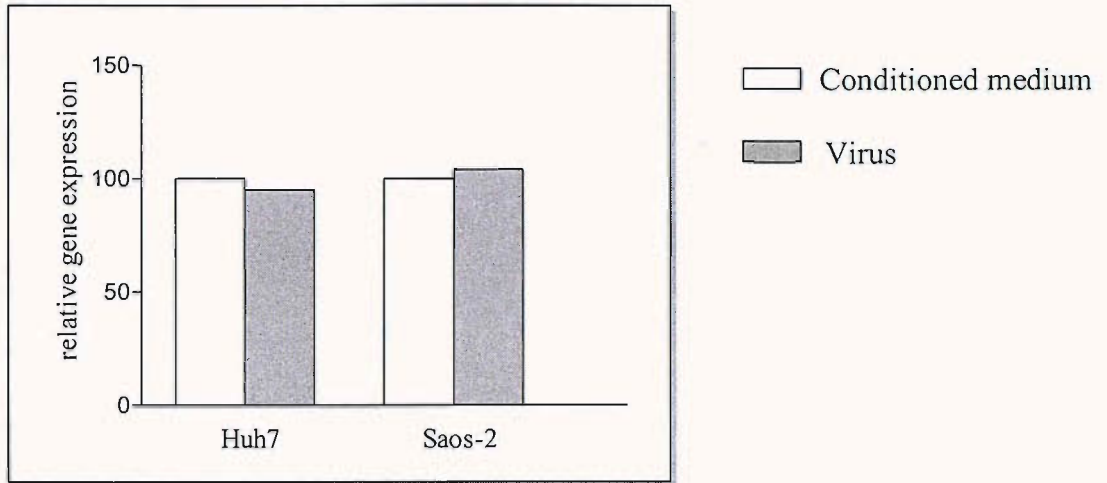
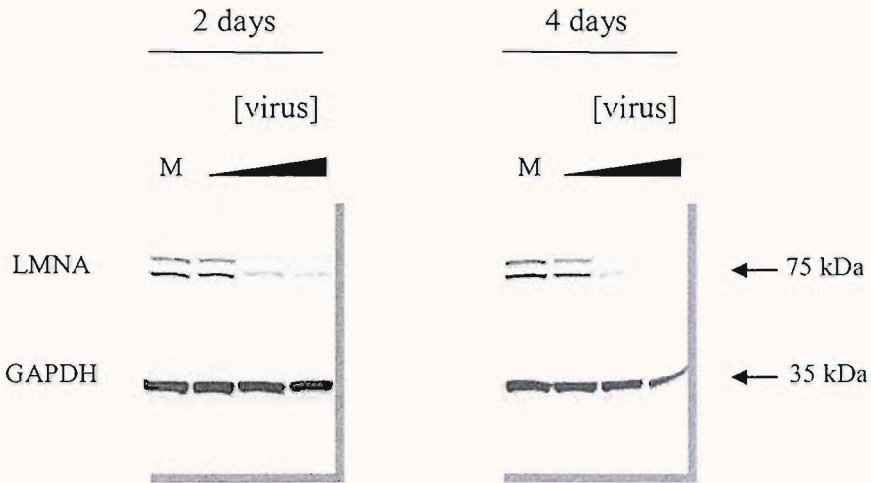


Figure 6.5. LMNA gene expression in Huh7 and Saos-2 cells after 1 h incubation in media alone or containing recombinant virus. Cells were incubated for 1 h at 37°C with conditioned medium (medium preincubated with sf-9 cells) or P0 recombinant virus shRNA targeting LMNA gene containing 2 mismatches at a MOI of 40. 2 days post transfection cells were harvested and RNA extract was prepared. 1 µg RNA was reverse transcribed into cDNA and 20 ng of cDNA was used as a template in TaqMan PCR with either LMNA and FAM probe. Gene expression was normalised with ACTB gene expression and calculated as relative expression to the control (conditioned medium).

a.



b.

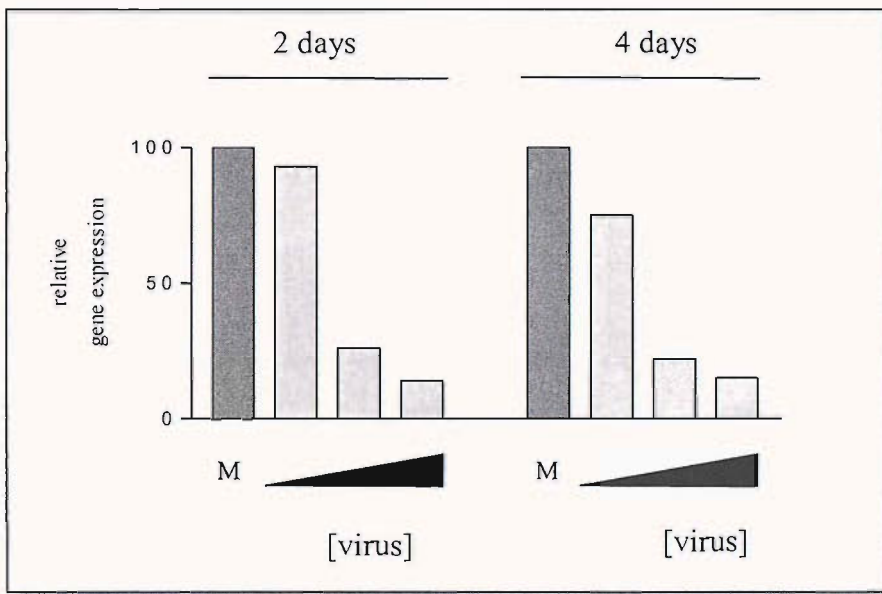
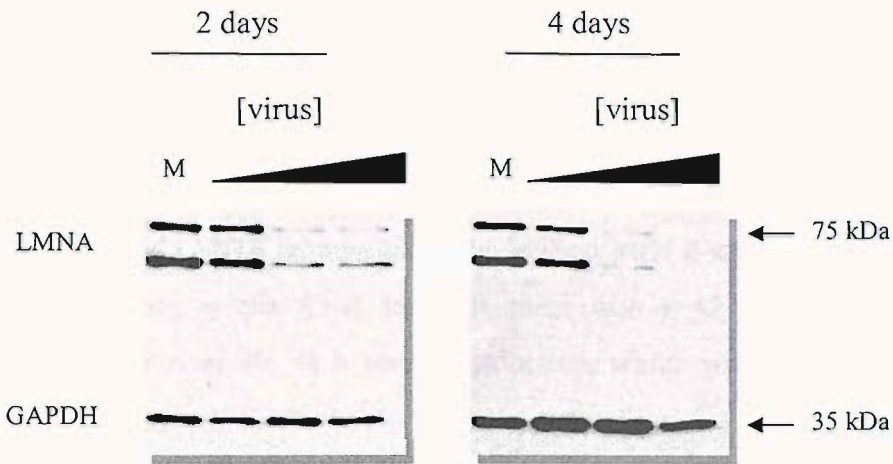


Figure 6.6. LMNA expression level in Huh7 after infection with recombinant baculovirus. Huh7 cells were incubated for 1 h at 37°C with P0 recombinant virus generating shRNA targeting LMNA or LMNA containing 2 mismatches (M). Cells were incubated with increasing concentrations of virus at a MOI of 0.4 4 and 40. 2 or 4 days post-infection cells were harvested and split into 2 samples from which protein and RNA extract were prepared. (a) whole cell protein extracts (25 µg) were used for SDS-PAGE and immunoblot detection of LMNA using an anti-LMNA antisera. Equal loading was controlled with the detection of GAPDH using GAPDH anti sera. (b) 1 µg RNA was reverse transcribed into cDNA and 20 ng of cDNA was used as a template in TaqMan PCR with LMNA specific primers and FAM probe. Gene expression was normalised with ACTB gene expression and calculated as relative expression to the control (gene expression in cells treated with virus containing LMNA mismatch shRNA).

a.



b.

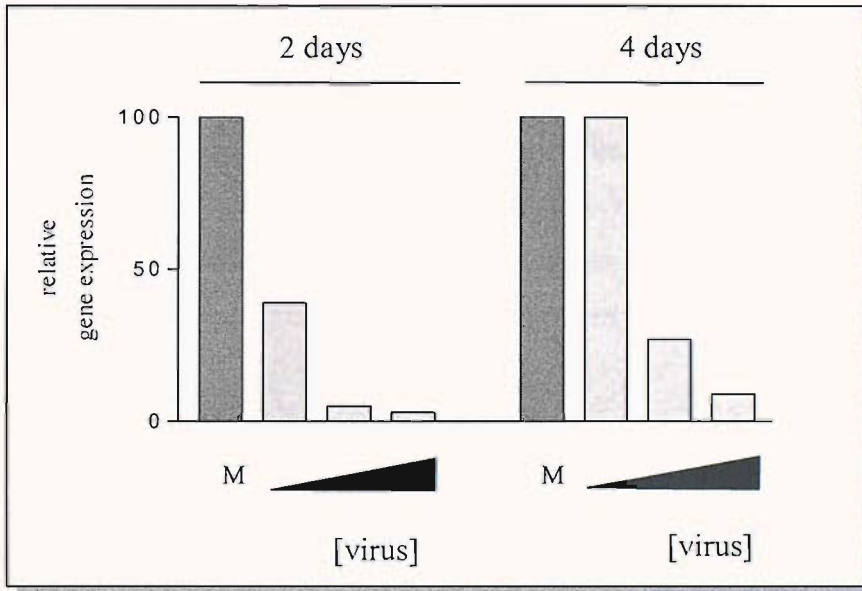


Figure 6.7. LMNA expression level in Saos-2 after infection with recombinant baculovirus. Saos-2 cells were incubated for 1 h at 37°C with P0 recombinant virus generating shRNA targeting LMNA or LMNA containing 2 mismatches (M). Cells were incubated with increasing concentrations of virus at a MOI of 0.4 4 and 40. 2 or 4 days post-infection cells were harvested and split into 2 samples from which protein and RNA extract were prepared. (a) whole cell protein extracts (25 µg) were used for SDS-PAGE and immunoblot detection of LMNA using an anti-LMNA antisera. Equal loading was controlled with the detection of GAPDH using GAPDH anti sera. (b) 1 µg RNA was reverse transcribed into cDNA and 20 ng of cDNA was used as a template in TaqMan PCR with LMNA specific primers and FAM probe. Gene expression was normalised with ACTB gene expression and calculated as relative expression to the control (gene expression in cells treated with virus containing LMNA mismatch shRNA). Western blot were done by L. Nicholson (London).

LMNA gene. In this experiment, cells were infected for 1 h with concentrated P1 viruses at a MOI of 0.4 or 4 and 40 (LMNA WT) or at a MOI of 40 (LMNA mismatch) as a control. As shown on Figure 6.8.a., the LMNA protein level was not significantly modified after treatment with the recombinant virus although there was a slight decrease of LMNA expression at the highest MOI 2 day post infection. This was also noticeable at the RNA level as there was a 42 % decrease in gene expression at a MOI of 40, 48 h post transduction, which was lost after another 2 days of growth (Figure 6.8.b.).

These results could be explained by either a cell specific effect of the LMNA shRNA or more likely by an impaired transduction of LX2 of the recombinant viruses.

Overall, the baculovirus system was proven to be a successful system to deliver shRNA into cells although the degree of the gene knockdown was dependant upon the efficiency of transduction, which varied with the cell type. Then, this system was tested on primary cells which were known to be fairly resistant to transfection.

6.2.3. LMNA silencing in primary HSC

Taking into account the previous experiment which showed that LX2 HSC were difficult to transduce, primary HSC were incubated for 1 h with concentrated P1 virus at a MOI of 150 and 300. After 2 days of growth the cells were harvested and the expressions of LMNA protein and RNA were investigated. Figure 6.9.a. showed a decrease in LMNA protein level, detectable at the highest MOI, i.e. 300, whereas TaqMan PCR revealed a 50 % knock down of the level of RNA messenger at both MOI tested (Figure 6.9.b.). These data confirmed that baculovirus transduced primary HSC and expressed functional shRNA. However, further experiments would be necessary to optimise the transduction conditions (longer incubation of the virus, cell confluency) in order to obtain a gene knockdown at lower MOI.

Successful knocking down of LMNA gene expression using siRNA baculovirus expression vector in several cells line and primary HSC allowed us to demonstrate that shRNA could be delivered using the baculovirus system. Therefore, this new technology could be used to study the effect of RUNX gene silencing on cells.

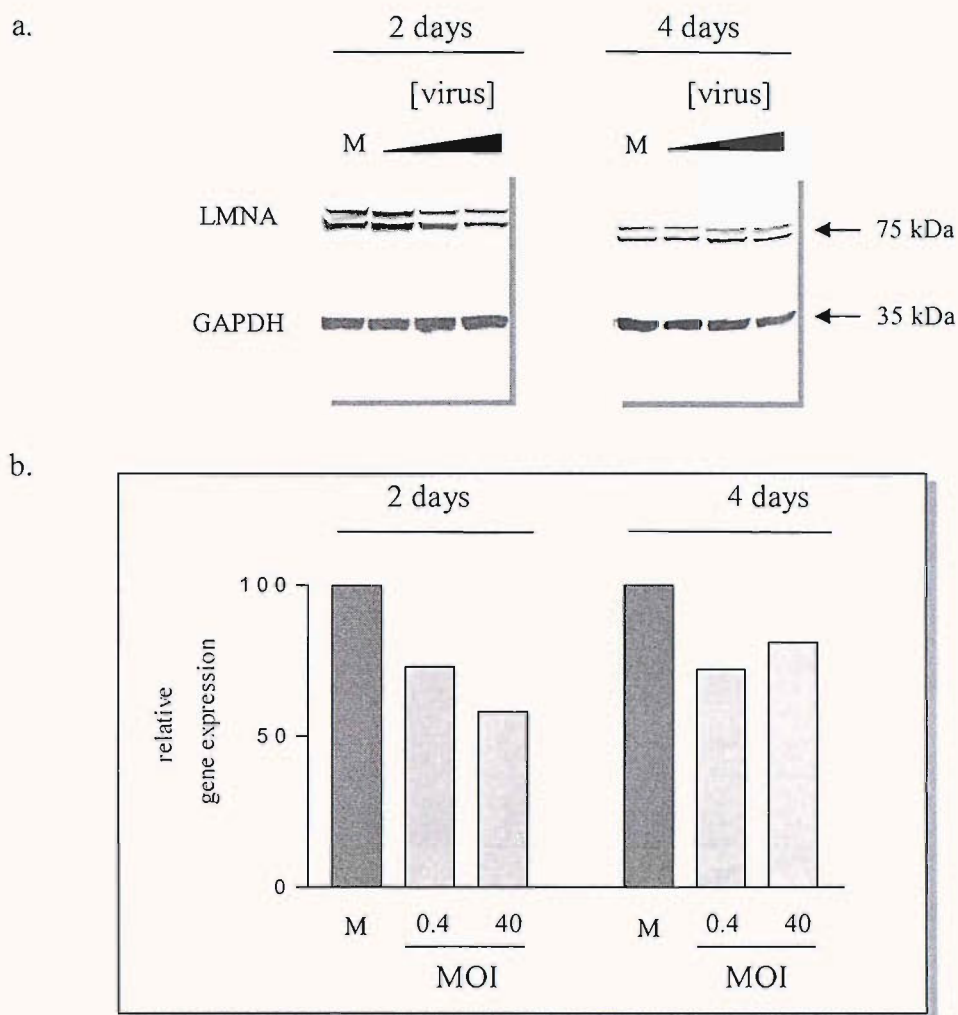


Figure 6.8. **LMNA expression level in LX2 after infection with recombinant baculovirus.** LX2 cells were incubated for 1 h at 37°C with P1 recombinant virus generating shRNA targeting LMNA or LMNA containing 2 mismatches (M). Cells were incubated with increasing concentrations of virus at a MOI of 0.4, 4 and 40. 2 or 4 days post-infection cells were harvested and split into 2 samples from which protein and RNA extract were prepared. (a) whole cell protein extracts (25 µg) were used for SDS-PAGE and immunoblot detection of LMNA using an anti-LMNA antisera. Equal loading was controlled with the detection of GAPDH using GAPDH anti sera. (b) 1 µg RNA was reverse transcribed into cDNA and 20 ng of cDNA was used as a template in TaqMan PCR with LMNA specific primers and FAM probe. Gene expression was normalised with ACTB gene expression and calculated as relative expression to the control (gene expression in cells treated with virus containing LMNA mismatch shRNA).

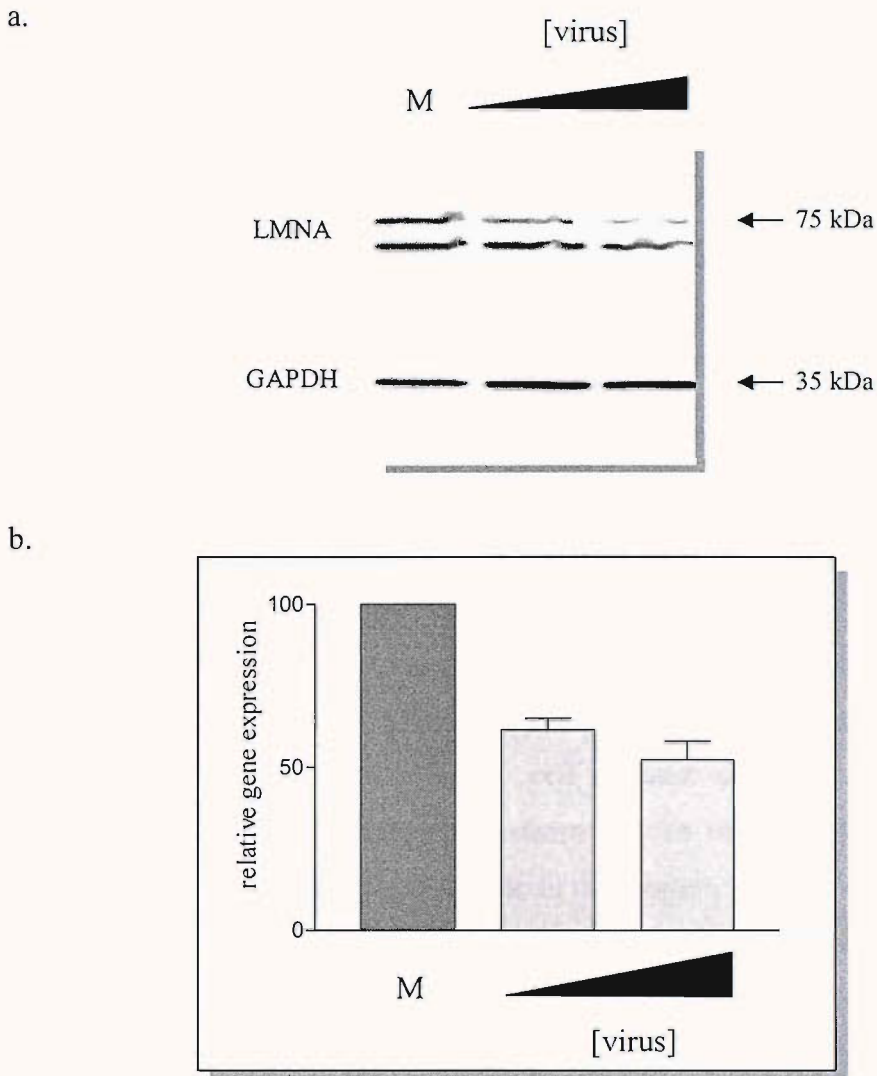


Figure 6.9. LMNA expression level in primary human HSC after infection with recombinant baculovirus. HSC cells were incubated for 1 h at 37°C with P1 concentrated recombinant virus generating shRNA targeting LMNA or LMNA containing 2 mismatches (M). Cells were incubated with increasing concentrations of virus at a MOI of 150 and 300. 2 post-infection cells were harvested. Protein or RNA extract were prepared. (a) whole cell protein extracts (15 µg) were used for SDS-PAGE and immunoblot detection of LMNA using anti-LMNA anti sera. Equal loading was controlled with the detection of GAPDH using GAPDH anti sera. (b) 1 µg RNA was reverse transcribed into cDNA and 20 ng of cDNA was used as a template in TaqMan PCR with LMNA specific primers and FAM probe. Gene expression was normalised with ACTB gene expression and calculated as relative expression to the control (gene expression in cells treated with virus containing LMNA mismatch shRNA). Data represent the mean (+/- SE) of 2 independent experiments.

6.3. RUNX silencing

Due to cost and time consuming it was decided to construct initially 2 recombinant baculovirus. Amongst the 3 RUNX proteins, RUNX2 was chosen as a target for shRNA as it was the one with the more reliable antibody available for western blot. One sequence was specific to RUNX2 and the other sequence was complementary to the runt domain, which, as a result, targeted also RUNX1 and RUNX3 mRNA.

However, it is well established that although several different siRNA can target one specific mRNA, only a few are able to knockdown the gene expression (McManus and Sharp, 2002). Therefore, the siRNA selected for our experiments had to be validated before being transduced into primary cells.

Saos-2, which was known to express predominantly RUNX2 (Geoffroy *et al.*, 1998), and LX2 were incubated with P0 or P1 recombinant virus at a MOI of 40 or 200 respectively. 2 days post infection cell extracts were prepared and the RUNX2 protein level was investigated by western blot. In contrast with the 64 kDa form of RUNX2, which was barely detectable in the western blot, the 40 and 30 kDa form of the protein reacted strongly with RUNX2 antisera but the expression of these proteins did not change significantly upon infection of both recombinant viruses (Figure 6.10.). These results indicated that the selected shRNA were not effective. Indeed, the lack of protein depletion could not be due to an inefficient transduction as Saos-2 cells were easily transduced by baculovirus as shown by previous experiments (6.2.2.1.).

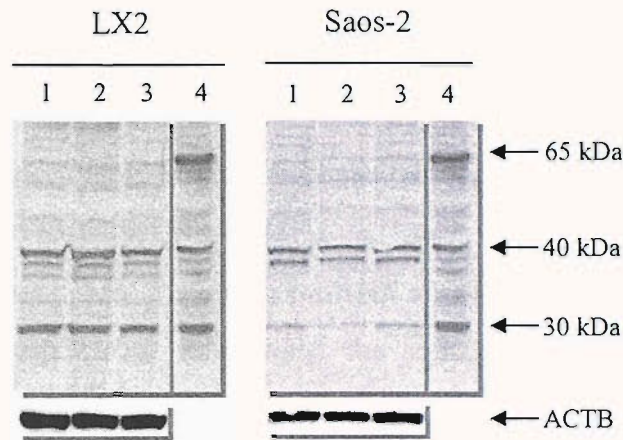
In conclusion, the siRNA selected did not decrease RUNX2 protein expression and therefore was not suitable for transduction in primary HSC. Unfortunately, the time framework of the studies did not allow us to design and test new sequences.

6.4. Interferon response triggered by shRNAi

6.4.1 Aim of the study

One of the claimed advantages of the siRNA was, because of their short length, that siRNA and shRNA were supposed to bypass the interferon/PKR response normally.

a.



1. No treatment
2. shRNA targeting RUNX2
3. shRNA targeting RUNT domain
4. Positive control

b.

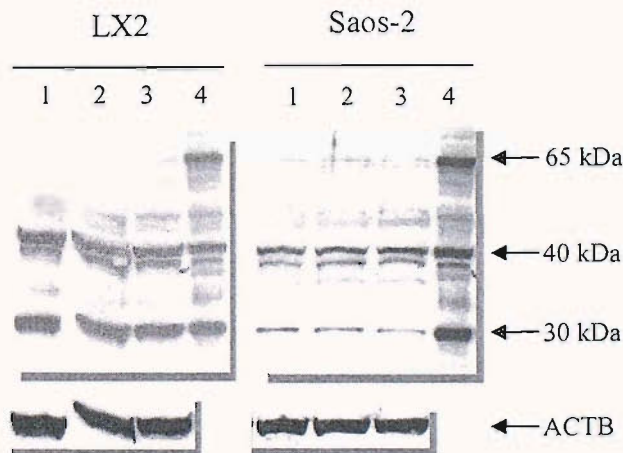


Figure 6.10. **RUNX2 expression level in LX2 and Saos-2 cells after infection by recombinant baculovirus.** LX2 or Saos-2 cells were incubated for 1 h at 37°C without (1) or with recombinant virus generating shRNA targeting RUNX2 (2), shRNA targeting RUNT domain (3). Western cell extracts were prepared 2 days post-infection. (4) overexpressing RUNX2 Cos cell extract as a positive control. Cells were incubated with recombinant viruses from clarified supernatant P0 at a MOI of 40 (a) or concentrated recombinant viruses P1 at a MOI of 200 (b). Equal loading was controlled with the detection of ACTB using ACTB anti sera.

triggered by the introduction of long (>30 bp) dsRNA into cells (Manche *et al.*, 1992; Song *et al.*, 2003). However, several studies pointed out the need for the validation of downstream effects mediated by siRNA as they showed that some siRNA could induced an interferon response (Bridge *et al.*, 2003; Sledz *et al.*, 2003) or off-target effect (Scacheri *et al.*, 2004).

Therefore, we investigated the level of mRNA expression of 2 proteins known to be upregulated in response to interferons: the signal transducers and activators of transcription (STAT1) and 2'-5' oligoadenylate synthetase 1 (OAS1). STAT1 is a mediator of interferon-induced signal in the JAK/STAT signalling pathway and a transcription factors which plays an important role in growth arrest and in promoting apoptosis (Bromberg and Darnell, Jr., 2000). OAS1 is an enzyme that catalyses the formation of oligoadenylate molecules that binds to and activated RNase L resulting in non-specific degradation of cellular RNA (Sledz *et al.* 2003).

6.4.2. Interferon response in Saos-2 and Huh7

In this experiment Saos-2 or Huh7 cells were treated for 1 h either with LMNA recombinant virus (mutant or WT), with serum free medium (untreated) or with conditioned media (Sf-900 II SFM preincubated with Sf-9 cells). After 2 days of growth, cells were harvested and the levels of LMNA, STAT1 and OAS1 mRNA of the different samples were determined by TaqMan PCR. Firstly, data shown in Figure 6.11. confirmed that in both cell lines, conditioned media, in which viruses were produced, had no effect on the cells compared to untreated samples. Neither did the mismatch recombinant virus on the LMNA RNA level, showing once again specificity of the shRNA mediated gene knockdown.

However, STAT1 mRNA level increased by 2 fold and OAS1 level by 5 to 10 fold in Saos-2 cells treated with the viruses compared to the corresponding mRNA level in untreated samples. This effect was not a consequence of LMNA inactivation *per se*, as suggested by the similar induction of STAT1 and OAS1 expression triggered by both WT and mismatch virus infections. In contrast, the interferon response was not activated in Huh7 cells as the expression of STAT1 and OAS1 did not change upon different treatments. This difference could be explained by a defective interferon response in Huh7 as suggested by Eguchi *et al.* studies (2000).

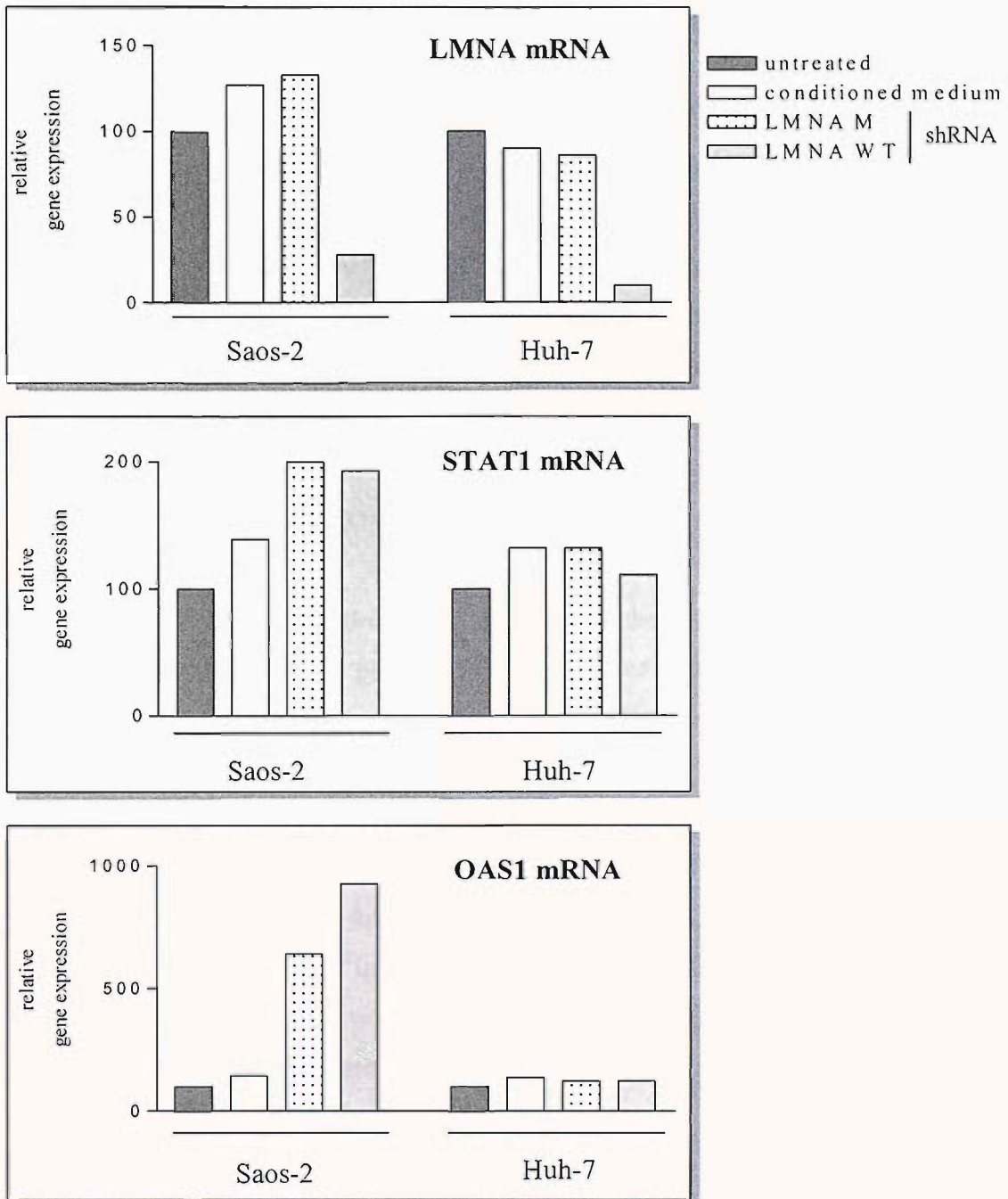


Figure 6.11. **Induction of OAS1 and STAT1 gene expression by recombinant baculovirus on Saos-2 or Huh7.** Cells were incubated for 1 h at 37°C with serum free medium (untreated), conditioned medium or P0 recombinant virus shRNA targeting either LMNA gene (WT) or LMNA gene containing 2 mismatches (M) at a MOI of 40. 2 days post transfection cells were harvested and RNA extract was prepared. 1 µg RNA was reverse transcribed into cDNA and 20 ng of cDNA was used as a template in TaqMan PCR with either LMNA, STAT1 or OAS1 specific primers and FAM probe. Gene expression was normalised with ACTB gene expression and calculated as relative expression to the control (serum free medium condition).

6.4.3. Interferon response in primary HSC

In a similar experiment, the expression of STAT1 and OAS1 was investigated in primary human HSC infected with LMNA recombinant viruses, WT or mismatch, and were compared to the level of STAT1 and OAS1 in untreated cells (Figure 6.12.). While LMNA shRNA knocked down efficiently and specifically the expression of LMNA in the cells, the presence of shRNA into the cells triggered the interferon response. Indeed STAT1 and OAS1 expression increased by 10 and 50 times respectively after incubation with the WT and mismatch viruses.

6.4.4. Mechanism of the siRNA mediated effects

Only a few studies had addressed the problem of the siRNA induced IFN-response, and the mechanism of this phenomenon was not yet clearly defined, although some evidence suggests that it was dependent on the siRNA sequence, their concentration and their method of delivery (Moss and Taylor, 2003). For instance, Bridge *et al.* (2003) showed that OAS1 expression induction was greater when the amount of siRNA delivered increased and Pebernard *et al.*, (2004) demonstrated that some of the effects were related to the U6 promoter. Indeed, shRNA driven by U6 promoter gave a higher induction of interferon-stimulated genes than the one under control of the H1 promoter. Whatever mechanism was underlying the effects, the need of careful validation of downstream effects was important, along with the development of new strategies to minimize the interferon response.

6.5. Conclusion

In order to clarify the role of RUNX in *TIMP1* gene regulation in HSC, we decided to develop a gene knockdown strategy using siRNA, a new powerful tool. However, transfection rate was still a limiting factor for the efficiency of gene silencing by siRNA, especially in primary cells. Previous work in our laboratory had shown that baculovirus were a good alternative to gene delivery in primary HSC compared to the chemical transfection methods. Therefore, in collaboration with Dr C. Dolphin team from King's college, London, we developed a new technology that coupled

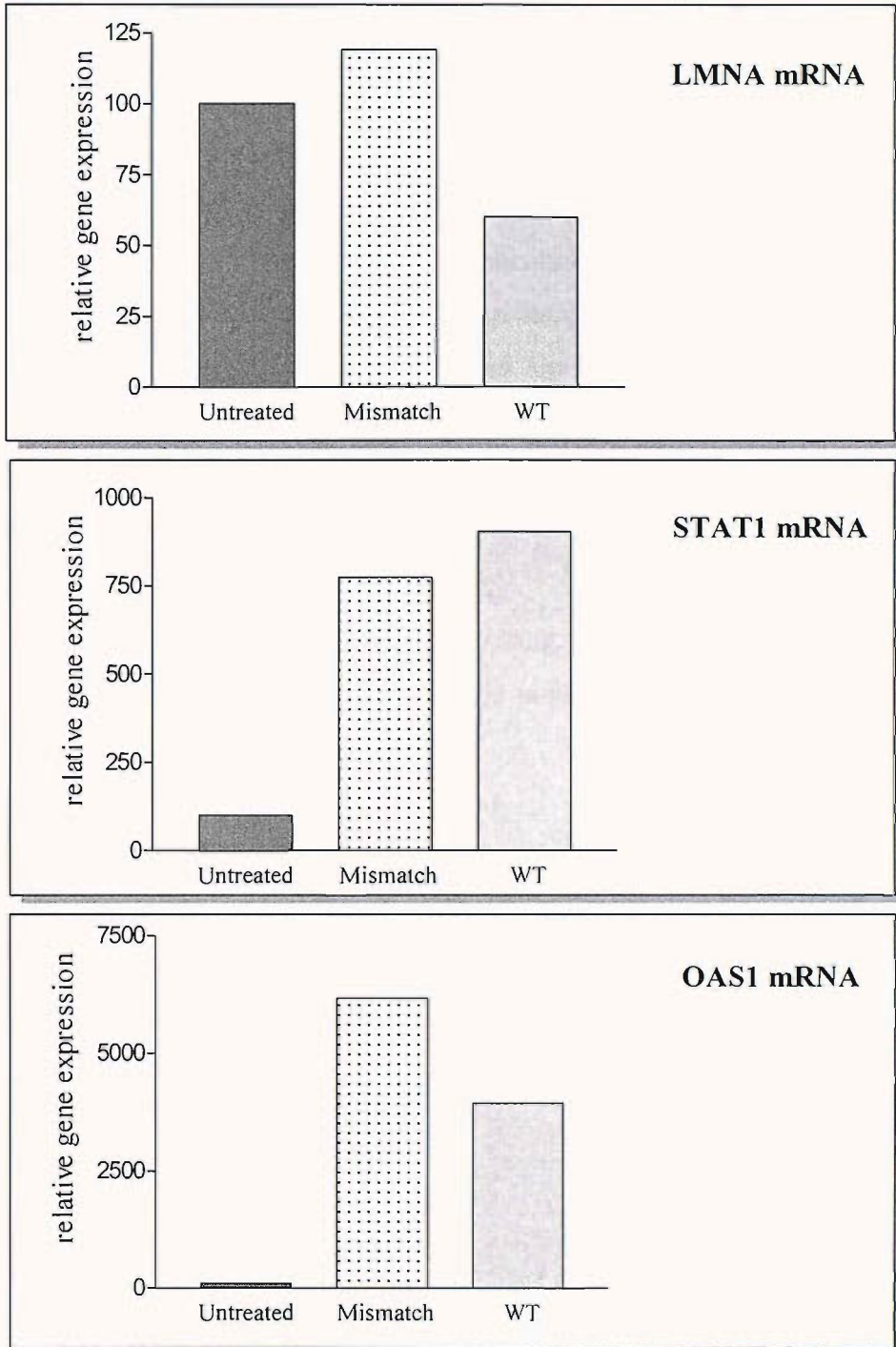


Figure 6.12. Induction of OAS1 and STAT1 gene expression by recombinant baculovirus on primary human HSC. Cells were incubated for 1 h at 37°C with serum free medium or P1 recombinant virus shRNA targeting either LMNA gene (WT) or LMNA gene containing 2 mismatches (M) at a MOI of 300. 2 days post transfection cells were harvested and RNA extract was prepared. 1 μ g RNA was reverse transcribed into cDNA and 20 ng of cDNA was used as a template in TaqMan PCR with either LMNA, STAT1 or OAS1 specific primers and FAM probe. Gene expression was normalised with ACTB gene expression and calculated as relative expression to the control (serum free medium condition).

two tools leading to siRNA delivery via recombinant baculovirus.

As a proof of principle, baculovirus expressing shRNA targeting LMNA gene were first constructed and successfully tested in several cell lines and in primary human HSC. Indeed more than 85 % LMNA knockdowns were measured in cell lines and 50 % in primary cells. Unfortunately the baculoviruses developed against RUNX turned out to be inefficient certainly due to an inappropriate targeted sequence of the shRNA. Another problem encountered was the detection of global interferon-stimulated genes in response to the intracellular presence of shRNA. Further experiments should focussed on the selection of efficient shRNA which also minimize the induction of non-specific gene along with the improvement of the delivery vector.

Overall, this new technology was very promising, but needs deeper investigation to improve the system. Certainly, this could be possible in the near future as siRNA technology is a rapidly expanding field.

Chapter 7

General discussion

Liver fibrosis is characterised by an excessive deposition of extracellular matrix (ECM) proteins within the liver, which disrupts its normal architecture and function leading to organ failure and death. The formation of fibrotic bands is the result of an increased production of ECM by Hepatic Stellate Cells (HSC) and its impaired degradation by Matrix metalloproteinases (MMP). The Tissue inhibitor of metalloproteinases (TIMP1), which inhibits MMP activity, is upregulated in fibrotic tissue, and therefore plays a critical role in the pathology of the disease. Understanding the regulation of *TIMP1* gene expression can lead to the characterisation of crucial transcription regulators of the fibrogenic process. Previous studies have already identified a key DNA binding element within the *TIMP1* promoter called UTE-1, essential for the promoter activity, which binds an unknown 30 kDa protein.

The aim of this thesis was to identify this protein in HSC, and to determine its role in the control of *TIMP1* expression.

Using the One-Hybrid system, we determined that the UTE-1 DNA element was recognised by the members of the RUNX transcription factor family which includes RUNX1, RUNX2 and RUNX3. While these factors bind to a common DNA motif, which matches perfectly the UTE-1 sequence, each RUNX specifically controls the expression of genes involved in hematopoiesis (RUNX1), osteogenesis (RUNX2) or neurogenesis and gastric cancer (RUNX3). Their intrinsic ability to affect promoter activity is weak. However, they act as organizing factors which recruit other transcription factors and co-factors forming an enhanceosome that drives transcription. The gene transcription specificity of RUNX is in part due to tissue specific expression of the different factors. To assess which RUNX is involved in *TIMP1* expression during liver fibrosis, we next investigated the presence and functionality of the different RUNX proteins in human and rat HSC and monitored the change of expression of the main variants in cultured activated rat HSC.

RT-PCR and Western blot revealed the presence of different spliced forms of RUNX1 and RUNX2 at the RNA and protein levels, whereas RUNX3 RNA expression was downregulated upon activation of HSC. In addition, post-transcriptional and post-translational regulation might occur, as the variation in protein expression upon activation was not detectable at a RNA level. The presence

of endogenous RUNX1 that binds to UTE-1 in rat and human activated HSC was confirmed by a supershift EMSA, whereas functional endogenous RUNX2 was only detectable in rat activated HSC. Moreover, ChIP experiments confirmed that RUNX1 but not RUNX2 was associated with the *TIMP1* promoter *in situ*. According to the experiments, RUNX1 appeared to be the functional protein expressed in HSC whereas the importance of RUNX2 was not demonstrated due to technical limitations (i.e. antibody likely to be not suitable for supershift EMSA and ChIP experiments). Further investigations need to be carried out using new developed antibody to draw clear conclusions regarding the specificity of expression of endogenous RUNX2. Meanwhile, the influence of RUNX1 and RUNX2 on *TIMP1* promoter activity was assessed by reporter gene assays.

Overexpression of RUNX1A (a short isoform of RUNX1) increased *TIMP1* promoter activity when overexpressed in HeLa and culture-activated rat HSC, whereas RUNX1B (the main variant of RUNX1) acted as an inhibitor of transcription. Moreover, as the RUNX and AP1 binding sites are in close proximity within the *TIMP1* promoter, we also looked at the influence of RUNX on JunD-induced *TIMP1* promoter activation. RUNX1A did not affect the JunD-induced activation of the *TIMP1* promoter activity while RUNX1B blunted it. Interestingly, immunoprecipitation experiments indicated that JunD interacted with RUNX1A but not RUNX1B and this loss of interaction correlated with the specific inhibitory effect of RUNX1B on JunD-induced transcription. Hence, these data suggested that RUNX1B contained a C-terminal region that was responsible for the inhibition of both transcription and interaction with JunD.

We next investigated the effect of MOZ and CBP, two histones acetyl transferases that are known to interact with RUNX1B and enhanced its induction of several promoters. Interestingly, RUNX1B reduced MOZ-induced transcription and synergistic activation of MOZ and JunD on the *TIMP1* promoter. Recently, it has been shown that a non phosphorylated form of RUNX1B is associated with mSin3, a co-repressor of transcription, and that the phosphorylation of RUNX1B results in the dissociation of mSin3 from RUNX1B. This could explain the inhibitory effect of RUNX1B on the *TIMP1* promoter detected under our experimental conditions suggesting that RUNX1B might recruit a co-repressor within the *TIMP1* promoter. Moreover the association of mSin3 with RUNX1B could prevent the interaction of

JunD with RUNX1B as supported by the fact that RUNX1A interacts with JunD, but not mSin3. In the same way, MOZ cannot interact with RUNX1B due to the presence of the co-repressor. In contrast, CBP and RUNX1B synergistically activate *TIMP1* promoter activity. As RUNX1B interacting domains with CBP and mSin3 are overlapping, a competition between the two cofactors for the binding with RUNX1B can occur with a higher affinity for CBP under our experimental conditions.

Several experiments need to be carried out to confirm this model. For example, the effect of phosphorylation of RUNX1B on its ability to drive the *TIMP1* promoter or to interact with JunD or MOZ has to be investigated. The effect of RUNX1A, which does not bind mSin3, on MOZ-induced transcription still needs to be characterised. Moreover, the JunD/MOZ interaction has not been demonstrated yet. Finally, it would be interesting to look at the effect of the simultaneous presence of JunD, MOZ, RUNX1B and CBP on *TIMP1* promoter activity. All these experiments would give us a better understanding of the regulation of *TIMP1* by RUNX1B.

Less evidence has been gathered regarding the role of RUNX2 on *TIMP1* transcription. An induction of the *TIMP1* promoter activity by RUNX2 has been detected, suggesting that, unlike RUNX1B, it does not recruit any co-repressor to the promoter. However, the activation was modest, and this can be explained by the fact that RUNX2 is more active when phosphorylated as shown by other studies. This hypothesis still needs to be investigated in the context of the *TIMP1* promoter. The absence of a cooperative effect between RUNX2 and JunD on the *TIMP1* promoter activity was surprising, but correlated with a lack of physical interaction between the two proteins. The investigation of functional interplay of RUNX2 with other members of the AP-1 family may help understanding the way RUNX2 regulates *TIMP1* expression.

Overall, our data suggest that the influence of RUNX2 and RUNX1 on *TIMP1* transcription does not involve the same mechanism since interactions with different factors and coregulators might take place. As both RUNX1B and RUNX2 are expressed in activated rat HSC, the level of *TIMP1* transcription could depend on the balance between RUNX proteins present at the promoter. RUNX expression has been shown to be controlled by different extracellular signals such as TGF β , BMP

and FGF2. Therefore, the effect of these growth factors on RUNX expression in HSC should be determined in order to see whether these factors could affect the ratio between RUNX1 and RUNX2 present in HSC.

The reporter gene assay is a rapid method to investigate the role of RUNX on the *TIMP1* promoter, but presents some disadvantages as it is limited by the amount of transfected DNA and by the cell transfection rate. An alternative approach to understand the role of RUNX on *TIMP1* promoter activity was to work on the endogenous gene by inhibiting *RUNX* gene expression, and to analyse the effect of the absence of RUNX in the cells.

Small interfering RNA (siRNA) targeting the *RUNX2* gene or *LMNA* gene (Lamin), as a control gene, were introduced into HSC using baculovirus vectors in order to overcome the problem of transfection efficiency. Although the knock down of LMNA was successful using this new technology, the silencing of the *RUNX2* gene expression was not achieved, probably due to an inappropriate targeted sequence of the siRNA. New bioinformatics tools are currently being developed for choosing efficient target sequences. Therefore, a preliminary screening of several potential targets selected via these programs should be performed before construction of new recombinant baculoviruses. Another problem that needs to be addressed is the induction of interferon-stimulated genes due to the presence of siRNA, which can lead to misinterpretation of the effect of RUNX silencing on the expression of other genes. For instance, we showed that STAT1 expression is induced when siRNA is introduced in the cells. This protein has been previously shown to interact with RUNX2 and downregulates its activity. Therefore, the knockdown of RUNX1 gene could also affect the activity of RUNX2, and the subsequent effects monitored would not be RUNX1 specific. However, siRNA is a new promising biologic tool, and a lot of effort by different groups focuses on the improvement of this new technology. Unfortunately, at the time of the study, we were unable to add further information on RUNX influence on *TIMP1* expression using siRNA.

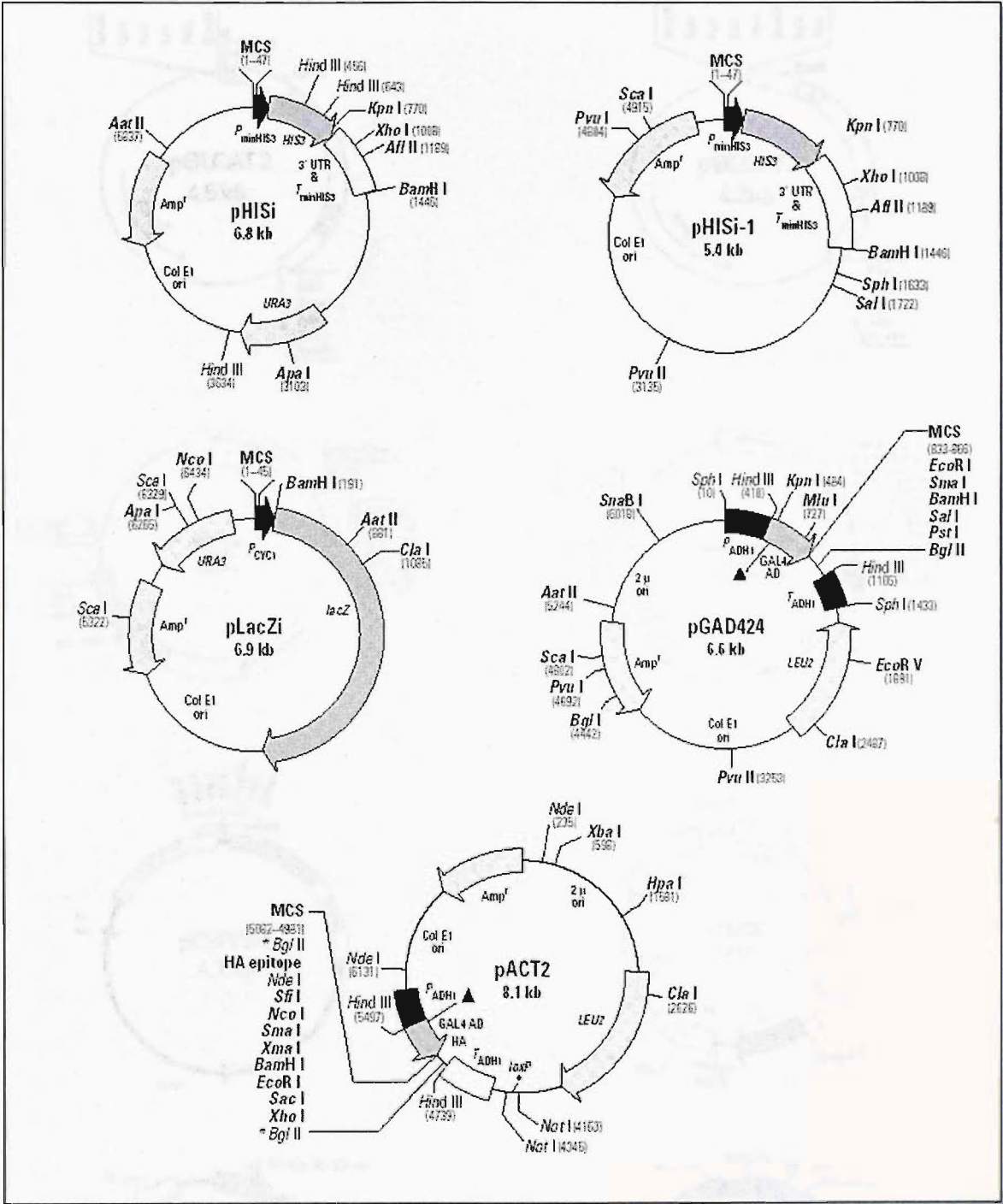
Taken together, our data strongly suggest that UTE-1 is recognised by RUNX proteins, and therefore RUNX factors are involved in the control of *TIMP1* expression in HSC. Interestingly, *RUNX* expression is regulated by TGF β and FGF,

which are upregulated in fibrotic liver and induced *TIMP1* gene expression. These factors may increase RUNX expression that then act on *TIMP1* expression. In addition, RUNX proteins have been shown to increase *collagen-1*, and *TGF β receptor 1* gene expression resulting in the accumulation of the ECM and increasing the cellular response to TGF β . Moreover, the activity of RUNX is enhanced by phosphorylation induced by cytokines such as IGF α and FGF, but also by changes in the ECM. Concurrently, these cytokines are released by activated HSC and injured hepatocytes during liver fibrosis, not to mention ECM modifications.

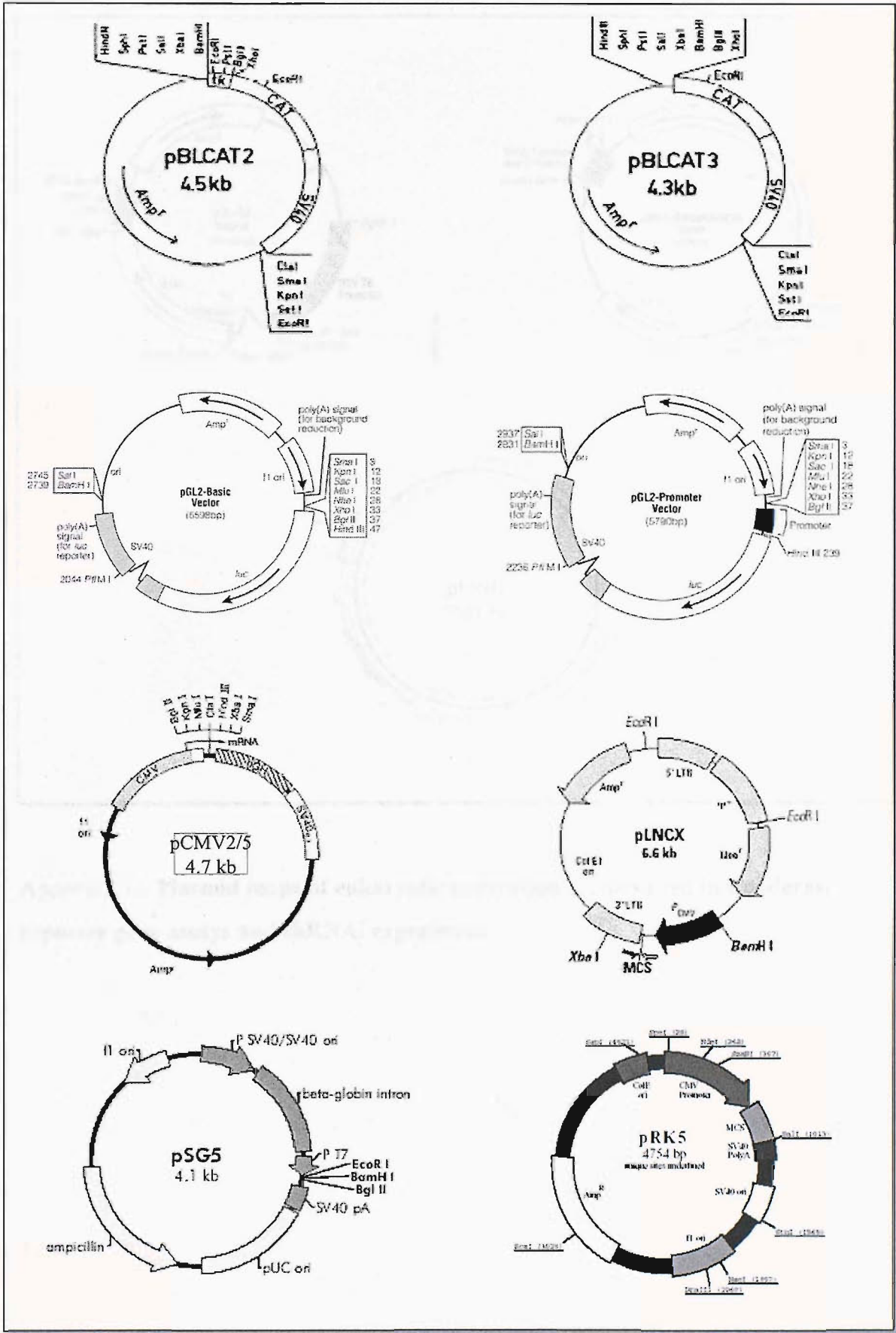
Further investigations are needed to complete the mechanism by which *TIMP1* gene expression is regulated. It is important to move away from reporter gene assay experiments as the role of RUNX as an organizer of the enhanceosome can not be fully understood via these methods. ChIPs assay may identify which factors are recruited within the *TIMP1* promoter in HSC. More importantly, this study is lacking an *in vivo* approach, although the use of knockout mice was not possible since they are not viable. However, a mice model of *in vivo* imaging of NF- κ B activity has been developed by a Norwegian group where transgenic mice express luciferase under control of NF- κ B. It would be interesting to use this technology to detect expression of RUNX in the liver and to determine the influence of TGF β or other cytokines on the expression pattern of RUNX in intact animals. Collaborative work with this Norwegian group should be set up in order to develop transgenic mice expressing luciferase gene under control of RUNX.

The identification of RUNX as the UTE-1 binding protein is a step towards the understanding of *TIMP1* regulation and the fibrosis process. For the first time, we have established a link between TIMP1 and RUNX, two key proteins involved in cancer, thus opening a new exciting area of research.

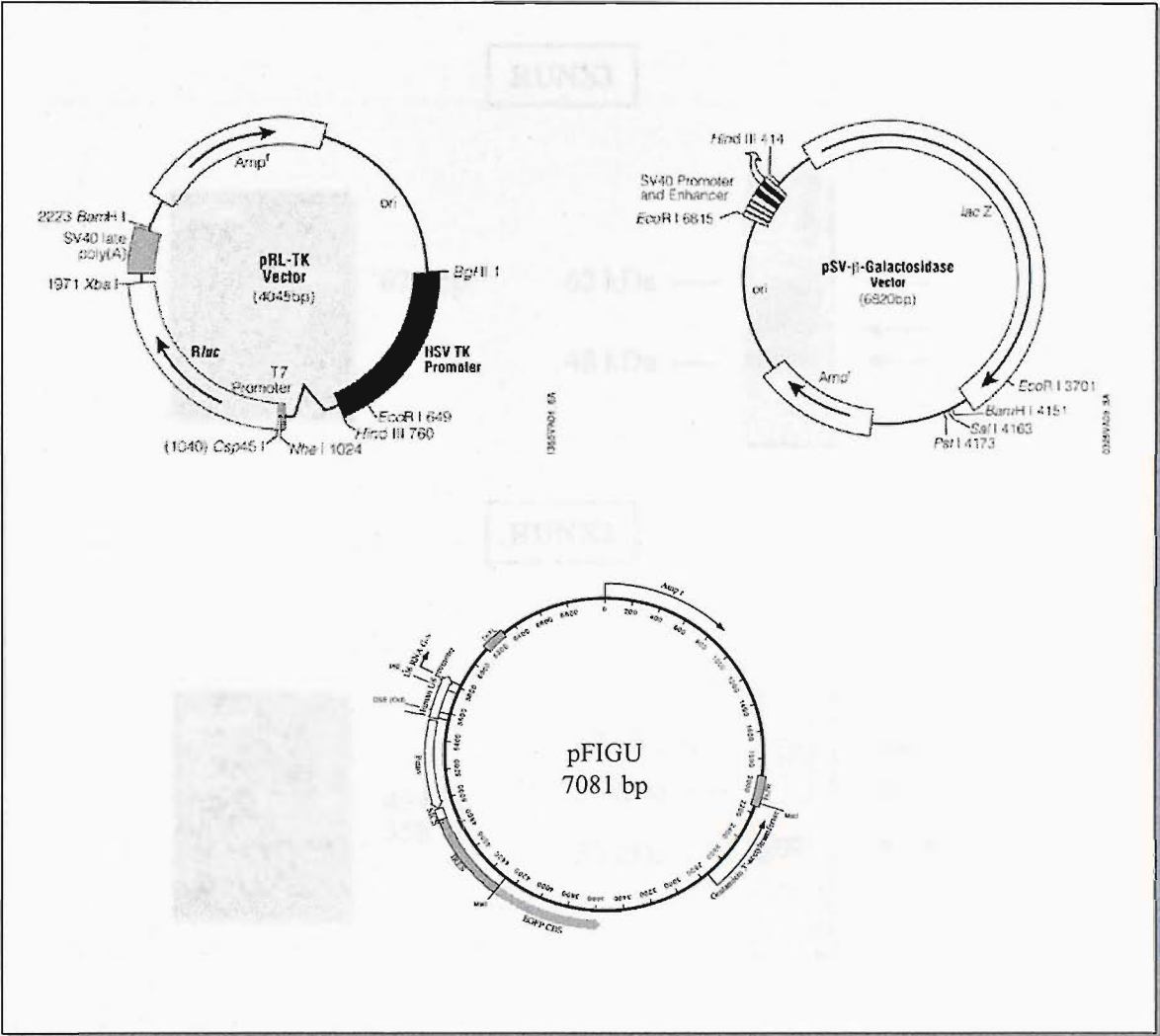
Appendices



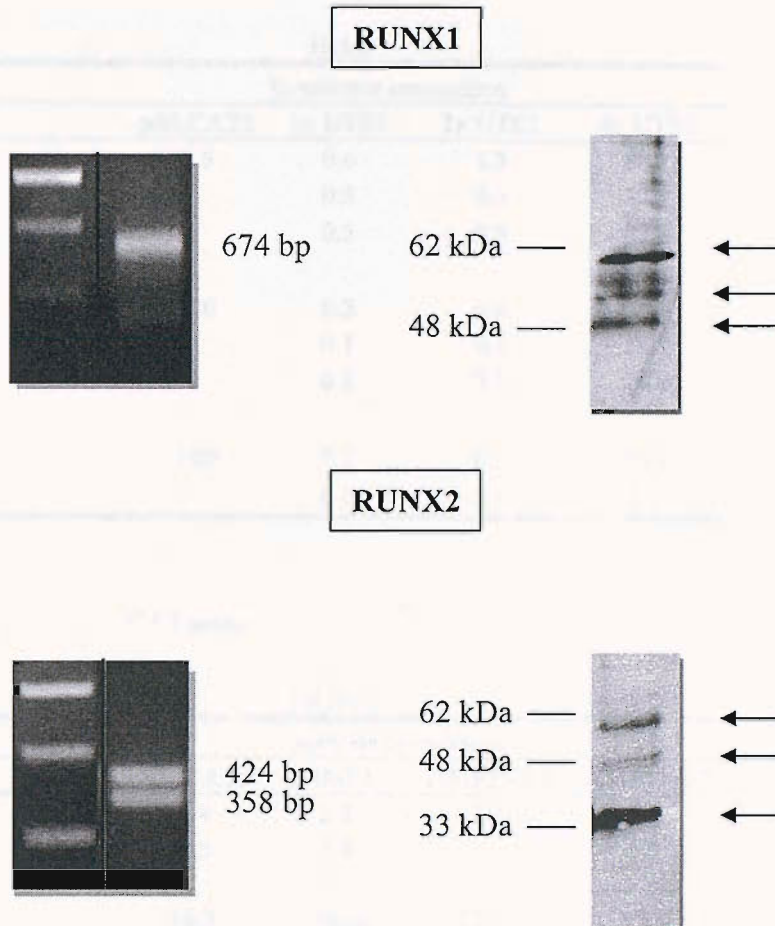
Appendix 1a. Plasmid maps of vectors used in the One-Hybrid System.



Appendix 1b. Plasmid maps of eukaryotic expression vectors used in CAT, Luciferase reporter gene assays and immunoprecipitation experiments.



Appendix 1c. **Plasmid maps of eukaryotic expression vectors used in Luciferase reporter gene assays and shRNAi experiments.**



Appendix 2. Expression of RUNX1 and RUNX2 in LX2 cells. cDNA was synthesised from RNA extracted from LX2 cells and PCR were performed using specific primers for *RUNX1* or *RUNX2* genes. PCR were run for 40 cycles at 60°C and 61°C. PCR products were run on an 1 % (w/v) agarose gel and visualized by ethidium bromide staining. Whole cell protein extracts (20 µg) prepared from LX2 cells were used for SDS-PAGE and immunoblot detection of RUNX1 using an anti-RUNX1 antisera and RUNX2 using an anti-RUNX2 antisera.

Figure 3.3. CAT assay

HeLa				
% substrate conversion				
	pBLCAT2	1x UTE1	2x UTE1	4x UTE1
	3.5	0.6	1.3	88.7
		0.5	0.5	87.2
		0.5	0.5	83.8
relative	100	0.2	0.4	25.3
data		0.1	0.1	24.9
		0.1	0.1	24.0
mean	100	0.2	0.2	24.7
stderror		0.0	0.1	0.5

Figure 3.8. CAT assay

rat HSC				
% substrate conversion				
	pBLCAT3	TIMP1	TIMP1+A/1	TIMP1+A/2
	0.4	2.4	3.3	0.9
	0.5	2.4		1.2
relative	16.7	100.0	137.5	37.5
data	20.8	100.0		50.0
mean	18.7	100.0	137.5	43.8
stderror	1.4			4.2

Cos-1				
% substrate conversion				
	pBLCAT3	TIMP1	TIMP1+A/1	TIMP1+A/2
	0.3	26.1	25.9	9.6
	1.0	16	9.8	3.2
relative	1.1	100	99.2	36.8
data	6.3	100	61.2	20
mean	3.7	100	80.2	28.4
stderror	2.6	0	19	8.4

Figure 5.1. Luciferase assay

pTIMP1-Luc	RLU	RLU	mean	std error
0 µg	48	55.1	51.6	3.6
0.25 µg	872.5	949.6	911.1	38.6
0.5 µg	2709	2557.7	2633.4	75.7
0.75 µg	4370.3	5254.7	4812.5	442.2
1 µg	6267.7	6821.7	6544.7	277.0

Figure 5.2. CAT assay

Eff DNA	TIMP1-CAT								
	0.25 µg			0.5 µg			0.1 µg		
	% substrate conversion			% substrate conversion			% substrate conversion		
	HeLa	Cos-1	rHSC	HeLa	Cos-1	rHSC	HeLa	Cos-1	rHSC
1:10	2.9	1.6	1.4	38.4	5.8	5.2	59.5	61.2	4
	1.9	1.3	3.6	12.4	9.6	3	56.2	54.1	4.3
mean	2.4	1.5	2.5	25.4	7.7	4.1	57.9	57.7	4.2
std error	0.5	0.2	1.1	13	1.9	1.1	1.7	3.6	0.2
1:25	2.8	0.8	2.1	24.7	13.6	6.2	66.7	66.7	3.5
	2.5	1	2.2		7.6		68.7		4.9
mean	2.7	0.9	2.2	24.7	10.6	6.2	67.7	66.7	4.2
std error	0.2	0.1	0.1	0.0	3.0	0.0	1.0	0.0	0.7
1:50	2.6	1.1	2.1	26	17.5	7.1	31.8	13.8	4.4
	2.8	0.7	1	23	18.6	7.3	30.1	22.1	2.2
mean	2.7	0.9	1.6	24.5	18.05	7.2	31.0	18.0	3.3
std error	0.1	0.2	0.6	1.5	0.6	0.1	0.9	4.2	1.1

Figure 5.4. Luciferase, renilla and β galactosidase assays

RUNX1B	exp1				exp2			
	Luc	%	β gal	%	Luc	%	β gal	%
0 μ g	40.9	100	0.89	100	41.5	100	0.9	100
0.5 μ g	42.7	104	0.61	69	39.45	95	0.6	67
1 μ g	25.0	61	0.45	51	32.75	79	0.45	51
1.5 μ g	18.5	45	0.35	39	22.05	53	0.32	36

RUNX1B	mean		std error	
	Luc		β gal	
0 μ g	100.0	0.0	100.0	0.0
0.5 μ g	99.7	4.7	68.0	0.6
1 μ g	70.0	8.9	50.6	0.0
1.5 μ g	49.1	4.0	37.6	1.7

RUNX2	exp1				exp2			
	Luc	%	Ren	%	Luc	%	Ren	%
0 μ g	5.3	100	75	100	6.5	100	77	100
1 μ g	7.8	147.4	95.4	127.2	8.4	129.5	67	87.0
1.5 μ g	15.4	289.6	125	166.7	14.9	231.0	108.8	141.3
2 μ g	27.1	511.3	165	220	38.1	589.9	265.7	345.1

RUNX2	mean		std error	
	Luc		Ren	
0 μ g	100.0	0.0	100.0	0.0
1 μ g	138.4	9.0	107.1	20.1
1.5 μ g	260.3	29.3	154.0	12.7
2 μ g	550.6	39.3	282.5	62.5

Figure 5.5. Luciferase assay

	pTIMP1-Luc WT		pTIMP1-Luc Mutant	
	RLU	%	RLU	%
exp1	76	100	37.1	48.8
exp2	60	100	38.4	64.0
exp3	23.2	100	12.4	53.4
mean		100		55.4
stderror				5.7

CAT assay

	pTIMP1-CAT WT		pTIMP1-CAT Mutant	
		%		%
exp1	12.8	100	8.7	68.0
exp2	52.7	100	38.4	72.9
exp3	47.1	100	28.5	60.5
mean		100		67.1
stderror				4.4

Figure 5.6. Luciferase assay HeLa cells

pTIMP1 WT		exp1		exp2		exp3		exp4	
RUNX1B	RLU	%	RLU	%	RLU	%	RLU	%	
0 µg	13.4	100.0	21.2	100.0	40.8	100.0	41.5	100.0	
0.5 µg	14	104.5	16.1	75.9	42.7	104.7	39.5	95.2	
1 µg	5.5	41	8.4	39.6	25	61.3	32.7	78.8	
1.5 µg	2.6	19.4	4.8	22.6	18.4	45.1	22.1	53.3	
2 µg	0.9	6.7	2.1	9.9					

pTIMP1 mutated		exp1		exp2		exp3	
RUNX1B	RLU	%	RLU	%	RLU	%	
0 µg	2.8	100.0	2.2	100.0	47.5	100.0	
2 µg	5.3	189.0	4.2	191	114.1	240.0	

pTIMP1 WT			pTIMP1 mut	
RUNX1B	mean	std error	mean	std error
0 µg	100.0	0.0	100.0	0.0
0.5 µg	95.1	9.6	n/a	n/a
1 µg	55.2	14.9	n/a	n/a
1.5 µg	35.1	14.1	n/a	n/a
2 µg	8.3	1.6	206.7	22.2

pTIMP1 WT		exp1		exp2	
RUNX1A	RLU	%	RLU	%	
0 µg	15.4	100.0	13.4	100.0	
0.5 µg	17.1	111	18	134.3	
1 µg	20.1	130.5	26.6	198.5	
1.5 µg	24.6	159.7	17.6	131.3	

pTIMP1 mutated		exp1		exp2		exp3	
RUNX1A	RLU	%	RLU	%	RLU	%	
0 µg	2.8	100.0	2.2	100.0	12.4	100.0	
1.5 µg	2.6	92.8	2.5	113.6	9.6	77.4	

pTIMP1 WT			pTIMP1 mut	
RUNX1A	mean	std error	mean	std error
0 µg	100.0	0.0	100.0	0.0
0.5 µg	122.7	11.7	n/a	n/a
1 µg	164.5	34.0	n/a	n/a
1.5 µg	145.5	14.2	94.6	12.7

Figure 5.6. CAT assay rat HSC

pTIMP1 WT		exp1		exp2		exp3	
RUNX1B	% conv.	%	% conv.	%	% conv.	%	
0 µg	49.6	100.0	3.8	100.0	41.6	100.0	
0.5 µg	26.3	53.0	1.8	47.4	32.4	77.9	
1 µg	22.6	45.6	1.4	36.8	26.8	64.4	
1.5 µg	19.4	39.1			23.2	55.8	
2 µg	12.7	25.6	1.6	42.1			

pTIMP1 mutated		exp1		exp2	
RUNX1B	% conv.	%	% conv.	%	
0 µg	22.2	100.0	28.5	100.0	
2 µg	22.4	101.0	18	63.2	

pTIMP1 WT			pTIMP1 mutated	
RUNX1B	mean	std error	mean	std error
0 µg	100.0	0	100.0	0.0
0.5 µg	59.4	12.3	n/a	n/a
1 µg	48.9	10.3	n/a	n/a
1.5 µg	47.5	8.4	n/a	n/a
2 µg	33.9	8.3	82.1	18.9

pTIMP1 WT		exp1		exp2	
RUNX1A	% conv.	%	% conv.	%	
0 µg	1.9	100.0	100.0	100.0	
0.5 µg	2.3	121.1	121.1	188	
1 µg	2.8	147.4	147.4	207.5	
1.5 µg	3.5	184.2	184.2	175	
2 µg	5.0	263.1	263.1	170	

pTIMP1 mutated		exp1		exp2	
RUNX1A	% conv.	%	% conv.	%	
0 µg	22.2	100.0	28.5	100.0	
2 µg	8.5	38.0	14.0	49.0	

pTIMP1 WT			pTIMP1 mutated	
RUNX1A	mean	std error	mean	std error
0 µg	100.0	0.0	100.0	0.0
0.5 µg	154.6	33.5	n/a	n/a
1 µg	177.5	30.1	n/a	n/a
1.5 µg	179.6	4.6	n/a	n/a
2 µg	216.6	46.6	43.5	5.5

Figure 5.7. Luciferase assay HeLa cells

pTIMP1 WT		exp1		exp2		exp3	
RUNX2	RLU	%	RLU	%	RLU	%	
0 µg	5.3	100.0	15.4	100.0	15.4	100.0	
0.5 µg	8.4	158.5	21.95	142.5	20.4	132.5	
1 µg	7.8	147.2	26.25	170.5	21.85	141.9	
1.5 µg	15.35	289.6	31.8	206.5	34.1	221.4	
2 µg	27.1	511.3	32.85	213.3	53.3	346.1	

pTIMP1 mutated		exp1		exp2		exp3	
RUNX2	RLU	%	RLU	%	RLU	%	
0 µg	2.7	100.0	12.6	100.0	12.6	100.0	
2 µg	3.85	142.6	13.8	109.5	16.6	131.2	

pTIMP1 WT			pTIMP1 mutated	
RUNX2	mean	std error	mean	std error
0 µg	100.0	0.0	100.0	0.0
0.5 µg	144.5	9.3	n/a	n/a
1 µg	153.2	11.5	n/a	n/a
1.5 µg	239.2	33.6	n/a	n/a
2 µg	356.9	102.9	127.8	12.2

CAT assay rat HSC

pTIMP1 WT		exp1		exp2		exp3	
RUNX2	% conv.	%	% conv.	%	% conv.	%	
0 µg	3.8	100.0	41.6	100.0	49.6	100.0	
0.5 µg	2.8	73.7	42.5	102.2	60.6	122.2	
1 µg	4.1	107.9	65	156.3	63.3	127.6	
1.5 µg			59.1	142.1	65.1	131.3	
2 µg	6.8	178.9			56.9	114.7	

pTIMP1 mutated		exp1		exp2	
RUNX2	% conv.	%	% conv.	%	
0 µg	29.7	100.0	28.5	100.0	
2 µg	30.1	113.7	31.6	111.0	

pTIMP1 WT			pTIMP1 mutated	
RUNX2	mean	std error	mean	std error
0 µg	100.0	0.0	100.0	0.0
0.5 µg	99.3	17.1	n/a	n/a
1 µg	130.6	17.1	n/a	n/a
1.5 µg	136.7	5.4	n/a	n/a
2 µg	146.8	32.1	112.4	1.4

Figure 5.8. Luciferase assay HeLa cells

	exp1		exp2		exp3	
	RLU	%	RLU	%	RLU	%
pTIMP1 WT	9.5	12.4	23.5	21.7	13.6	26.8
JunD	76.7	100.0	106.8	100.0	50.8	100.0
JunD +RUNX1B	17.7	22.8	37.9	35.0	29.0	57.1
pTIMP1 mutated	12.1	20.6	12.4	22.5	7.9	8.5
JunD	58.8	100.0	55.1	100.0	92.0	100.0
JunD +RUNX1B	72.4	123.0	69.5	126.0	175	190.0
pTIMP1 WT	50.4	32.5	23.5	21.7	13.6	26.8
JunD	155.1	100.0	106.8	100.0	50.8	100.0
JunD +RUNX1A	239.5	154.4	144.3	135.1	76	149.6

	mean	std error
pTIMP1 WT	20.3	5.3
JunD	100.0	0.0
JunD +RUNX1B	38.3	12.5
pTIMP1 mutated	17.2	5.8
JunD	100.0	0.0
JunD +RUNX1B	146.3	29.1
pTIMP1 WT	27.0	3.7
JunD	100.0	0.0
JunD +RUNX1A	146.4	7.5

Figure 5.8. CAT assay rHSC

	exp1		exp2		exp3	
	% conv.	%	% conv.	%	% conv.	%
pTIMP1 WT	4.0	17.6	45.7	67.3	41.6	76.2
JunD	22.7	100	67.9	100	54.6	100
JunD +RUNX1B	10.8	47.6	30.3	44.6	26.4	48.4
pTIMP1 mutated	8.7	77.7	22.5	42.7	28.5	61.8
JunD	11.2	100.0	52.0	100.0	46.1	100.0
JunD +RUNX1B	11.5	102.7	35.2	67.7	39.3	85.2
pTIMP1 WT	39.3	72.0	4.0	20.1	49.6	73.0
JunD	67.2	100.0	19.9	100.0	67.9	100.0
JunD +RUNX1A	52.1	95.4	19.2	96.5	59.5	87.6

	mean	std error
pTIMP1 WT	53.7	24.1
JunD	100.0	0.0
JunD +RUNX1B	46.9	1.5
pTIMP1 mutated	60.7	12.0
JunD	100.0	0.0
JunD +RUNX1B	85.2	11.7
pTIMP1 WT	55.0	23.3
JunD	100.0	0.0
JunD +RUNX1A	93.2	3.7

Figure 5.9. Luciferase assay HeLa cells

	expl		exp2		exp3	
	RLU	%	RLU	%	RLU	%
pTIMP1 WT	20.4	13.5	50.4	32.5	36.8	23.1
JunD	150.8	100.0	155.1	100.0	159.2	100.0
JunD +RUNX2	193.2	128.1	213.4	137.4	230.7	144.9
pTIMP1 mutated	12.1	20.6	12.6	31.6	12.4	22.5
JunD	58.8	100.0	39.8	100.0	55.1	100.0
JunD +RUNX2	46.2	78.6	30.7	77.1	35.6	64.6

	mean	std error
pTIMP1 WT	23.0	6.4
JunD	100.0	0.0
JunD +RUNX2	136.8	5.8
pTIMP1 mutated	24.9	4.5
JunD	100.0	0.0
JunD +RUNX2	73.4	5.9

CAT assay rHSC

	expl		exp2		exp3	
	% conv.	%	% conv.	%	% conv.	%
pTIMP1 WT	4.0	17.6	49.6	73	1.3	68.4
JunD	22.7	100	67.9	100	1.9	100
JunD +RUNX2	28.7	126.4	67.7	99.7	2.3	121.1
pTIMP1 mutated	22.2	42.7	28.5	61.8		
JunD	52	100.0	46.1	100.0		
JunD +RUNX2	55.8	107.3	41.4	89.8		

	mean	std error
pTIMP1 WT	53.0	23.6
JunD	100.0	0.0
JunD +RUNX2	115.7	10.7
pTIMP1 mutated	52.3	9.6
JunD	100.0	0.0
JunD +RUNX2	98.6	8.8

Figure 5.11. Luciferase assay HeLa cells

a.

	exp1		exp2	
	RLU	%	RLU	%
pTIMP1 WT	36.8	41.2	50.4	65.2
MOZ	89.2	100	77.3	100
RUNX1B	14.3	16.0	14.7	19.0
MOZ + RUNX1B	35.5	39.8	16.6	21.5
MOZ + RUNX1A	234	262.3	239.5	309.8
MOZ + RUNX2	76.4	85.6	87.3	112.9

	mean	std error
pTIMP1 WT	53.2	12
MOZ	100	0.0
RUNX1B	17.5	1.5
MOZ + RUNX1B	30.7	9.2
MOZ + RUNX1A	286.1	23.8
MOZ + RUNX2	99.3	13.7

b.

	exp1		exp2	
	RLU	%	RLU	%
pTIMP1 WT	13.7	39.7	50.4	62.6
MOZ	34.2	100	80.5	100
RUNX1B	12.2	35.7	14.7	18.3
JunD	47.8	139.8	155.5	193.2
MOZ + JunD	243.8	712.9	289.2	359.3
MOZ + JunD+	29.7	86	34.9	43.4
RUNX1B				

	mean	std error
pTIMP1 WT	51.15	11.45
MOZ	100	0.0
RUNX1B	27	8.7
JunD	166.5	26.7
MOZ + JunD	536.1	176.8
MOZ + JunD+	64.7	21.3
RUNX1B		

Figure 5.12. Luciferase assay HeLa cells

	exp1		exp2	
	RLU	%	RLU	%
pTIMP1 WT	55.6	100	13.6	100
CBP	86.6	155.7	40.8	300
RUNX1B	80	144	9.8	72.1
CBP+RUNX1B	372	669.1	75.1	552.2

	mean	std error
pTIMP1 WT	100	0.0
CBP	227.9	72.2
RUNX1B	108.1	36.0
CBP+RUNX1B	610.7	58.5

Figure 6.4. TaqMan efficiency

		LMNA		
cDNA (ng) Log (cDNA)		Ct		
30	1.5	19.581	19.388	19.298
10	1	21.137	20.981	21.223
5	0.7	21.995	22.25	22.37
0.5	-0.3	25.889	26.054	25.956
0.05	-1.3	29.667	29.459	30.122
0.005	-2.3	33.476	33.233	33.057

		STAT1		
cDNA (ng) Log (cDNA)		Ct		
30	1.5	26.901	26.384	
10	1	29.308	29.166	
1	0	33.299	33.589	33.407
0.1	-1	35.406	36.524	36.284

		OAS1	
cDNA (ng) Log (cDNA)		Ct	
10	1	29.859	30.081
1	0	33.558	34.356
0.5	-0.3	35.303	34.42
0.1	-1	37.574	37.731

Figure 6.5. TaqMan Huh7/Saos-2

Ct				
Huh7			Saos-2	
	cond.	media virus	cond.	media virus
LMNA	22.131	21.904	20.761	20.033
	22.057		21.472	20.104
			21.449	20.116
%	100	95	100	104
ACTB	19.191	18.547	20.09	19.335
	18.369	18.323	20.617	19.181
	18.679	18.368	20.077	19.001

Figure 6.6. TaqMan Huh7

Ct								
	Mismatch	day2			Mismatch	day4		
		0.4	4	40		0.4	4	40
LMNA	20.574	22.426	22.516	24.191	20.743	20.804	22.489	23.531
	20.486	22.55	23.083	23.984	20.936	21.176	22.363	22.471
	20.669	22.298	22.534	23.738	21.096	20.727	23.87	23.505
ACTB	16.616	18.42	17.033	17.26	17.941	17.204	17.5	17.252
	17.079	18.449	16.631	17.153	17.515	17.25	17.142	17.229
	17.077	19.204	17.102	17.13	17.86	17.37		17.459
%	100	93	26	14	100	75	22	15

Figure 6.7. TaqMan Saos-2

Ct								
	Mismatch	day2			Mismatch	day4		
		0.4	4	40		0.4	4	40
LMNA	19.347	21.021	22.831	24.894	19.859	20.354	23.204	24.223
	19.402	21.102	22.836	24.722	20.087	20.314	22.844	24.202
	19.582	20.783	23.063	24.384	20.085	20.215	23.067	24.199
ACTB	19.295	19.153	17.976	19.262	18.181	18.376	19.118	18.539
	19.151	19.588	17.889	18.527	18.029	18.416	19.062	18.83
	19.278	19.024	18.243	18.462	18.246	18.572	19.072	18.296
%	100	39	5	3	100	101	27	9

Figure 6.8. TaqMan LX2

Ct						
	Mismatch	day2		Mismatch	day4	
		0.4	40		0.4	40
LMNA	24.076	23.036	24.431	24.142	26.309	24.72
	24.104	24.003	24.363	24.528	26.258	24.804
ACTB	33.2	31.661	32.71	33.064	34.641	33.157
	33.834	32.222	33.201	33.01	34.343	33.104
%	100	73	58	100	72	81

Figure 6.9. TaqMan human HSC

Ct						
	Mismatch	expl		Mismatch	exp2	
		150	300		150	300
LMNA	20.47	21.517	21.316	23.116	22.689	23.335
	20.815	21.655	21.329	23.067	22.566	23.587
ACTB	18.689	18.795	18.602	20.441	19.623	20.37
	19.164	19.234	18.411		19.632	20.455
%	100	58	50	100	65	63

Figure 6.11. TaqMan Saos-2 Huh7

Ct								
	untreated	Saos-2			untreated	Huh-7		
		cond.media	mismatch	40		cond. media	mismatch	40
LMNA	20.35	20.761	20.033	22.902	21.558	22.131	21.904	26.167
	20.107	21.472	20.104	22.998	21.912	22.057		26.264
	20.448	21.449	20.116	23.115				
%	100	127	133	28	100	90	86	10
STAT1	27.46	27.248	25.94	25.987	25.261	25.097	25.235	25.449
	26.245	27.359	25.55	25.654	24.936	24.759	23.372	26.006
	26.243	27.777	25.642	25.886	25.124	24.696	24.948	25.625
%	100	139	206	193	100	132	132	111
OAS1	33.479	33.359	29.959	29.588	29.124	29.075	28.589	29.798
	33.007	33.453	30.264	29.537	29.446	29.024	29.127	29.924
	32.273	34.22	30.068	29.392	29.292	28.861	28.693	29.375
%	100	144	641	927	100	136	123	124
ACTB	19.049	20.09	19.335	19.195	18.742	19.191	18.547	19.121
	18.777	20.617	19.181	19.189	18.654	18.369	18.323	19.562
	18.949	20.077	19.001	20.362	18.239	18.679	18.368	19.223

Figure 6.12. TaqMan human HSC

	Ct		
	untreated	mismatch	300
LMNA	19.997	20.47	21.316
	20.259	20.815	21.329
%	100	119	60
STAT1	24.651	21.991	21.938
	24.433	22.053	21.497
	24.827	22.241	22.087
%	100	774	904
OAS1	35.598	22.17	23.036
		22.343	23.175
%	100	616500	394203
ACTB	18.047	18.689	18.602
	18.19	19.164	18.411

List of references

- Ahn,M.Y., Huang,G., Bae,S.C., Wee,H.J., Kim,W.Y., Ito,Y. (1998). Negative regulation of granulocytic differentiation in the myeloid precursor cell line 32Dcl3 by ear-2, a mammalian homolog of *Drosophila* seven-up, and a chimeric leukemogenic gene, AML1/ETO. *Proc.Natl.Acad.Sci.U.S.A* 95, 1812-1817.
- Alarcon-Riquelme,M.E. (2003). A RUNX trio with a taste for autoimmunity. *Nat.Genet.* 35, 299-300.
- Alcolado,R., Arthur,M.J., Iredale,J.P. (1997). Pathogenesis of liver fibrosis. *Clin.Sci.(Colch.)* 92, 103-112.
- Alexander,C., Howard,E.W., Bissell,M.J., Werb Z. (1996). Rescue of mammary epithelial cell apoptosis and entactin degradation by a tissue inhibitor of metalloproteinase-1 transgene. *J. Cell. Biol.* 135, 1669-1677.
- Armesilla,A.L., Calvo,D., Vega,M.A. (1996). Structural and Functional characterisation of the human CD36 gene promoter: Identification of a proximal PEBP2/CBF site. *J. Biol. Chem.* 271, 7781-7787.
- Aronson,B.D., Fisher,A.L., Blechman,K., Caudy,M., Gergen,J.P. (1997). Groucho-dependent and -independent repression activities of Runt domain proteins. *Mol.Cell Biol.* 17, 5581-5587.
- Arthur,M.J., Mann,D.A., Iredale,J.P. (1998). Tissue inhibitors of metalloproteinases, hepatic stellate cells and liver fibrosis. *J.Gastroenterol.Hepatol.* 13 Suppl, S33-S38.
- Bae,S.C., Ogawa,E., Maruyama,M., Oka,H., Satake,M., Shigesada,K., Jenkins,N.A., Gilbert,D.J., Copeland,N.G., Ito,Y. (1994). PEBP2 alpha B/mouse AML1 consists of multiple isoforms that possess differential transactivation potentials. *Mol.Cell Biol.* 14, 3242-3252.
- Bae,S.C., Choi,J.K. (2004). Tumor suppressor activity of RUNX3. *Oncogene* 23, 4336-4340.
- Bahr,M.J., Vincent,K.J., Arthur,M.J., Fowler,A.V., Smart,D.E., Wright,M.C., Clark,I.M., Benyon,R.C., Iredale,J.P., Mann,D.A. (1999). Control of the tissue inhibitor of metalloproteinases-1 promoter in culture-activated rat hepatic stellate cells: regulation by activator protein-1 DNA binding proteins. *Hepatology* 29, 839-848.
- Banerjee,C., McCabe,L.R., Choi,J.Y., Hiebert,S.W., Stein,J.L., Stein,G.S., Lian,J.B. (1997). Runt homology domain proteins in osteoblast differentiation: AML3/CBFA1 is a major component of a bone-specific complex. *J.Cell Biochem.* 66, 1-8.
- Banerjee,C., Javed,A., Choi,J.C., Green,J., Rosen,V., van Wijnen,A.J., Stein,J.L., Lian,J.B., Stein,G.S. (2001). Differential regulation of the two principal Runx2/Cbfa1 n-terminal isoforms in response to bone morphogenetic protein-2 during development of the osteoblast phenotype. *Endocrinology* 142, 4026-4039.
- Bangsow,C., Rubins,N., Glusman,G., Bernstein,Y., Negreanu,V., Goldenberg,D., Lotem,J., Ben Asher,E., Lancet,D., Levanon,D., Groner,Y. (2001). The RUNX3 gene-sequence, structure and regulated expression. *Gene* 279, 221-232.
- Barnes,G.L., Javed,A., Waller,S.M., Kamal,M.H., Hebert,K.E., Hassan,M.Q., Bellahcene,A., van Wijnen,A.J., Young,M.F., Lian,J.B., Stein,G.S., Gerstenfeld,L.C. (2003). Osteoblast-related transcription factors Runx2 (Cbfa1/AML3) and MSX2 mediate the expression of bone sialoprotein in human metastatic breast cancer cells. *Cancer Res.* 63, 2631-2637.
- Barnes,G.L., Hebert,K.E., Kamal,M., Javed,A., Einhorn,T.A., Lian,J.B., Stein,G.S., Gerstenfeld,L.C. (2004). Fidelity of Runx2 activity in breast cancer cells is required for the generation of metastases-associated osteolytic disease. *Cancer Res.* 64, 4506-4513.
- Benyon,R.C., Iredale,J.P., Goddard,S., Winwood,P.J., Arthur,M.J. (1996). Expression of tissue inhibitor of metalloproteinases 1 and 2 is increased in fibrotic human liver. *Gastroenterology* 110, 821-831.

- Benyon,R.C., Arthur,M.J. (1998). Mechanisms of hepatic fibrosis. *J.Pediatr. Gastroenterol. Nutr.* 27, 75-85.
- Benyon,R.C., Iredale,J.P. (2000). Is liver fibrosis reversible? *Gut* 46, 443-446.
- Benyon,R.C., Arthur,M.J. (2001). Extracellular matrix degradation and the role of hepatic stellate cells. *Semin.Liver Dis.* 21, 373-384.
- Bertrand-Philippe,M., Ruddell,R.G., Arthur,M.J., Thomas,J., Mungalsingh,N., Mann,D.A. (2004). Regulation of tissue inhibitor of metalloproteinase 1 gene transcription by RUNX1 and RUNX2. *J.Biol.Chem.* 279, 24530-24539.
- Bigg,H.F., McLeod,R., Waters,J., Cawston,T.E., Nolan,J.F., Clark,I.M. (1999). Induction of human tissue inhibitor of metalloproteinase-1 gene expression by all-trans retinoic acid in combination with basic fibroblast growth factor involves both p42/44 and p38 MAP kinases. *Ann.N.Y.Acad.Sci.* 878, 506-509.
- Bigg,H.F., McLeod,R., Waters,J.G., Cawston,T.E., Clark,I.M. (2000). Mechanisms of induction of human tissue inhibitor of metalloproteinases-1 (TIMP-1) gene expression by all-trans retinoic acid in combination with basic fibroblast growth factor. *Eur.J.Biochem.* 267, 4150-4156.
- Borrow,J., Stanton,V.P., Jr., Andresen,J.M., Becher,R., Behm,F.G., Chaganti,R.S., Civin,C.I., Distèche,C., Dube,I., Frischauf,A.M., Horsman,D., Mitelman,F., Volinia,S., Watmore,A.E., Housman,D.E. (1996). The translocation t(8;16)(p11;p13) of acute myeloid leukaemia fuses a putative acetyltransferase to the CREB-binding protein. *Nat.Genet.* 14, 33-41.
- Boyce,F.M., Bucher,N.L. (1996). Baculovirus-mediated gene transfer into mammalian cells. *Proc.Natl.Acad.Sci.U.S.A* 93, 2348-2352.
- Brew,K., Dinakarbandian,D., Nagase,H. (2000). Tissue inhibitors of metalloproteinases: evolution, structure and function. *Biochim. Biophys. Acta.* 1477, 267-283.
- Bridge,A.J., Pebernard,S., Ducraux,A., Nicoulaz,A.L., Iggo,R. (2003). Induction of an interferon response by RNAi vectors in mammalian cells. *Nat.Genet.* 34, 263-264.
- Bristow,C.A., Shore,P. (2003). Transcriptional regulation of the human MIP-1alpha promoter by RUNX1 and MOZ. *Nucleic Acids Res.* 31, 2735-2744.
- Britos-Bray,M., Friedman,A.D. (1997). Core binding factor cannot synergistically activate the myeloperoxidase proximal enhancer in immature myeloid cells without c-Myb. *Mol.Cell Biol.* 17, 5127-5135.
- Bromberg,J., Darnell,J.E., Jr. (2000). The role of STATs in transcriptional control and their impact on cellular function. *Oncogene* 19, 2468-2473.
- Bruhn,L., Munnerlyn,A., Grosschedl,R. (1997). ALY, a context-dependent coactivator of LEF-1 and AML-1, is required for TCRalpha enhancer function. *Genes Dev.* 11, 640-653.
- Butler,G.S., Butler,M.J., Atkinson,S.J., Will,H., Tamura,T., van Westrum,S.S., Crabbe,T., Clements,J., d'Ortho,M.P., Murphy,G. (1998). The TIMP2 membrane type 1 metalloproteinase "receptor" regulates the concentration and efficient activation of progelatinase A. A kinetic study. *J.Biol.Chem.* 273, 871-880.
- Cameron,E.R., Neil,J.C. (2004). The Runx genes: lineage-specific oncogenes and tumor suppressors. *Oncogene* 23, 4308-4314.
- Campbell,C.E., Flenniken,A.M., Skup,D., Williams,B.R. (1991). Identification of a serum- and phorbol ester-responsive element in the murine tissue inhibitor of metalloproteinase gene. *J.Biol.Chem.* 266, 7199-7206.

- Carmeliet,P., Moons,L., Lijnen,R., Janssens,S., Lupu,F., Collen,D., Gerard,R.D. (1997). Inhibitory role of plasminogen activator inhibitor-1 in arterial wound healing and neointima formation: a gene targeting and gene transfer study in mice. *Circulation* 96, 3180-3191.
- Chandrasoma,P., Taylor,C.R. (1995) Concise pathology, Second edition. Appleton and Lange
- Chang,D.J., Ji,C., Kim,K.K., Casinghino,S., McCarthy,T.L., Centrella,M. (1998). Reduction in transforming growth factor beta receptor I expression and transcription factor Cbfa1 on bone cells by glucocorticoid. *J.Biol.Chem.* 273, 4892-4896.
- Cho,J.Y., Akbarali,Y., Zerbini,L.F., Gu,X., Boltax,J., Wang,Y., Oettgen,P., Zhang,D.E., Libermann,T.A. (2004). Isoforms of the Ets transcription factor NERF/ELF-2 physically interact with AML1 and mediate opposing effects on AML1-mediated transcription of the B cell-specific blk gene. *J.Biol.Chem.* 279, 19512-19522.
- Clark,I.M., Rowan,A.D., Edwards,D.R., Bech-Hansen,T., Mann,D.A., Bahr,M.J., Cawston,T.E. (1997). Transcriptional activity of the human tissue inhibitor of metalloproteinases 1 (TIMP-1) gene in fibroblasts involves elements in the promoter, exon 1 and intron 1. *Biochem.J.* 324 (Pt 2), 611-617.
- Comer,F.I., Hart,G.W. (2000). O-Glycosylation of nuclear and cytosolic proteins. Dynamic interplay between O-GlcNAc and O-phosphate. *Biol. Chem.* 275, 29179-29182.
- Condreay,J.P., Witherspoon,S.M., Clay,W.C., Kost,T.A. (1999). Transient and stable gene expression in mammalian cells transduced with a recombinant baculovirus vector. *Proc.Natl.Acad.Sci.U.S.A* 96, 127-132.
- Crocker,S.J., Pagenstecher,A., Campbell,I.L.(2004). The TIMPs tango with MMPs and more in the central nervous system. *J. Neurosci. Res.* 75, 1-11.
- D'Alonzo,R.C., Selvamurugan,N., Karsenty,G., Partridge,N.C. (2002). Physical interaction of the activator protein-1 factors c-Fos and c-Jun with Cbfa1 for collagenase-3 promoter activation. *J. Biol. Chem.* 277, 816-822.
- Dean,G., Young,D.A., Edwards,D.R., Clark,I.M. (2000). The human tissue inhibitor of metalloproteinases (TIMP)-1 gene contains repressive elements within the promoter and intron 1. *J.Biol.Chem.* 275, 32664-32671.
- Denhardt,D.T., Feng,B., Edwards,D.R., Cocuzzi,E.T., Malyankar,U.M. (1993). Tissue inhibitor of metalloproteinases (TIMP, aka EPA): structure, control of expression and biological functions. *Pharmacol.Ther.* 59, 329-341.
- Dignam,J.D., Lebovitz,R.M. and Roeder,R.G. (1983). Accurate transcription initiation by RNA polymerase-II in a soluble extract from isolate mammalian nuclei. *Nucleic Acids. Res.* 5, 1475-1489.
- Dillin,A. (2003). The specifics of small interfering RNA specificity. *Proc.Natl.Acad.Sci.U.S.A* 100, 6289-6291.
- Drissi,H., Luc,Q., Shakoori,R., Chuva De Sousa,L.S., Choi,J.Y., Terry,A., Hu,M., Jones,S., Neil,J.C., Lian,J.B., Stein,J.L., van Wijnen,A.J., Stein,G.S. (2000). Transcriptional autoregulation of the bone related CBFA1/RUNX2 gene. *J.Cell Physiol* 184, 341-350.
- Drissi,H., Pouliot,A., Koolloos,C., Stein,J.L., Lian,J.B., Stein,G.S., van Wijnen,A.J. (2002). 1,25-(OH)₂-vitamin D3 supresses the bone related Runx2/Cbfa1 gene promoter. *Exp. Cell Res.* 274, 323-333.
- Ducy,P., Zhang,R., Geoffroy,V., Ridall,A.L., Karsenty,G. (1997). Osf2/Cbfa1: a transcriptional activator of osteoblast differentiation. *Cell* 89, 747-754.

- Edwards,D.R., Murphy,G., Reynolds,J.J. Whitham,S.E., Docherty,A.J., Angel,P., Heath,J.K. (1987). Transforming growth factor beta modulates the expression of collagenase and metalloproteinase inhibitor. *EMBO J.* 6, 1899-1904.
- Eguchi,H., Nagano,H., Yamamoto,H., Miyamoto,A., Kondo,M., Dono,K., Nakamori,S., Umeshita,K., Sakon,M., Monden,M. (2000). Augmentation of antitumor activity of 5-fluorouracil by interferon alpha is associated with up-regulation of p27Kip1 in human hepatocellular carcinoma cells. *Clin. Cancer Res.* 6, 2881-2890.
- Elbashir,S.M., Harborth,J., Lendeckel,W., Yalcin,A., Weber,K., Tuschl,T. (2001). Duplexes of 21-nucleotide RNAs mediate RNA interference in cultured mammalian cells. *Nature* 411, 494-498.
- Fears,S., Gavin,M., Zhang,D.E., Hetherington,C., Ben David,Y., Rowley,J.D., Nucifora,G. (1997). Functional characterization of ETV6 and ETV6/CBFA2 in the regulation of the MCSFR proximal promoter. *Proc.Natl.Acad.Sci.U.S.A* 94, 1949-1954.
- Franceschi,R.T., Xiao,G. (2003). Regulation of the osteoblast-specific transcription factor, Runx2: Responsiveness to multiple signal transduction pathways. *J.Cell Biochem.* 88, 446-454.
- Friedman,S.L. (1996). Hepatic stellate cells. *Prog.Liver Dis.* 14, 101-130.
- Friedman,S.L. (2000). Molecular regulation of hepatic fibrosis, an integrated cellular response to tissue injury. *J.Biol.Chem.* 275, 2247-2250.
- Gabele,E., Brennar,D.A., Rippe,R.A. (2003). Liver Fibrosis: Signals leading to the amplification of the fibrogenic hepatic stellate cell. *Frontiers in Bioscience.* 8, 69-77.
- Gamou,T., Kitamura,E., Hosoda,F., Shimizu,K., Shinohara,K., Hayashi,Y., Nagase,T., Yokoyama,Y., Ohki,M. (1998). The partner gene of AML1 in t(16;21) myeloid malignancies is a novel member of the MTG8(ETO) family. *Blood* 91, 4028-4037.
- Gao,R., McCormick,C.J., Arthur,M.J., Ruddell,R., Oakley,F., Smart,D.E., Murphy,F.R., Harris,M.P., Mann,D.A. (2002). High efficiency gene transfer into cultured primary rat and human hepatic stellate cells using baculovirus vectors. *Liver* 22, 15-22.
- Geoffroy,V., Corral,D.A., Zhou,L., Lee,B., Karsenty,G. (1998). Genomic organization, expression of the human CBFA1 gene, and evidence for an alternative splicing event affecting protein function. *Mamm.Genome* 9, 54-57.
- Ghozi,M.C., Bernstein,Y., Negreanu,V., Levanon,D., Groner,Y. (1996). Expression of the human acute myeloid leukemia gene AML1 is regulated by two promoter regions. *Proc.Natl.Acad.Sci.U.S.A* 93, 1935-1940.
- Giese,K., Kingsley,C., Kirshner,J.R., Grosschedl,R. (1995). Assembly and function of a TCR alpha enhancer complex is dependent on LEF-1-induced DNA bending and multiple protein-protein interactions. *Genes Dev.* 9, 995-1008.
- Goldberg,G.I., Strongin,A., Collier,I.E., Genrich,L.T., Marmer,B.L. (1992). Interaction of 92-kDa type IV collagenase with the tissue inhibitor of metalloproteinases prevents dimerization, complex formation with interstitial collagenase, and activation of the proenzyme with stromelysin. *J.Biol.Chem.* 267, 4583-4591.
- Golub,T.R., Barker,G.F., Bohlander,S.K., Hiebert,S.W., Ward,D.C., Bray-Ward,P., Morgan,E., Raimondi,S.C., Rowley,J.D., Gilliland,D.G. (1995). Fusion of the TEL gene on 12p13 to the AML1 gene on 21q22 in acute lymphoblastic leukemia. *Proc.Natl.Acad.Sci.U.S.A* 92, 4917-4921.
- Gomez,D.E., Alonso,D.F., Yoshiji,H., Thorgeirsson,U.P. (1997). Tissue inhibitors of metalloproteinases: structure, regulation and biological functions. *Eur.J.Cell Biol.* 74, 111-122.

- Guede, L., Courtemanch, L., Stetler-Stevenson, M. (1998). Tissue inhibitor of metalloproteinase (TIMP)-1 induces differentiation and an antiapoptotic phenotype in germinal center B cells. *Blood* 92, 1342-1349.
- Gutierrez, S., Liu, J., Javed, A., Montecino, M., Stein, G.S., Lian, J.B., Stein, J.L. (2004). The vitamin D response element in the distal osteocalcin promoter contributes to chromatin organization of the proximal regulatory domain. *J. Biol. Chem.*
- Hall, M.C., Young, D.A., Waters, J.G., Rowan, A.D., Chantry, A., Edwards, D.R., Clark, I.M. (2003). The comparative role of activator protein 1 and Smad factors in the regulation of Timp-1 and MMP-1 gene expression by transforming growth factor-beta 1. *J. Biol. Chem.* 278, 10304-10313.
- Hanai, J., Chen, L.F., Kanno, T., Ohtani-Fujita, N., Kim, W.Y., Guo, W.H., Imamura, T., Ishidou, Y., Fukuchi, M., Shi, M.J., Stavnezer, J., Kawabata, M., Miyazono, K., Ito, Y. (1999). Interaction and functional cooperation of PEBP2/CBF with Smads. Synergistic induction of the immunoglobulin germline Calpha promoter. *J. Biol. Chem.* 274, 31577-31582.
- Hayakawa, T., Yamashita, K., Tanzawa, K., Uchijima, E., Iwata, K. (1992). Growth-promoting activity of tissue inhibitor of metalloproteinase-1 (TIMP-1) for a wide range of cells. A possible new growth factor in serum. *FEBS Lett.* 298, 29-32.
- Hayakawa, T., Yamashita, K., Ohuchi, E., Shinagawa, A. (1994). Cell growth-promoting activity of tissue inhibitor of metalloproteinases-2 (TIMP-2). *J. Cell. Sci.* 107, 2373-2379.
- Hellemans, K., Grinko, I., Rombouts, K., Schuppan, D., Geerts, A. (1999). All-trans and 9-cis retinoic acid alter rat hepatic stellate cell phenotype differentially. *Gut.* 45, 134-42.
- Hendriks, H.F., Verhoofstad, W.A., Brouwer, A., de Leeuw, A.M., Knook, D.L. (1985). Perisinusoidal fat-storing cells are the main vitamin A storage sites in rat liver. *Exp. Cell Res.* 160, 138-149.
- Hernandez-Munain, C., Krangel, M.S. (1994). Regulation of the T-cell receptor delta enhancer by functional cooperation between c-Myb and core-binding factors. *Mol. Cell Biol.* 14, 473-483.
- Hernandez-Munain, C., Krangel, M.S. (1995). c-Myb and core-binding factor/PEBP2 display functional synergy but bind independently to adjacent sites in the T-cell receptor delta enhancer. *Mol. Cell Biol.* 15, 3090-3099.
- Hess, J., Porte, D., Munz, C., Angel, P. (2001). AP-1 and Cbfa/runt physically interact and regulate parathyroid hormone-dependent MMP13 expression in osteoblasts through a new osteoblast-specific element 2/AP-1 composite element. *J. Biol. Chem.* 276, 20029-20038.
- Hirai, H. (2004). AML1 is functionally regulated through p300-mediated acetylation on specific lysine residues. *J. Biol. Chem.* 279, 15630-15638.
- Houglum, K., Badossa, P., Chojkier, M. (1994) TGF-beta and collagen-alpha 1 (I) gene expression are increased in hepatic acinar zone 1 of rats with iron overload. *Am. J. Physiol.* 267, G908-13.
- Howard, E.W., Banda, M.J. (1991). Binding of tissue inhibitor of metalloproteinases 2 to two distinct sites on human 72-kDa gelatinase. Identification of a stabilization site. *J. Biol. Chem.* 266, 17972-17977.
- Huang, G., Shigesada, K., Ito, K., Wee, H.J., Yokomizo, T., Ito, Y. (2001). Dimerization with PEBP2beta protects RUNX1/AML1 from ubiquitin- proteasome-mediated degradation. *EMBO J.* 20, 723-733.
- Hui, A.Y., Friedman, S.L. (2003). Molecular basis of hepatic fibrosis. *Expert reviews in molecular medicine* 1-23.
- Imai, K., Hiramatsu, A., Fukushima, D., Pierschbacher, M.D., Okada, Y. (1997). Degradation of decorin by matrix metalloproteinases: identification of the cleavage sites, kinetic analyses and transforming growth factor-beta1 release. *Biochem. J.* 322, 809-814.

- Imai,Y., Kurokawa,M., Yamaguchi,Y., Izutsu,K., Nitta,E., Mitani,K., Satake,M., Noda,T., Ito,Y., Hirai,H. (2004). The corepressor mSin3A regulates phosphorylation-induced activation, intranuclear location, and stability of AML1. *Mol.Cell Biol.* 24, 1033-1043.
- Inman,C.K., Shore,P. (2003). The osteoblast transcription factor Runx2 is expressed in mammary epithelial cells and mediates osteopontin expression. *J.Biol.Chem.* 278, 48684-48689.
- Inoue,K., Ozaki,S., Shiga,T., Ito,K., Masuda,T., Okado,N., Iseda,T., Kawaguchi,S., Ogawa,M., Bae,S.C., Yamashita,N., Itoharu,S., Kudo,N., Ito,Y. (2002). Runx3 controls the axonal projection of proprioceptive dorsal root ganglion neurons. *Nat.Neurosci.* 5, 946-954.
- Iredale,J.P., Murphy,G., Hembry,R.M., Friedman,S.L., Arthur,M.J. (1992). Human hepatic lipocytes synthesize tissue inhibitor of metalloproteinases-1. Implications for regulation of matrix degradation in liver. *J.Clin.Invest* 90, 282-287.
- Iredale,J.P., Goddard,S., Murphy,G., Benyon,R.C., Arthur,M.J. (1995). Tissue inhibitor of metalloproteinase-I and interstitial collagenase expression in autoimmune chronic active hepatitis and activated human hepatic lipocytes. *Clin.Sci.(Lond)* 89, 75-81.
- Iredale,J.P., Benyon,R.C., Pickering,J., McCullen,M., Northrop,M., Pawley,S., Hovell,C., Arthur,M.J. (1998). Mechanisms of spontaneous resolution of rat liver fibrosis. Hepatic stellate cell apoptosis and reduced hepatic expression of metalloproteinase inhibitors. *J.Clin.Invest* 102, 538-549.
- Irigoyen,J.P., Munoz-Canoves,P., Montero,L., Koziczak,M., Nagamine,Y. (1999). The plasminogen activator system: biology and regulation. *Cell Mol.Life Sci.* 56, 104-132.
- Ito,Y. (1999). Molecular basis of tissue-specific gene expression mediated by the runt domain transcription factor PEBP2/CBF. *Genes Cells* 4, 685-696.
- Ito,Y. (2004). Oncogenic potential of the RUNX gene family: 'overview'. *Oncogene* 23, 4198-4208.
- Javed,A., Gutierrez,S., Montecino,M., van Wijnen,A.J., Stein,J.L., Stein,G.S., Lian,J.B. (1999). Multiple Cbfa/AML sites in the rat osteocalcin promoter are required for basal and vitamin D-responsive transcription and contribute to chromatin organization. *Mol.Cell Biol.* 19, 7491-7500.
- Javed,A., Guo,B., Hiebert,S., Choi,J.Y., Green,J., Zhao,S.C., Osborne,M.A., Stifani,S., Stein,J.L., Lian,J.B., van Wijnen,A.J., Stein,G.S. (2000). Groucho/TLE/R-esp proteins associate with the nuclear matrix and repress RUNX (CBF(alpha)/AML/PEBP2(alpha)) dependent activation of tissue-specific gene transcription. *J.Cell Sci.* 113 (Pt 12), 2221-2231.
- Javed,A., Barnes,G.L., Jasanya,B.O., Stein,J.L., Gerstenfeld,L., Lian,J.B., Stein,G.S. (2001). Runt homology domain transcription factors (Runx, Cbfa, and AML) mediate repression of the bone sialoprotein promoter: evidence for promoter context-dependent activity of Cbfa proteins. *Mol.Cell Biol.* 21, 2891-2905.
- Ji,C., Casinghino,S., Chang,D.J., Chen,Y., Javed,A., Ito,Y., Hiebert,S.W., Lian,J.B., Stein,G.S., McCarthy,T.L., Centrella,M. (1998). CBFa(AML/PEBP2)-related elements in the TGF-beta type I receptor promoter and expression with osteoblast differentiation. *J.Cell Biochem.* 69, 353-363.
- Jimenez,M.J., Balbin,M., Lopez,J.M., Alvarez,J., Komori,T., Lopez-Otin,C. (1999). Collagenase 3 is a target of Cbfa1, a transcription factor of the runt gene family involved in bone formation. *Mol.Cell Biol.* 19, 4431-4442.
- Kanno,T., Kanno,Y., Chen,L.F., Ogawa,E., Kim,W.Y., Ito,Y. (1998). Intrinsic transcriptional activation-inhibition domains of the polyomavirus enhancer binding protein 2/core binding factor alpha subunit revealed in the presence of the beta subunit. *Mol.Cell Biol.* 18, 2444-2454.
- Kim,R., Trubetskoy,A., Susuki,T., Jenkins, N.A., Copeland,N.G., Lenz,J. (2003). Genome-based identification of cancer genes by proviral tagging in mouse retrovirus-induced T-cell lymphomas. *J. virol.* 77, 2056-2062.

- Kim,W.Y., Sieweke,M., Ogawa,E., Wee,H.J., Englmeier,U., Graf,T., Ito,Y. (1999). Mutual activation of Ets-1 and AML1 DNA binding by direct interaction of their autoinhibitory domains. *EMBO J.* 18, 1609-1620.
- Kitabayashi,I., Yokoyama,A., Shimizu,K., Ohki,M. (1998). Interaction and functional cooperation of the leukemia-associated factors AML1 and p300 in myeloid cell differentiation. *EMBO J.* 17, 2994-3004.
- Kitabayashi,I., Aikawa,Y., Nguyen,L.A., Yokoyama,A., Ohki,M. (2001). Activation of AML1-mediated transcription by MOZ and inhibition by the MOZ-CBP fusion protein. *EMBO J.* 20, 7184-7196.
- Komori,T., Yagi,H., Nomura,S., Yamaguchi,A., Sasaki,K., Deguchi,K., Shimizu,Y., Bronson,R.T., Gao,Y.H., Inada,M., Sato,M., Okamoto,R., Kitamura,Y., Yoshiki,S., Kishimoto,T. (1997). Targeted disruption of Cbfa1 results in a complete lack of bone formation owing to maturational arrest of osteoblasts. *Cell* 89, 755-764.
- Kristensen,D.B., Kawada,N., Imamura,K., Miyamoto,Y., Tateno,C., Seki,S., Kuroki,T., Yoshizato,K. (2000). Proteome analysis of rat hepatic stellate cells. *Hepatology* 32, 268-277.
- Kundu,M., Chen,A., Anderson,S., Kirby,M., Xu,L., Castilla,L.H., Bodine,D., Liu, P.P. (2002) *Blood* 7, 2449-2456.
- Le,X.F., Groner,Y., Kornblau,S.M., Gu,Y., Hittelman,W.N., Levanon,D., Mehta,K., Arlinghaus,R.B., Chang,K.S. (1999). Regulation of AML2/CBFA3 in hematopoietic cells through the retinoic acid receptor alpha-dependent signaling pathway. *J.Biol.Chem.* 274, 21651-21658.
- Lee,J. (2000). Metabolic powerhouse. *New Scientist* 1-4.
- Lee,K.S., Buck,M., Houglum,K., Chojkier,M. (1995). Activation of hepatic stellate cells by TGF alpha and collagen type I is mediated by oxidative stress through c-myc expression. *J.Clin.Invest* 96, 2461-2468.
- Lee,K.S., Kim,H.J., Li,Q.L., Chi,X.Z., Ueta,C., Komori,T., Wozney, J.M., Kim,E.G., Choi,J.Y., Ryoo,H.M., Bae,S.C. (2000). Runx2 is a common target of transforming growth factor beta1 and bone morphogenetic protein 2, and cooperation between Runx2 and Smad5 induces osteoblast-specific gene expression in the pluripotent mesenchymal precursor cell line C2C12. *Mol Cell Biol* 20, 8783-8792.
- Lee,S.J., Friedman,S.L., Whalen,R., Boyer,T.D. (1994). Cellular sources of glutathione S-transferase P in primary cultured rat hepatocytes: localization by in situ hybridization. *Biochem.J.* 299 (Pt 1), 79-83.
- Levanon,D., Negreanu,V., Bernstein,Y., Bar-Am,I., Avivi,L., Groner,Y. (1994). AML1, AML2, and AML3, the human members of the runt domain gene-family: cDNA structure, expression, and chromosomal localization. *Genomics* 23, 425-432.
- Levanon,D., Goldstein,R.E., Bernstein,Y., Tang,H., Goldenberg,D., Stifani,S., Paroush,Z., Groner,Y. (1998). Transcriptional repression by AML1 and LEF-1 is mediated by the TLE/Groucho corepressors. *Proc.Natl.Acad.Sci.U.S.A* 95, 11590-11595.
- Levanon,D., Glusman,G., Bangsow,T., Ben Asher,E., Male,D.A., Avidan,N., Bangsow,C., Hattori,M., Taylor,T.D., Taudien,S., Blechschmidt,K., Shimizu,N., Rosenthal,A., Sakaki,Y., Lancet,D., Groner,Y. (2001). Architecture and anatomy of the genomic locus encoding the human leukemia-associated transcription factor RUNX1/AML1. *Gene* 262, 23-33.
- Levanon,D., Groner,Y. (2004). Structure and regulated expression of mammalian RUNX genes. *Oncogene* 23, 4211-4219.
- Li,G., Fridman,R. (1999). Tissue inhibitor of metalloproteinase-1 inhibits apoptosis of human breast epithelial cells. *Cancer Res.* 15, 6267-6275.

- Li,J., Kleeff,J., Guweidhi,A., Esposito,I., Berberat,P.O., Giese,T., Buchler,M.W., Friess,H. (2004a). RUNX3 expression in primary and metastatic pancreatic cancer. *J.Clin.Pathol.* 57, 294-299.
- Li,Q.L., Ito,K., Sakakura,C., Fukamachi,H., Inoue,K., Chi,X.Z., Lee,K.Y., Nomura,S., Lee,C.W., Han,S.B., Kim,H.M., Kim,W.J., Yamamoto,H., Yamashita,N., Yano,T., Ikeda,T., Itohara,S., Inazawa,J., Abe,T., Hagiwara,A., Yamagishi,H., Ooe,A., Kaneda,A., Sugimura,T., Ushijima,T., Bae,S.C., Ito,Y. (2002). Causal relationship between the loss of RUNX3 expression and gastric cancer. *Cell* 109, 113-124.
- Li,Q.L., Kim,H.R., Kim,W.J., Choi,J.K., Lee,Y.H., Kim,H.M., Li,L.S., Kim,H., Chang,J., Ito,Y., Youl,L.K., Bae,S.C. (2004b). Transcriptional silencing of the RUNX3 gene by CpG hypermethylation is associated with lung cancer. *Biochem.Biophys.Res.Comm.* 314, 223-228.
- Libermann,T.A., Pan,Z., Akbarali,Y., Hetherington,C.J., Boltax,J., Yergeau,D.A., Zhang,D.E. (1999). AML1 (CBFalpha2) cooperates with B cell-specific activating protein (BSAP/PAX5) in activation of the B cell-specific BLK gene promoter. *J Biol Chem* 274, 24671-24676.
- Linggi,B., Muller-Tidow,C., van de Locht,L., Hu,M., Nip,J., Serve,H., Berdel,W.E., van der Reijden,B., Quelle,D.E., Rowley,J.D., Cleveland,J., Jansen,J.H., Pandolfi,P.P., Hiebert,S.W. (2002). The t(8;21) fusion protein, AML1 ETO, specifically represses the transcription of the p14(ARF) tumor suppressor in acute myeloid leukemia. *Nat. Med.* 8, 743-750.
- Liu,H., Holm,M., Xie,X.Q., Wolf-Watz,M., Grundstrom,T. (2004). AML1/Runx1 recruits calcineurin to regulate granulocyte macrophage colony-stimulating factor by Ets1 activation. *J.Biol.Chem.* 279, 29398-29408.
- Logan,S.K., Garabedian,M.J., Campbell,C.E., Werb,Z. (1996). Synergistic transcriptional activation of the tissue inhibitor of metalloproteinases-1 promoter via functional interaction of AP-1 and Ets-1 transcription factors. *J.Biol.Chem.* 271, 774-782.
- Lutterbach,B., Sun,D., Schuetz,J., Hiebert,S.W. (1998). The MYND motif is required for repression of basal transcription from the multidrug resistance 1 promoter by the t(8;21) fusion protein. *Mol.Cell Biol.* 18, 3604-3611.
- Lutterbach,B., Hiebert,S.W. (2000). Role of the transcription factor AML-1 in acute leukemia and hematopoietic differentiation. *Gene* 245, 223-235.
- Lutterbach,B., Westendorf,J.J., Linggi,B., Isaac,S., Seto,E., Hiebert,S.W. (2000). A mechanism of repression by acute myeloid leukemia-1, the target of multiple chromosomal translocations in acute leukemia. *J.Biol.Chem.* 275, 651-656.
- Manche,L., Green,S.R., Schmedt,C., Mathews,M.B. (1992). Interactions between double-stranded RNA regulators and the protein kinase DAI. *Mol.Cell Biol.* 12, 5238-5248.
- Mann,D.A., Smart,D.E. (2002). Transcriptional regulation of Hepatic Stellate cell activation. *Gut.* 50, 891-896.
- McCarthy,T.L., Ji,C., Chen,Y., Kim,K.K., Imagawa,M., Ito,Y., Centrella,M. (2000). Runt domain factor (Runx)-dependent effects on CCAAT/enhancer-binding protein delta expression and activity in osteoblasts. *J. Biol. Chem* 275, 21746-21753.
- McGuire,R.F., Bissell,D.M., Boyles,J., Roll,F.J. (1992). Role of extracellular matrix in regulating fenestrations of sinusoidal endothelial cells isolated from normal rat liver. *Hepatology* 15, 989-997.
- McManus,M.T., Sharp,P.A. (2002). Gene silencing in mammals by small interfering RNAs. *Nat.Rev.Genet.* 3, 737-747.
- Melnick,A., Carlile,G.W., McConnell,M.J., Polinger,A., Hiebert,S.W., Licht,J.D. (2000). AML-1/ETO fusion protein is a dominant negative inhibitor of transcriptional repression by the promyelocytic leukemia zinc finger protein. *Blood* 96, 3939-3947.

- Mengshol,J.A., Vincenti,M.P., Brinckerhoff,C.E. (2001). IL-1 induces collagenase-3 (MMP-13) promoter activity in stably transfected chondrocytic cells: requirement for Runx-2 and activation by p38 MAPK and JNK pathways. *Nucleic Acids Res.* 29, 4361-4372.
- Meyers,S., Downing,J.R., Hiebert,S.W. (1993). Identification of AML-1 and the (8;21) translocation protein (AML- 1/ETO) as sequence-specific DNA-binding proteins: the runt homology domain is required for DNA binding and protein-protein interactions. *Mol.Cell Biol.* 13, 6336-6345.
- Meyers,S., Lenny,N., Hiebert,S.W. (1995). The t(8;21) fusion protein interferes with AML-1B-dependent transcriptional activation. *Mol.Cell Biol.* 15, 1974-1982.
- Mink,S., Haenig,B., Klempnauer,K.H. (1997). Interaction and functional collaboration of p300 and C/EBPbeta. *Mol.Cell Biol.* 17, 6609-6617.
- Miyahara,T., Schrum,L., Rippe,R., Xiong,S., Yee,H.F. Jr, Motomura,K., Anania,F.A., Willson,T.M., Tsukamoto,H. (2000). Peroxisome proliferator-activated receptors and hepatic stellate cell activation. *J. Biol. Chem.* 275,35715-35722.
- Miyoshi,H., Shimizu,K., Kozu,T., Maseki,N., Kaneko,Y., Ohki,M. (1991). t(8;21) breakpoints on chromosome 21 in acute myeloid leukemia are clustered within a limited region of a single gene, AML1. *Proc.Natl.Acad.Sci.U.S.A* 88, 10431-10434.
- Miyoshi,H., Ohira,M., Shimizu,K., Mitani,K., Hirai,H., Imai,T., Yokoyama,K., Soeda,E., Ohki,M. (1995). Alternative splicing and genomic structure of the AML1 gene involved in acute myeloid leukemia. *Nucleic Acids Res.* 23, 2762-2769.
- Moss,E.G., Taylor,J.M. (2003). Small-interfering RNAs in the radar of the interferon system. *Nat.Cell Biol.* 5, 771-772.
- Mundlos,S., Otto,F., Mundlos,C., Mulliken,J.B., Aylsworth,A.S., Albright,S., Lindhout,D., Cole,W.G., Henn,W., Knoll,J.H., Owen,M.J., Mertelsmann,R., Zabel,B.U., Olsen,B.R. (1997). Mutations involving the transcription factor CBFA1 cause cleidocranial dysplasia. *Cell* 89, 773-779.
- Murphy,F.R., Issa,R., Zhou,X., Ratnarajah,S., Nagase,H., Arthur,M.J., Benyon,C., Iredale,J.P. (2002). Inhibition of apoptosis of activated hepatic stellate cells by tissue inhibitor of metalloproteinase-1 is mediated via effects on matrix metalloproteinase inhibition: implications for reversibility of liver fibrosis. *J.Biol.Chem.* 277, 11069-11076.
- Murphy,G., Docherty,A.J. (1992). The matrix metalloproteinases and their inhibitors. *Am.J.Respir.Cell Mol.Biol.* 7, 120-125.
- Murphy,G., Nguyen,Q., Cockett,M.I., Atkinson,S.J., Allan,J.A. (1994). Assessment of the role of the fibronectin-like domain of gelatinase A by analysis of deletion mutant. *J. Biol. Chem.* 269, 6632-6636.
- Murphy,G., Willenbrock,F. (1995). Tissue inhibitors of matrix metalloendopeptidases. *Methods Enzymol.* 248, 496-510.
- Nagase,H., Woessner,J.F., Jr. (1999). Matrix metalloproteinases. *J.Biol.Chem.* 274, 21491-21494.
- Nisson,P.E., Watkins,P.C., Sacchi,N. (1993). Transcriptionally active chimeric gene derived from the fusion of the AML gene and a novel gene on chromosome 8 in t(8;21) leukemic cells. *Cancer Genet.Cytogenet.* 66, 81.
- North,T., Gu,T.L., Stacy,T., Wang,Q., Howard,L., Binder,M., Marin-Padilla,M., Speck,N.A. (1999). Cbfa2 is required for the formation of intra-aortic hematopoietic clusters. *Development* 126, 2563-2575.

- Nuchprayoon,I., Meyers,S., Scott,L.M., Suzow,J., Hiebert,S., Friedman,A.D. (1994). PEBP2/CBF, the murine homolog of the human myoleid AML1 and PEBP2 beta/CBF beta proto-oncoproteins, regulates the murine myeloperoxidase and neutrophil elastase genes in immature myeloid cells. *Mol. Cell Biol.* 14, 5558-5568.
- Nucifora,G., Begy,C.R., Erickson,P., Drabkin,H.A., Rowley,J.D. (1993). The 3;21 translocation in myelodysplasia results in a fusion transcript between the AML1 gene and the gene for EAP, a highly conserved protein associated with the Epstein-Barr virus small RNA EBER 1. *Proc.Natl.Acad.Sci.U.S.A* 90, 7784-7788.
- Nucifora,G., Rowley,J.D. (1994). The AML1 gene in the 8;21 and 3;21 translocations in chronic and acute myeloid leukemia. *Cold Spring Harb.Symp.Quant.Biol.* 59, 595-605.
- Nucifora,G., Rowley,J.D. (1995). AML1 and the 8;21 and 3;21 translocations in acute and chronic myeloid leukemia. *Blood* 86, 1-14.
- O'Reilly,M.S., Wiederschain,D., Stetler-Stevenson,W.G., Folkman,J., Moses,M.A. (1999). Regulation of angiostatin production by matrix metalloproteinase-2 in a model of concomitant resistance. *J. Biol. Chem.* 274, 29568-29571.
- Oelgeschlager,M., Janknecht,R., Krieg,J., Schreek,S., Luscher,B. (1996). Interaction of the co-activator CBP with Myb proteins: effects on Myb-specific transactivation and on the cooperativity with NF-M. *EMBO J.* 15, 2771-2780.
- Ogawa,E., Inuzuka,M., Maruyama,M., Satake,M., Naito-Fujimoto,M., Ito,Y., Shigesada,K. (1993a). Molecular cloning and characterization of PEBP2 beta, the heterodimeric partner of a novel *Drosophila* runt-related DNA binding protein PEBP2 alpha. *Virology* 194, 314-331.
- Ogawa,E., Maruyama,M., Kagoshima,H., Inuzuka,M., Lu,J., Satake,M., Shigesada,K., Ito,Y. (1993b). PEBP2/PEA2 represents a family of transcription factors homologous to the products of the *Drosophila* runt gene and the human AML1 gene. *Proc.Natl.Acad.Sci.U.S.A* 90, 6859-6863.
- Okuda,T., van Deursen,J., Hiebert,S.W., Grosveld,G., Downing,J.R. (1996). AML1, the target of multiple chromosomal translocations in human leukemia, is essential for normal fetal liver hematopoiesis. *Cell* 84, 321-330.
- Okuda,T., Takeda,K., Fujita,Y., Nishimura,M., Yagyu,S., Yoshida,M., Akira,S., Downing,J.R., Abe,T. (2000). Biological characteristics of the leukemia-associated transcriptional factor AML1 disclosed by hematopoietic rescue of AML1-deficient embryonic stem cells by using a knock-in strategy. *Mol.Cell Biol.* 20, 319-328.
- Osato,M., Yanagida,M., Shigesada,K., Ito,Y. (2001). Point mutations of the RUNx1/AML1 gene in sporadic and familial myeloid leukemias. *Int.J.Hematol.* 74, 245-251.
- Otto,F., Thornell,A.P., Crompton,T., Denzel,A., Gilmour,K.C., Rosewell,I.R., Stamp,G.W., Beddington,R.S., Mundlos,S., Olsen,B.R., Selby,P.B., Owen,M.J. (1997). Cbfa1, a candidate gene for cleidocranial dysplasia syndrome, is essential for osteoblast differentiation and bone development. *Cell* 89, 765-771.
- Otto,F., Lubbert,M., Stock,M. (2003). Upstream and downstream targets of RUNX proteins. *J.Cell Biochem.* 89, 9-18.
- Pardali,E., Xie,X.Q., Tsapogas,P., Itoh,S., Arvanitidis,K., Heldin,C.H., ten Dijke,P., Grundstrom,T., Sideras,P. (2000). Smad and AML proteins synergistically confer transforming growth factor beta1 responsiveness to human germ-line IgA genes. *J. Biol. Chem.* 275, 3552-3560.
- Pebernard,S., Iggo,R.D. (2004). Determinants of interferon-stimulated gene induction by RNAi vectors. *Differentiation* 72, 103-111.

- Pei,D., Weiss,S.J. (1995). Furin-dependant intracellular activation of the human stromelysin-3 zymogen. *Nature* 18, 244-247.
- Pendas,A.M., Balbin,M., Llano,E., Jimenez,M.G., Lopez-Otin,C. (1997). Structural analysis and promoter characterization of the human collagenase-3 gene (MMP13). *Genomics* 40, 222-233.
- Petrovick,M.S., Hiebert,S.W., Friedman,A.D., Hetherington,C.J., Tenen,D.G., Zhang,D.E. (1998). Multiple functional domains of AML1: PU.1 and C/EBPalpha synergize with different regions of AML1. *Mol.Cell Biol.* 18, 3915-3925.
- Pinzani,M., Milani,S., Grappone,C., Weber,F.L. Jr, Gentilini,P., Abboud,H.E. (1994). Expression of platelet-derived growth factor in a model of acute liver injury. *Hepatology* 19, 701-707.
- Pinzani,M., Marra,F., Carloni,V. (1998). Signal transduction in hepatic stellate cells. *Liver* 18, 2-13.
- Prince,M., Banerjee,C., Javed,A., Green,J., Lian,J.B., Stein,G.S., Bodine,P.V., Komm,B.S. (2001). Expression and regulation of Runx2/Cbfa1 and osteoblast phenotypic markers during the growth and differentiation of human osteoblasts. *J.Cell Biochem.* 80, 424-440.
- Qiao,M., Shapiro,P., Kumar,R., Passaniti,A. (2004). Insulin-like growth factor-1 regulates endogenous RUNX2 activity in endothelial cells through a PI3K/ERK-dependent and Akt-independent signaling pathway. *J.Biol.Chem.*
- Rescan,P.Y., Loreal,O., Hassell,J.R., Yamada,Y., Guillouso,A., Clement,B. (1993) . Distribution and origin of the basement membrane component perlecan in rat liver and primary hepatocyte culture. *Am. J. Pathol.* 142, 199-208.
- Rockey,D.C., Boyles,J.K., Gabbiani,G., Friedman,S.L. (1992). Rat hepatic lipocytes express smooth muscle actin upon activation in vivo and in culture. *J.Submicrosc.Cytol.Pathol.* 24, 193-203.
- Romana,S.P., Poirel,H., Leconiat,M., Flexor,M.A., Mauchauffe,M., Jonveaux,P., Macintyre,E.A., Berger,R., Bernard,O.A. (1995). High frequency of t(12;21) in childhood B-lineage acute lymphoblastic leukemia. *Blood* 86, 4263-4269.
- Sasaki,K. Yagi,H., Bronson,R.T., Tominaga,K., Matsunashi,T., Deguchi,K., Tani,Y., Kishimoto,T., Komori,T. (1996). Absence of fetal liver hematopoiesis in mice deficient in transcriptional coactivators core-binding factor beta. *Proc.Natl.Acad.Sci.U.S.A.* 93, 12359-12363.
- Sato,H., Takino,T., Okada,Y., Cao,J., Shinagawa,A., Yamamoto,E., Seiki,M. (1994). A matrix metalloproteinase expressed on the surface of invasive tumour cells. *Nature* 370, 61-65.
- Scacheri,P.C., Rozenblatt-Rosen,O., Caplen,N.J., Wolfsberg,T.G., Umayam,L., Lee,J.C., Hughes,C.M., Shanmugam,K.S., Bhattacharjee,A., Meyerson,M., Collins,F.S. (2004). Short interfering RNAs can induce unexpected and divergent changes in the levels of untargeted proteins in mammalian cells. *Proc.Natl.Acad.Sci.U.S.A* 101, 1892-1897.
- Schroeder,T.M., Kahler,R.A., Li,X., Westendorf,J.J. (2004). Histone deacetylase 3 interacts with Runx2 to repress the osteocalcin promoter and regulate osteoblast differentiation. *J.Biol.Chem.*
- Schuppan,D. (1990). Structure of the extracellular matrix in normal and fibrotic liver: collagens and glycoproteins. *Semin.Liver Dis.* 10, 1-10.
- Schuppan,D., Ruehl,M., Somasundaram. (2001). Matrix as Modulator of Stellate Cell and Hepatic Fibrogenesis. *Seminars in Liver Disease.* 21, 351-372.
- Selvamurugan,N., Chou,W.Y., Pearman,A.T., Pulumati,M.R., Partridge,N.C. (1998). parathyroid hormone regulates the rat collagenase-3 promoter in osteoblastic cells through the cooperative interaction of the activator protein-1 site and the runt domain binding sequence. *J. Biol. Chem.* 273, 10647-10657.

- Sevetson,B., Taylor,S., Pan,Y. (2004). Cbfa1/RUNX2 directs specific expression of the sclerosteosis gene (SOST). *J.Biol.Chem.* 279, 13849-13858.
- Shaulian,E., Karin,M.(2001). AP-1 in cell proliferation and survival. *Oncogene.* 19, 2390-2400.
- Sledz,C.A., Holko,M., de Veer,M.J., Silverman,R.H., Williams,B.R. (2003). Activation of the interferon system by short-interfering RNAs. *Nat.Cell Biol.* 5, 834-839.
- Smart,D.E., Vincent,K.J., Arthur,M.J., Eickelberg,O., Castellazzi,M., Mann,J., Mann,D.A. (2001). JunD regulates transcription of the tissue inhibitor of metalloproteinases-1 and interleukin-6 genes in activated hepatic stellate cells. *J.Biol.Chem.* 276, 24414-24421
- Smith,M.R., Kung,H., Durum,S.K., Colburn,N.H., Sun,Y. (1997). TIMP-3 induces cell death by stabilizing TNF-alpha receptors on the surface of human colon carcinoma cells. *Cytokine* 9, 770-780.
- Song,S.U., Shin,S.H., Kim,S.K., Choi,G.S., Kim,W.C., Lee,M.H., Kim,S.J., Kim,I.H., Choi,M.S., Hong,Y.J., Lee,K.H. (2003). Effective transduction of osteogenic sarcoma cells by a baculovirus vector. *J.Gen.Virol.* 84, 697-703.
- Stein,G.S., Lian,J.B., van Wijnen,A.J., Stein,J.L., Montecino,M., Javed,A., Zaidi,S.K., Young,D.W., Choi,J.Y., Pockwinse,S.M. (2004). Runx2 control of organization, assembly and activity of the regulatory machinery for skeletal gene expression. *Oncogene* 23, 4315-4329.
- Sterner,D.E., Berger,S.L. (2000). Acetylation of histones and transcription-related factors. *Microbiol.Mol.Biol.Rev.* 64, 435-459.
- Sternlicht,M.D., Lochter,A., Sympton,C.J., Huey,B., Rougier,J.P. Gray,J.W., Pinkel,D., Bissell,M.J., Werb,Z. (1999). The stromal proteinases MMP-3/Stromelysin-1 promotes mammary carcinogenesis. *Cell.* 98, 137-146.
- Sternlicht,M.D., Werb,Z. (2001). How matrix metalloproteinases regulate cell behaviour. *Annu. Rev. Cell Dev. Biol.* 17,463-516.
- Stöcker,W., Grams,F., Baumann,U., Reinemer,P., Gomis-Rüth,F.X. McKay,D.B., Bode,W. (1995). The metzincins-topological and sequential relations between the astacins, adamlynsins, serralyins and matrixins (collagenases) defines a superfamily of zinc peptidases. *Protein Sci.* 4, 823-840.
- Strom,D.K., Nip,J., Westendorf,J.J., Linggi,B., Lutterbach,B., Downing,J.R., Lenny,N., Hiebert,S.W. (2000). Expression of the AML-1 oncogene shortens the G(1) phase of the cell cycle. *J.Biol.Chem.* 275, 3438-3445.
- Sun,L., Vitolo,M.I., Qiao,M., Anglin,I.E., Passaniti,A. (2004). Regulation of TGFbeta1-mediated growth inhibition and apoptosis by RUNX2 isoforms in endothelial cells. *Oncogene* 23, 4722-4734.
- Suzuji,K. Enghild,J.J., Morodomi,T., Salvesen,G., Nagase,H.(1990). Mechanisms of activation of tissue procollagenase by matrix metalloproteinase-3 (stromelysin). *Biochemistry.* 29, 10261-10270.
- Taimr,P., Higuchi,H., Kocova,E., Rippe,R.A., Friedman,S., Gores,G.J. (2003). Activated stellate cells express the TRAIL receptor-2/death receptor-5 and undergo TRAIL-mediated apoptosis. *Hepatology.* 37, 87-95.
- Takahara,T., Furui,K., Yata,Y., Jin,B., Zhang,L.P., Nambu,S., Sato,H., Seiki,M., Watanabe,A. (1997). Dual expression of matrix metalloproteinase-2 and membrane-type matrix metalloproteinase in fibrotic human livers. *Hepatology* (26), 1521-1529.
- Tanaka,T., Mitani,K., Kurokawa,M., Ogawa,S., Tanaka,K., Nishida,J., Yazaki,Y., Shibata,Y., Hirai,H. (1995a). Dual functions of the AML1/Evi-1 chimeric protein in the mechanism of leukemogenesis in t(3;21) leukemias. *Mol.Cell Biol.* 15, 2383-2392.

- Tanaka,T., Tanaka,K., Ogawa,S., Kurokawa,M., Mitani,K., Nishida,J., Shibata,Y., Yazaki,Y., Hirai,H. (1995b). An acute myeloid leukemia gene, AML1, regulates hemopoietic myeloid cell differentiation and transcriptional activation antagonistically by two alternative spliced forms. *EMBO J.* *14*, 341-350.
- Tanaka,T., Kurokawa,M., Ueki,K., Tanaka,K., Imai,Y., Mitani,K., Okazaki,K., Sagata,N., Yazaki,Y., Shibata,Y., Kadowaki,T., Hirai,H. (1996). The extracellular signal-regulated kinase pathway phosphorylates AML1, an acute myeloid leukemia gene product, and potentially regulates its transactivation ability. *Mol. Cell Biol.* *16*, 3967-3979.
- Tang,Y.Y., Crute,B.E., Kelley,J.J., Huang,X., Yan,J., Shi,J., Hartman,K.L., Laue,T.M., Speck,N.A., Bushweller,J.H. (2000). Biophysical characterization of interactions between the core binding factor alpha and beta subunits and DNA. *FEBS Lett.* *470*, 167-172.
- Taniuchi,I., Littman,D.R. (2004). Epigenetic gene silencing by Runx proteins. *Oncogene* *23*, 4341-4345.
- Terry,A., Kilbey,A., Vaillant,F., Stewart,M., Jenkins,A., Cameron,E., Neil,J.C. (2004). Conservation and expression of an alternative 3' exon of Runx2 encoding a novel proline-rich C-terminal domain. *Gene* *336*, 115-125.
- Tjia,S.T., zu Altschiltsche,G.M., Doerfler,W. (1983). Autographa californica nuclear polyhedrosis virus (AcNPV) DNA does not persist in mass cultures of mammalian cells. *Virology.* *125*, 107-117.
- Trim,J.E., Samra,S.K., Arthur,M.J., Wright,M.C., McAulay,M., Beri,R., Mann,D.A. (2000). Upstream tissue inhibitor of metalloproteinases-1 (TIMP-1) element-1, a novel and essential regulatory DNA motif in the human TIMP-1 gene promoter, directly interacts with a 30-kDa nuclear protein. *J.Biol.Chem.* *275*, 6657-6663.
- Uchida,H., Zhang,J., Nimer,S.D. (1997). AML1A and AML1B can transactivate the human IL-3 promoter. *J. Immunol.* *158*, 2251-2258.
- Wang,Q., Stacy,T., Binder,M., Marin-Padilla,M., Sharpe,A.H., Speck,N.A. (1996). Disruption of the Cbfa2 gene causes necrosis and hemorrhaging in the central nervous system and blocks definitive hematopoiesis. *Proc.Natl.Acad.Sci.U.S.A* *93*, 3444-3449.
- Wagnier,A., Legros-Maida,S., Bosselut,R., Bourge,J.F., Lafaurie,C., Ghysdael,C.J., Sasportes,M., Paul,P. (1995). Identification of human granzyme B promoter regulatory elements interacting with activated T-cell specific proteins: Implication of Ikaros and CBF binding sites in promoter activation. *Proc.Natl.Acad.Sci.U.S.A* *92*, 6930-6934.
- Wee,H.J., Huang,G., Shigesada,K., Ito,Y. (2002). Serine phosphorylation of RUNX2 with novel potential functions as negative regulatory mechanisms. *EMBO Reports* *kvf193*.
- Westendorf,J.J., Yamamoto,C.M., Lenny,N., Downing,J.R., Selsted,M.E., Hiebert,S.W. (1998). The t(8;21) fusion product, AML1-ETO, associates with C/EBP-alpha, inhibits C/EBP-alpha-dependent transcription, and blocks granulocyte differentiation. *Mol. Cell Biol.* *18*, 322-333.
- Westendorf,J.J., Hiebert,S.W. (1999). Mammalian runt-domain proteins and their roles in hematopoiesis, osteogenesis, and leukemia. *J.Cell Biochem. Suppl* *32-33*, 51-58.
- Williams,E.J., Iredale,J.P. (1998). Liver cirrhosis. *Postgrad.Med.J.* *74*, 193-202.
- Woolf,E., Xiao,C., Fainaru,O., Lotem,J., Rosen,D., Negreanu,V., Bernstein,Y., Goldenberg,D., Brenner,O., Berke,G., Levanon,D., Groner,Y. (2003). Runx3 and Runx1 are required for CD8 T cell development during thymopoiesis. *Proc.Natl.Acad.Sci.U.S.A* *100*, 7731-7736.

- Wotton,S.F., Blyth,K., Kilbey,A., Jenkins,A., Terry,A., Bernardin-Fried,F., Friedman,A.D., Baxter,E.W., Neil,J.C., Cameron,E.R. (2004). RUNX1 transformation of primary embryonic fibroblasts is revealed in the absence of p53. *Oncogene* 23, 5476-5486.
- Xia,H., Mao,Q., Paulson,H.L., Davidson,B.L. (2002). siRNA-mediated gene silencing in vitro and in vivo. *Nat.Biotechnol.* 20, 1006-1010.
- Xiao,G., Wang,D., Benson,M.D., Karsenty,G., Franceschi,R.T. (1998a). Role of the alpha2-integrin in osteoblast-specific gene expression and activation of the Osf2 transcription factor. *J.Biol.Chem.* 273, 32988-32994.
- Xiao,G., Jiang,D., Thomas,P., Benson,M.D., Guan,K., Karsenty,G., Franceschi,R.T. (2000). MAPK pathways activate and phosphorylate the osteoblast-specific transcription factor, Cbfa1. *J. Biol. Chem.* 275, 4453-4459.
- Xiao,Z.S., Thomas,R., Hinson,T.K., Quarles,L.D. (1998b). Genomic structure and isoform expression of the mouse, rat and human Cbfa1/Osf2 transcription factor. *Gene* 214, 187-197.
- Yagi,R., Chen,L.F., Shigesada,K., Murakami,Y., Ito,Y. (1999). A WW domain-containing yes-associated protein (YAP) is a novel transcriptional co-activator. *EMBO J.* 18, 2551-2562.
- Yamaguchi,Y., Kurokawa,M., Imai,Y., Izutsu,K., Asai,T., Ichikawa,M., Yamamoto,G., Nitta,E., Yamagata,T., Sasaki,K., Mitani,K., Ogawa,S., Chiba,S., Hirai,H. (2004). AML1 is functionally regulated through p300-mediated acetylation on specific lysine residues. *J.Biol.Chem.* 279, 15630-15638.
- Yamauchi,M., Potter,J.J., Mezey,E. (1988). Characteristics of alcohol dehydrogenase in fat-storing (Ito) cells of rat liver. *Gastroenterology* 94, 163-169.
- Ye,S. (2000). Polymorphism in matrix metalloproteinase gene promoters: Implication in regulation of gene expression and susceptibility of various diseases. *Matrix Biol.* 19, 623-629.
- Yoshiji,H., Kuriyama,S., Miyamoto,Y., Thorgeirsson,U.P., Gomez,D.E., Kawata,M., Yoshii,J., Ikenaka,Y., Noguchi,R., Tsujinoue,H., Nakatani,T., Thorgeirsson,S.S., Fukui,H. (2000). Tissue inhibitor of metalloproteinases-1 promotes liver fibrosis development in a transgenic mouse model. *Hepatology* 32, 1248-1254.
- Yoshiji,H., Kuriyama,S., Yoshii,J., Ikenaka,Y., Noguchi,R., Nakatani,T., Tsujinoue,H., Yanase,K., Namisaki,T., Imazu,H., Fukui,H. (2002). Tissue inhibitor of metalloproteinases-1 attenuates spontaneous liver fibrosis resolution in the transgenic mouse. *Hepatology.* 36, 850-860.
- Zambotti,A., Makhluf,H., Shen,J., Ducy,P. (2002). Characterization of an osteoblast-specific enhancer element in the CBFA1 gene. *J. Biol. Chem.* 277, 41497-41506.
- Zhang,D.E., Hetherington,C.J., Chen,H.M., Tenen,D.G. (1994). The macrophage transcription factor PU.1 directs tissue-specific expression of the macrophage colony-stimulating factor receptor. *Mol.Cell Biol.* 14, 373-381.
- Zhang,D.E., Hetherington,C.J., Meyers,S., Rhoades,K.L., Larson,C.J., Chen,H.M., Hiebert,S.W., Tenen,D.G. (1996). CCAAT enhancer-binding protein (C/EBP) and AML1 (CBF alpha2) synergistically activate the macrophage colony-stimulating factor receptor promoter. *Mol.Cell Biol.* 16, 1231-1240.